REGULATION OF THE ESSENTIAL TWO-COMPONENT REGULATORY SYSTEM VICRK IN *STREPTOCOCCUS MUTANS*

by

Yannick Tremblay

Submitted in partial fulfilment of the requirements
for the degree of Doctor of Philosophy

at

Dalhousie University
Halifax, Nova Scotia
September 2009

Your file Votre référence
ISBN: 978-0-494-56458-5
Our file Notre référence
ISBN: 978-0-494-56458-5

DALHOUSIE UNIVERSITY

To comply with the Canadian Privacy Act the National Library of Canada has requested that the following pages be removed from this copy of the thesis:

Preliminary Pages
- Examiners Signature Page (pii)
- Dalhousie Library Copyright Agreement (piii)

Appendices
- Copyright Releases (if applicable)

TABLE OF CONTENTS

LIST OF TABLES

LIST OF FIGURES

ABSTRACT

Streptococcus mutans is considered to be the major etiological agent of dental caries. As an inhabitant of the human oral cavity, *S. mutans* faces frequent environmental changes. Two-component regulatory systems (TCS) play a critical role in responding to these changes. The *S. mutans* genome encodes 14 TCSs including ComDE and LiaFSR which have been linked to acid stress response and biofilm formation, key virulence traits for *S. mutans*. Another TCS, VicRK, has been shown to be essential for growth.

The main objective of this study was to identify environmental and bacterial factors regulating the expression of the *vicRKX* operon. The promoter of the *vicRKX* operon was fused to a promoterless *lacZ* reporter gene and introduced into *S. mutans* strain UA159. LacZ-plate assays identified pH, vancomycin, ampicillin, penicillin G, and polymyxin B, but not carbohydrates, as factors affecting expression. Using an RNA dot blot approach, it was observed that transcript levels of the response regulator gene, *vicR*, were at their highest in exponential-phase cells cultured in HEPES-buffered tryptone-vitamin media with glucose at pH 7.8 (HTVG). The pH-dependent expression of *vicR* implicated the LiaFSR TCS in its regulation. To investigate this further, the associated genes were deleted. The LiaFSR system mutant and the histidine kinase mutant (Δ*liaS*) exhibited up-regulation of *vicR* in HTVG whereas the response regulator mutant (Δ*liaR*) exhibited down-regulation of *vicR* expression in tryptone-vitamin media with glucose at pH 6.0 ($TVG_{6.0}$). Given that several TCSs autoregulate their expression, the role of the histidine kinase VicK and the accessory protein VicX was assessed. Expression was unchanged in Δ*vicK*, Δ*vicX* and Δ*vicKX* mutants suggesting that VicRK does not autoregulate its expression. The role of another TCS (ComDE) associated with virulence was also assessed. It was observed that the competence-stimulating peptide down-regulated *vicR* expression in a ComX-independent manner.

It was concluded that in the absence of stress, *vicR* expression was growth-phase dependent and regulation of *vicR* expression is embedded in the cell-division process. Furthermore, *vicR* expression is induced indirectly by the LiaFSR system during cell-envelope stress.

LIST OF ABBREVIATIONS USED

18-CSP	18-amino-acid CSP
2DGE	Two-Dimensional Gel Electrophoresis
21-CSP	21-amino-acid CSP
ATR	Acid Tolerance Response
BHI	Brain Heart Infusion broth
CHAPS	3-[(3-Cholamidopropyl)dimethylammonio]-1-propanesulfonate
CSP	Competence-Stimulating Peptide
DBM	Defined Biofilm Medium
DEPC	Diethyl Pyrocarbonate
DIG	Digoxigenin
DTT	Dithiothreitol
FBS	Fetal Bovine Serum
GBP	Glucan-Binding Protein
GTF	Glucosyltransferases
HEPES	4-(2-hydroxyethyl)-1-piperazineethanesulfonic acid
HK	Histidine Kinase
HTVG	HEPES-buffered TVG
IEF	Isoelectric Focusing
IPTG	Isopropyl β-D-1-thiogalactopyranoside
LC-MS/MS	Liquid Chromatography followed by Tandem Mass Spectrometry
LB	Lysogeny Broth
MBP	Maltose-binding Protein
MES	2-(*N*-morpholino)ethanesulfonic acid

MIC	Minimal Inhibitory Concentration
MOPS	3-(N-morpholino)propanesulfonic acid
ONPG	Ortho-Nitrophenyl-β-galactoside
PBS	Phosphate-buffered Saline
PPB	Potassium Phosphate Buffer
PMSF	Phenylmethylsulfonyl Fluoride
PTS	Phosphoenolpyruvate-sugar Phosphotransferase System
RR	Response Regulator
SEM	Scanning Electron Microscopy
sHA	Saliva-coated Hydroxyapatite
SOC	Super Optimal Broth with Catabolite Repression
TBS	Tris-buffered Saline
TCS	Two-component Regulatory System
THB	Todd-Hewitt Broth
THY	Todd-Hewitt Broth with Yeast extract
TSG	Tryptone-Salt-Glucose medium
TTBS	TBS containing Tween 20
TV	Tryptone-vitamins based media
TVG	TV with Glucose
$TVG_{5.0}$	TVG with pH adjusted to 5.0
$TVG_{6.0}$	TVG with pH adjusted to 6.0
$TVG_{7.8}$	TVG with pH adjusted to 7.8
TY	Tryptone broth medium
TYEG	Tryptone-yeast-extract-glucose media

ACKNOWLEDGEMENTS

I would like to thank my supervisor, Dr. Song Lee, for giving me an opportunity to work in his laboratory and his guidance. My supervisory committee (Drs. Scott Halperin, Jessica Boyd, Yung-Hua Li and Rafael Garduno) is also acknowledged for their advice and guidance. Past and present graduate students (Matthew Mayer, Elisabeth Davis, Ahmad Hussein, Mahdi Aminian, Karenn Chan, Jennifer Knight and Nicole McCormick) and post-doctoral fellow (Elisoa Andrian) in the Lee/Halperin laboratory are thanked for providing stimulating conversations, technical assistance, and their patience. I would also like to acknowledge past undergraduate students in the Lee/Wang/Halperin laboratory, Jason David, Henry Lo and Alexandra Vivhelin, for testing my knowledge, skills and patience. Yi-Jing Li, Anette Morris, Carrie Philips and Rebecca Townsend are also thanked for their technical assistance. Members of Dr. Nikhil Thomas' laboratory, especially Jenny-Lee Thomassin and Darren Starty, generously provided their time for training me to use their Western blotting equipment and the VersaDoc MP Imaging system, and for general scientific discussion. Dr. Celia Lima from Dr. Rafael Garduno's laboratory, and Dr. Joanna Potrykus and Craig Steeves from Dr. Steve Bearne's laboratory are thanked for teaching me the technical aspect of two-dimensional gel electrophoresis. Technical assistance with the preparation of the scanning electron samples and analysis from Mary Ann Trevors, Dr. Ping Li and Patricia Scallion was also greatly appreciated. I would also like to thank Audrey Chong, Matthew Mayer and Elisabeth Davis for critically reading my comprehensive exam answers, and Jenny-Lee Thomassin for critically reading my thesis. The Natural Sciences and Engineering Research Council of Canada (NSERC) supported this work.

Chapter 1. Introduction

1.1 *Streptococcus mutans*

Streptococcus mutans is a Gram-positive coccus belonging to the family *Streptococcaceae* in the *Lactobacillales* sub-class of the *Bacilli*. *S. mutans* is a resident of the oral cavity microbiota of humans. It is considered to be the major etiological agent of dental caries and a cause of infective endocarditis. *S. mutans* was first isolated in 1924 by Clarke (as cited by Banas, 2004) and was confirmed as the bacterium causing carious lesions in a clinical setting in the 1960's (Banas, 2004). Clinical findings were later confirmed using germ-free rats as an animal model.

1.1.1 Virulence Factors

It is generally accepted that *S. mutans* possesses three key virulence determinants: its ability to attach to teeth, to generate acid (acidogenicity) and to tolerate acid (aciduricity). Specific genes involved in these traits are summarized in Table 1.1. Attachment of *S. mutans* is mediated by both sucrose-independent and sucrose-dependent mechanisms. *S. mutans* is able to form tenacious biofilms in which attachment plays a key role. Biofilm formation has an impact on the ability of *S. mutans* to resist acids produced from its own fermentation by-products. The production of acids is the key event associated with demineralization of the tooth enamel and the development of carious lesions (Quivey et al., 2001).

1.1.1.1 Attachment

In the absence of sucrose, adherence of *S. mutans* is mediated by ionic and lectin-

Table 1.1. Virulence factors of *S. mutans*

Virulence Categories and Factors	Gene(s)	Function
Sucrose-independent attachment		
Antigen I/II	*spaP*	Binds to salivary agglutinin and pellicle
130 kDa Fibronectin-binding protein	Not identified	Binds to fibronectin
63 kDa Fibronectin-binding protein	*fbp*	Binds to fibronectin
Collagen-binding protein	*wapA*	Binds to collagen
Sucrose-dependent attachment		
Glucosyltransferase B	*gtfB*	Synthesis of water-insoluble glucan
Glucosyltransferase C	*gtfC*	Synthesis of water-insoluble glucan
Glucosyltransferase D	*gtfD*	Synthesis of water-soluble glucan
Glucan-binding protein A	*gbpA*	Binds to glucan; biofilm architecture
Glucan-binding protein B	*gbpB*	Binds to glucan; peptidoglycan hydrolase
Glucan-binding protein C	*gbpC*	Binds to glucan; biofilm architecture
Glucan-binding protein D	*gbpD*	Binds to glucan and lipoteichoic acid
Acidogenicity and aciduricity		
Lactate dehydrogenase	*ldh*	Lactic acid production
F_1F_0-ATPase proton pump	*atpBHA GDC* and *uncEF*	proton-translocation across the membrane
Acid-inducible DNA repair	*recA* and others	Repair of DNA damage

Virulence Categories and Factors	**Gene(s)**	**Function**
Enrichment of fatty acid with mono-saturated and longer chain fatty acids	many	Decrease permeability of membrane
Addition of D-alanyl to lipoteichoic acid	*dltABCD*	Modify the charge of the cell-wall
Diacylglycerol kinase	*dgk*	Phospholipid turn-over
Heat shock proteins	many	Undefined role but likely prevent protein misfolding
Translocation machinery	many	Role undefine but likely help exportation of needed surface protein
Biofilm formation		
Fructosyltransferase (Ftf)	*ftf*	Fructan synthesis
Biofilm regulatory protein	*brpA*	Biofilm formation
Regulation of virulence		
ComDE TCS	*comDE*	Regulation of ATR and biofilm
LuxS-quorum sensing system	*luxS* and others	Regulation of biofilm formation
Trigger factor	*ropA*	Regulation of biofilm formation
Orphan RR CovR	*covR*	Regulation of *gtfB*,*gtfC*, *gtfD* and *gbpC* expression
Magnesium and iron regulator, SloR	*sloR*	Regulation of *covR* expression
VicRK TCS	*vicRK*	Regulation of GTF gene expression
LiaSR TCS	*liaSR*	Regulation of GTF and GbpC genes expression

like interactions to salivary agglutinin, other oral bacteria, extracellular matrix and epithelial cell-surface receptors. The main adhesin for the sucrose-independent mechanisms is the streptococcal protein antigen P1 (SpaP) also know as antigen I/II. In the presence of sucrose, cell-surface-associated glucosyltransferases (GTFs) synthesize glucans which are used by glucan-binding proteins (GBPs) to mediate attachment (Banas and Vickerman, 2003). The molecular architecture of the surface proteins involved in attachment is depicted in Fig 1.1.

1.1.1.1.1 Sucrose-Independent Attachment

In the oral cavity, the initial adhesion of *S. mutans* is considered to be mainly influenced by SpaP which is also known as P1, PAc and antigen I/II. SpaP is a 185 kDa surface protein and similar proteins are found in other oral streptococci (Ma et al., 1991). As a group, the SpaP homologues are usually refered to as the antigen I/II family and all members of the family share similar structural amino-acid domains (Fig 1.1); however, their ability to bind salivary agglutinin, salivary pellicle and other plaque bacteria varies among oral streptococcal species (Whittaker et al., 1996; Petersen et al., 2002). Proteins of the antigen I/II family are secreted by the aid of a typical N-terminal signal peptide. Once secreted, the protein is anchored to the cell wall by sortases (Lee and Boran, 2003) and the anchoring process is directed by a typical C-terminal LPXTG motif (Homonylo-McGavin and Lee, 1996). The proteins are also characterized by a highly charged N-terminal region followed by multiple alanine-rich repeats. A variable region separates the alanine-rich repeat region and the multiple proline-rich repeat region (Okahashi et al., 1989; Demuth and Irvine, 2002; Troffer-Charlier et al., 2002). Both the alanine-rich and

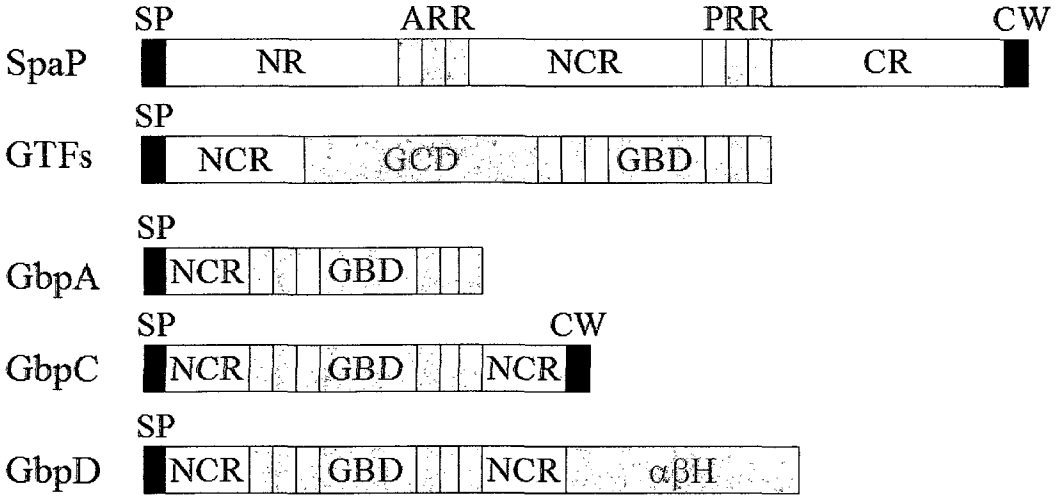

Fig 1.1 Molecular architecture of SpaP, GTFs, GbpA, GbpC and GbpD. Depiction of SpaP and GTFs show the general architecture for the antigen I/II family and GTF family, respectively. GBP are drawn individually because each protein has distinct architecture. GbpB was omitted because it does not possess the typical glucan-binding domain. Signal peptide (SP), N-terminal region (NR), alanine-rich repeats (ARR), non-conserved region (NCR), proline-rich repeats (PRR), conserved region (CR), GTF catalytic domain (GCD), repeat-rich glucan-binding domains (GBD), α/β hydrolase family domain (αβH) and cell wall anchor motif (CW) are shown where appropriate. Proteins are not drawn to scale.

proline-rich repeats are thought to be responsible for the binding of antigen I/II proteins to salivary components (Brady et al., 1992; Crowley et al., 1993; Nakai et al., 1993; Hajishengallis et al., 1994; Yu et al., 1997).

The role of SpaP as an adhesion protein was first discovered in a *S. mutans* mutant exhibiting reduced ability to bind to saliva-coated hydroxyapatite (Lee et al., 1989; Ohta et al., 1989). The loss of SpaP is also characterized by the disappearance of the fuzzy fibrillar surface layer on *S. mutans* cells as observed by electron microscopy. It was later discovered that *in situ* synthesis of glucan improved the ability of a Δ*spaP* mutant to adhere to saliva-coated hydroxyapatite, suggesting SpaP did mediate glucan-independent attachment (Bowen et al., 1991). The same study also investigated the impact of the *spaP* deletion on virulence and it was observed that the mutant was as virulent as the parent strain in a rat model fed a high (56%) sucrose diet indicating that SpaP was not required for virulence. The contribution of SpaP to virulence was, however, determined when a Δ*spaP* mutant could not invade human root dentinal tubules (Love et al., 1997). The designation of SpaP as a virulence factor was confirmed when rats fed a low (5%) sucrose diet were infected with a Δ*spaP* mutant. It was found that the mutant was less virulent than the parent strain (Crowley et al., 1999). It has also been reported that deletion of *spaP* resulted in changes in the biofilm achitecture (Banas, 2004).

Although the role of SpaP as a virulence factor for dental lesions has been established, SpaP does not play a role in infective endocarditis or bacteremia (Nakano et al., 2006). The loss of SpaP reduced *S. mutans* phagocytosis by human polymorphonuclear leukocytes . The deletion of *spaP* also resulted in increased survival in blood and severity of systemic inflammation. Similarly, clinical isolates lacking SpaP

or possessing a truncated SpaP have reduced rates of phagocytosis. It was, therefore, concluded that SpaP increased the susceptibility of *S. mutans* phagocytosis by human polymorphonuclear leukocytes (Nakano et al., 2006).

Attachment of *S. mutans* to the heart during bacteremia and to the extracellular matrix is probably mediated by other surface proteins. It has been demonstrated that the loss of SpaP results in reduced adhesion of *S. mutans* to fibronection, collagen and fibrinogen (Beg et al., 2002). SpaP is not the only factor contributing to the binding of *S. mutans* to the extracellular matrix. Two other fibronectin-binding proteins (Chia et al., 2000; Miller-Torbert et al., 2008) and a collagen-binding protein, WapA (Han et al., 2006), have also been identified.

1.1.1.1.2 Sucrose-Dependent Attachment

When sucrose is available, GTFs located on the surface of *S. mutans* will synthesize glucans. As consequence of their activity, GTFs offer a ligand for GBPs which mediate the sucrose-dependent attachment. Using their sucrase activity, the GTFs are capable of hydrolyzing their natural substrate, sucrose, into glucose and fructose (Monchois et al., 1999). Once hydrolyzed, glucose is added to a growing polymer chain of glucan. One of the functions of glucan is to facilitate bacterium-bacterium interaction. Three GTFs have been identified and characterized in *S. mutans*. Based on secondary structure prediction, GTFs are thought to belong in the α-amylase superfamily (MacGregor et al., 1996). The amino acid sequences among *S. mutans* and oral streptococci GTFs are highly similar and are characterized by the presence of a series of direct repeats at the C-terminus. The repeats function as a glucan-binding domain (Ferretti et al., 1987). Additionally, alteration in the number of repeats resulted in a

decrease or a lack of GTF activity. Alterations in the repeats also changed the structure of the glucan (Monchois et al., 1999). At the N-terminus of GTFs, a signal peptide is present which is followed by a non-conserved region. The catalytic domain is located after the non-conserved region and is necessary for sucrose metabolism (Mooser et al., 1991; Funane et al., 1993; MacGregor et al., 2001). Interestingly, the GTFs lack the typical cell-wall anchoring motif despite being associated with the cell surface.

Two GTFs (GtfB and GtfC) are known to produce water-insoluble glucans (Loesche, 1986) and one GTF (GtfD) produces water-soluble glucans (Banas, 2004). The water-insoluble glucans, also known as mutans, are highly branched polymers with α-1,3-glycosidic linkages whereas the water-soluble glucans are mostly linear polymers with few branches and α-1,6-glycosidic linkages. Both types of glucans participate in sucrose-mediated attachment and dental caries development; however, water-insoluble glucans have been associated with more tenacious adhesion to the tooth surface and dental plaque development (Loesche, 1986), and with smooth surface caries (Munro et al., 1995). It is not known why *S. mutans* possess three GTFs producing different types of glucans but all three proteins appear to be needed for optimal attachment. It has been established that GTFs must be expressed at a certain ratio (20:1:4, GtfB:GtfC:GtfD) for optimal colonization. Alteration to this ratio results in changes to the adherence properties of the dental biofilms (Ooshima et al., 2001). Genes encoding GtfB and GtfC are arranged in tandem and are separated by 198 base pairs. Expression of these two genes is under the control of their own promoters (Fukushima et al., 1992; Smorawinska and Kuramitsu, 1995; Goodman and Gao, 2000). Although the expression of both *gtfB* and *gtfC* appears to be independent of each other, their expression is coordinated,

suggesting that a *gtfB-gtfC* polycistronic transcript exist. However, the existence of a *gftB-gtfC* polycistronic transcript has yet to be determined (Goodman and Gao, 2000).

Unlike GTFs, GBPs have not been identified in non-mutans oral streptococci. GBPs are considered to be an important component of sucrose-dependent attachment. Deletion of GBP genes results in altered plaque structure and decreased cariogenesis (Munro et al., 1991). In *S. mutans*, four GBPs (GbpA, GbpB, GbpC, GbpD) have been isolated and characterized. GbpA was the first GBP to be identified and was isolated by glucan-affinity chromatography (Russell, 1979; Douglas and Russell, 1982; Rusell et al., 1985). The glucan-binding domain of GbpA is located at the C-terminus (Haas and Banas, 2000). Inactivation of *gbpA* caused an increase in virulence and altered the biofilm architecture (Hazlett et al., 1998; 1999). Although GbpB was isolated using glucan-affinity chromatography, GbpB has homology to a peptidoglycan hydrolase and appears to be involved in cell-wall homeostasis rather than attachment (Chia et al., 2001). However, the abilities of clinical isolates to form biofilms is correlated with GbpB levels (Mattos-Graner et al., 2001). Additionally, the gene appears to be essential in some strains (Mattos-Graner et al., 2006). GbpC was the third GBP to be identified and is involved in the dextran-dependent aggregation phenotype (Sato et al., 1997). As expected of surface proteins, GbpC has a membrane anchor and cell-wall-binding domain (Sato et al., 1997). Deletion of the *gbpC* gene impacted biofilm architecture and resulted in a biofilm twice as thick as the parent strain biofilm (Banas et al., 2001). A Δ*gbpC* mutant exhibited a reduce ability to adhere in a sucrose-dependent or sucrose-independent manner or to form carie lesions (Matsumura et al., 2003). It has been shown that deletion of *gbpC* and *gbpA* resulted in reduction of development of dental caries in a rat model (Nakano et al., 2002). Furthermore, GbpC has a higher affinity for water-soluble glucan

produced by GtfD than water-insoluble glucan produced by GtfB and GtfC (Matsumoto et al., 2006). GpbD was the last GBP to be identified and the glucan-binding domain is located in the middle of the protein (Shah and Russell, 2004). GbpD is also characterized by a signal sequence at its N-terminal and a domain with homology to the α/β hydrolase family (including lipases and carboxylesterases) at its C-terminal. In addition to binding glucan, GbpD is also able to bind lipoteichoic acid of *Streptococcus sanguinis* and release fatty acids. Therefore, it has been proposed that GbpD is directly involved in interspecies competition within the plaque biofilm (Shah and Russell, 2004).

1.1.1.2 Acidogenicity and Aciduricity

S. mutans is adapted to metabolize a wide array of carbohydrates. Analysis of the *S. mutans* genome has revealed that this bacterium has a complete glycolytic pathway and can metabolize a wider variety of carbohydrates than any other Gram-positive bacteria (Ajdic et al., 2002). Based on the genomic analysis, *S. mutans* can potentially transport and metabolise glucose, fructose, sucrose, lactose, galactose, mannose, cellobiose, β-glucosides, trehalose, maltose, raffinose, ribulose, mellobiose, starch, isomaltosaccharides, and sorbose. Carbohydrates are almost the sole source of carbon and energy for *S. mutans* (Jacobson et al., 1989). The fermentation of carbohydrates results in the production of pyruvate which is then converted to lactate, formate, acetate or ethanol (Ajdic et al., 2002). Lactate is the major fermentation by-product produced by *S. mutans* when glucose is the primary carbohydrate source (Dashper and Reynolds. 1996). Furthermore, the deletion of lactate dehydrogenase (LDH) is lethal in *S. mutans* (Chen et al., 1994).

Production of lactate reduces the dental plaque pH and, once the pH drops below 5.4, demineralization of the tooth enamel begins and may result in the development of dental lesions. It is generally accepted that the acidogenicity of *S. mutans* is one of the reasons for the decrease of dental plaque pH. As a consequence, the low plaque pH alters the plaque microbiota. Acidification of the plaque microenvironment usually leads to an increased proportion of *S. mutans* and other acidogenic and aciduric species. The change in microbiota further drops the pH and prolongs or prevents recovery of the plaque back to a neutral pH (Loesche et al., 1986; Banas, 2004). The ability of *S. mutans* to survive the acidification of the plaque microenvironment is another determinant of *S. mutans* virulence.

The aciduric ability of *S. mutans* appears to be mediated by the F_1F_0-ATPase proton pump and the up-regulation of several other genes. The process by which *S. mutans* responds and adapts to an acid environment is refered to as the acid-tolerance response (ATR). The ATR appears to be more effective in biofilm cells than planktonic cells (Li et al., 2001a; McNeill and Hamilton, 2003). It has been hypothesized that ATR is mediated by LuxS-quorum sensing (Wen and Burne, 2004) and the two-component regulatory systems (TCSs) ComDE and LiaSR (Li et al., 2001a; 2002a). Furthermore, the contribution of GbpA to biofilm formation also appears to improve aciduricity (Banas et al., 2007).

During acidification of the growth environment, external protons will start to permeate inside *S. mutans* cytoplasm and, consequently, acidify the cytoplasm. An acidic cytoplasm presents a sub-optimal condition for glycolysis and other cellular functions. The F_1F_0-ATPase proton pump is essential for removing the excess protons and establishing and maintaining a pH gradient across the membrane. In *S. mutans*, it has

been shown that the activity of the F_1F_0-ATPase proton pump increases and maintains a pH gradient of one unit (Hamilton and Buckley, 1991; Belli and Marquis, 1991; Dashper and Reynolds, 1992). In response to acidification, the fatty acid content of the membrane is enriched with mono-saturated and longer chain fatty acids within one generation without requiring *de novo* protein synthesis (Quivey et al., 2000; Fozo and Quivey, 2004). The shift in fatty acid composition results in a decreased permeability to protons (Quivey et al., 2000) and in an increased secretion of acidic end products (Dashper and Reynolds, 1996). In addition to membrane fatty acid content, the addition of D-alanyl to lipoteichoic acid (Boyd et al., 2000) and phospholipid turn-over by diacylglycerol kinase (Yamashita et al., 1993) have also been associated with improvement in survival under acid pH. Defects in protein translocation (Gutierrez et al, 1996; 1999; Kremer et al., 2001) and heat-shock proteins (Jayaraman et al, 1997; Lemos et al., 2001; Lemos and Burne, 2002) have also been linked to a decrease in ATR. Furthermore, a DNA repair mechanism has also been hypothesized to play a key role during the ATR. It was noted that the resistance to UV killing of a Δ*recA* mutant could be increased if the mutant underwent ATR (Quivey et al., 1995). It has been proposed that an acid-inducible DNA repair system existed.

1.1.1.3 Biofilm Formation

In its natural environment, *S. mutans* grows and participates in development of a multispecies biofilm, the dental plaque. Therefore, the virulence capability of *S. mutans* is linked to its ability to initiate and develop a biofilm. Components of both sucrose-independent and -dependent attachment have been associated with biofilm development (Banas, 2004; Lynch et al., 2007). Furthermore, the ATR of *S. mutans* has been reported

to be more effective in biofilm grown cells (Li et al., 2001a; McNeill and Hamilton, 2003). In addition to virulence, biofilm formation also appears to impact other biological processes, such as competence. For example, Li et al. (2001b) observed that several *S. mutans* strains grown in a biofilm had a greater transformation frequency that their planktonic counter-parts.

Biofilm formation is a tightly coordinated and regulated process and several factors have been associated with proper biofilm architecture. In *S. mutans*, two TCSs, ComDE and LiaRS (Li et al., 2001b; 2002a), the LuxS-quorum sensing system (Merritt et al., 2003), the trigger factor, RopA (Wen et al., 2005), and a novel regulatory protein (Wen and Burne, 2002) have been identified as regulators of biofilm development. The deletion of the LiaRS TCS, the LuxS-quorum sensing or RopA results in a differential regulation of GTFs or GBPs (Wen et al., 2005; Yoshida et al., 2005; Chong et al., 2008). The GTF genes and fructosyltransferase gene (*ftf*) are up-regulated in biofilm grown cells. Furthermore, secretion of GTFs and Ftf appear to be critical for biofilm development. For example, Huang et al. (2008) correlated an increased expression of the secretory system gene *secA* with an increased expression of the GTF genes, *ftf* and *spaP* in biofilm cells when compared to planktonic cells. The correlation suggests that GTFs, Ftf and SpaP are secreted during biofilm development and that these proteins play a key role during biofilm formation. An increase in the secretion of the GTFs is critical for the synthesis of glucan and, consequently, for the development of the biofilm matrix. The matrix is essential for the cohesiveness of the bacteria. Recently, the role of the GBPs in biofilm formation has been investigated (Lynch et al., 2007). Single, double and triple GBP deletion mutants produced biofilms with a significant loss of thickness, but the reduction in height was dependent on specific GBPs. For example, mutants lacking

GbpA or GbpD occupied a reduced surface area. Mutants missing GbpC individually or in combination with another GBP formed biofilms with increased ratio of surface area to biovolume. Additionally, a Δ*gbpA* mutant formed a biofilm with a reduced ratio of surface area to biovolume. Based on these findings, it has been proposed that GbpA acts as a link between glucan molecules of individual *S. mutans* cells, GbpC acts as a bond between the cells and glucan, and GbpD provides a bond for *S. mutans* to adhere to the exopolysaccharide. It has also been hypothesized that GbpA and GbpD contribute to the scaffolding that allows the biofilm to build outward. Therefore, each GBPs has a unique contribution to the development of proper biofilm achitecture (Lynch et al., 2007).

In addition to the role of GTFs and GBPs, other cellular functions are needed for biofilm formation. For example, the major autolysin, AtlA, was identified as an important component for biofilm formation (Brown et al., 2005; Shibata et al., 2005). It was later found that the production of several surface proteins was reduced in a Δ*atlA* mutant (Ahn and Burne, 2006). These changes in the surface protein profile were suggested to be the reason for the defect in biofilm formation by the mutant.

Given that gene expression is controlled by regulators whose activities are influenced by environmental conditions, the effect of several environmental conditions on biofilm formation have been investigated. For example, the presence of iron and iron-saturated lactoferrin in saliva decreased biofilm formation by *S. mutans* (Francesca et al., 2004). Additionally, manganese supplementation of defined growth media improved biofilm formation in the presence or absence of sucrose; however, the effect of manganese varied among *S. mutans* strains (Arirachakaran et al., 2007a). Changes in iron and other metal ion concentrations is generally considered to be a host signal detected by commensal and pathogenic bacteria (Wandersman and Delepelaire, 2004). The host

influences biofilm formation by *S. mutans* in other ways. For example, the presence of the dietary carbohydrate, starch, in combination with sucrose was associated with up-regulation of *gtfB* and increased accumulation of biofilm biomass on a saliva-coated hydroxyapatite disc. However, *S. mutans* biofilms developed poorly when cultured in the presence of starch alone or in combination with glucose and fructose (Duarte et al., 2008). Furthermore, it has been noted that the presence of sucrose in growth media improved the competitiveness of *S. mutans* in mixed spectococcal biofilms, which contained *Streptococcus oralis*, *Streptococcus gordonii*, *Streptococcus mitis*, and *Streptococcus sobrinus*. In the presence of sucrose, *S. mutans* formed microcolonies whereas in the absence of sucrose, *S. mutans* formed single-cell chains (Kreth et al., 2008a). Interestingly, *S. mutans* biofilms formed in the presence of sucrose were more resistant to Listerine and chlorhexidine treatment (Kreth et al., 2008a). It has been found that dual species biofilms containing *S. mutans* and the benevolant plaque bacterium, *Veillonella parvula*, were more resistant to antimicrobial treatment than their single species counterpart (Kara et al., 2006; 2007; Luppens et al., 2008). To the benefit of *S. mutans*, *V. parvula* does not ferment glucose or most sugars, and metabolizes lactate into weaker acids such as acetic and propionic acids (Distler and Kroncke, 1981). However, not all oral commensal bacteria are beneficial to *S. mutans* biofilm. For example, *S. sanguinis* and *S. gordonii* have been shown to produce hydrogen peroxide (H_2O_2) to compete against, and prevent, *S. mutans* biofilm formation (Kreth et al., 2008b).

1.1.2 Regulation of Virulence-Associated Genes

It has been demonstrated that the expression of GTFs is influenced by several environmental factors including carbohydrate sources, pH and metal ions. It was first

observed that *ftf*, *gtfB* and *gtfC* expression was up-regulated in the presence of sucrose (Hudson and Curtiss, 1990). In addition to sucrose, it was also noted that *gtfB* and *gtfC* expression was influenced by the pH of the growth media (Li and Burne, 2001). Shemesh et al. (2006) also observed that *ftf* expression was strongly induced in the presence of sorbitol and mannitol and moderately induced in the presence of glucose and sucrose. The expression of *gtfB* and *gtfC* was markedly up-regulated in the presence of sorbitol, glucose, sucrose, fructose and mannitol whereas the expression of *gtfD* was only up-regulated in the sorbitol and mannitol (Shemesh et al., 2006). Goodman & Gao (2000) observed that *gtf* expression was growth phase specific and suggested that intercellular signaling was involved in the expression of GTF genes. Shemesh et al. (2006) also noted a growth-phase dependent expression of *ftf*, *gtfB*, *gtfC*, and *gtfD* but the level of induction was dependent on the carbohydrate supplied. Furthermore, it has been observed that GTF gene expression reached its peak during stationary-phase; however, the expression pattern varied among *S. mutans* strains (Stipp et al., 2008).

In addition to growth-phase and carbohydrates, the influence of copper and manganese ions on the expression of GTF genes has also been investigated. In the case of copper, the transcription and translation of *gtfD* but not *gtfB* or *gtfC* was induced by the presence of copper ions (Chen et al., 2006). In contrast, the expression of *gtfB* was up-regulated by manganese in planktonic and biofilm cells whereas the expression of *gtfC* was only induced by manganese in planktonic cells (Ariachakaran et al., 2007b). Manganese also induced the expression of *spaP* in planktonic cells. Levels of *gbpC* transcripts were increased in both planktonic and biofilm cells cultured in the presence of manganese. The expression of *gbpC* was at its maximum at mid-exponential growth phase, induced under thermal stress and repressed at low pH (Biswas et al., 2007).

Interestingly, the carbohydrate source had no impact on *gbpC* expression. On the other hand, the expression of *gbpA* is optimal when *S. mutans* is cultured under an anaerobic atmosphere in neutral pH condition (Banas et al., 1997). A decrease in the expression of *gbpA* and *gbpD* by biofilm cells cultured in the presence of manganese was also observed. (Ariachakaran et al., 2007b).

For *gtfB*,*gtfC*, *gtfD* and *gbpC* regulation, the orphan response regulator, CovR, binds directly to the promoters of *gtfB*, *gtfC*, *gtfD* and *gbpC*, and represses the expression of each gene (Idone et al., 2003; Biswas and Biswas, 2006; Biswas et al, 2007; Chong et al., 2008b). As with the expression of GTF genes and *gbpC*, the concentration of magnesium also impacted the expression of *covR* (Chong et al., 2008b). Recently, it has been observed that the magnesium and iron regulator SloR directly regulates the expression of *covR* (Dunning et al., 2008). The involvement of SloR offers an explanation for the influence of magnesium on the expression of the GTF and GBP genes. SloR has also been shown to directly bind to the promoter of the ComDE TCS genes, *ropA* and *spaP* (Idone et al., 2003). Deletion of trigger factor, RopA, results in decreased levels of GtfB and GtfD (Wen et al., 2005). Furthermore, deletion of *sloR* resulted in biofilm defects of *S. mutans* cultured in sucrose or glucose and therefore, establishes another association between SloR and the GTFs and GBPs.

The regulation of the *gtfB*, *gtfC*, *gtfD* and *gbpC* expression in response to manganese, and possibly iron, can be sumarized by a hierarchical model. Briefly, changes in manganese and iron concentration would result in changes in the binding affinity of SloR towards its targeted sites resulting in up-regulation of *covR, comDE* and *ropA* expression. Changes in *covR* expression in response to SloR would consequently result in similar changes in the CovR regulon. This regulon includes GTFs and GbpC. A

hierarchical model for the SloR-CovR relationship has been proposed for the ATR (Dunning et al., 2008).

In addition to CovR and RopA, the *lux*-quorum sensing system has also been implicated in the regulation of GTF gene expression. In this case, the transcription of *gtfB* and *gtfC* , but not *gtfD*, was upregulated in the mid-exponential phase in the absence of *luxS* (Yoshida et al., 2005). The precise regulatory mechanism has yet to be determined. Other TCS (VicRK and LiaSR) have also been associated with differential expression of the GTFs and GbpC genes (Senadheera *et al.*, 2005; Chong et al., 2008a).

1.1.3 Summary of Pathogenesis of *S. mutans* in the Oral Cavity

It is generally accepted that the pathogenesis of *S. mutans* occurs in three stages: attachment, accumulation and dental plaque formation (summarized in Fig 1.2). During the initial phase, *S. mutans* colonizes the tooth surface by attaching to salivary agglutinin glycoproteins. This adhesion is mediated by SpaP. Once *S. mutans* has attached to the tooth surface, *S. mutans* produces GTFs and, if sucrose is present, the GTFs will synthesize glucans. *S. mutans* will also start producing GBPs. *S. mutans* then start to multiply and accumulate. As glucans are synthesized, GBPs interact with these glucans and *S. mutans* starts to aggregate. This aggregation leads to formation of a biofilm knowns as dental plaque. After a meal, carbohydrates are available and are metabolized into lactic acid. The pH of the dental plaque rapidly decreases (see the Stephan curve; Stephan, 1944) and if the production of acid drops the pH below a critical point (pH 5.4), the tooth enamel demineralizes. The damage to enamel becomes more permanent when *S. mutans* reaches a critical threshold in the multispecies dental plaque.

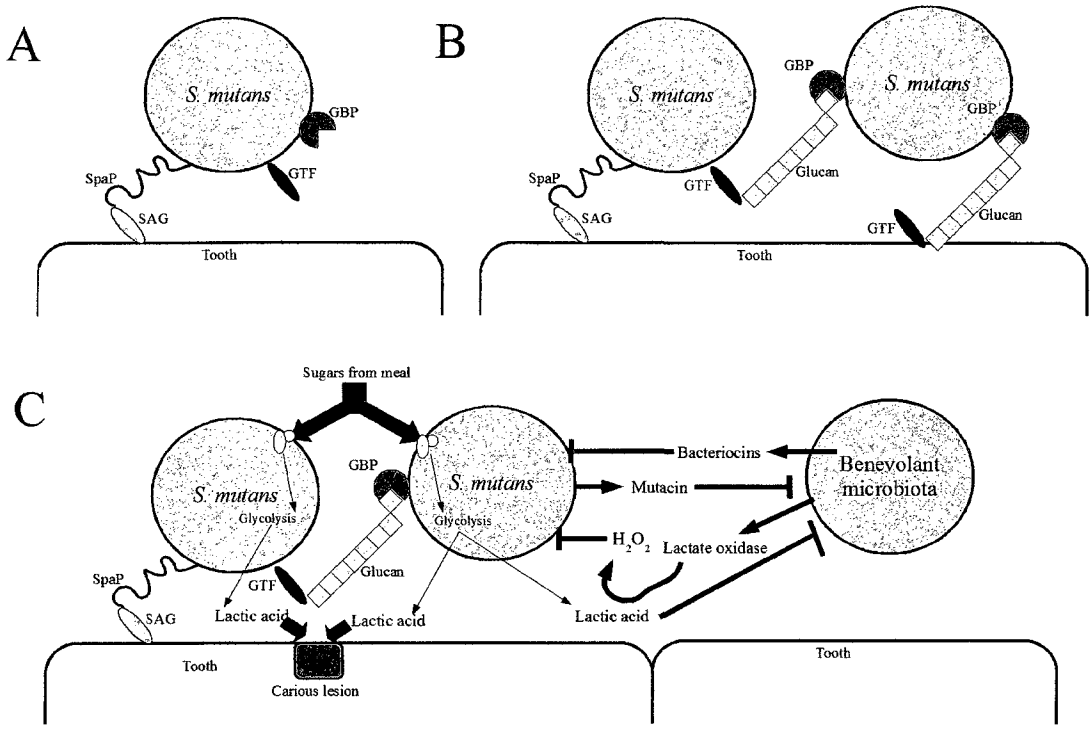

Fig 1.2 Molecular pathogenesis of *S. mutans* in the oral cavity. (A) *S. mutans* colonizes the tooth surface by attaching via SpaP to salivary agglutinin glycoproteins (SAG). (B) GTFs will synthesize glucans, GBPs interact with glucans and *S. mutans* starts to aggregate, multiply and accumulate. (C) After a meal, sugars are metabolized into lactic acid by glycolysis. The pH decreases and the tooth enamel demineralizes. Through the process, *S. mutans* competes with the benevolant microbiota. The figure was adapted from Taubman and Nash (2006) and Mitchell (2003).

Through the process mentioned above, *S. mutans* competes with several other oral microorganisms. For example, the lactic acid produced by *S. mutans* has a bacteriostatic effect on beneficial bacteria (Horiuchi et al., 2009); however, some benevolant organisms such as *Streptococcus oligofermentans* produce H_2O_2 using the lactic acid produced by *S. mutans* (Tong et al., 2007). The production of H_2O_2 kills *S. mutans*. Furthermore, *S. mutans* also produces an array of bacteriocins, known as mutacin, that kill beneficial bacteria. Benevolant bacteria also produce bacteriocins that have bactericidal effect on *S. mutans*. This constant competition between the benevolant population and the harmful bacteria greatly influences the composition of the dental plaque. Consequently, the composition of the dental plaque has a major role in disease outcome.

1.2 Two-Component Regulatory Systems (TCS)

TCS typically contain a membrane-associated sensor-histidine kinase (HK) that transfers information from stimuli to a cytoplasmic-response regulator (RR). The steps in signal transduction performed by TCS are summarized in Fig 1.3. The HK senses environmental changes, nutritional stimuli or peptides. These stimuli are detected by the sensory domain of the HK. In response to these stimuli, the HK undergoes a conformational change and it then autophosphorylates by transferring the γ-phosphoryl group from an ATP molecule to a conserved histidine residue (Bijlsma & Groisman, 2003). The RR then catalyzes the transfer of the phosphoryl group from the phospho-histidine residue to a conserved aspartate residue in the RR regulatory domain (Stock et al., 2000). Normally, the regulatory domain inhibits the activity of the output domain. Once the regulatory domain of the RR is phosphorylated, a conformational change

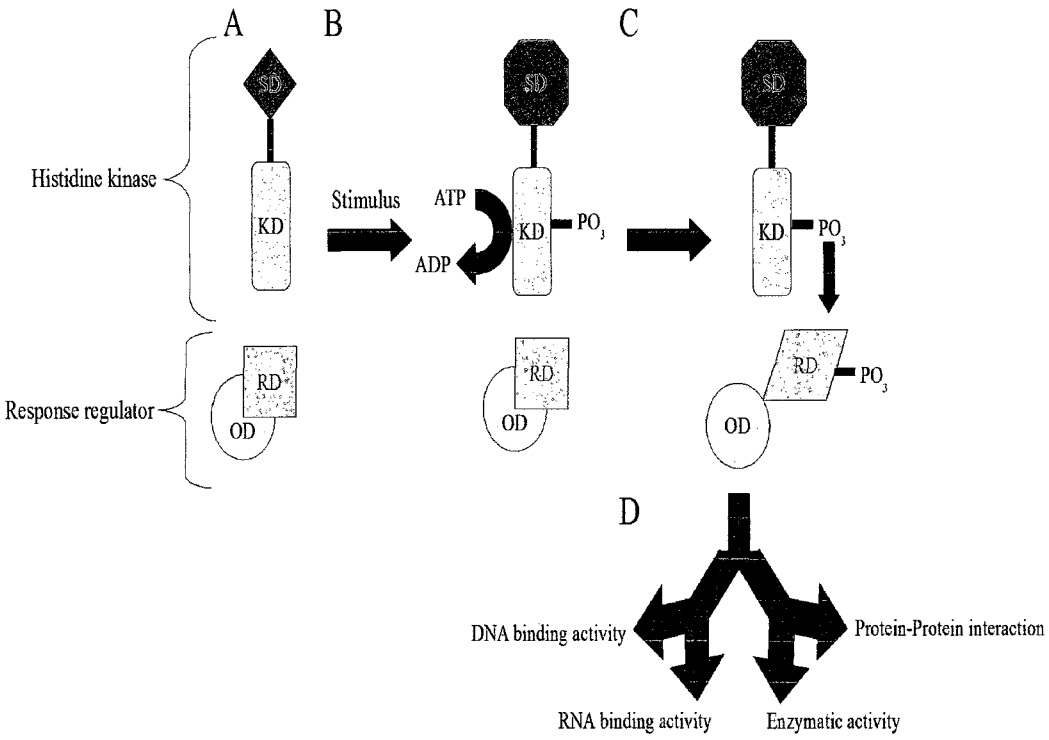

Fig 1.3 Schematic of signal transduction by two-component regulatory system (TCS). TCS composes a histidine kinase and a response regulator. (A) In the absence of stimulus, the regulatory domain (RD) of the response regulator (RR) inhibits the activity of the output domain (OD). (B) Once a stimulus is detected by the sensory domain (SD), the histidine kinase (HK) undergoes a conformational change and the kinase domain (KD) transfers the γ-phosphoryl group from an ATP molecule. (C) The RR catalyzes the transfer of the phosphoryl group from the HK to the RD. This initiates a conformational change which relieves the inhibition OD. (D) The RR is activated and can have an affect on its target. RR can have DNA or RNA binding activity, enzymatic activity or can interact with other proteins.

occurs in the RR relieving the inhibition of the output domain (Hoch, 2000). The RR is now activated. Some RRs can also be phosphorylated by phosphoryl donors such as acetyl phosphate and carbamoyl phosphate (Lukat *et al.*, 1992; McCleary *et al.*, 1993). Furthermore, the phosphoryl transfers require divalent metal ions (Stock et al., 2000). Mg^{2+} is considered to be the most relevant cation *in vivo*. Once activated, the RR via its output domain can have an affect on its target. In approximately 60% of the cases, RRs bind to specific conserved DNA sequence found in promoter regions (Gao et al, 2007). Some RRs prevent the binding of RNA polymerase and other transcription factors to the promoter region whereas other RRs act as accessory proteins in transcription by improving the binding of RNA polymerase binding to the promoter region. In the remaing 40%, RRs interact with proteins and RNA or act as an enzyme (Gao et al, 2007). In response to non-activating signals, the RR is inactivated by its dephosphorylation. The removal of the phosphoryl group is performed by the specific phosphatase activity of HK or aspartyl-phosphatases (Stephenson and Hoch 2002).

As mentioned above, stimuli are sensed by the HK via its sensory domain. An array of sensory domains have been identified and novel domains are reported frequently (Galperin, 2004). The most common sensory domain is the PAS domain (Galperin, 2004). This domain is usually located in the cytoplasm and this domain is thought to sense stimuli arising from the cytoplasm. The PAS domain is characterized by its ligand-binding pocket. This pocket is thought to accommodate an array of flat heterocyclic molecules such as haem, flavin, cinnamic acid and the adenine moiety of ATP (Galperin, 2004). The PAS domain is thought to sense the changes in oxygen concentration, redox potential, proton motive force and light or the presence of specific ligands (Taylor and

Zhulin, 1999). The signals sensed by the PAS domain are considered to be representative of the cell energy status.

In addition to the sensory domain, the signal transduction domain of HK also plays a key role in phosphorelay. One of the most common signal transduction domains is the HAMP domain (Taylor, 2007). This domain is considered to play a role in dimerization or oligomerization events (Aravind and Ponting, 1999). The HAMP domain is usually found in transmembrane receptors (Aravind and Ponting, 1999). Despite recent advancement in the identifcation of domains in HK, the functions of domains are poorly characterized and the nature of the sensed signals is often unknown. Furthermore, experimental evidence gathered for one system often does not apply to a different system with similar domains.

1.2.1 TCS and Virulence

TCS are ubiquitous in bacteria and have been shown to control several cellular processes including chemotaxis, nitrogen fixation, sporulation and virulence in both Gram-negative and Gram-positive pathogens (Bijlsma & Groisman, 2003; Galperin and Gomelsky, 2005). A typical TCS associated with virulence in Gram-negative bacteria is PhoPQ which is found in *Salmonella enterica* serova Typhimurium. The PhoPQ TCS is composed of PhoP (the RR) and PhoQ (the HK) (see Miller et al., 1989). The PhoPQ system controls over 40 genes which enables *S. typhimurium* to successfully enter epithelial cells, survive within macrophages and resist antimicrobial peptides by modifying its lipopolysaccharide composition (see Groisman, 1998; Ernst et al., 1999). PhoP also plays a role in invasion of eukaryotic cells by *Salmonella enterica* serova

Typhi because a *phoP* mutant of this organism has a reduced ability to invade HT-29 cells (Lee et al., 2007).

In Gram-positive bacteria, several TCS have been linked to virulence and the typical example is the CovRS (Control Of Virulence) TCS. In *Streptococcus pyogenes* and *Streptococcus agalactiae*, the CovRS TCS has been established as an important regulator of virulence. In *S. pyogenes*, CovRS regulates the *has* operon, which encodes proteins required for capsule synthesis, other surface-expressed proteins and secreted factors that are required for survival and virulence in animal models and in humans (Levin et al., 1998; Federie et al., 1999; Graham et al., 2002). Isogenic *covRS* mutant have been shown to be hypervirulent in the murine skin infection model (Levin et al., 1998; Federle et al., 1999; Graham et al., 2002). In *S. agalactiae*, Lamy et al. (2004) and Jiang et al. (2005) have demonstrated that a *covRS* deletion mutant had increased haemolytic activity and decreased activity on the Christie-Atkins-Munch-Petersen (CAMP) test. The CAMP test is routinely used to identify *S. agalactiae* and is used to test increased hemolytic activity in the presence of beta-hemolysin produced by some strains of *Staphylococcus aureus*. The *covRS*-deletion mutant was also hyperadherent to epithelial cells and, in animal models, the mutant was attenuated (Lamy et al., 2004; Jiang et al., 2005)

Therefore, it is clear that TCSs play a key a role in the regulation of bacterial virulence and that TCSs are worthy of investigation due to their importance.

1.2.2 TCS in *S. mutans*

A total of 13 TCSs and one orphan response regulator were first identified in the completed genome of *S. mutans* strain UA159 (Ajdic *et al.*, 2002). An additional

response regulator, which is absent from strain UA159, has been predicted in strain CH43 (Qi *et al.*, 2000). Biswas et al. (2008) also found that the genome of *S. mutans* strain UA159 encodes an additional TCS, which was omitted during the initial annotation. This TCS would bring the total number of potential TCSs in strain UA159 to 14. TCS found in *S. mutans* strain UA159 are summarized in Table 1.2. It, however, appears that strain UA159 possesses more TCSs than other *S. mutans* strains. Using the genome of 11 serotype c strains (including UA159, NG8 and GS5), 1 serotypte e strain (V100) and 1 serotype f strain (OMZ175) as template, PCR-amplification of HK genes was only succeseful for only 11 HK of the 13 strains tested and results were confirmed with Southern hybridization. Notably, SMu0041 and SMu1652 were present only in strain UA159 and 8VS3, and SMu0946 was present in all but one strain. Therefore, HK variability exists among *S. mutans* strains.

The study of TCS in *S. mutans* was first initiated by Bhagwat *et al* (2001). Bhagwat and co-workers (2001) were interested in the effect of the deletion of six putative RRs on formation of biofilm; however, only five RRs could be deleted. It was observed that one of the RR mutants was significantly impaired in its ability to form biofilm (*tcbR*, currently known as *comE*). In addition to the study by Bhagwat *et al* (2001), Biswas et al. (2008) and Lévesque et al. (2007) have also systematically deleted all sensor HK in *S. mutans* to characterize their role in stress tolerance response or in expression of virulence determinants, respectively. Biswas et al. (2008) found that the deletion of *liaS* or *ciaH* had the greatest impact on the ability of *S. mutans* to respond to stress. Lévesque et al. (2007) found that deletion of *ciaH* had the greatest impact on the ability of *S. mutans* to grow in the presence of high salt concentration or H_2O_2. Despite the interesting results of the study by Bhagwat *et al.* (2001), Biswas et al. (2008) and

Table 1.2. Two-component regulatory systems of *Streptococcus mutans*

LANL Gene ID[1]	Gene Name[2]	Protein Function	Role[4]	Signal[4]
SMu0041	-----[3]	Histidine Kinase	Not characterized	Unknown
SMu0042	-----	Response Regulator		
SMu0440	*liaS*	Histidine Kinase	Envelope-stress response	Lipid II cycle disruption
SMu0441	*liaR*	Response Regulator		
SMu0525	*lytT*	Response Regulator	Not characterized	Unknown
SMu0526	*lytS*	Histidine Kinase		
SMu0601	*spaR*	Response Regulator	Not characterized	Unknown
SMu0602	*spaK*	Histidine Kinase		
SMu0841	*sptR*	Response Regulator	Survival in saliva	Unknown
SMu0842	*sptS*	Histidine Kinase		
SMu0918	*mbrC*	Response Regulator	Bacitracin resistance	bacitracin-UPP complex
SMu0919	*mbrD*	Histidine Kinase		
SMu0946	*bfrB*	Histidine Kinase	Biofilm formation	Unknown
SMu0947	*bfrA*	Response Regulator		
SMu1031	*ciaH*	Histidine Kinase	Biofilm formation,	Salivary protein or serum protein
SMu1032	*ciaR*	Response		

LANL Gene ID[1]	Gene Name[2]	Protein Function	Role[4]	Signal[4]
		Regulator	competence and mutacin production	
SMu1048	*scnK*	Histidine Kinase	Oxidative-stress response	Unknown
SMu1049	*scnR*	Response Regulator		
SMu1378	*vicK*	Histidine Kinase	Control of cell division and cell-envelope homeostasis	Peptidoglycan biosynthetic precusors
SMu1379	*vicR*	Response Regulator		
SMu1406	-----	Response Regulator	Not characterized	Unknown
SMu1407	-----	Histidine Kinase		
SMu1652	-----	Histidine Kinase	Not characterized	Unknown
SMu1653	-----	Response Regulator		
SMu1740	*comD*	Histidine Kinase	Biofilm formation, competence and mutacin production	CSP
SMu1741	*comE*	Response Regulator		
SMu1748	*covR*	Response Regulator	Regulation of virulence factors	Not applicable

LANL Gene ID[1]	Gene Name[2]	Protein Function	Role[4]	Signal[4]
SMu1782	*levR*	Response Regulator	Utilization of fructan	Inulin and low concentration of fructose
SMu1783	*levS*	Histidine Kinase		

[1] Los Alamos National Laboratory (LANL) gene number

[2] The names are based on the literature, homologue, and names assigned in the oral pathogen database

[3] The name was omitted because it was either absent from the database or the literature or naming was conflicting with the naming of other system

[4] Identification of the function and signal is based on the literature or homologous systems

Lévesque et al. (2007), researchers have focused their investigation on 7 of the 14 TCS identified, namely CiaHR, ComDE, VicRK, LiaSR (also known as Hk11-Rr11 or Hk03-Rr03), LevRS, ScnKR and MbrCD, and the orphan response regulator, CovR. In this thesis, only the TCSs known to control virulence factors will be reviewed. Their regulatory pathways are summarized and depicted in Fig 1.4.

1.2.2.1 ComDE (BlpRH)

The ComDE TCS was first identified in *Streptococcus pneumoniae* as a key regulator in early-growth phase competence development (Pestova *et al.*, 1996). In *S. mutans*, a system similar to ComDE was first associated with biofilm formation (Bhagwat *et al.*, 2001) and later, associated with competence development and acid stress adaptation (Li *et al.*, 2001a and 2001b). Recent phylogenetic studies have, however, found that the ComDE TCS identified in *S. pneumoniae* is only found in the mitis and anginosus group. The system in *S. mutans* is universally found in other *Streptococcus* and is a paralogue of ComDE (Martin et al., 2006). In some cases, members of the mitis and anginosus group possess both systems. For clarity, Martin et al. (2006) proposed that the system found in mitis and anginosus group keeps the ComDE name and that the ubiquitous system be renamed BlpRH. In contrast to ComDE, the BlpRH system is not at all or only indirectly connected to competence. Althought the ComDE and BlpRH systems appear to be different, the alternative sigma factor, ComX, is universally conserved among the streptococci. For the sake of clarity, the *S. mutans* system and signaling peptide will be called ComDE and CSP, respectively, to be consistent with the current *S. mutans* literature.

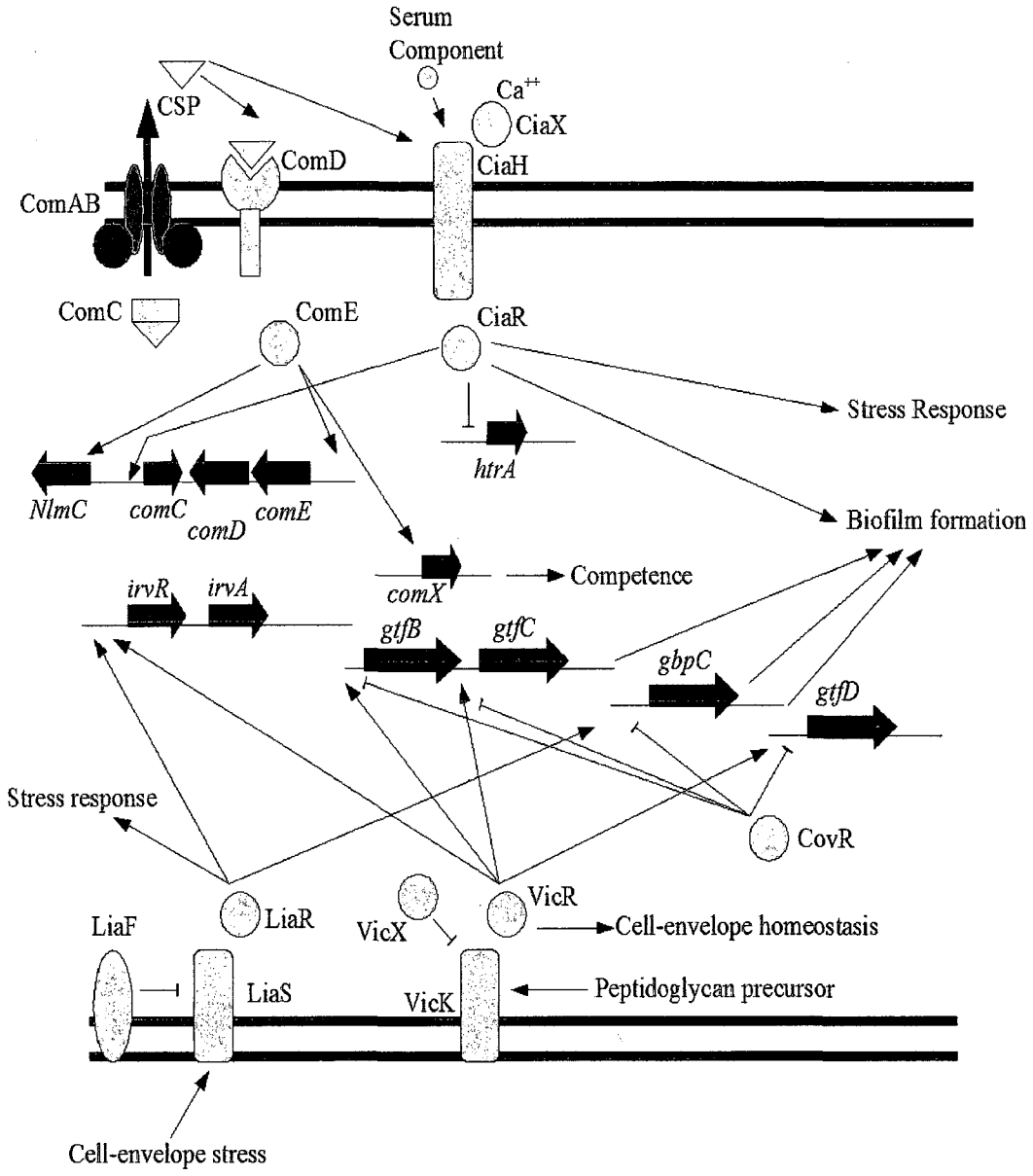

Fig 1.4 Regulation of virulence by TCSs in *S. mutans*. Only the TCSs known to control virulence factors and the orphan RR are depicted. See text for details.

1.2.2.1.1 Identification of the Components

Petersen and Scheie (2000) observed that the deletion of the competence-related ABC-transporter genes, *comAB*, resulted in a decrease in transformation efficiency and hypothesized that a peptide, similar to the CSP, was involved in competence development. Li et al. (2001a) confirmed that peptide induced transformation development. Deletion of *comC*, *comD* or *comE* resulted in a decreased in transformation frequency and addition of exogenous CSP improved transformation frequency in a wild-type strain and a *comC*-deletion mutant. It was also observed that exogenous CSP did not complement deletion of *comD* or *comE*, which suggested that the CSP was sensed by ComD TCS.

The biological function the ComDE TCS has been extensively investigated. Similarly, the function of the CSP to act as a signal for the ComDE TCS has been well established in *S. mutans*. CSP is created by the processing of its precursor, ComC, which results in the 21-amino-acid long CSP (21-CSP). Furthermore, the length and the amino acid sequence of the CSP appears to be well conserved among strains of *S. mutans* (Allan et al., 2007). However some strains appear to encode an 18-amino-acid CSP (18-CSP; Petersen et al., 2006; Allan et al., 2007). The 18-CSP variant lacks the last three amino acids at the C-terminus (Petersen et al., 2006; Allan et al., 2007). Allan et al (2007) observed that the three amino acid deletion at the C-terminud did not impair the function of 18-CSP. In contrast, Syvitski et al. (2007) observed that the same deletion impaired the function of the CSP but not its binding to ComD. Both groups used synthetic CSP and tested the activity of the CSP on strain UA159. It is possible that the different observations were due to subtle differences in experimental conditions. The reason for this discrepancy has yet to be investigated.

Syvitski et al. (2007) also observed that the deletion of the first four amino acids at the N-terminus impaired the function of the CSP. In addition to the importance of the amino acids at the N-terminal or C-terminal regions, phenylalanine residues in the hydrophobic face of the CSP also play a key role in the activity the signal molecule (Syvitski et al., 2007). Based on functional analysis, it is clear that the amino acid content and length of the CSP are crucial for optimal signaling.

1.2.2.1.2 Role of ComDE in Acid Stress Response

The ComDE TCS has also been associated with acid stress response in *S. mutans*. Li et al. (2001b) observed that culture supernatant of *S. mutans* grown in a chemostat under acidic pH was able to induce acid tolerance whereas the culture supernatant of *S. mutans* cultured in a chemostat at neutral pH did not induce acid tolerance. It was also found that the component was sensitive to heat and proteinase, which suggested that it was proteinaceous in nature. It was also observed that acid stress adaptation was cell-density dependent. Therefore, it was hypothesized that a quorum sensing molecule induced the adaptation and the CSP was the primary candidate. The hypothesis was confirmed when *comC*, *comD* or *comE* deletion mutants had a reduced ability to adapt to acid stress. Additionaly, the CSP was able to complement a *comC*-deletion mutant. However, the culture supernatant of a *comC*-deletion mutant cultured at pH 5.2 was still able to induce the ATR in a Δ*comC* mutant. However, the presence of exogenous CSP improved survival during acid stress. It was, therefore, concluded that the ComDE TCS plays a key role in acid-stress adaptation but a second signal molecule is also important for acid stress adaptation.

1.2.2.1.3 Role of ComDE in Biofilm Formation

In *S. mutans*, the association of ComDE with biofilm formation was first observed by Bhagwat *et al.* (2001) and later confirmed by Li et al. (2002b). It was first observed that the deletion of the response regulator gene, *comE*, resulted in a greatly reduced ability to accumulate biomass in microwells (Bhagwat *et al.*, 2001). The role of the CSP was later established. Deletion of the CSP-encoding gene, *comC*, resulted in a noticeable difference in biofilm achitecture; however, the presence of exogenous CSP did not fully complement the ability of a Δ*comC* mutant to form a properly structured biofilm (Li et al., 2002b). In addition to *comE*, deletion of *comD* or *comX* also resulted in a decrease in the ability of the mutants to accumulate biomass (Li et al., 2002b). The idea that the ComDE signaling pathway plays a role in biofilm is well supported by the fact that *comDE* is up-regulated in biofilm cells compared to planktonic cells (Shemesh et al., 2007).

1.2.2.1.4 Role of ComDE in Mutacin Production

CSP has been shown to induce production of the non-lantibotic bacteriocin, mutacin IV (van der Ploeg, 2005; Kreth et al., 2006), and mutacin V (Kreth et al., 2007). The expression of mutacin IV associated genes, *nlmAB* were induced by CSP in a concentration dependent manner (van der Ploeg, 2005). Expression of the mutacin V gene, *nlmC* was also induced by the presence of CSP in the growth media (Kreth et al., 2007). In the case of *nlmAB* expression, the induction was dependent on the presence of *comC*, *comDE* and *comA*. Induction of *nlmAB* could be restored with the addition of CSP to the growth medium in a *comC*- and, in some cases, *comA*-deletion mutant but not in a *comDE*-deleletion mutant (van der Ploeg, 2005). Similarly, expression of *nlmC* was not

restored by the addition of CSP in a *comE*- or *comD*- deleletion mutant (Kreth et al., 2007). Expression of *nlmAB* was unaffected by the deletion of *comX*. It has been concluded that expression of *nlmAB* is regulated by the ComDE TCS in a ComX-independent manner (van der Ploeg, 2005).

1.2.2.1.5 Induction of Cell Lysis by ComDE

In addition to stimulating competence, the CSP can induce cell death when supplied exogenously above the concentration required to induce competence (Qi et al., 2005). It was demonstrated that the presence of CSP resulted in a significant reduction in the rate of cell division (concentration of 0.4 mM) or cell death (concentration of 1.6 mM). Additionally, Ahn et al. (2006) observed a noticeable increase in the length of the growth cycle when CSP was supplied exogenously at a concentration required to induce competence. Furthermore, Qi et al. (2005) observed the induction of cell death in both planktonic and biofilm cells. The inhibitory effect of the CSP was associated with ComDE but was independent of ComX or the presence of the ComC gene in the genome (Qi *et al.*, 2005). It was concluded that cell-death was induced by CSP in a ComX-independent manner. The mechanism by which CSP inhibits cell division has been recently investigated. Perry et al. (2009a) have demonstrated that CSP-induced cell lysis is due to the up-regulation of mutacin V, *nlmC*, by the ComDE TCS.

1.2.2.1.6 Model of ComDE Signaling

Based on the *S. pneumoniae* model of competence induction, a signaling pathway for the ComDE system has been described in *S. mutans* (see Li et al., 2002b; Fig 1.4). Briefly, the ComD HK senses a competence-stimulating peptide (CSP) encoded as a

precursor by the *comC* gene. The precursor CSP is secreted by an ABC-transporter encoded by the *comA* and *comB* genes. Once the CSP is secreted, it is processed into the mature and active form. The binding of the CSP to ComD induces autophosphorylation of the HK and, consequently, the phosphorylation of the RR, ComE, by the HK. Once activated, ComE initates the transcription of *comAB*, *comDE, comX* and genes associated with mutacin production such as *nlmAB* and *nlmC* (Kreth et al., 2007). ComE also represses the expression of signal peptide gene, *comC* (Kreth et al., 2007). ComX recognizes a DNA sequence termed the *com* box and induces the transcription of genes encoding proteins required for genetic competence such as DNA transporters and enzymes responsible for recombination (see Li et al., 2002b).

1.2.2.2 LiaSR

The LiaSR TCS was first characterized by Li et al. (2002a) and was initially named Hk11-Rr11. Based on amino acid sequence similarity, the LiaSR TCS belongs to the family of TCS associated with envelope stress response in the low G+C Gram-positive bacteria. This TCS family is characterized by HK that have unusually short input (sensing) domain composed of two putative transmembrane helices separated by 25 amino acids. Most of the sensing domain is buried within the cytoplasmic membrane. It has been suggested that these HKs sense perturbations that affect cell envelope synthesis by interacting with the lipid interface of the membrane (Mascher, 2006). It is unlikely that these HKs sense extracellular signals but could be dependent on intracellular or cytoplasmic membrane-associated stimuli. Additionally, the intracellular signal could potentially be a result of disruption of the cell membrane. Furthermore, these HKs are considered to be a novel family of cell envelope stress sensors and have been named

intramembrane-sensing histidine kinase (IM-HK; Mascher, 2006). The IM-HK family can be sub-divided into two distinct groups: the ABC-transporter linked IM-HK and the LiaS-like IM-HK.

In *S. mutans*, the LiaSR TCS has been associated with biofilm formation and acid resistance (Li *et al.*, 2002a). Although both *liaR* and *liaS* deletion mutants had defects in biofilm formation, the biofilm architecture of each mutant was noticeably different. The defect in biofilm formation in the Δ*liaS* mutant is likely a consequence of the up-regulation of *gbpC* gene during growth (Chong et al., 2008a). Furthermore, the *liaS* isogenic mutant was sensitive to acid and exhibited a reduced capacity to activate the acid stress response (Li *et al.*, 2002a). Deletion of the ComDE system in a Δ*liaS* mutant resulted in a mutant that was unable to grow at pH 5.0 (Li et al., 2008). Therefore, it has been hypothesized that LiaS acts as a pH sensor (Li *et al.*, 2002a).

Recently, LiaS has also been linked to mutacin I production in strain UA140 (Tsang et al., 2005) which occurs via the repression of the IrvA regulator (Tsang et al., 2006). IrvA is a repressor of mutacin I and, thus, repression of *irvA* results in increased mutacin I production. The repression of IrvA by LiaS may, however, be indirect because four different proteins, including VicK, have been associated with repression of IrvA (Tsang *et al.*, 2006). Chong et al. (2008a) also observed decreased production of mutacin IV in a Δ*liaS* but not in Δ*liaR* mutant. The decrease in mutacin IV production was linked to a decrease in the expression of the mutacin IV associated gene, *nlmA*.

Biswas et al. (2008) also characterized a *liaS* mutant. In their studies, Biswas et al. (2008) noticed that the mutant did not grown in an oxygen-rich atmosphere (20% O_2), was more sensitive to oxidative stress and thermal stress, and did not produce mutacin. Surprisingly, the Δ*liaS* mutant grew faster than the parent in a chemically defined

medium. Additionally, characterization of a Δ*liaR* mutant demonstrated that the mutant had a decreased transformation efficiency in the absence of CSP and that genes associated with stress-response were differentially regulated in the absence of LiaR.

As described above, the LiaSR system has been associated with the regulation of several virulence factors in *S. mutans* and the ability of mutants to cause dental caries has been investigated. Li et al. (2008) found that the mutants had a reduced fitness and could not out-compete the parent strain in a dental biofilm. The role of the LiaRS system in modulating response to antibiotic-induced cell envelope stress has just been investigated but it has yet to be fully characterized (Suntharalingam et al., 2009).

The role of LiaRS TCS in modulating response to antibiotic stress has been characterized in more details in *B. subtilis* (Mascher et al., 2003). It has been showed that the LiaRS response can be activated by cationic antimicrobial peptides such as LL-37 and PG-1 (Pietiainen et al., 2005), bacitracin, and vancomycin (Mascher et al., 2003). LiaS is thought to sense the lipid II cycle and any disruptions of the normal cycle, which are representative of cellular damage (Mascher et al., 2004). A recent study has demonstrated that in *S. aureus*, VraS, a LiaS homologue, can act both as kinase and phosphatase, and regulates VraR, a LiaR homologue, phosphorylation and dephosphorylation events (Belcheva and Golemi-Kotra, 2008). Furthermore, VraR can auto-dephosphorylate. Phosphorylation of VraR has also been shown to be important to initiate the dimerization of VraR. The dimer configuration of VraR is required for DNA-binding activity (Belcheva and Golemi-Kotra, 2008). The binding of LiaR to its own promoter has been shown to positively autoregulate its expression and that of its cognate HK (Jordan et al., 2006). A third protein, LiaF, has also been shown to play a role in the LiaRS response. In *B. subtilis*, LiaF negatively regulates expression of genes belonging

to the LiaR regulon by directly interacting with LiaS and hypothetically preventing the autophosphorylation of LiaS (Jordan et al., 2006). Furthermore, the LiaR-dependent regulation in a mutant lacking LiaF did not depend on the presence of a stimulus (Jordan et al., 2006).

A recent study has demonstrated that *liaSR* is normally repressed during growth in the exponential phase and induced during the transition phase from the exponential phase to the stationary phase of *B. subtilis* (Jordan et al., 2007). It was demonstrated that the regulator, AbrB, directly binds to the promoter of the operon and represses *liaSR* expression during the exponential phase (Jordan et al., 2007). In addition to being repressed during exponential phase, the LiaSR TCS appears to be activated by a small peptide found in *B. subtilis* which is expressed during the stationary phase (Butcher et al., 2007). Futhermore the expression of the small peptide is also repressed by AbrB and it appears to be conserved in other Gram-positive bacteria including *S. aureus*, *Bacillus cereus* and *Streptococcus agalactiae* (Butcher et al., 2007).

LiaRS homologues have been identified in *Streptococcus pneumoniae* (Haas et al., 2005), *Staphylococcus aureus* (Kuroda et al., 2003), *Lactococcus lactis* (Martinez et al., 2007) and *Listeria monocytogenes* (Gravesen et al., 2004). Despite being widely conserved among Firmicutes (see Jordan et al., 2006), it appears that the streptococcal, lactococcal and staphylococcal LiaR belong to a sub-group distinct from the *Bacillus* LiaR (see Martinez et al., 2007). For example, the DNA sequence bound by the *Bacillus* LiaR appears to be absent from the *Streptococcus* and *Staphylococcus* genome (Jordan et al., 2006) and the DNA motif recognized by the *Lactococcus* LiaR is absent from the *Bacillus* genome but present in the *Staphylococcus* genome (Martinez et al., 2007). In addition, the LiaRS TCS regulon of *Staphylococcus* (46 genes; Kuroda et al., 2003) and

Lactococcus (23 genes; Martinez et al., 2007) appears to encapsulate more genes than the *Bacillus* one (2 genes; Mascher *et al.*, 2003). Therefore, the LiaRS response of *S. mutans* may resemble the one observed in *Lactococcus* and *Staphylococcus* rather than the one observed in *Bacillus*.

Despite the differences mentioned, all LiaSR systems appear to respond to at least one common signal: disruption of the normal cycle of lipid II. In all characterized systems, the LiaSR homologues appear to modulate cell wall homeostasis in response to envelope stress caused by vancomycin (Haas et al., 2005; Kuroda et al., 2003; Mascher *et al.*, 2003), bacteriocin Lcn972 (Martinez et al., 2007) or nisin (Gravesen et al., 2004). Furthermore, it is likely that LiaRS TCS plays a key role in natural resistance to vancomycin and other antimicrobial compounds that disrupt the lipid II cycle.

1.2.2.3 CiaHR

In *S. mutans*, the CiaHR system was initially associated with mutacin I production (Qi et al., 2004). It was observed that deletion of *ciaH* resulted in reduced production of mutacin I in strain UA140 whereas the introduction of a similar deletion in a mutacin II producing strain T8 had no impact. Deletion of *ciaR* did not, however, result in decreased production of mutacin I rather a noticeable increase was observed (Qi et al., 2004). In addition to lower mutacin I production, deletion of *ciaH* resulted in reduced competence development and acid stress tolerance, and altered biofilm formation in the presence of sucrose (Qi et al., 2004). Like the results obtained for mutacin production, deletion of *ciaR* did not impact biofilm formation or acid stress tolerance. The role of CiaH in competence development was surprising because it has been hypothesized, and

to a certain extent established, that the ComDE TCS was essential for competence development (Li et al., 2001b).

Recently, Ahn et al. (2006) have demonstrated that the both CiaHR and ComED systems are required for optimal competence development. Ahn et al. (2005) had previously observed that CSP induced expression of *htrA*. HtrA is a surface protease found in Gram-positive bacteria and is involved in the processing and maturation of extacellular proteins. HtrA also degrades abnormal or misfolded proteins. In *S. mutans*, the deletion of *htrA* resulted in increased sensitivity to various environmental stresses, such as thermal shock, and also affected the expression of cell-surface proteins such as GbpB (Biswas and Biswas, 2005). Ahn et al. (2006) observed a 100-fold increase in *htrA* expression when *ciaH* was deleted and therefore, the CiaHR system appears to repress the expression of *htrA*. Furthermore, Ahn et al. (2006) confirmed that CiaH controls competence development in the absence of CSP but the addition of CSP improved competence development. Therefore, CiaH is not required for the transduction of the CSP signal; however, CiaH is required for the induction of the *comDEC* gene expression. Thus, the lack of competence in the *ciaH* mutant is due to down-regulation of the *comDEC* genes in the absence of exogenous CSP.

In addition to CSP, horse serum or purified bovine serum albumin is required for optimal competence development (Ahn et al., 2006). Since CiaH and a serum protein is required for induction of the *com* gene expression, it was suggested that CiaH senses the presence of either peptides released from salivary proteins, which could be a quorum-sensing signal, or specific serum components present in gingival fluid.

The CiaRH TCS role is not limited to competence development and is likely an important regulator during stress response. Biswas et al. (2008) assessed the ability of the

HK-deletion mutants to grow on a solid media in the presence of O_2 and found that the Δ*ciaH* mutant did not grow.

In addition to stress response, the CiaRH TCS also appears to play a role in biofilm formation. A third component is required for the CiaRH signaling cascade. Using a microarray screen for environmental factors, He et al. (2008) found that calcium was a key factor inducing *ciaRH* expression. Based on an *in silico* analysis, a third gene, *ciaX*, preceding the *ciaRH* operon was identified and the encoded protein had multiple serine-aspartate (SD) and serine-asparagine (SN) repeats. Since proteins containing SD repeats often have calcium-binding properties, it was hypothesized that CiaX was a calcium binding peptide involved in the calcium-mediated signal transduction of CiaHR TCS (He et al., 2008). The ability of CiaX to bind calcium was confirmed in a calcium-binding assay. Deletion of *ciaX* resulted in decreased expression of the *ciaRH* in the absence of calcium. Additionally, the Δ*ciaX* mutant had a reduced ability to form biofilms in the absence of calcium and the addition of calcium suppressed this effect. He et al. (2008) also demonstrated that the CiaXRH signal autoregulates in response to calcium and that CiaR could potentially binds two direct repeats 10 bp upstream of the the -10 region of the promoter of the *ciaXRH* operon. Interestingly, He et al. (2008) also identified a potential CiaR-binding site located upstream of *htrA*, which is regulated by CiaR (Ahn et al., 2006).

1.2.2.4 CovR

The RR, CovR, of *S. mutans* has yet to be associated with a cognate HK and is refered to as the orphan RR (Chong et al., 2008b). In *S. mutans*, the orphan RR was first identified in a glucan-dependent aggregation-negative merodiploid mutant and it was

first named *gcrR* (Sato et al., 2000). In this mutant, a gain of function suggested that CovR was responsible for repressing *gbpC* expression and Δ*covR* mutant exhibited a constitutive glucan-aggregation phenotype, which confirmed the latter statement (Sato et al., 2000). The repression was later confirmed by a different group of researchers, which renamed the system *tarC*. The group also identified CovR as a repressor of GtfD expression and, consequently, a regulator of biofilm formation (Idone et al., 2003). Additionally, the Δ*covR* mutant was less virulent in a germ-free rat model. Later, CovR was associated with the regulation of two additional virulence factors, GtfB and GtfC, and the role of CovR in the regulation of biofilm formation was confirmed (Biswas and Biswas, 2006). As in the case of *gtfD* and *gbpC*, CovR represses the expression of *gtfB* and *gtfC* by directly binding to each promoter. Recently, CovR has been associated with the ATR (Dunning et al., 2008). It was observed that a *covR*-deletion mutant was sensitive to acid and was deficient in its ATR when compared to the parental strain. Additionally, the Δ*covR* mutant, when compared to the parent strain, had differential expression of acid tolerance response associated genes, *atpA/E* and *ffh*.

In addition to controlling *gtfB*, *gtfC*, *gtfD* and *gbpC*, CovR also autoregulates its own expression by binding directly to its own promoter (Chong et al., 2008b). The expression of *covR* was also up-regulated during the exponential phase and repressed during the stationary phase. Stipp et al. (2008) have also recorded a growth-phase dependent pattern of *covR* expression but the pattern varied among strains. The culture pH and the concentration of magnesium also had an impact on the expression of *covR* whereas temperature had no significant impact. In the case of the culture pH, a neutral pH induced the expression of *covR*. In the case of magnesium, *covR* expression increased as magnesium concentration increased. In contrast to Chong et al. (2008b), Dunning et

al. (2008) observed that *covR* expression was not responsive to acidic pH and significantly increased when *S. mutans* was cultured in a manganese-restricted medium. Interestingly, the autoregulation of *covR* was independent of magnesium, and this suggests that another regulator, which may be magnesium dependent, modulates *covR* expression. The regulator is likely to be the ferric iron regulator, SloR because it has been determined that SloR binds to the promoter of *covR* and it has been hypothesized that SloR regulates *covR* expression in response to stress (Dunning et al., 2008). Furthermore, a homologue of SloR, named MtsR, appears to respond to magnesium in *S. pyogenes* (Bates et al., 2005).

In *S. pyogenes*, it has been observed that the ratio of phosphorylated CovR (CovR-P) to unphosphorylated CovR was reduced in a Δ*covS* mutant (Churchward, 2007). Therefore, it indicates that CovR is phosphorylated by low-molecular weight compounds such as acetyl phosphate or a different phospho-relay system in the absence of CovS (Churchward, 2007). However mathematical modelling suggested that CovS was primarily responsible for the phosphorylation of CovR (Mitrophanov et al., 2007). Given this information, it has been proposed that, in the absence of stress, CovS acts as a kinase by phosphorylating CovR. In the presence of a stress, CovS acts as a phosphatase and dephosphorylates CovR (Churchward, 2007). In the absence of CovS, CovR is not dephosphorylated. In *S. mutans*, CovR is able to repress virulence-associated genes despite the absence of its cognate HK. Therefore, CovR in *S. mutans* may either be phosphorylated by an unidentified phosphoryl donor or has a mutation that makes it constitutively active. The *S. pyogenes* model further suggest that the *S. mutans* CovR may be dephosphorylated by an unidentified phosphatase.

1.2.2.5 VicRK

The VicRK TCS is a ubiquitous system among the Firmicutes and the system has been demonstrated to be essential for viability in several species such as *B. subtilis* and *S. aureus* (Fabret and Hoch, 1998; Martin et al., 1999). In some species, only the RR, VicR, is essential and the HK, VicK, can be deleted. For example, previous attempts to obtain a VicR-deficient *S. mutans* have failed but the *vicK* was eliminated from the genome (Bhagwat et al, 2001; Senadheera et al., 2005). The deletion of the system has, however, been reported in some species including *S. pyogenes* and *Lactococcus lactis* (O'Connell-Motherway *et al.*, 2000; Liu et al., 2006). In the case of *S. pyogenes*, the system was dispensable *in vitro* but it was not in a mouse model (Liu et al., 2006). In addition to variations in the essential nature of the VicRK system, the operon composition also varies among species. In *Bacillus* and *Listeria*, the operon is composed of 6 genes (*vicR*, *vicK*, yycH, *yycI*, *vicX* and *yycK*). In staphylococci and enterococci, *yycK* is not present. In streptococci and lactococci, *yycH*, *yycI* and *yycK* are absent. The VicRK TCS can also be distinguished among species according to the structural features of VicK. VicK appears to belong to the HK subgoup Class IIIA and it has been hypothesized that VicK possesses the function of both a kinase and a phosphatase (Alves and Savageau, 2004). Additionally, the *vicK* HK family can be divided in two sub-categories: class I and class II (Ng and Winkler, 2004).

In class I, VicK is essential and possesses two predicted transmembrane domains and one extracellular domain. Computational-modelling has also predicted that the extracellular domain contains a PAS sensory domain (Szurmant et al., 2008). Class I VicK is found in *Bacillus*, *Staphylococcus*, *Listeria*, *Lactobacillus* and *Enterococcus*. Class II VicK is dispensable and possesses only one transmembrane domain with 4-12

extracellular residues. The Class II sub-group has been identified in *Streptococcus* and *Lactococcus*. In both sub-groups, VicK is predicted to possess in its cytoplasmic portion a HAMP domain (signal transduction), a PAS domain (sensor domain), a HisKA domain (dimerization and phospho-acceptor domain) and HATPase_C domain (histidine kinase-like ATPase domain).

The source of signal sensed by the VicK PAS domain has yet to be identified; however, the presence of dithiothreitol (DTT) in an *in vitro* assay stimulated the autophosphorylation of *Enterococcus faecalis* VicK and consequently the phosphorylation of VicR suggesting that redox potential modulates VicK activity (Ma et al., 2008). The importance of the PAS domain has also been demonstrated in *S. pneumoniae*. Substitution of a conserved residue in the N-terminal cap of the PAS domain resulted in a defect in *in vitro* autophosphorylation and in competence repression under microaerobiosis (Echenique and Trombe, 2001). However, the substitution did not impact the autophosphorylation of the isolated cytoplasmic HK domain (Clausen et al., 2003).

In *S. mutans*, deletion of *vicK* resulted in decreased transformation efficiency. The deletion caused up-regulation of *gtfB* and *gtfC* in the presence of glucose but not in the presence of sucrose. Additionally, down-regulation of *gtfD*, *ftf* and *gbpB* was also reported (Senadheera et al., 2005). The expression of the virulence factors and surface proteins was deregulated in a Δ*vicK* mutant and, consequently, affected accumulation of extracellular polysaccharides. Changes in surface protein expression and extracellular polysaccharides likely caused the clumping of the Δ*vicK* mutant observed at the on set of stationary phase and reduced the ability of the mutant to form properly structured biofilm (Senadheera et al., 2005; Biswas et al., 2008).

Given that VicK possesses a PAS domain, it has been suggested that the VicRK TCS plays a role during oxidative stress. However, the deletion of *vicK* did not affect paraquat sensitivity (Senadheera et al., 2007). Biswas et al. (2008) also assessed the ability of the *vicK*-deletion mutant to grow on a solid media in the presence of O_2 or thermal stress, and it was found that the mutant was not affected by either stress. It was noted that phenotypes of a Δ*vicK* mutant were affected by the presence of O_2 when compared to the phenotypes of a Δ*vicK* mutant cultured in absence of O_2 (Ahn and Burne, 2007).

VicK also appears to play a role in other biological processes and has been linked to mutacin I production (Tsang et al., 2005) via the repression of the IrvA regulator (Tsang et al., 2006). Additionally, VicK appears to play a role in antibiotic resistance. Deletion of *vicK* increased the sensitivity of *S. mutans* to several antibiotics including penicillin, cefotaxime, ceftazidime, meropenem, mezlocillin, and trimethroprim. Deletion of *vicK* also appears to have a consequence during infection. In *S mutans*, a Δ*vicK* mutant formed more surface plaque with a reduced amount of CFU in a germ-free rat model (Senadheera et al., 2005).

The role of the RR, VicR, in virulence has also been investigated in *S. pyogenes*. In *S. pyogenes*, *vicR* is dispensible which allowed Lui et al (2006) to investigate the role of VicR in an infection model. It was observed that mice infected with a Δ*vicR* mutant had an increase survival rate compared to mice infected with the parent strain. Furthermore, complementing the Δ*vicR* mutant *in trans* restored virulence. Additionally, the *vicR* mutant generated using a transposon exhibited a high rate of reversion during an infection. It, therefore, indicates that *vicR* inactivation was deleterious and that VicR is required for the survival of *S. pyogenes* in an animal model (Lui et al., 2006).

As expected in RR, VicR possesses a receiver domain (REC, CheY-homologue domain) and a DNA-binding domain (Trans_reg_c). The DNA sequence recognized by the VicR DNA-binding domain has been characterized as two hexanucleotide direct repeats separated by five nucleotides. Based on sequences identified in *S. mutans*, *S. aureus*, *S. pneumoniae* and *B. subtilis*, it has been proposed that the consensus sequence is 5'-TGTNDH-N5-BKBWRN-3' (Dubrac et al., 2008). The consensus sequence suggested that VicR binds to DNA as a dimer (Watanabe et al., 2003). In *B.subtilis*, VicR can also act as a repressor or an activator of gene expression depending on the location of the recognized site (Bisicchia et al., 2007). In *S. mutans*, it was observed that VicR directly bound to the *gtfC*, *gtfB* and *ftf* promoters, which are genes that have been shown to be differentially regulated in the absence of VicK (Senadheera et al., 2005). Senadheera *et al.* (2005) also showed that the expression of *gbpB* (*pcsB*) is controlled by VicRK TCS. In *S. pneumoniae*, it was found that VicR controls the expression of peptidoglycan hydrolase gene (*pcsB*), which encodes a protein required for growth and the constitutive expression of *pcsB* removes the *vicR* requirement (Ng *et al.* 2003, 2004, 2005). Thus, the essential nature of *vicR* in *S. pneumoniae* appears to be due to its ability to induce *pcsB* expression. The *S. mutans pcsB* homologue also appears to be required for viability (Mattos-Graner et al., 2006) but the requirement may vary among strains (Chia et al., 2001; Fujita et al., 2007). It is, however, unknown if VicR binds to the *gbpB* promoter or if the constitutive expression of *gbpB* would alleviate the *vicR* requirement. Control of *pcsB* was also observed in *S. pyogenes*; however, *pcsB* is not required in *S. pyogenes* (Lui et al., 2006). The role of VicR in modulating the expression of peptidoglycan hydrolase (*pcsB*) in streptococci demonstrated that the VicRK TCS plays a key role in modulating cell-wall metabolism.

In addition to controlling the expression of *gbpB* in *S. mutans*, the VicRK system also appears to control the expression of the major autolysin gene, *atlA*, and a gene encoding a protein involved in AtlA production and maturation (Ahn and Burne, 2007). Furthermore, deletion of *vicK* or *atlA* resulted in similar changes in cell morphologies. Changes in cell morphology were observed in *S. pneumoniae* mutants expressing a reduced amount of *vicR* or *pcsB* transcript. For example, when *vicR* or *pcsB* mRNA levels were not detectable, *S. pneumoniae* cells lost their ovoid shape and had irregular morphology. Additionally, cell-size uniformity in the population decreased and large defective and hollow cells were observed (Ng *et al.* 2003, 2004, 2005).

The association between the VicRK TCS and cell division has been recently demonstrated. In *B. subtilis*, VicR regulates expression of the cell-division proteins *ftsAZ* (Fukuchi et al., 2000; Howell et al., 2003). The *ftsAZ* operon is preceded by three different promoters. VicR controls *ftsAZ* expression from one of these promoters whih is non-essential promoter. It has been shown that VicK could be co-immunoprecipitated with FtsZ and that VicK localizes at the septum in a FtsZ-dependent manner (Fukushima et al., 2008). It is thought that the VicRK TCS in *B. subtilis* modulates cell-wall synthesis and elongation. Therefore, differential regulation of VicRK has observable consequences. For example, an increase in *vicR* expression leads to excessive cellular division (i.e. mini-cells) whereas a decrease in *vicR* expression leads to an increase in the number of ghost cells (Fukuchi et al., 2000).

As mentioned above, the *vicRK* genes are part of 6-, 5- or 3-gene operons and, most of the proteins encoded by the other genes appear to control the activity of the VicRK TCS. YycK is the protein encoded by the last gene in the bacilli and listeria operons and it is the only member of the operon that appears to have no effect on VicRK

activity (Szurmant et al., 2005). In *Bacillus*, *Listeria*, *Staphylococcus*, *Enterococcus* and *Lactobacillus*, two genes, *yycH* and *yycI*, are immediatley downstream of *vicRK* and the proteins encoded by each gene play a critical role in modulating VicK activity and, consequently, VicR activity (Howell et al., 2003; Szurmant et al., 2005; 2006; 2007; 2008; Santelli et al., 2007). In contrast to the genera mentioned above, the gene immediately downstream of the streptococci and lactococci *vicRK* genes is named *vicX* and it encodes an uncharacterized protein, which has been identified as a member of the metallo-β-lactamase family (Senadheera et al., 2005). In species other than the streptococci and lactococci, *vicX* is immediately downstream of *yycI* (Dubrac et al., 2008). Phenotypic effects of the *vicX* deletion in *S. mutans* include the following: sensitivity to paraquat-induced oxidative stress, reduced competence development in the absence of exogenous CSP and defects in biofilm formation (Senadheera et al., 2007). Additionally, deletion of *vicX* resulted in up-regulation of *gtfB* and *gtfC* when cultured with glucose. Based on these findings, it has been suggested VicX participates in the signaling pathway by acting as a negative regulator of the VicRK TCS (Dubrac et al., 2008).

In addition to VicK and VicX, modulation of VicR phosphorylation may also occur through other HKs. For example, a recent study has demonstrated that *B. subtilis*VicR can be phosphorylated by PhoR during phosphate limitation (Howell et al., 2006). Furthermore, *S. pneumoniae* VicR could be phosphorylated by the *E. faecalis* HK, VanS, *in vitro* (Wagner et al., 2002).

Despite progress in identifiying components regulating, and the target of, the VicRK signaling cascade, elements and environmental conditions controlling *vicRK* expression have not been investigated in detail. In *B. subtilis*, it has been determined that

three transcripts are produced: one containing all 6 genes, one containing only *vicR* and one containing only *yycK* (Fabret and Hoch, 1998; Fukuchi et al., 2000). Both transcripts containing *vicR* are detected during the exponential growth and expression from the *vicR* promoter is typical of a SigA-type promoter (Fabret and Hoch, 1998; Fukuchi et al., 2000). Despite a decrease in *vicRK* transcript during the transition phase, the amount of VicR and VicK protein does not decrease (Fabret and Hoch, 1998; Szurmant et al., 2005; Howell et al., 2006). Growth-phase dependent expression of *vicR* has been noted in *S. mutans* (Stipp et al., 2008). It was observed that *vicR* expression decreases once the cells enter either the transition or the stationary phase; however, transcript patterns varied among strains (Stipp et al., 2008). Expression of *vicR* did not respond to different carbohydrate sources, with the exception of xylitol (Shemesh et al., 2006). The presence of xylitol in the growth media induced *vicR* expression. Recently, two potential inducers of *vicR* have been identified: paraquat (Senadheera et al., 2007) and hydrogen peroxide (Deng et al., 2007). However, the expression of *vicR* by aerobically grown *S. mutans* was only marginally lower than that produced by anaerobically grown cells (Ahn and Burne, 2007). Therefore, it appears that activation of *vicR* expression by oxidative stress is a transient response caused by the side effect of paraquat and hydrogen peroxide. It was also noted that *vicR* was significantly down-regulated in a thicker biofilm (400 micron) compared to a thiner biofilm (100 micron; Shemesh et al., 2007). It was also observed that the 100 micron biofilm had more vitality and, thus the down-regulation in the 400 micron biofilm might be due to a lower growth rate and cell-wall turnover.

Althought *vicR* expression is known to be growth-phase dependent, regulators have yet to be identified. It has, however, been established in *S. mutans* (Senadheera et al., 2007), *B. subtilis* (Fabret and Hoch, 1999) and *S. pneumoniae* (Ng et al., 2005) that

VicR does not autoregulate its own expression. The regulation of *vicRK* could potentially be regulated by other TCS. In *S. pyogenes*, the Irr-IhK TCS has been associated with *vicR* regulation and *vicR* was up-regulated in a *irr*-deletion mutant (Voyich et al., 2004); however, the distribution of the system among the streptococci is unknown and homologues of Irr and Ihk appear to be absent in the *S. mutans* genome. Therefore, it is unlikely that the Irr and Ihk homologues have an impact on the regulation of *vicR* in *S. mutans*.

1.3. Rationale and Objectives of this Study

During an infection, the expression of virulence must be precisely coordinated. Several TCSs have been identified as controllers of virulence in both Gram-positive and Gram-negative bacteria. In *S. mutans*, 4 TCSs (CiaHR, ComDE, LiaSR and VicRK) and the orphan RR (CovR) have been established as regulators of virulence factors. Therefore, the charaterization of any of the TCSs mentioned above was worthy due to their importance.

The deletion of the *vicRKX* operon had been previously attempted using a suicide vector (Lee et al., 2004); however, the attempt failed and resulted in insertion of the suicide plasmid in a unknown site. Therefore, the first objective of this thesis was to identify the site of insertion. Given that several RR share significant homology, the hypothesis was that the suicide vector had recombined within another RR gene found in the *S. mutans* genome. If the hypothesis was correct, the second objective was to characterize the mutant obtained. However, the hypothesis was disproved. The suicide plasmid did not insert into a TCS and therefore, the characterization of the mutant was limited to confirmation of the phenotype and measurement of biofilm formation.

At the onset of this project, the knowledge regarding the expression of *vicRKX* was very limited. It was known only that *vicR* expression in *B. subtilis* was growth-phase dependent and the involvement of Irr-IhK TCS in *S. pyogenes* in *vicR* regulation had just been revealed (Voyich et al., 2004). Furthermore, *vicR* is an essential gene and all characterization of the VicR regulon had been done through indirect means. Given that a student in this laboratory had constructed a P_{vicR}-*lacZ* fusion, it was, therefore, decided that the second part of the project would be to identify environmental factors influencing *vicR* expression. Growth-phase, pH and cell-envelope acting antibiotics were identified as environmental factors affecting *vicR* expression. Cell-envelope stress and pH are considered to be signals sensed by the LiaSR TCS. It was hypothesized that the LiaSR TCS modulates *vicR* expression. The third objective was to characterize the phenotypes of mutants lacking component(s) of the LiaSR TCS and, if possible, link the phenotype observed with the differential expression of *vicR*.

Chapter 2. Materials and Methods

2.1 Bacteria and growth Conditions

2.1.1 Growth of *S. mutans*

S. mutans (Table 2.1) was routinely cultured in Todd-Hewitt broth (THB), Brain Heart infusion broth (BHI) or tryptone-vitamin based (TV) media (Burne et al., 1999) supplemented with 27.5 mM glucose (TVG) at 37°C without shaking under normal atmospheric conditions. Growth was monitored turbidimetrically at 600 nm (HP8452A, Hewlett-Parkard Co, Mississauga Ontario, Canada, or UV-1700, Shimadzu Corporation, Kyoto, Japan). Late-exponential phase ($OD_{600}\approx1.0$) cultures were stored frozen at −80°C as large aliquots (5 ml) supplemented with glycerol (to 15% (w/v)). When required, kanamycin, tetracycline or erythromycin was added to 500 μg/ml, 10 μg/ml and 5 μg/ml, respectively.

2.1.2 Growth of *E. coli*

E. coli (Table 2.1) was routinely cultured in Lysogeny broth (LB; 1% (w/v) tryptone, 0.5% (w/v) yeast extract, 1% (w/v) NaCl) at 37°C with shaking (200 rpm). When required, kanamycin, tetracycline or ampicillin was added to 50 μg/ml, 15 μg/ml and 100 μg/ml, respectively

2.1.3 Growth Kinetics

For the growth-kinetic assay, strains (5% (v/v) inoculum) were cultured in TVG, HEPES-(100 mM) buffered TVG at pH 7.8 (HTVG) or TVG at pH 6.0 ($TVG_{6.0}$) at 37°C without shaking. The culture volumes were 30 mL in a 50-mL screw-cap Erlenmeyer

Table 2.1. Bacterial strains and plasmids used in this study

Strains/Plasmids	Description	Source
E.coli		
XL1-blue	Cloning strain	Strategene
BL21 (DE3)	Protein expression strain	Strategene
DH10β	Cloning strain	Invitrogen
DH5α	Cloning strain	Invitrogen
S. mutans		
NG8	Serotype C	A. S. Bleiweis, University of Florida
murA1 mutant	NG8, *murA1*::pCovR/981	Lee et al., 2004
UA159	Serotype C, sequenced strain	Ajdic et al., 2002
HLO001	UA159, pSL	Lo and Lee (unpublished data)
HLO002	UA159, pP_{vicR}LacZ	Lo and Lee (unpublished data)
YDNT004	HLO002, *vicX*::*ermAM*	This study
YDNT005	HLO002, *liaS*::*ermAM*	This study
YDNT006	HLO002, *vicK*::*ermAM*	This study
YDNT008	HLO002, *comX*::*ermAM*	This study
YDNT009	HLO002, *liaR*::*ermAM*	This study
YDNT010	HLO002, P_{liaF}-*liaF*::*ermAM*	This study
YDNT011	UA159, pYH2	This study
YDNT016	HLO002, *vicKX*::*ermAM*	This study

Strains/Plasmids	**Description**	**Source**
Plasmids		
pVA981	*S. mutans* suicide vector, ColE1 *ori*, *tet*^{r}	Tobian et al., 1984
pCovR/981	pVA981 containing a *vicR* fragment, *tet*^{r}	Lee et al., 2004
pCovR/981-A2	pCovR/981 extracted from the *murA1* mutant containing a *murA1-epuA* fragment, *tet*^{r}	This study
pSL	pDL276, *kan*^{r}, promoterless LacZ gene	Syvitski et al., 2007
pP_{vicR}LacZ	pSL, *kan*^{r}, P_{vicR}-*lacZ* promoter fusion	Lo and Lee (unpublished data)
pYH2	pSL, *kan*^{r}, P_{comDE}-*lacZ* promoter fusion	Syvitski et al., 2007
pMALc	Expression vector, *amp*^{r}, maltose-binding protein tag	NEB
pMALcVicR	pMALc, *amp*^{r}, MBP-VicR fusion	This study
pMALcLiaR	pMALc, *amp*^{r}, MBP-LiaR fusion	This study
pET16b	Expression vector, *amp*^{r}, 10-His tag	Novagen
pET-LiaR	pET16b, *amp*^{r}, His_{10}-LiaR	This study

flask. Growth was monitored turbidimetrically at 600 nm (UV-1700, Shimadzu) at the indicated time intervals.

2.2 Genetic Manipulation of *E. coli* and *S. mutans*

2.2.1 Plasmid Isolation and Transformation of *E. coli*

Plasmids were routinely isolated by alkaline lysis (Birnboim and Doly, 1979). For sequencing, plasmids were isolated using the QIAprep Spin miniprep kit as following the manufacturer instructions (QIAGEN, Mississauga, Ont., Canada) and were sent to the DNA Sequencing Facility at Robarts Research Institute (London, Ontario). Transformation of *E. coli* was performed as described by Sambrook *et al.* (1989).

2.2.2 Creation of an *E. coli* Library Containing the Suicide Vector pCovR/981 Rescued from *S. mutans*

S. mutans genomic DNA (2.5 µL) isolated as described in section 2.2.3.1 was treated with HindIII (20 U, 37°C, 2h). The restriction enzyme was inactivated with heat (80°C, 40 min). The HindIII-treated genomic DNA (5 µL) was then mixed with water (3 µL) and incubated at 65°C for 20 min. Once the mixture reached room temperature, T4 DNA ligase (400 U; New England Biolabs Inc. (NEB), Pickering, Ontario, Canada) and 10X ligase buffer (1 µL) were added for a total reaction volume of 10 µL. After 16h at 4°C, the DNA was precipitated with 2 volumes of 95% ethanol containing 2.5% (w/v) potassium acetate and washed twice with 75% ethanol. The DNA was resuspended in 1 µL of DNase free water. The DNA (1 µL) was then mixed with 50 µL of electro-competent *E. coli* DH10β (Invitrogen Life Technologies, Burlington, ON) and 50 µL of

deionized distilled water. The resulting mixture was then subjected to electroporation (0.1 cm cuvette, 2.25 kV, 25 μF and 100 Ω) using a BioRad Gene Pulser II (BioRad, Hercules, CA). The electroporated cells were mixed with a 1-mL volume of super optimal broth with catabolite repression (SOC) medium (2% (w/v) tryptone, 0.5% (w/v) yeast extract, 10 mM NaCl, 2.5 mM KCl, 10 mM $MgCl_2$, 20 mM glucose, pH 7.0 with NaOH) and incubated at 37°C for 1 h. A volume (60 μL) was spread on solid (1.5% (w/v) agar) LB medium containing tetracycline (15 μg/mL). The plates were incubated at 37°C for 16-32h.

For PCR analysis, isolated colonies for each clone were suspended in 25 μL of 10 mM HEPES (pH 7.4 with KOH). Primer pairs SL369/SL370 and SL370/SL161 (Table 2.2) were then used in PCR with the cell suspensions (5-μL volumes) serving as DNA templates. The typical PCR (50-μL volume) contained 2 μL of template DNA, 0.5 μM upstream primer, 0.5 μM downstream primer, 2 μM dATP, 2 μM dGTP, 2 μM dCTP, 2 μM dTTP, 5 μL of 10 × ThermoPol reaction buffer (NEB), and 2.5 U of *Taq* DNA polymerase (NEB). The PCR mixture was subjected to 5 min at 95°C, 30 cycles of 30 s at 95°C, 30 s at 54°C and 3 min at 72°C, and a final 5 min at 72°C using a thermocycler. The resulting PCR products were analyzed by means of electrophoresis using 0.8% (w/v) agarose.

For restriction digest analysis, plasmids were isolated by alkaline lysis as described in section 2.2.1. The typical restriction digest reaction (10-μL volume) contained 5 μL of plasmid DNA, 10 U of restriction enzyme (*EcoRI*, *ClaI* or *HincII*) and 1 μL of 10X reaction buffer. Following a 3h incubation at 37°C, the reactions were analyzed by means of electrophoresis using 0.8% (w/v) agarose.

Table 2.2. List of primers used in this study

Name	Description	Sequence (5' → 3')[a]
SL160	*vicR* probe forward	TATGACACGATTACAGCCTT
SL161	*vicR* probe reverse	CGGTGAGTTAACTCTACCTC
SL178	*vic* operon forward, SmaI	AGCCCGGGTTCTAACATAAAGTTTA
SL179	*vic* operon reverse, KpnI	ACGGTACCTAAAGTCTTCTGCCAGT
SL180	*vicK* reverse, KpnI	ACGGTACCACTATTGCCACTTGAACC
SL357	*liaS* knock-out and *liaF* probe, forward	CTGAAGGAAGCCTTATGCG
SL358	*liaS* knock-out, reverse	CATAGACAACGGCTTGGGTC
SL368	primer walking sequencing	AGCTCGGTACCCCGGTGAGTTAA
SL369	TetR region of pVA981, reverse	GAGGGCAATGGCTGATATGGAAAC
SL370	pBR325 region of pVA981, forward	TCTGAGAATAGTGTATGCGGCGAC
SL410	pBR325 region at NruI site of pVA981, forward	GGATGGCCTTCCCCATTATGATTC
SL417	*epuA*, forward	GCTGTTTTCGCTGAGACTTGTTCG
SL418	SMu1387, reverse	GAGCTTCTGAGAATATAGGACGTC
SL524	*16S rRNA* probe forward	CTATGGCTCAACCATAGTGTGCTC
SL525	*16S rRNA* probe reverse	GAATTAAACCACATGCTCCACCGC
SL550	*erm*AM forward, SfiI	CTGGGCCCAGGCGGCCGGGCCCAAAA TTTGTTTGAT
SL551	*erm*AM reverse, SfiI	CCTGGCCGGCCTGGCCGGCAGCGACTC ATAGAAT

Name	Description	Sequence (5' → 3')[a]
SL560	*vicK* knock-out reverse, SfiI	TATACCGGCCGGAGGCCCCAGGGACTT GATTCAAACACATTAG
SL561	*vicK* knock-out forward, SfiI	ATATGGCCGCCTGGGCCAATAGTGAGG AAGGCGAAGGGTC
SL562	*vicX* knock-out forward	CCAGATTTTTCTTCACCCTTAC
SL563	*vicX* knock-out reverse, SfiI	ATATGGCCGCCTGGGCCATGATACCTC GCCAGATACTG
SL564	*vicX* knock-out forward, SfiI	TATACCGGCCGGAGGCCCACTTTTCGG TCTATTTCTGC
SL565	uptsream of *liaFSR* operon forward, EcoRI	GCGTGAATTCCTAGTTCAAGTGCGACG ACAAC
SL567	*liaR* knock-out and *liaS* probe forward	CGCTTCTTGCTGCCTTTATTTCC
SL568	*liaR* knock-out reverse	TTCATGCCAACGTACCAAACGGAC
SL569	*liaR* expression and probe forward, EcoRI	GCGCGAATTCATGCTGATGAGTAAAAC AAAAG
SL570	*liaR* expression and probe reverse, BamHI	CGCTGGATCCCTAATTTTCGTCCTGTGG CACTAA
SL571	*vicR* expression forward, EcoRI	GCGCGAATTCATGAAGAAAATTCTAAT CGTTGAC
SL572	*vicR* expression reverse, BamHI	GCGCGGATCCTTAGTCATATGATTTCA TGTAATA
SL573	*comX* knock-out forward	CCACAAACAATTGAGACACG
SL574	*comX* knock-out reverse	GAGAATGGGCTAATGGTTTCTCC

Name	Description	Sequence (5' → 3') [a]
SL588	*liaF* knock-out region forward	CAAGGTTGTCAAAGTCACTATGCC
SL589	*liaF* knock-out and *liaR* probe reverse	CATAGCAAGTCCTTCTGAAAGTG
SL590	*liaF* knock-out reverse, SfiI	GATACCGGCCCGGAGGCCCCAGAATTTTTCAAATATCAAAGACG
SL591	*liaF* knock-out forward, SfiI	ATAGGCCGCCTGGGCCGACTGTCTGATCATATAGATGG
SL616	*liaR* expression forward, NdeI	CGCGCATATGCTGATGAGTAAAACAAAAG
SL622	*liaS* probe, reverse	TTCTAGACGACTAGCCTTGGCATG
SL623	*liaF* probe, reverse	CTTCCATCTATATGATCAGACAGTC

[a]Restriction sites are underlined

2.2.3 Construction of Deletion Mutants in *S. mutans*

2.2.3.1 Genomic DNA Isolation and Transformation of S. mutans

For polymerase-chain reaction (PCR) purposes, genomic DNA was isolated as follows: cells from an overnight culture (20 mL) were harvested by centrifugation (14 000 × g, 5 min) and washed once with phosphate-buffered saline (PBS; 145mM NaCl, 8.7 mM Na_2HPO_4 and 1.5 mM NaH_2PO_4, pH 7.4). Cells were then resuspended in 600 µL of GTE (50 mM glucose, 25 mM Tris, pH 8.0, 10 mM EDTA) with 5 µL of RNase (10 mg/mL) and transferred to a 1.5-mL tube containing 0.3 g of glass beads. The cells were then disrupted mechanically by vortexing the mixture for 1 min. The cell debris and glass beads were removed by centrifugation (2 000 × g, 15 sec). The supernatant was transferred to a 1.5-mL tube and centrifuged. The supernatant was again collected and the DNA was extracted with phenol:chloroform followed by chloroform alone. The DNA was precipitated with 2 volumes of 95% ethanol containing 2.5% (w/v) potassium acetate and washed with 75% ethanol. The DNA was resuspended in 100 µL of DNase-free water.

For primer walking sequencing and restriction digest, genomic DNA was isolated as described previously (Vats and Lee, 2000) with modifications. Briefly, 50 mL of fresh pre-warmed BHI broth was added to 50 mL of an overnight culture. After 2 h at 37°C, glycine (to 5% w/v) was added and the culture was incubated for an additional 2 h. Cells were then harvested by centrifugation (14 000 × g, 10 min) and washed once with PBS. The pellet was resuspended in GTE containing 10 kU of lysozyme, 1 kU mutanolysin, 5 µL of RNase (10 mg/mL) and 25 µL EDTA (0.5 M, pH 8.0) per mL. The suspension was incubated at 37°C for 1 hour. Cells were lysed with 2 % (w/v) SDS at room temperature

for a minimum of 30 min. The cell lysate was collected by centrifugation (14 000 × g, 10 min) and the DNA was then extracted thrice with 1 volume of phenol-chloroform (1:1) followed by 1 volume of chloroform. The DNA was precipitated with 1 volume of iso-propyl alcohol. The DNA pellet was washed twice with 75% (v/v) ethanol and resuspended in TE (10 mM Tris, pH 8.0, 10 mM EDTA) buffer. Primer walking sequencing was performed as described by Heiner et al. (1998) using primer SL368 (Table 2.2) and the resulting reactions were analyzed by the DalGEN Microbial Genetics Centre (Dalhousie University, Halifax, Canada).

S. mutans was transformed as described by Ahn et al. (2006) with some modifications. Briefly, *S. mutans* was grown in BHI to early-exponential phase ($OD_{600}\approx0.1$) and a volume (9 mL) was transfered to a 13-mL test tube (Startsedt, Monreal, Québec, Canada) containing 1 mL of heat-inactivated fetal bovine serum (FBS) and 10 µg of CSP. The CSP was generously provided by Dr. Yung-Hua Li (Dalhousie University). Following a 20 min incubation at 37°C, a volume (750 µL) of the CSP-induced bacteria was added to a 1.5-mL tube containing the desired DNA. The bacteria were incubated for an additional 2h, harvested (14 000 × g, 1 min), resuspended in 200 µL of BHI and plated as 100 µL aliquots on solid BHI (1.5% (w/v) agar) containing the appropriate antibiotic(s). The plates were incubated for 24-72h (37°C, 5% CO_2).

2.2.3.2 Construction of the LiaFSR Negative Mutant

To construct the LiaFSR$^-$ mutant, upstream and downstream regions of *liaF* were amplified from the UA159 chromosomal DNA by PCR with the primer pairs SL588/SL590 and SL591/SL589, respectively (Table 2.2). An erythromycin resistance cassette (*erm*) was PCR amplified from a synthetic construct template (Claverys et al.,

1995) with the primer pair SL550/SL551. The PCR products were extracted with phenol:chloroform, digested with SfiI (50°C for 16 h), and ligated. The ligation products were amplified by PCR using the primer pair SL588/SL589 to obtain a 2.2-kb product (Lau et al., 2002). The resulting PCR product carries the *ermAM* gene flanked by the upstream and downstream sequences of *liaF*. The construct was used to transform strain HLO002. Transformants were selected on BHI containing erythromycin and kanamycin.

2.2.3.3 Construction of the ΔliaS, ΔliaR *and ΔcomX Mutants*

Genomic DNA was isolated from the Δ*liaS* (hk11), the Δ*liaR* (*rr11*) or Δ*comX* mutants of *S. mutans* strain NG8 (Li et al., 2002a; 2001b). The regions containing the *liaS* (2.3 kb), the *liaR* (2.4 kb) or the *comX* (2.0 kb) genes with the inserted *ermAM* gene as described above were amplified by PCR with the primer pairs SL357/SL358, SL567/SL568 or SL573/SL574, respectively (Table 2.2). The PCR products were subsequently transformed into strain HLO002 to obtain the Δ*liaS*, Δ*liaR* and Δ*comX* mutants.

2.2.3.4 Construction of the ΔvicK, ΔvicX *and ΔvicKX Mutants*

To construct the Δ*vicK* and Δ*vicX* mutants, upstream and downstream regions of the *vicK* or *vicX* genes were amplified from the UA159 chromosomal DNA by PCR with the primer pairs SL560/SL179 and SL561/SL178 for *vicK*, and pair SL562/SL563 and SL564/SL179 for *vicX* (Table 2.2). The *ermAM* casette was PCR amplified from a synthetic construct template (Claverys et al., 1995) with the primer pair SL550/SL551. The PCR products were extracted with phenol:chloroform, digested with SfiI (50°C for 16 h), and ligated. The ligated products were amplified by PCR using the primer pair

SL178/SL179 or SL562/SLSL179 to obtain a 1.8-kb and a 2.2-kb product, respectively (Lau et al., 2002). The constructs were used to transform strain UA159.

To construct the Δ*vicKX* mutant, genomic DNA was isolated from the Δ*vicK* and Δ*vicX* mutants. The genomic DNA from the Δ*vicK* mutant was used to PCR-amplify the upstream fragment containing the *ermAM* cassette using primers SL571 and SL550. The downstream fragment containing the *ermAM* cassette was PCR-amplified using genomic DNA from the Δ*vicX* mutant and primer pair SL562/SL551. The resulting PCR products were purified by ethanol precipitation and were mixed at a 1:1 ratio. The mixture was diluted tenfold and 1.5μL was used as the DNA template in the PCR reaction. These fragments were self-annealed and extended by preparing a PCR mixture as described above and ommiting the primers. The PCR mixture was first subjected to 5 min at 95°C, 15 cycles of 30 s at 95°C, 30 s at 60°C and 3.25 min at 72°C using a thermocycler. Once the cycles were completed, 0.5 μM of primer SL562 and 0.5 μM of primer SL571 were added to the reaction mixture. The resulting PCR mixture was subjected to an additional 15 cycles of 30 s at 95°C, 30 s at 54°C and 3.25 min at 72°C, and a final 10 min at 72°C using a thermocycler. The PCR products were subsequently transformed into strain HLO002.

2.2.3.5 Confirmation of Gene Deletions

The transformants obtained were first verified to contain the *ermAM* cassette inserted into the chromosome by PCR using primer pairs and transformant genomic DNA as template as outlined in Table 2.3. PCR was performed as described above. Transformants were considered to have a deleted gene when PCR yielded amplicons of

Table 2.3. Primers used to confirm the deletion mutants

Strains	Verification	Primers		Expected Amplicon Size	
		Forward	Reverse	Parent	Mutant
YDNT010	PCR	SL565	SL623	1102 bp	1259 bp
	Sequencing	SL565	SL550	-----[1]	1235 bp
	Sequencing	SL551	SL622	-----	1730 bp
YDNT005	PCR	SL591	SL358	1685 bp	1667 bp
	PCR	SL550	SL358	-----	1526 bp
	PCR	SL591	SL551	----	1001 bp
	Sequencing	SL550	SL358	-----	1526 bp
	Sequencing	SL591	SL551	----	1001 bp
YDNT009	PCR	SL569	SL570	570 bp	1003 bp
	Sequencing	SL550	SL570	-----	969 bp
	Sequencing	SL569	SL551	----	894 bp
YDNT008	PCR	SL574	SL573	1508 bp	2058 bp
	Sequencing	SL550	SL574	-----	1425 bp
	Sequencing	SL573	SL551	----	1493 bp
YDNT006	PCR	SL160	SL180	2030 bp	1666 bp
	Sequencing	SL160	SL550	-----	1512 bp
	Sequencing	SL551	SL180	----	1014 bp
YDNT004	PCR	SL160	SL179	2920 bp	3171 bp
	Sequencing	SL160	SL550	-----	2985 bp
	Sequencing	SL551	SL179	----	1046 bp
YDNT016	PCR	SL160	SL179	2920 bp	1698 bp
	Sequencing	SL160	SL550	-----	1512 bp
	Sequencing	SL551	SL179	-----	1046 b

[1] Absence of amplification

the expected sizes in both the parent and the mutants (Table 2.3), and when PCR with the primer pair SL550/SL551 yielded a product only in the mutant strains.

Inactivations were subsequently confirmed by sequencing. To do so, the deleted genes were amplified by PCR as outlined Table 2.3. The resulting PCR products were sent to the McGill University and Genome Québec Innovation Centre (Montreal, Québec, Canada). Purification of PCR products, sequencing reaction and analysis was carried by the McGill University and Genome Québec Innovation Centre.

2.3 LacZ Assay

2.3.1 LacZ Plate Assay

HLO001 and HLO002, which contained the promoterless *lacZ* and the P_{vicR}-*lacZ* fusion, respectively, were streaked on FMC (Terleckyj et al., 1975) or TV agar buffered with 100 mM HEPES and supplemented with 25 mM glucose, 15 mM sucrose, or 15 mM maltose. The agar also contained 200 µM of 5-bromo-4-chloro-3-indolyl-β-D-galactopyranoside (X-Gal). When required, the pH of medium was adjusted with NaOH or HCl prior to autoclaving. Both strains were subsequently streaked on unbufferred FMC or TVG agar at pH 7.0, pH 6.0, or pH 5.0. The plates were incubated at 37°C for 36 h in a candle jar. The presence (blue colonies) or the absence (white colonies) of X-Gal hydrolysis exhibited by the isolated colonies was recorded.

The filter paper disc diffusion assay was adapted from Cao et al. (2002). This method was chosen because several anti-bacterial agents could be tested on one plate. Briefly, strains were grown to mid-exponential phase ($OD_{600}\approx0.5$) in TVG and diluted to an OD_{600} of 0.2 in PBS. The bacteria were inoculated to the entire surface of the HEPES-

buffered TVG agar at pH 7.8 containing X-Gal using a cotton swab. Filter paper discs were then placed onto the agar surface and tetracycline (30 μg), erythromycin (15 μg), ampicillin (10 μg), penicillin G (10 U), vancomycin (30 μg), polymyxin B (15 000 U), bacitracin (3 400 U), hydrogen peroxide (9 mg), or Triton X-100 (8 mg) was added to the discs. For controls, sterile water was added to the discs. The plates were incubated at 37°C for 24 h in a 5% CO_2 incubator. The presence or absence of X-Gal hydrolysis around the zone of inhibition was recorded.

2.3.2 LacZ Liquid Assay

For the growth experiment, *S. mutans* HLO002 was grown in the unbuffered TVG at pH 7.8 ($TVG_{7.8}$), unbuffered TVG at pH 6.0 ($TVG_{6.0}$) or HEPES-buffered-TVG at pH 7.8 (HTVG) at 37°C. At the indicated time points, cells were harvested by centrifugation (3 000 × g, 10 min), resuspended in PBS to an $OD_{600}\approx3.0$, and stored at -80°C. Once these frozen cells were thawed, a volume (600 μL) was centrifuged (14 000 × g, 1 min) and resuspended in the Z buffer (600 μL; 60 mM Na_2HPO_4, 40 mM NaH_2PO_4, 10 mM KCl, 1 mM $MgCl_2$ and 2.6 mM β-mercaptoethanol, pH 6.9). Cells were mechanically broken with glass beads (setting 7, 2 min; Mickle High Speed Vibratory Tissue Disintegrator, Mickle Laboratory Engineering Co. Ltd., Gonshall, Surrey, UK) and cell debris was removed by centrifugation (6 000 × g, 3 min). The cleared cell lysate (400 μL) was diluted with Z buffer (800 μL). Aliquots (150 μL) of the diluted cell lysate were added to a 96-well microplate and incubated at 37°C for 30 min. O-nitrophenyl-β-D-galactopyranoside (ONPG; 2 μM) was then added to the samples and incubated at 37°C for up to 60 min. The level of ONPG hydrolysis was measured at 405

nm (A_{405}) using a microplate reader Model 3550 (BioRad) or Synergy HT (Bio-Tek, Instruments Inc, Winooski, VT, USA) every 15 minutes. The protein concentrations of the diluted cell lysates were measured using a modified Bradford method (Spector, 1978). LacZ activity was calculated as [(A_{405} × 1000)/(mg of proteins × incubation time)] and is reported as Modified Miller Unit.

For LiaFSR$^-$, Δ*liaS*, Δ*liaR*, Δ*comX*, Δ*vicK*, Δ*vicX* and Δ*vicKX* mutants experiment, *S. mutans* strains were grown in HTVG or $TVG_{6.0}$ to mid-exponential phase (OD_{600}≈0.5). For the experiment involving early-exponential phase and CSP, *S. mutans* strains were cultured in HTVG or $TVG_{6.0}$ to an optical density of OD_{600}≈0.100 and harvested or, when required, CSP was added to 500 ng/mL and the cells were harvested 1 hour later. Cells were harvested by centrifugation (3 000 × g, 15 min), resuspended in PBS to an OD_{600}≈2.0, and stored at -80°C. A volume (1 mL) of washed cells was centrifuged (14 000 × g, 1 min), resuspended in 1 mL of Z-buffer, and transferred to a 2-mL screw-cap tube containing 250 µL of glass beads. Cells were mechanically broken with glass beads (45 sec, 6000 × g; FastPrep FP120, BIO101, Thermo Scientific, Milford, MA, USA) and the cell debris was removed by centrifugation (6 000 × g, 3 min). A volume (300 µL) of Z buffer was then added to the collected cell lysates (700 µL). The LacZ activity was measured as described above.

2.4 RNA Isolation and RNA Dot Blot

RNA was extracted using the method as described by Peterson et al. (2000) with modifications. *S. mutans* strains were cultured in $TVG_{6.0}$ or HTVG and when the cultures reached the early-exponential phase (OD_{600}≈0.1 to 0.2), mid-exponential phase

($OD_{600}\approx0.5$ for the $TVG_{6.0}$ culture, $OD_{600}\approx1.0$ for the HTVG culture), or late-exponential phase ($OD_{600}\approx1.0$ for the $TVG_{6.0}$, culture $OD_{600}\approx2.0$ for the HTVG culture), cells were collected by centrifugation (14 000 × g, 5 min). The cells (> 3.0×10^{10} CFU) were resuspended in 500 µL of diethyl pyrocarbonate (DEPC)-treated water and 1.5 mL of phenol, which contained 0.1% (w/v) SDS and saturated with citric acid buffer (0.05 M sodium citrate and 0.05 M citric acid, pH 4.3 with citric acid). The suspensions were boiled for 10 minutes and then cooled on ice. The aqueous phase was separated by centrifugation (3 000 × g, 10 min), extracted once with 2 volumes of acidic phenol with chloroform (1:1; 3 000 × g, 7.5 min), and then with 2 volumes of chloroform (3 000 × g, 7.5 min). Sodium acetate (to 0.3 M) was added to the aqueous phase and the RNA was precipitated with 2 volumes of isopropyl alcohol. The mixture was incubated on ice for 20 minutes. The RNA was collected by centrifugation (15 000 × g, 20 min) and washed with 75% ethanol. The precipitated RNA was resuspended in DEPC-treated water (50 µL) and stored at –80°C. Prior to use, the RNA was treated with 100 U of RNase-free DNase I (Sigma-Aldrich Chemical Co., Oakville, Ontario, Canada) for 15 minutes at room temperature. The RNA was further extracted with acidic phenol:chloroform, followed by chloroform extraction. The RNA was used immediately after the last extraction. The RNA was also analyzed by means of agarose gel electrophoresis to verify its integrity.

For the RNA dot blot, RNA was denatured with 3 volumes of RNA denaturing solution (600 µL of deionized formamide, 210 µL of 37% (w/v) of formaldehyde, 130 µL of 10 X 3-(N-Morpholino) propanesulfonic acid (MOPS) buffer (0.2M MOPS, 20 mM sodium acetate, 10 mM EDTA, pH 7.0) at 65°C for 5 min. Following the incubation,

20X SSC (3 M NaCl. 300 mM sodium citrate, pH 7.0) was added immediately to the denatured RNA to a final concentration of 10X SSC. The RNA was then blotted onto a piece of Hybond H+ nylon-membrane (GE Healthcare Bio-Science, Baie-d'Urfé, Québec, Canada) using a Bio-Dot Microfiltration Apparatus (Bio-Rad) according to the manufacturer's instruction. The blots were blocked and reacted with the digoxigenin (DIG)-labelled DNA probes using protocols suggested by Roche Applied Science (Laval, Québec, Canada). The DIG-labelled DNA probes were PCR-synthesized as suggested by Roche Applied Science. Probes were amplified using the following primer pairs (Table 2.2): SL160/SL161 (*vicR*), SL623/SL357 (*liaF*), SL622/SL567 (*liaS*), SL569/SL570 (*liaR*) and SL524/SL525 (*16S rRNA*). *16S rRNA* was selected as the loading control given that its expression is relatively constant regardless of growth phase (Stipp *et al.*, 2008). Images of RNA dot blots were obtained using a FluorChem SP and the AlphaPartIIEase Software (Alpha Innotech Corp., San Leandro, CA) or the VersaDoc MP Imaging system (BioRad). The intensity of RNA dots were estimated using Image J software (National Institutes of Health, Bethesda, MD) and the relative intensity of *vicR, liaF, liaS* or *liaR* dots were calculated as [(Intensity of the gene of interest dot)/(Intensity of *16s rRNA* dot)].

2.5 Biomass Accumulation Assay

Biomass accumulation assay was adapted from Li et al. (2002a). Briefly, strains (1% (v/v) inoculum) were grown in 2-mL volumes of 70% FMC, defined biofilm medium (DBM) or DBM supplemented with Mn (25 μM) or Fe (5 μM; for 70% FMC and DBM composition see Table 2.4) for 16 h (37°C, 5% CO_2) in a 24-well microwell plate (Falcon 353847). Following incubation, the liquid medium was removed using a

vacuum and the planktonic cells were removed by washing the well once with sterile Millipore water. The plates were air dried at 37°C for 15 min. and the dry biofilms were fixed with 10% (v/v) formaldehyde and 5% (v/v) acetic acid in PBS. After a 15 min. incubation, the wells were washed twice with Millipore water and air dried at 37°C for 15 min. The biofilms were then stained with 0.1% (wt/vol) safranin for 10 min. The biofilms were washed thrice with distilled water and then dried at 37°C for 15 min. The stain was then released using 50% (v/v) acetic acid and 50% (v/v) ethanol solution and the amount of released stain was quantified by measuring the absorbance at 490 nm with a microplate reader Synergy HT (Bio-Tek, Instruments Inc, Winooski, VT, USA).

The detachment assay was adapted from Mitrakul et al., (2004) with modifications. Briefly, *S. mutans* strains (1% (w/v) inoculum) were grown in 200 µL of 70% FMC for 16 hours at 37°C with 5% CO_2 in a 96-well microwell plate (Falcon 353872). A Calgary biofilm device was used as the lid (Innovotech Inc., Calgary, AB). After the biofilms were formed, the Calgary biofilm device was transferred to a new 96-well microwell plate with fresh and pre-warmed 70% FMC. The biofilms were then incubated for 8 hours (37°C, 5% CO_2). The Calgary biofilm device was removed and the 96-well microwell plate was processed as described above with the exception that 0.1% (wt/v) crystal violet solution was used instead of safranin.

2.6 Scanning Electron Microscopy (SEM)

Biofilms were formed on microscope-cover-glass slides deposited in wells of a 24-well plate. The culture volume was 2-mL of 70% FMC with 14 mM glucose. After 16-h or 24-h incubation, the media was removed by suction and the biofilms were gently

Table 2.4 Defined Medium composition

Ingredients	Concentration	
	70% FMC	DBM
KH_2PO_4	1.77 mM	15 mM
K_2HPO_4	1.70 mM	58 mM
NaH_2PO_4	10 mM	--------[1]
Na_2HPO_4	15 mM	--------
Sodium citrate	0.536 mM	--------
Sodium acetate	30 mM	--------
$(NH_4)_2SO_4$	3.2 mM	10 mM
$MgSO_4$	0.570 mM	2 mM
NaCl	0.121 mM	35 mM
$MnSO_4$	0.025 mM	--------
$FeSO_4$	0.004 mM	--------
Glucose	14 mM	20 mM
Riboflavin	0.28 mg/L	0.4 mg/L
Biotin	0.007 mg/L	0.01 mg/L
Folic acid	0.07 mg/L	0.1 mg/L
Pantothenate	0.56 mg/L	0.8 mg/L
p-Aminobenzoic acid	0.07 mg/L	0.1 mg/L
Thiamine	0.28 mg/L	0.4 mg/L
Nicotinamide	1.4 mg/L	2.0 mg/L
Pyridoxamide	0.56 mg/L	0.8 mg/L
Adenine	24.5 mg/L	35.0 mg/L
Guanine	18.9 mg/L	27.0 mg/L
Uracil	21.0 mg/L	30.0 mg/L
Glutamine	3.5 mg/L	5 mg/L
L-Glutamic acid	210 mg/L	300 mg/L
L-lysine; L-aspartate; L-isoleucine; L-leucine; L-methionine; L-serine; L-phenylalanine; L-threonine; L-	70.0 mg/L[2]	100 mg/L[2]

Ingredients	Concentration	
	70% FMC	DBM
L-alanine; L-arginine; L-cysteine; L-histidine; glycine; L-hydroxyproline; L-proline; L-tryptophan; L-tyrosine	140 mg/L[2]	200 mg/L[2]

[1] Absent from the media unless otherwise indicated in the Materials and methods section

[2] Concentration for each ingredient

washed once with PBS. The biofilms were fixed (24 hours, room temperature) with 2.5% glutaraldehyde in 90 mM sodium cacodylate buffer (pH 7.3). The samples were osmicated and dehydrated to 100% ethanol using standard methods. These steps were performed by Mary-Ann Trevors (Dalhousie University, Halifax, NS). Once dehydrated, samples were processed by critical point freezing, and the glass slides were mounted and coated with gold. The samples were processed by Dr. Ping Li (Dalhousie University). The samples were examined using a Hitachi S-4700 Field Emission Scanning Electron Microscope (Hitachi High-Technologies Canada, Inc., Toronto, Ontario, Canada) at the Institute for Research in Materials at Dalhousie University.

2.7 Autolysis Assay and Zymogram Analysis

Autolysis assay was carried as described by Ahne and Burne (2007) with modifications. Briefly, late-exponential phase ($OD_{600}\approx1.0$) cells were harvested by centrifugation (14 000 × g, 1 min), washed twice with PBS and resuspended in pre-warmed (44°C) autolysis buffer (20 mM potassium phosphate buffer (pH 6.5), 1 M KCl, 1 mM $CaCl_2$, 1 mM $MgCl_2$, 0.4% (w/v) sodium azide and 0.4% (v/v) Triton X-100) to an $OD_{600}\approx1.0$. The cell suspensions were incubated at 44°C and cell density was monitored turbidimetrically at 600 nm over the indicated period of time. Culture density remaining was calculated as a percentage of OD_{600} at t=X, where X is desired time point, over OD_{600} at t=0 h.

The preparation of crude autolysin extracts was performed as described by Shibata et al. (2005) with modifications. Briefly, the *S. mutans* strains were cultured in 30-mL volume of TVG, HTVG or $TVG_{6.0}$ to late-exponential phase and harvested by centrifugation (3 000 × g, 15 min). The supernatant was discarded and the pellet was

resuspended in 250 µL of 4% (w/v) of SDS. The cell suspension was incubated at room temperature and after 30 min, the samples were centrifuged (10 000 × g, 1 min). The supernatant was collected and an equal volume of 50 mM Tris-HCl (pH 6.5) containing 10% (w/v) glycerol was added.

Zymogram analysis was performed as described by Shibata et al. (2005). Briefly, *S. mutans* strain UA159 was cultured in TVG (900 mL) to late-exponential phase and harvested by centrifugation (14 000 × g, 5 min). The pellet was washed thrice with Millipore water and resuspended in 60 mL of 4% (w/v) of SDS. The resulting suspension was incubated in boiling water for 30 min. The bacteria were collected by centrifugation, washed five times with Millipore water and resuspend in 8 mL of 46% hydrofluoric acid. After a 12-h incubation (4°C), the cells were harvested by centrifugation and washed five times with Millipore water. The resulting cell pellet was directly incorporated into 10% SDS-polyacrylamide gels. Crude-autolysin extracts were applied to the gels. After electrophoresis, the gels were washed twice with Millipore water and incubated in 0.2 M sodium phosphate buffer (pH 7.0) for 12 h at room temperature to allow digestion of the cell wall by autolysins. A zone of clearing was considered to be indicative of enzymatic activity.

2.8 Acid Stress Assay

Acid sensitivity assays were performed essentially as described by Li et al. (2002a). Briefly, parent and deletion mutant strains were grown in HTVG to mid-exponential phase of growth, serially diluted, and aliquots (10 µL) were inoculated onto

$TVG_{5.0}$ or $TVG_{7.8}$ agar. Growth was determined after 36-h incubation at 37°C with 5% CO_2.

2.9 Acid Adaptation and Tolerance Assay

The acid-tolerance-response assay was performed as described by Li et al. (2002a) with modifications. To test acid adaptation, *S. mutans* strains were cultured (10% (v/v) inoculum) in 100 mM HEPES-buffered (pH 7.8) tryptone-yeast-extract-glucose media (TYEG; 1% (w/v) tryptone, 0.5% (w/v) yeast extract and 20 mM glucose) to mid-exponential phase (OD_{600}≈0.5-0.75) at 37°C with 5% CO_2, and cells were then harvested by centrifugation (14 000 × g, 1 min). To induce the acid-tolerance response, cells were resuspended in 3-mL of 100 mM MES-buffered TYEG (pH 5.5) to an OD_{600}≈1.0 and incubated for 2 h (37°C, 5% CO_2). To assess acid resistance, cells from pH 5.5 and 7.8 cultures were resuspended in 2-mL of 100 mM citrate-buffered TYEG (pH 3.5) to an OD_{600}≈1.0 and incubated for 1.5 h (37°C, 5% CO_2). Colony forming units (CFU) were determined immediately after resuspension (t=0 h) and after 1.5 h (t=1.5 h) incubation at pH 3.5. Survival was calculated as a percentage of CFU recovered (t=1.5 h) over original CFU (t=0 h).

2.10 Antibiotic Sensitivity Assay

For the disc diffusion assay, strains were cultured to mid-exponential phase (OD_{600}≈0.5) in TVG and diluted to an OD_{600} of 0.2 in PBS. The bacteria were inoculated onto the entire surface of the HTVG agar at pH 7.8 using a cotton swab. Filter-paper discs were then placed onto the agar surface and polymyxin B (3 750 U, 7 500 U, 15 000

U), phosphomycin (100 μg, 200 μg, 400 μg), penicillin G (50 ng, 100 ng, 200 ng), vancomycin (25 μg, 50 μg, 100 μg) or erythromycin (3.75 μg, 7.5 μg, 15 μg) was added to the discs. The plates were incubated at 37°C for 24 h in a 5% CO_2 incubator. Zone of inhibition was measured from the edge of the filter-paper disc to the edge of the cleared zone.

For the minimal inhibitory concentration assay for polymyxin B, *S. mutans* strains were cultured to mid-exponential phase ($OD_{600}\approx0.5$) in TVG and diluted to $\approx5 \times 10^6$ CFU per mL in TVG, $TVG_{6.0}$ or HTVG. Volumes (100 μL) of each strain were aliquoted in sterile 96-well microwell plates. Polymyxin B was serially diluted two fold with a starting concentration of 1600 μg/mL. Volumes (100 μL) were distributed in the microwell plates containing the bacterial strains. Wells containing only the bacterial inoculum were used as positive controls and wells containing only the antibiotic dilution were used as negative controls. The microwell plates were incubated for 24 h (37°C, 5% CO_2) and bacterial growth was measured turbidimetrically at 600 nm with a microplate reader (Synergy HT).The MIC was considered the lowest concentration that inhibited growth ($OD_{600}\leq0.1$)

The vancomycin and penicillin G E-tests were performed using standard practices by the IWK Health Centre Microbiology laboratory (Halifax, NS, Canada).

2.11 Deferred Antagonist Assay

To assay mutacin production, a deferred antagonist assays was carried as described by Chong et al. (2008a) with modifications. Briefly, *S. mutans* strains were stabbed into solid (1.5% (w/v) agar) Todd-Hewitt medium containing yeast extract (0.3%

(w/v); THY) or HTVG and grown overnight at 37°C in an atmosphere of 5% CO_2. *Streptococcus gordonii* strain DL-1 was used as the indicator strain and was grown overnight in THY or HTVG broth. The overnight cultures were used to inoculate (10% (v/v) inoculum) soft agar (0.4% (w/v)) which was poured over the surface of the THY or HTVG agar plate stabbed with the tester strains. After 36 h at 37°C with 5% CO_2, the diameters of the zones of inhibition were recorded in mm.

2.12 Isolation of Cytoplasmic Proteins

To prepare cytoplasmic protein extracts, *S. mutans* strains were cultured in 200 mL of HTVG or $TVG_{6.0}$ to mid-exponential phase (OD_{600}≈0.500) and harvested by centrifugation (14 000 × g, 5 min). The cells were washed twice with PBS and resuspended in a 1-mL volume of 10 mM HEPES buffer (pH 7.4 with KOH). The cell suspension was transferred to a 2-mL screw-cap tube containing 250 µL of glass beads. Cells were mechanically broken (5 cycles of 30 sec, 6000 × g and 1 min on ice; FastPrep FP120) and cell debris and glass beads were removed by centrifugation (2 000 × g, 5 min). The supernatant was transferred to new tubes and the water-insoluble proteins and cell debris were removed by centrifugation (15 000 × g, 15 min). The supernatant was collected and store frozen (−80°C) as small aliquots (100 µL). The protein concentration of cytoplasmic fractions was measured using a modified Bradford method (Spector, 1978).

2.13 Expression and Purification of Recombinant MBP-VicR and MBP-LiaR

The genes encoding VicR or LiaR were PCR amplified with the primer pairs SL571/SL572 or SL569/SL570, respectively (Table 2.2) and inserted into BamHI and EcoRI restriction sites of the pMALc expression vector (NEB). The ligated product was used to transform *E. coli* strain XL1-blue and positive transformants were selected on solid LB containing ampicillin. Plasmids containing the *vicR* or the *liaR* gene were named pMALcVicR or pMALcLiaR, respectively. Both plasmids were subsequently introduced into *E. coli* strain BL21 (DE3). To express the protein, *E. coli* strains carrying pMALcVicR or pMALcLiaR were grown overnight in tryptone-salt-glucose media (TSG; 0.8% (w/v) tryptone, 87 mM NaCl, 27.5 mM glucose) at 37°C with agitation (200 rpm). The overnight culture was transferred (4% (v/v) inoculum) to 200 mL of pre-warmed TSG and grown at 37°C with agitation (200 rpm) until the culture reached an $OD_{600} \approx 0.6$. Once the culture reached the desired OD, isopropyl β-D-1-thiogalactopyranoside (IPTG) was added to a final concentration of 1 mM and the culture was incubated for an additional 3 h. Following the incubation, the bacteria were harvested by centrifugation (14 000 × g, 5 min) and the cells were resuspended in 10 mL of column buffer (20 mM Tris-HCl, pH 7.4, 1 mM EDTA) containing 1 M NaCl, 500 μM of phenylmethylsulfonyl fluoride (PMSF) and 10 mg of lysozyme. The cell suspension was incubated at room temperature with gentle rocking for 10 min.

Cells were then disrupted by sonication (3 cycles of 30 sec, and 10 sec on ice). Unbroken cells and large debris were sedimented by centrifugation (9 000 × g, 30 min) and the supernatant was collected. The volume of the supernatant was adjusted to 50 mL

with column buffer containing 1 M NaCl and the resulting mixture was applied to a 10-mL amylose-resin column (NEB). Once the sample had completely moved through the column, the resin was first washed with 30 mL of column buffer containing 750 mM NaCl, followed by 30 mL of column buffer containing 500 mM NaCl and then 30 mL of column buffer containing 350 mM NaCl. The resin was finally washed with 30 mL of column buffer containing 200 mM NaCl or until no protein was detected, using a modified Bradford method (Spector et al., 1978), in the recovered column buffer. Proteins were eluted from the resin using 25 mL of column buffer containing 200 mM NaCl and 10 mM maltose. Fractions were collected as 500 µL aliquots. A volume (15 µL) of each fraction was analyzed by SDS-PAGE and stained with Coomassie Blue to verify the presence and purity of the MBP-VicR or MBP-LiaR.

2.14 Generation of Anti-MBP-VicR and Anti-MBP-LiaR Serum

Female BALB/c mice (n=3 for MBP-VicR immunization, n=5 for MBP-LiaR immunization; Charles River Laboratory, St-Constant, Québec, Canada) were injected subcutaneously on 3 sites on their back with 200 µL of a mixture containing 50% (v/v) of incomplete Freund's adjuvant and 10 µg of purified MBP-VicR or MBP-LiaR. The injections were done on days 1, 14 and 21 and mice were sacrificed on day 28. Blood was collected by heart puncture. The collected blood was incubated at 37°C for 1 h followed by an incubation at 4°C for 1 h. The serum was collected by centrifugation (10 000 × g, 5 min) and store frozen (-80°C) as small aliquots (25 µL).

2.15 Expression and Purification of Recombinant His_{10}-LiaR

The gene encoding LiaR was PCR amplified with the primer pair SL570/SL616 (Table 2.2), treated (20 U of BamHI, 20 U of NdeI, 3 h at 37°C) and inserted into BamHI and NdeI restriction sites of the pET16b expression vector (Novagen, Madison, WI, USA). The ligated product was used to transform *E. coli* strain DH5-α and positive transformants were selected on solid LB containing ampicillin. Plasmids containing the *liaR* gene were named pET-LiaR. The selected plasmid was subsequently introduced in *E. coli* strain BL21 (DE3).To express the protein, the *E. coli* strain carrying pET-LiaR was grown overnight in tryptone broth medium (TY; 0.8% (w/v) tryptone, 87 mM NaCl, 0.5% (w/v) yeast extract; Stojiljkovic et al., 1994) at 37°C with agitation (200 rpm). The overnight culture was transferred (4% (v/v) inoculum) into 200 mL of pre-warmed TY and grown at 37°C with agitation (200 rpm) until the culture reached an $OD_{600}\approx0.6$. Once the culture reached the desired OD, IPTG was added to a final concentration of 1 mM and the culture was incubated for an additional 3 h. Following the incubation, the bacteria were harvested by centrifugation (14 000 × g, 5 min) and washed twice with cold 50 mM Tris-HCl (pH 8.0). The cells were resuspended in 25 mL of talon buffer (30.5 mM Na_2HPO_4, 19.5 mM NaH_2PO_4, pH 7.0, 300 mM NaCl) containing 4.5 mM imidazole pH 7.0, 500 μM of PMSF, 10 U of DNase and 10 mg of lysozyme. The cell suspension was incubated at room temperature with gentle rocking for 10 min. Cells were then disrupted by sonication (3 cycles of 10 sec, and 30 sec on ice). Unbroken cells and large debris were sedimented by centrifugation (12 000 × g, 20 min) and the supernatant was collected.

The supernatant was mixed with 1 mL of TALON metal affinity resin (Clontech, Mountain View, CA, USA) and incubated at room temperature with gentle rocking for 20 min. The resin was collected by centrifugation (700 × g, 5 min), resuspended in 20 mL of talon buffer and incubated at room temperature with gentle rocking for 10 min, this step was repeated one more time. The resin was then transferred to a protein purification column (BioRad) and washed once more with 10 mL of talon buffer. The protein was eluted with 10 mL of talon buffer containing 150 mM imidazole. Fractions were collected as 500 µL aliquots. A volume (15 µL) of each fraction was analyzed by SDS-PAGE and stained with Coomassie blue to verify the presence and purity of the His_{10}-LiaR.

2.16 Western Immunoblotting

Cytoplasmic proteins (10 µg) were separated on 12.5% SDS-polyacrylamide gels and transferred (Trans-Blot SD Semi-Dry Electrophoretic Transfer Cell (BioRad); 15V, 60 min) to an Immobulon-P PVDF membrane (Millipore, Etobicoke, Ontario, Canada). After the transfer, the membrane was blocked with 5% (w/v) skim milk in Tris-buffered saline with Tween (TTBS; 145 mM NaCl, 100 mM Tris-HCl pH 7.4, 0.15% (v/v) Tween-20). Following blocking, the membrane was incubated with the anti-MBP-VicR serum or anti-MBP-LiaR serum (1:2000 dilution) in TTBS with 1% (w/v) bovine serum albumin (BSA), washed thrice (10 min) with Tris-buffered saline (TBS; 145 mM NaCl, 100 mM Tris-HCl pH 7.4), incubated with anti-mouse antibodies conjugated with alkaline phosphatase (1:8000 dilution; Sigma-Aldrich) and washed thrice (10 min) with TTBS. After the last wash, the membrane was equilibrated in developing buffer (100

mM NaCl, 100 mM Tris-HCl, pH 9.5) for 3 min. and reacted with CSP-Star (Roche). Images were captured with the VersaDoc MP Imaging system (BioRad).

Duplicate SDS-polyacrylamide gels were stained with colloidal Coomassie Blue as described by Anderson (1991). Briefly, the SDS-polyacrylamide gels were incubated in the fixing solution (50% (v/v) ethanol, 2% (v/v) phosphoric acid) for 16 h at room temperature with gentle agitation. After the incubation, the gels were incubated in Mili-Q water for 1 h and the gels were then stained with the staining solution (34% (v/v) methanol, 2% (v/v) phosphoric acid, 17% (w/v) ammonium sulphate and 0.15% (w/v) Coomassie brilliant blue G-250) until saturation was reached (~3 days).

2.17 Two-Dimensional-Gel Electrophoresis (2DGE)

Sample preparation and 2DGE was performed as described by Potrykus et al. (2007). Briefly, 110 µg of cytoplasmic proteins were adjusted to 239 µL with isoelectric focusing (IEF) buffer (7 M urea, 2 M thiourea, 4% (w/v) 3-[(3-cholamidopropyl) dimethylammonio]-1-propanesulfonate (CHAPS), 0.5% (v/v) Amersham 3-10 Pharmalyte (GE Healthcare) and 11 µL of 33% (w/v) of dithiothreitol (DTT) solution was added to the mixture. The final mixture (250 µL) was loaded onto a 13-cm Immobiline Dry Strip (GE Healthcare) with a linear pH gradient of 4-7. The strip hydration (passive, 16 h, 20°C) and the IEF (500V for 1h, 1000V for 1h and 8000V for 2.5 h) were conducted using the Ettan IPGphor (GE Healthcare). Once the IEF was completed, the strips were equilibriated in buffer A (6 M urea, 2% (w/v) SDS, 375 mM Tris-HCl, pH 8.8, 20% (v/v) glycerol, 130 mM DTT) for 15 min and then buffer B (buffer A with 135 mM iodoacetamide instead of DTT) for 15 min. Following the strip

hydration, the proteins were separated on 12% SDS-polyacrylamide gels and proteins were stained with colloidal Coomassie Blue as described by Anderson (1991). The stained gels were scanned with a EPSON Expression 1680 scanner and the scanned gels were analyzed using the ImageMaster 2D software (GE Healthcare). Protein spots showing differential expression were excised using a surgical scalpel and sent to the DalGEN Proteomics Facility (Dalhousie University) for LC-MS/MS analysis. Briefly, the polypeptides were digested with trypsin and the digested peptides were separated by reverse-phase high-performance liquid chromatography and analyzed by tandem mass spectrometry on a hybrid quadrupole linear ion trap mass spectrometer (Applied Biosystems) equipped with a nanospray ion source. The peptides were identified by searching the NCBI nonredundant protein database with the MASCOT (version 1.6b21) algorithm.

2.18 Glycolytic Enzyme Activity Assay

To obtain cytoplasmic protein, strain HLO002 and the Δ*liaS* mutant were cultured in 30 mL of HTVG to mid-exponential phase ($OD_{600}\approx0.500$) and harvested by centrifugation (14 000 × g, 5 min). The cells were washed twice with potassium phosphate buffer (PPB; 50 mM potassium phosphate, pH 7.4, 2 mM EDTA, 2 mM β-mercaptoethanol) and stored overnight at −80°C. The next day, cells were thawed and resuspended in a 1-mL volume of PPB. Cytoplasmic protein were then isolated as described in section 2.12. Protein concentration of the cytoplasmic extract was estimated using a modified Bradford method (Spector, 1978).

Triose-phosphate isomerase, glyceraldehyde-3-phosphate dehydrogenase and phosphoglycerate kinase activity was assayed as described by Maitra and Lobo (1971) and modified by Nakano et. al (1999). Enzyme activities were measured in a buffer containing 50 mM triethanolamine hydrochloride (pH 7.4) and 10 mM $MgCl_2$. The total volume of the reaction was 1-mL and every reaction contained 5 μg of cytoplasmic protein. For triose-phosphate isomerase activity, the reaction contained 0.15 mM NADH, 0.4 mM glyceraldehyde-3-phosphate, and 2 U of α-glycerophosphate dehydrogenase. In the case of GAPDH activity, the mixture contained 0.15 mM NADH, 5 mM cysteine, 1 mM 3-phosphoglycerate, 1 mM ATP, and 2 U of PGK. Phosphoglycerate kinase activity was assayed in the same reaction mixture as the glyceraldehyde-3-phosphate dehydrogenase assay but phosphoglycerate kinase was replace with 2 U of glyceraldehyde-3-phosphate dehydrogenase. Native NADH oxidase activity in the cytoplasmic extract was measured in reaction mixture mentioned above that contained no substrates and enzymes. The rate of disappearance of NADH was monitored for up to 10 min at 340 nm. NADH was quantified by using an extinction coefficient of 6,220 M^{-1} cm^{-1}. Reaction rate was corrected using the rate of the control reaction. The following formula was used to calculate enzymatic activity: [(ΔA_{340nm}/min Test)-(ΔA_{340nm}/min Control)]/6,220/0.005mg.

2.19 *In silico* Analysis

For the *murA1* mutant study, the sequences obtained were searched for homologue matches in the Oral Pathogen Sequence database (http://www.oralgen.lanl.gov/oralgen/). Sequences used to build the predicted sites of

insertion were obtained at the Oral Pathogen Sequence database and GenBank (http://www.ncbi.nlm.nih.gov/Genbank/index.html). Once the sequence was constructed, it was stored and analyzed for restriction digest site using SDSC Biology WorkBench (http://workbench.sdsc.edu/).

For promoter analysis, the sequences were obtained at Oral Pathogen Sequence database and were analyzed for transcriptional start site using the Neural Network Promoter Prediction tool at the Berkeley Drosophila Genome Project (http://www.fruitfly.org/seq_tools/promoter.html) (Reese, 2001), DNA folding pattern at the DNA mfold server (http://frontend.bioinfo.rpi.edu/applications/mfold/cgi-bin/dna-form1.cgi) (Zuker, 2003) and DNA-binding protein sites using the promoter analysis tool at Virtual Footprint (http://www.prodoric.de/vfp/index2.php) (Münch et al., 2005)

2.20 Statistical Analysis

The results were analyzed by the Student's *t*-test for a two-sample equal variant population with a two-tailed distribution with a P value ≤ 0.05 was considered significant. When required, the statistical significance was established by analysis of variance (ANOVA; 95% confidence interval) followed by a Tukey's post-hoc comparison ($P \leq 0.05$) using the Minitab 15.0 software for Windows.

Chapter 3. Results

3.1 Characterization of a *murA1* Mutant

3.1.1 The Suicide Plasmid Inserted into *murA1*.

A previous study (Lee et al., 2004) made an attempt to inactivate the gene encoding VicR. However, the suicide plasmid containing a fragment of *vicR* inserted elsewhere in the chromosome. It was first hypothesized that the suicide vector had recombined within another RR gene found in the *S. mutans* genome. Therefore, primer-walking sequencing using primer SL368 from the *vicR* gene located on pCovR/981 was done in order to identify the insertion site. The analysis of the DNA sequence revealed that the recombination event did not occur at the plasmid-linked *vicR* fragment. Given that the hypothesis was false, a second hypothesis was formulated. It was hypothesized that the suicide vector had integrated using the region encoding the tetracycline resistance cassette because the cassette came from the transposon Tn916 (Tobian et al., 1984). In order to rescue the integrated plasmid, genomic DNA of the mutant was isolated and digested with HindIII. The fragments were ligated and transformed into *E. coli*. A total of 84 clones were obtained and analyzed by PCR using primer pair SL369/SL370 which amplified the intact tetracycline resistance cassette carried on the suicide vector. Every clone possessed an intact tetracycline resistance cassette, therefore, disproving the second hypothesis.

To finally identify an insertion site, a few clones were selected for further analysis using PCR and restriction digest. The PCR analysis revealed that the *vicR* fragment was intact and linked to the tetracycline resistance marker. The restriction-enzyme analysis indicated that at least one additional HincII site and at least one more

ClaI site were present in the rescued plasmids. Both PCR and restriction analyses indicated that the pBR325 region of the suicide vector was used during the recombination event. A primer was created at the border of the region and was used to sequence a clone that did not contain any extra fragment. Analysis of the sequence revealed that the insertion occurred in the *murA1* (SMu1386) gene and that a 9 base-pair homology was sufficient for a recombination event (Fig 3.1 and 3.2). The genomic DNA of the parent and the *murA1* mutant strains were analyzed by PCR using the primer pairs SL417/SL418 and SL417/SL410. For the parent strain, PCR using the primer pair SL417/SL418 yielded the expected amplicon (1.7 Kp) whereas the PCR using the primer pair SL417/SL410 yielded no product as predicted (Fig 3.3). For the *murA1* mutant strain, PCR using the primer pair SL417/SL418 did not yield an amplicon whereas the PCR using the primer pair SL417/SL410 yielded an amplicon of the predicted size (2.5 kb; Fig 3.3). Therefore, PCR analysis further confirmed that the suicide vector had integrated into the *murA1* gene.

In the previous study (Lee et al., 2004), Southern blot analysis of digested genomic DNA of the parent and mutant strains was performed. To correlate the restriction map obtained previously and the new data, the DNA sequence of the insertion site was determined using data available for the *murA1* gene in strain UA159 and for the suicide vector. A restriction map analysis of the inferred sequence was performed (Fig 3.2). In the previous study (Lee et al., 2004), labelled pVA981 annealed to two HindIII-cut fragments (7.0 and 2.5 kb), labelled *vicK* annealed to one SalI fragment (10.5 kb) and labelled *vicR* hybridyzed to three HindIII fragments (7.5, 2.6, and 0.9 kb). In this study, analysis of the cut site for HindIII of the reconstructed map indicated that two fragments

TTGGTTATATGGTTAGTACCTTTATCTGGTCTGTCATTTCGTTAAGTCAA
GATATCTTTTTTGCGATTTAATTTATTCGAATAGTGTCTTTATTGTGGTAT
epuA ⬅➡ intergenic sequence
AATGCAAGAATAAAATATAATAATTGGAGAAATTCGTGGATAGAATAAT
intergenic sequence ⬅ ➡*murA*
TATTGAAGGCGGAAATACACAACTTAAAGGGGAAGTCGTTATTGAAGG
GGCTAAAAATGCCGTTCTTCCGCTATTGGCAGCGGCTATTTTACCGACA
GAAGGGCAAACGCTTCTGAAGAATGTACCTATTTTGTCTGATGTTTTTA
CCATGAACAATGTTGTACGTGGTTTAAATGTTGCAGTCGATTTTGATGA
AGAAAGGAACCAAATACTGGTAGATGCAACAGGTGATATTTTAGATGT
GGCTCCTTATGAATATGTCAGTCAAATGCGAGCATCTATCGTTGTTTTG
GGACCTATTTTAGCACGAAATGGTCATGCTAAGGTTTCTATGCCCGGAG
GCTGTACAATTGGCAGTCGCCCCATTGATTTGCATTTAAAAGGCTTAGA
AGCTATGGGAGCAAAGATTCAACAGACAGGTGGTGATATTACAGCCAC
TGCCGATCGTTTAAAGGGTGCTAACATTTACATGGATTTTCCAAGTGTT
murA⬅
GGCGGGTGTCGGGGCGCAGCCATGACCCAGTCACGTAGCGATAGCGG
➡Plasmid Vector DNA
AGTGTATACTGGCTTAACTATGCGGCATCAGAGCAGATTGTACTGAGA
GTGCACCATATGCGGTGTGAAATACCGCACAGATGCGTAAGGAGAAAA
TACCGCATCAGGCGCTCTTCCGCTTCCTCGCTCACTGACTCGCTGCGC
TCGGTCGTTCGGCTGCGGCGAGCGGTATCAGCTCACTCNAAGGNGGTA
ATACGGNTATCCNCAGAATCNGGGGANAACGCAGGAAANAACATGTG
AGCAAAAGGCCAGCAAAAGGCCAGNAACCGTAAAAAGGCCGCGNTG
CTGGCGTTTTTCNTAGGCTCCGCCCCCCTGACNANCATCACAAAAATCG

Fig 3.1 Unedited DNA sequence of the pCovR/981-A2 generated from primer SL410. The DNA sequence was analyzed using the BLASTN function on the NCBI website (http://blast.ncbi.nlm.nih.gov/Blast.cgi) and the oral pathogen database website (http://www.oralgen.lanl.gov/cgi-bin/analyze.cgi?paralogs=paralogs&subdir=oralgen/bacteria). *S. mutans* genes are shaded in gray and arrows delineate specific DNA-sequence regions. The DNA sequence shared by *murA1* and pCovR/981, and the predicted site of insertion is underlined.

Fig 3.2. Insertion site of pCovR/981 in the *murA1* mutant. Restriction sites and their resulting fragments with the hybridyzed probe are indicated. Primer location (arrows) and amplicons are indicated between arrows. The image of the genetic map was adapted from the Gene Image Map application available at the Oral Pathogen Sequence Databases (http://www.oralgen.lanl.gov/oralgen/).

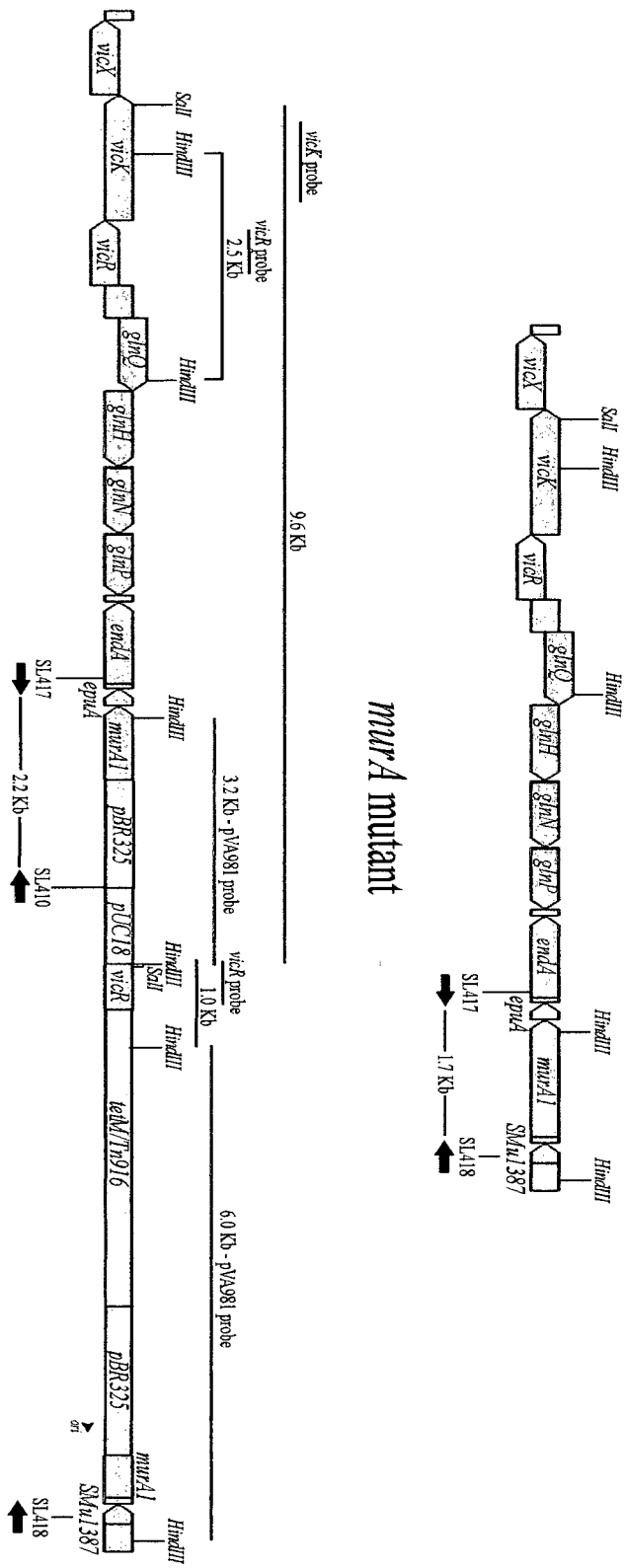
Parent
vicR probe
2.5 Kb
SalI
HindIII
vicX
vicK
vicR
glnQ
glnH
glnN
glnP
endA
epuA
murA1
SMu1387
SL417
1.7 Kb
SL418
murA mutant
vicK probe
9.6 Kb
vicR probe
2.5 Kb
3.2 Kb - pVA981 probe
1.0 Kb
6.0 Kb - pVA981 probe
pBR325
pUC18
tetM/Tn916
ori
SL410
2.2 Kb

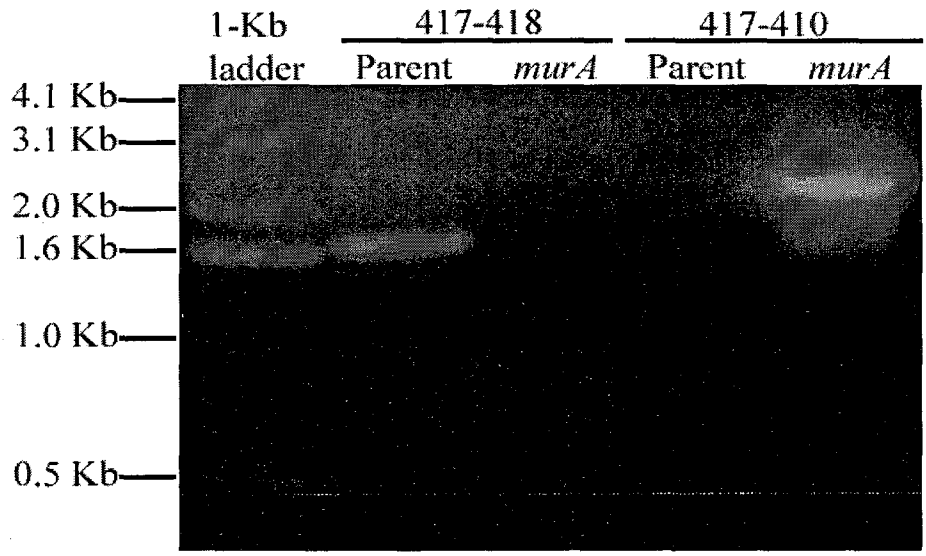

Fig 3.3. PCR amplification of *murA1-epuA* region at the site of pCovR/981 insertion. Genomic DNA of strain NG8 (parent) and *murA1* mutant (*murA*) served as templates for this PCR. The primer pairs SL417/418 (417-418) and SL417/SL410 (417-410) were chosen to amplify a 1.7 kb region in the parent and a 2.2 kb region present only the *murA1* mutant, respectively.

(6.5 and 2.5 kb) could potentially contain pVA981 sequence and two fragment (1.0 kb and 2.5 kb) could potentially contain the *vicR* sequence. If the digestion was incomplete, or if all predicted HindIII fragments are not present, a 7.0 kb fragment could also contain a *vicR* sequence. Analysis of the SalI site revealed that only one fragment (10.0 kb) would contain a *vicK* sequence. The SalI restriction sequence is rare within the *S. mutans* genome and is present in the suicide vector and the *vicK* sequence. Taken together, the *in silico* restriction analysis fit the results previously obtained by Lee et al. (2004)

In an attempt to further confirm that *murA1* was inactivated, complementation was attempted. PCR-amplicons containing either *murA1* alone or together with the gene immediately downstream, *epuA*, were ligated into pDL276 and the resulting construct were used to transform *E. coli*. However, *E. coli* transformants were never isolated despite nurmerous attempts and, therefore, complementation studies could not be performed.

3.1.2 Antibiotic Sensitivity

The *murA1* gene encodes a UDP-N-acetylglucosamine 1-carboxyvinyltransferase. This enzyme transfers carboxyvinyl from phosphoenolpyruvate to UDP-N-acetylglucosamine. This transfer is the first committed step of peptidoglycan synthesis. Given that the enzyme plays a key role in cell-wall synthesis and is the target of phosphomycin (Du et al., 2000, Kedar et al., 2008), the sensitivity to several antibiotics (phosphomycin, polymyxin B, penicillin G, vancomycin, and erythromycin) targeting different cellular processes was tested. The *murA1* mutant was more sensitive to phosphomycin than the parent but displayed a similar sensitivity to the other antibiotics (Fig 3.4; Table 3.1). The increase in phosphomycin sensitivity displayed by the mutant

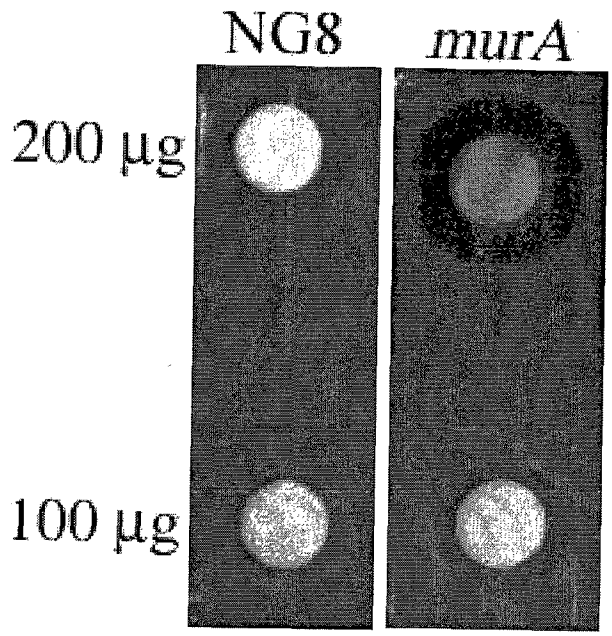

Fig 3.4. The *murA1* mutant is more sensitive to phosphomycin than the parent. Both the parent (NG8) and the *murA1* mutant (*murA*) were inoculated onto solid HTVG. Phosphomycin (100 or 200 µg) was added to the disc and the plates were incubated. The zone of inhibition was measured from the edge of the disc to the edge of the zone of inhibition.

Table 3.1. Antibiotic susceptibility of the *murA1* mutant

Antibiotic	Concentration	Strains	
		Parent	*murA1*
Phosphomycin	50 μg	≤ 1 mm[1]	1.5 mm
	100 μg	3 mm	4 mm
	200 μg	4 mm	7.5 mm
Polymyxin B	3750 U	3 mm	3 mm
	7500 U	4 mm	4 mm
	15000 U	6 mm	7 mm
Penicillin G	50 ng	≤ 1 mm	≤ 1 mm
	100 ng	3 mm	3 mm
	200 ng	5 mm	5 mm
Vancomycin	25 μg	3 mm	3 mm
	50 μg	4 mm	4.5 mm
	100 μg	5 mm	5.5 mm
Erythromycin	3.75 μg	10 mm	10 mm
	7.5 μg	11 mm	11 mm
	15 μg	11 mm	12 mm

[1]Distance from the edge of the disc to the edge of the zone of inhibition

supports the observation that the suicide vector inserted into the *murA1* gene. The insertion of the suicide plasmid in *murA1* also did not appear to affect other process as highlighted by the lack of change in sensitivity to the other antibiotics tested.

3.1.3 Biomass Accumulation and Biofilm Formation

In the previous study by Lee et al. (2004), the *murA1* mutant exhibited an increase in the expression of *ftf* and an autoaggregation phenotype. Such changes could affect the ability of the mutant to form biofilm. To first test if the mutant had lost its ability to attach and accumulate biomass, a biomass accumulation assay was performed. The *murA1* mutant did not lose its ability to accumulate biomass in any of the media tested (70% FMC, DBM, DBM+Fe, DBM+Mn, BHI and 25% BHI) and appeared to accumulate more biomass than the parent strains in most media (Fig 3.5). The exceptions were DBM+Fe and 25% BHI where biomass accumulation was greater for the parent and biomass accumulated equally, respectively. A detachment assay was also done using a Calgary Biofilm Apparatus and both the parent and *murA1* mutant strains had a similar rate of detachment (Fig 3.6).

Given that the *murA1* mutant strain was able to accumulate biomass, a SEM analysis was performed to examine the overall architecture of the biofilm (Fig 3.7 and 3.8). At 250X, the *murA1* mutant appeared to extensively cover the surface and formed a biofilm. However, when compared to the parent biofilm, the biofilm formed by the *murA1* mutant appears to be unstructured and disorganized. At 1000X, the *murA1*-mutant cells formed longer chains which are likely the cause of the difference in biofilm structure.

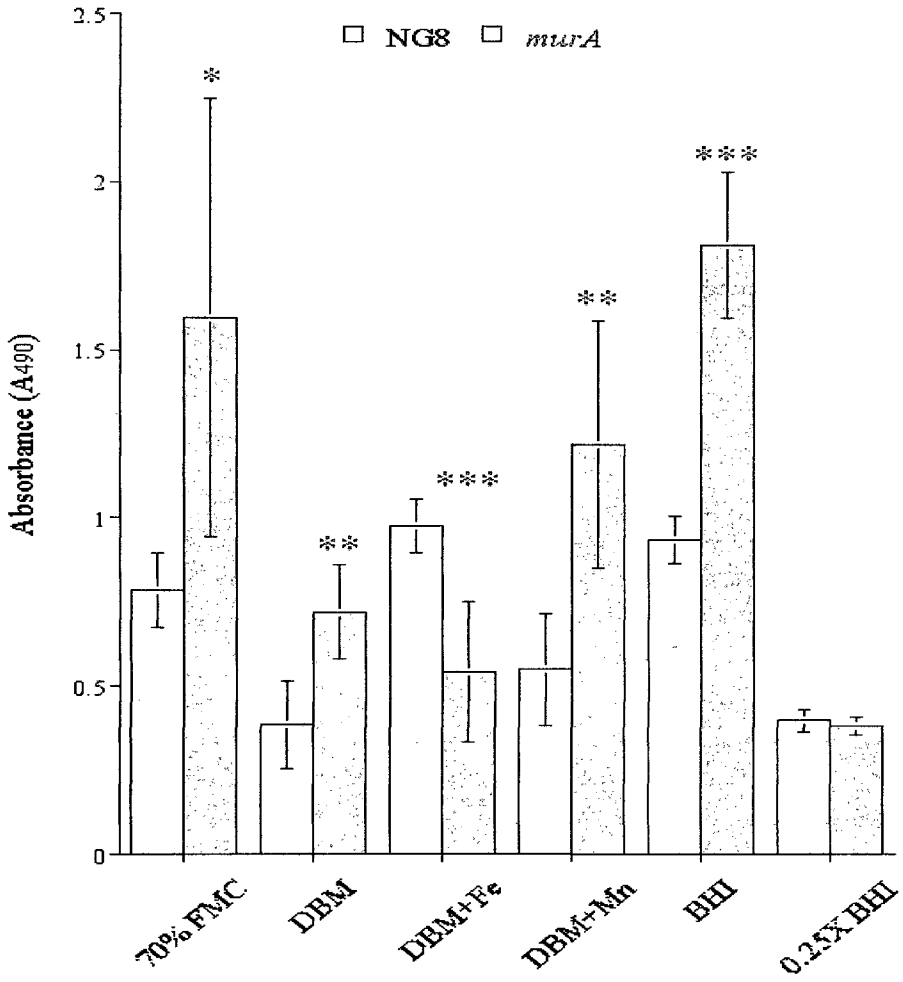

Fig 3.5. Biomass accumulation by the *murA1* mutant. *S. mutans* strains (parent, and *murA1* mutant) were grown in 70% FMC, DBM, DBM supplemented with 25 μM manganese sulfate (DBM with Mn), DBM supplemented with 5 μM ferrous sulfate (DBM with Fe), BHI or 0.25X BHI. The graph represents the level of stain absorbed and released by the biofilms. The results are the average of 6 replicates and representative of three independent experiments. The error bars represent the standard deviation. *, ** and *** indicate $P<0.05$, $P<0.01$ and $P<0.001$, respectively, when comparing the mutant and the parent cultured in the same media.

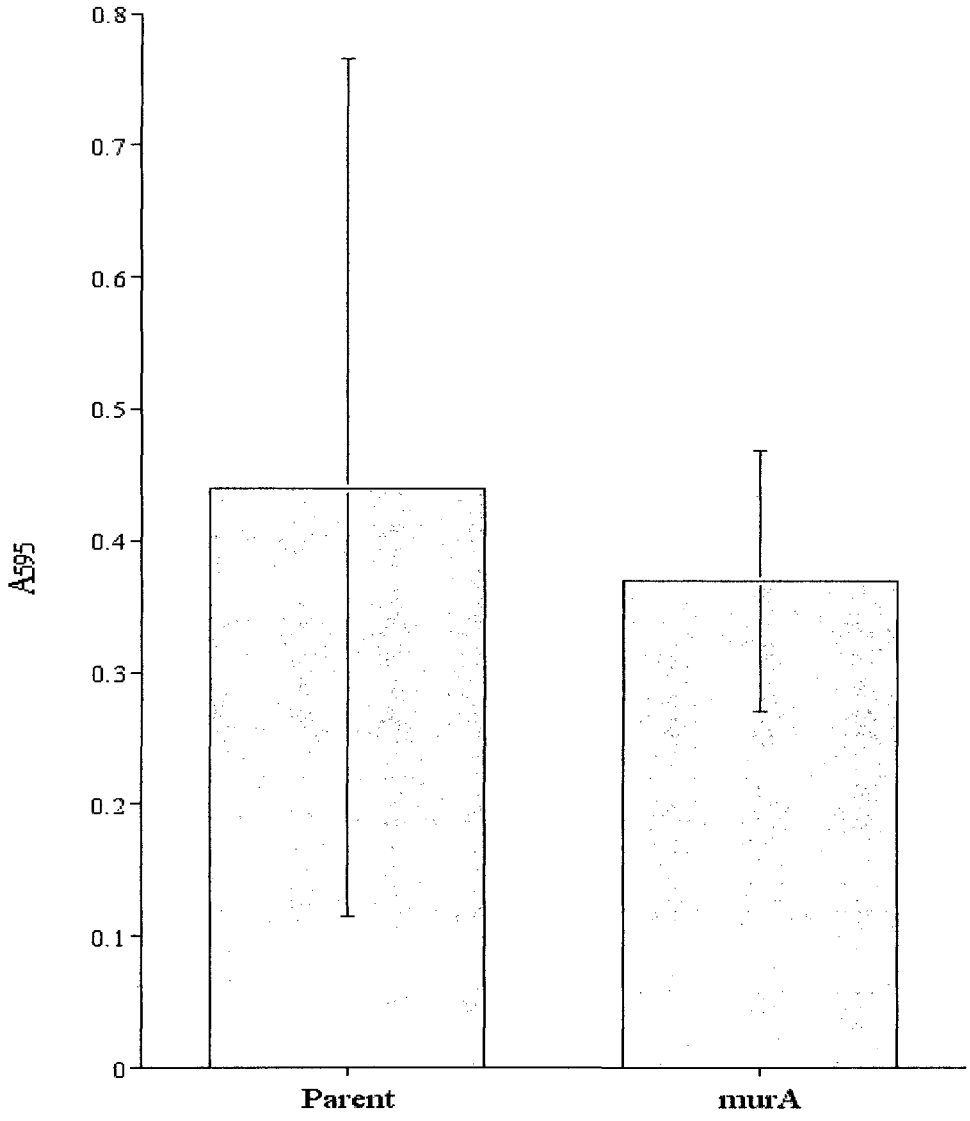

Fig 3.6. Biofilm detachment and quantification of the *murA1* mutant. *S. mutans* strains (parent, and *murA1* mutant) were grown in 70% FMC on a Calgary Biofilm Device. The graph represented the level of stain absorbed and released by the biofilm formed by the detached cells. The results are the average of 16 replicates and representative of three independent experiments. The error bars represent the standard deviation.

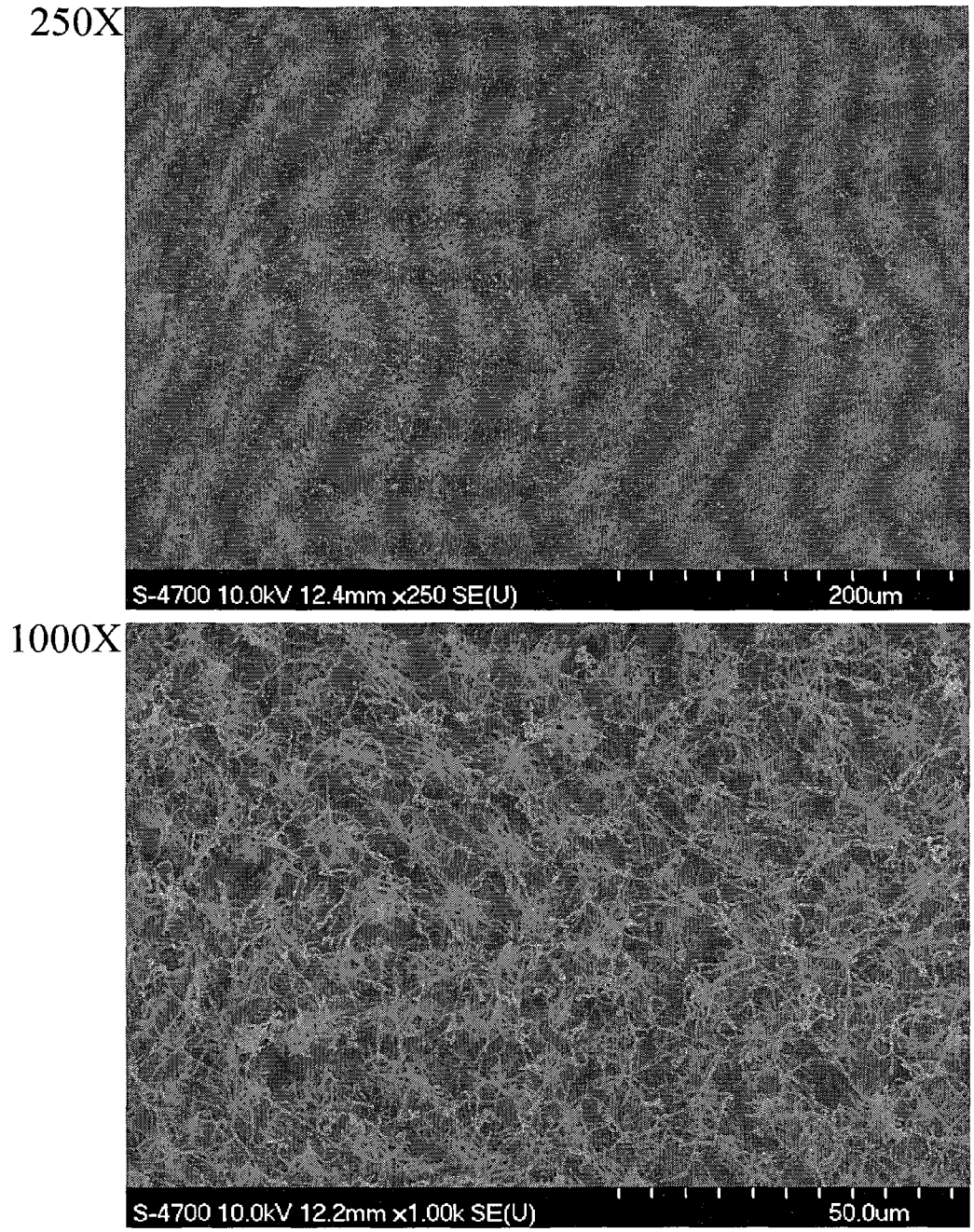

Fig 3.7. SEM of a 16h-biofilm formed by *S. mutans* strain NG8 cultured in 70% FMC. Representative fields of view at 250X and 1000X.

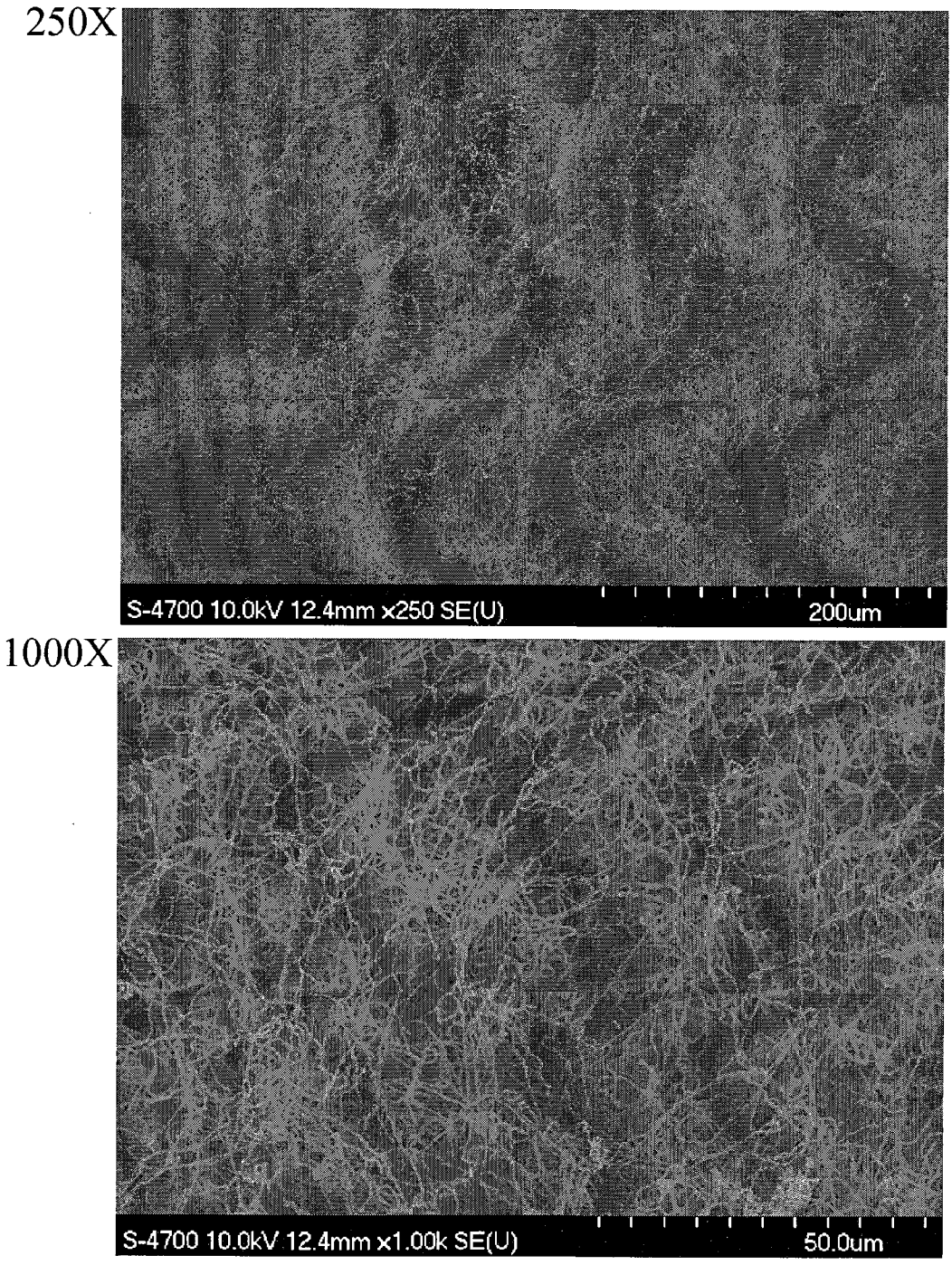

Fig 3.8. SEM of a 16h-biofilm formed by the *murA1* mutant cultured in 70% FMC.

Representative fields of view at 250X and 1000X.

3.2 Regulation and Expression of *vicR*

3.2.1 Effect of Media, pH, Carbohydrate and Antibiotics on Expression of *vicR*

3.2.1.1 LacZ Assay

Several environmental factors, such as pH and carbon sources, are known to regulate gene expression in *S. mutans*. To rapidly test some of these environmental factors on the expression of *vicR*, the reporter *lacZ* gene was fused to the *vicR* promoter and introduced into *S.mutans*. The strains carrying the fusion construct (HLO002) or the promoterless *lacZ* gene (HLO001) were tested for *lacZ* expression on FMC or TV agar containing glucose, sucrose, or maltose as the carbon source. In all cases, strain HLO001 showed no X-Gal hydrolysis confirming that in the absence of a promoter, *lacZ* was not expressed. In contrast, HLO002 colonies showed clear X-Gal hydrolysis. The degree of X-Gal hydrolysis was similar for all the tested carbon sources but was slightly stronger on FMC than the TV media. More interestingly, the LacZ activity was the strongest on plates at pH 7.0, weaker at pH 6.0, and absent at pH 5.0.

To further examine the effect of pH and growth on *vicRKX* expression, *S. mutans* HLO002 was grown in buffered (HTVG) and unbuffered ($TVG_{6.0}$ and $TVG_{7.8}$) media. HLO002 demonstrated a similar generation time when grown in HTGV and $TVG_{7.8}$ (1h 37min vs. 1h 34min) but the bacteria took longer to reach stationary phase in HTVG than in $TVG_{7.8}$ (Fig 3.9). HLO002 had a longer generation time (2 h 13 min) in $TVG_{6.0}$ and did not reach the same growth yield as in the other two media. During growth, the pH of the HTGV culture only dropped 1 pH unit to about pH 6.8, while the pH of the $TVG_{7.8}$ and $TVG_{6.0}$ cultures dropped rapidly to around pH 4.5 (Fig 3.10).

The LacZ activity of the HTVG culture remained relatively high and stable which coincided with the stable pH (Fig 3.11). In contrast, the LacZ activity of the $TVG_{6.0}$

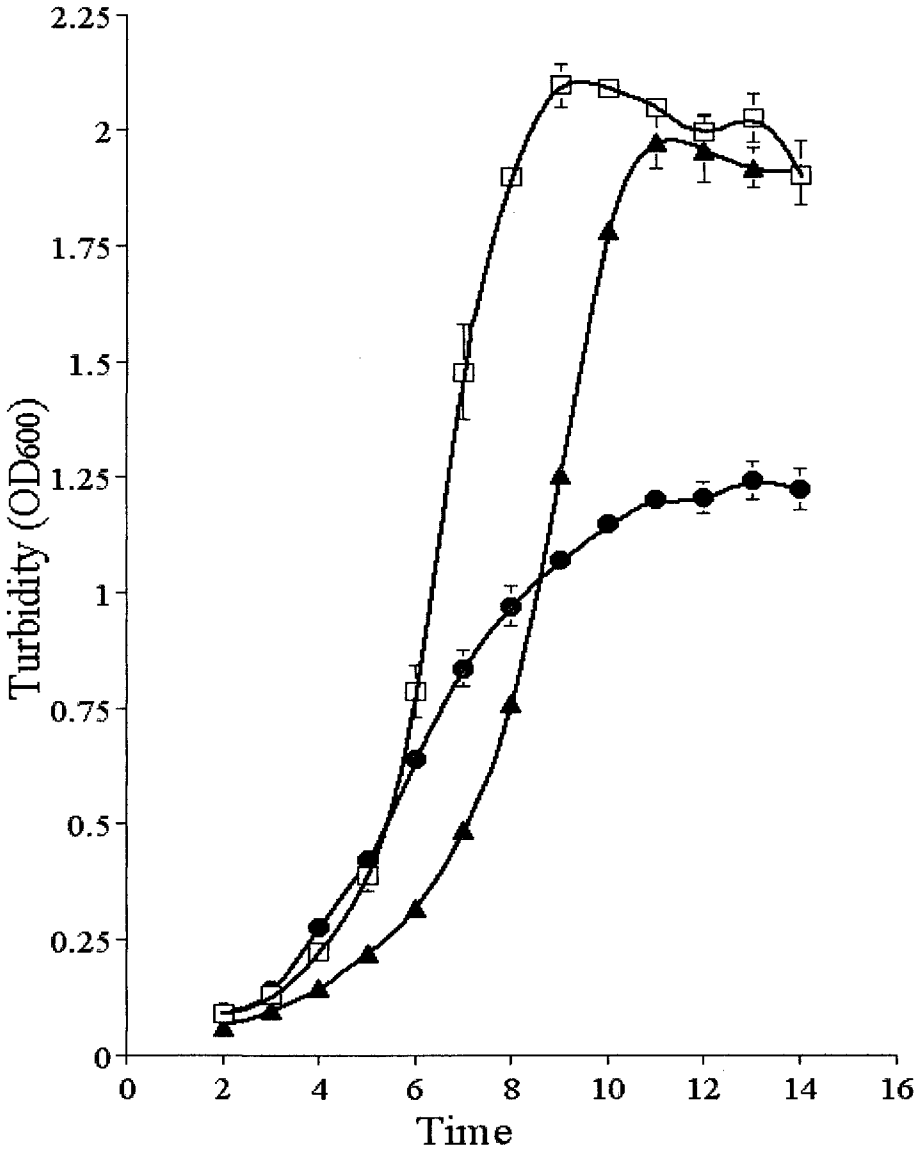

Fig 3.9. Growth kinetics of strain HLO002 cultured in $TVG_{7.8}$, $TVG_{6.0}$ and HTVG.

S. mutans HLO002 cultured in HTVG (closed triangles), $TVG_{7.8}$ (open squares), and $TVG_{6.0}$ (closed circles). The results are the means (± SE) of three independent experiments.

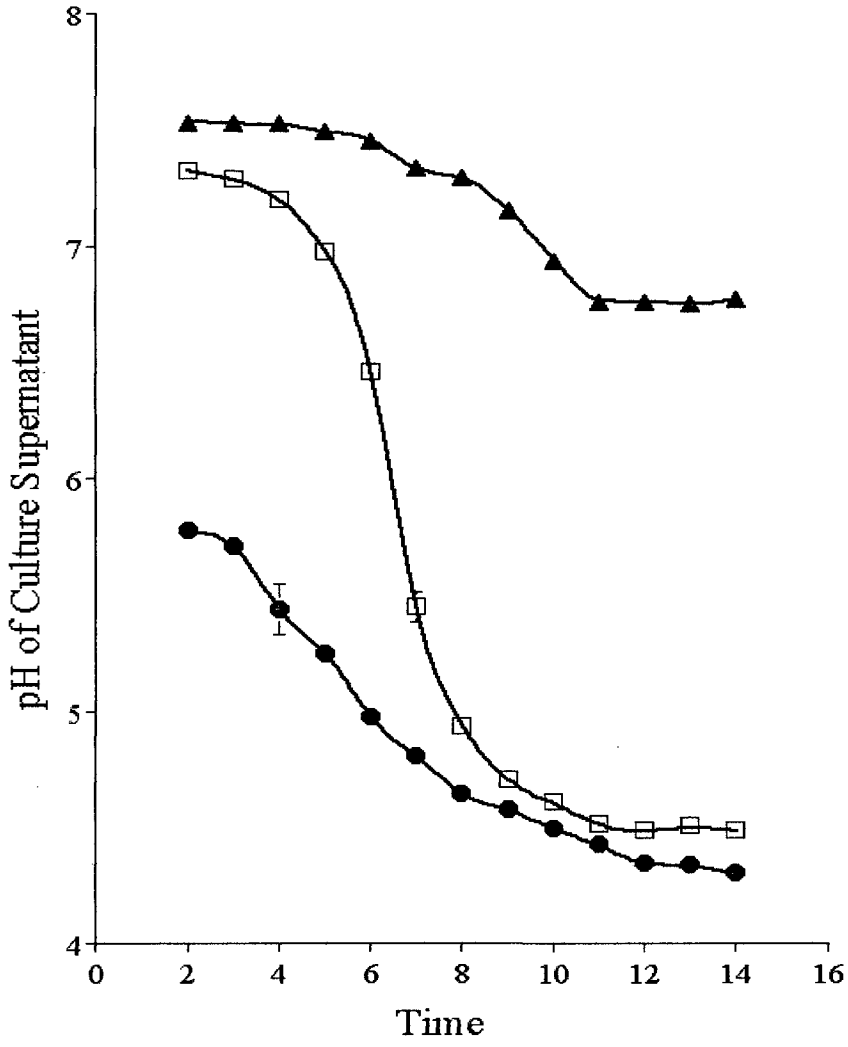

Fig 3.10. Kinetics of culture supernatant pH of strain HLO002 cultured in $TVG_{7.8}$, $TVG_{6.0}$ and HTVG. The pH of culture supernatant of *S. mutans* HLO002 cultured in HTVG (closed triangles), $TVG_{7.8}$ (open squares), and $TVG_{6.0}$ (closed circles). The results are the means (± SE) of three independent experiments.

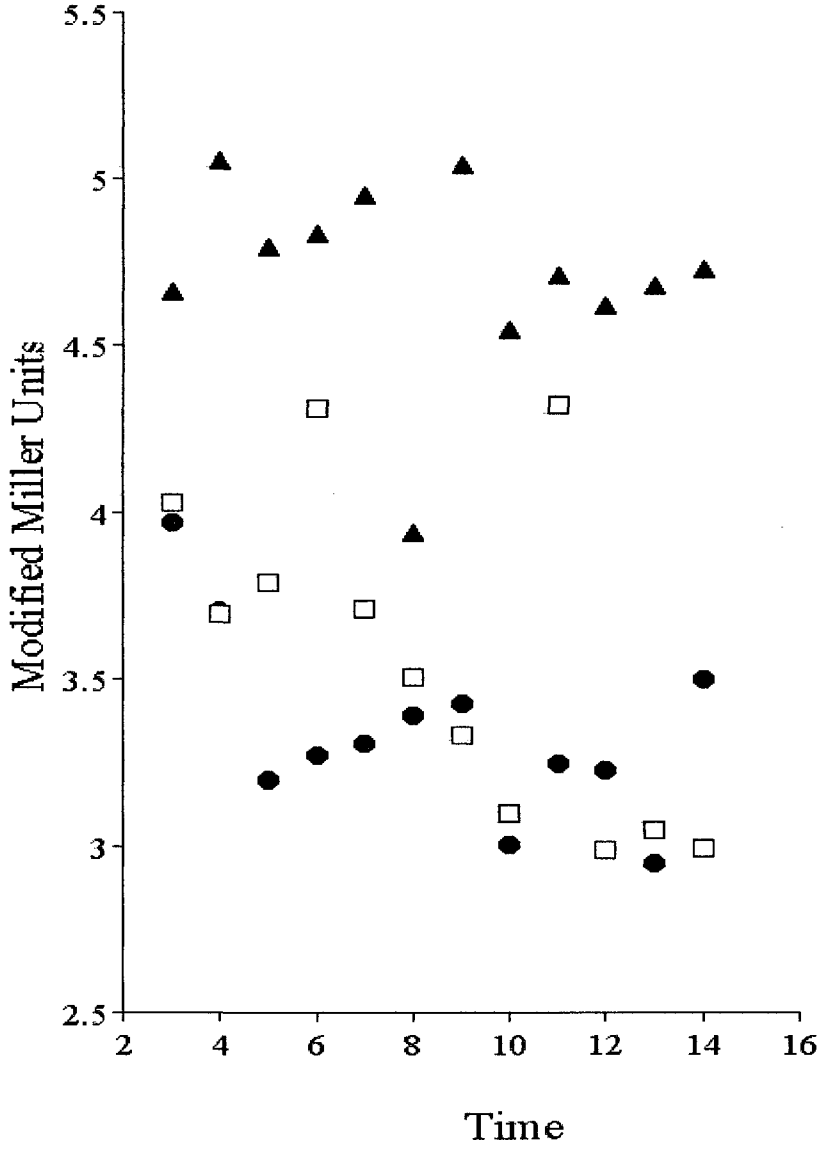

Fig 3.11. *lacZ* expression relative to time of strain HLO002 cultured in $TVG_{7.8}$, $TVG_{6.0}$ and HTVG. LacZ activity of *S. mutans* HLO002 cultured in HTVG (closed triangles), $TVG_{7.8}$ (open squares), and $TVG_{6.0}$ (closed circles).The results presented are the means of two independent experiments.

culture was much lower while that of the $TVG_{7.8}$ culture decreased rapidly as the culture pH dropped. A correlation between pH and LacZ activity was clearly evident from Figure 3.12.

3.2.1.2 RNA Levels

To verify the results of the LacZ experiments, the levels of *vicR* transcript in strain UA159 and HLO002 grown in $TVG_{6.0}$ or HTVG to early-, mid-, or late-exponential phase were analyzed by northern dot-blotting. As shown in Figure 3.13, *vicR* mRNA was present at the highest level in mid- and late-exponential cells grown in HTVG. *vicR* mRNA was only present in small quantities in early-exponential cells grown in HTVG. Consistent with the LacZ activity results, the level of *vicR* mRNA was much lower in cells grown in $TVG_{6.0}$ than in HTVG. Similar patterns of *viR* mRNA levels were observed for strain HLO002. These results further suggest that the *vicRKX* operon is down regulated at low pH and is growth-phase dependent.

3.2.1.3 Antibiotics that Induce Expression

Induction of the *vicR* promoter by antibacterial agents was also examined using the disc diffusion assay and the *lacZ* reporter construct. The results showed that vancomycin, penicillin G, ampicillin and polymyxin B induced the activity of P*vicR* whereas tetracycline, erythromycin, Triton X-100, bacitracin, and H_2O_2 did not (Fig 3.14 and Table 3.2).

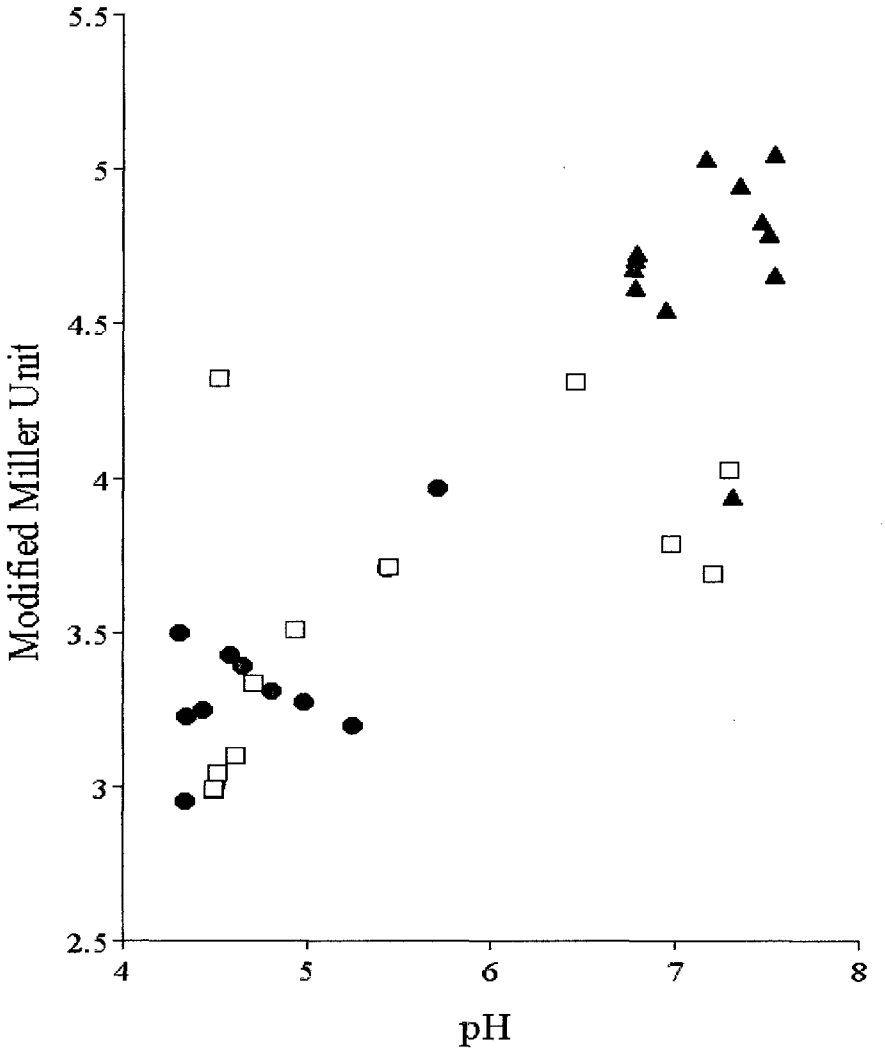

Fig 3.12. *lacZ* expression relative to pH of strain HLO002 cultured in $TVG_{7.8}$, $TVG_{6.0}$ and HTVG. LacZ activity of of *S. mutans* HLO002 cultured in HTVG (closed triangles), $TVG_{7.8}$ (open squares), and $TVG_{6.0}$ (closed circles).The results presented are the means of two independent experiments.

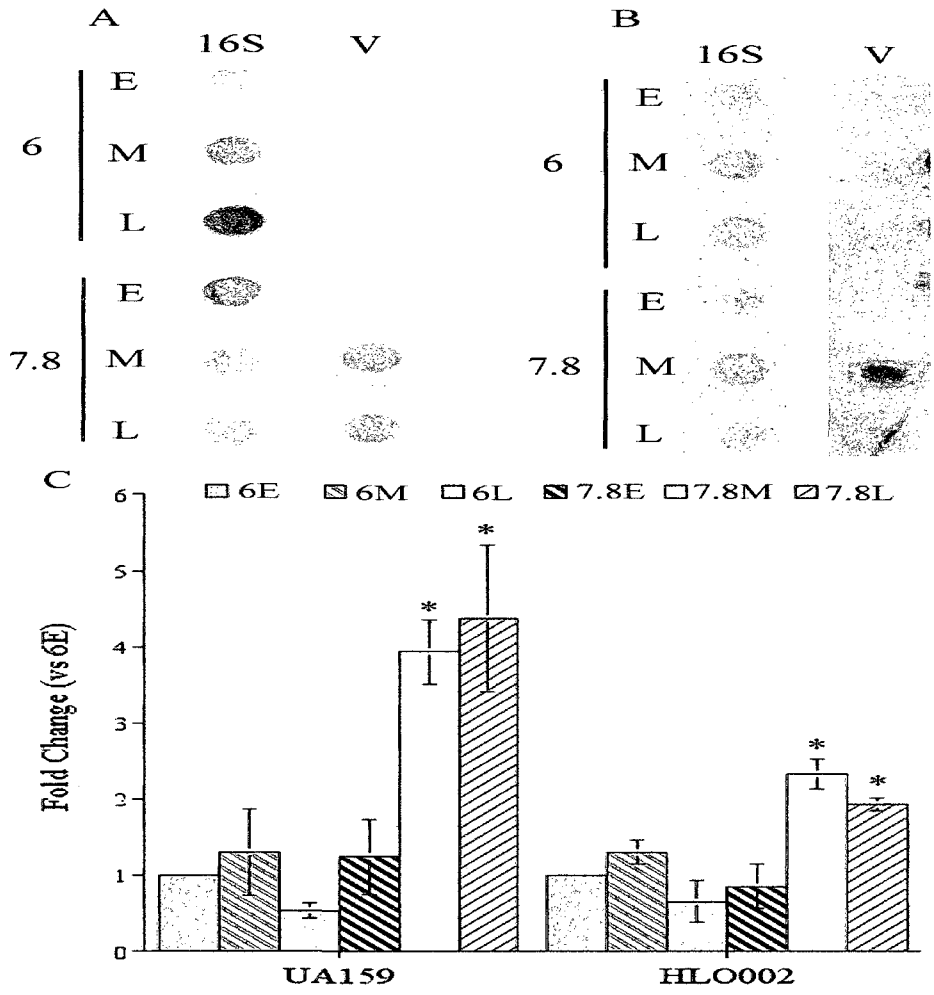

Fig 3.13. *vicR* expression in $TVG_{6.0}$ and HTVG at different growth phase in strains UA159 and HLO002. RNA dot blot of *vicR* (V) and *16S rRNA* (16S) transcripts from *S. mutans* UA159 (A) and *S. mutans* strain HLO002 (B). In both blots, RNA was detected from cells grown to early-exponential phase (E), mid-exponential phase (M) and late-exponential phase (L) in either unbuffered $TVG_{6.0}$ (6) or buffered HTVG (7.8). Relative intensities of the *vicR* transcripts were normalized against the 16S rRNA transcripts and reported as the mean (± SE) fold change compared to the early-exponential phase $TVG_{6.0}$ sample from three independent experiments (C). * , $P < 0.05$ between the sample and its counterpart in $TVG_{6.0}$.

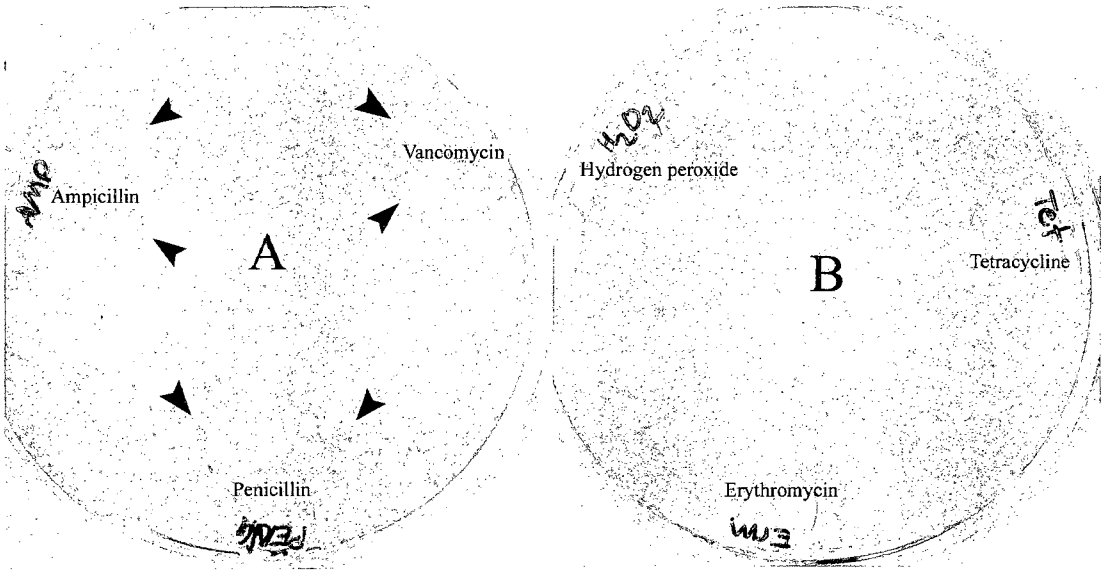

Fig 3.14. Induction of *lacZ* expression by antibiotics in strain HLO002. Typical results observed for antibiotics that induce (A) or do not induce (B) *lacZ* expression from P_{vicR}. Arrow heads indicate the intense blue color from X-Gal hydrolysis.

Table 3.2. Summary of LacZ activity assay using disc diffusion

Inducers	Induction
Sterile Water	-
Tetracycline (30 μg)	-
Erythromycin (15 μg)	-
Ampicillin (10 μg)	+
Penicillin G (10 U)	+
Vancomycin (30 μg)	+
Polymyxin B (15 000 U)	+
Bacitracin (3 400 U)	-
H_2O_2 (9 mg)	-
Triton X-100 (8 mg)	-

3.2.2 Deletion of *vicK, vicX* or *vicKX* has no Effect on *vicR* Expression

TCSs often have the ability to autoregulate their expression. To verify if the VicRKX TCS had such ability, *vicK* and *vicX* genes were deleted individually or in combination. Deletion of the genes was first confirmed by PCR (Fig 3.15). In the case of the *vicK* deletion, the PCR with primer pair SL160/SL180 yielded a 1.6 kb and a 2.0 kb amplicon for Δ*vicK* and the parent, respectively, indicating that *vicK* was deleted (Fig 3.15B). In the case of the *vicX* and *vicKX* deletion, the amplicons resulting from a PCR with primer pair SL160/SL179 were 2.9 kb, 3.1 kb and 1.7 kb for the parent, Δ*vicX* and Δ*vicKX*, respectively, indicating that *vicX* and *vicKX* were deleted in their respective mutants (Fig 3.15B). All three mutants are carrying the *ermAM* cassette which was absent from the parent genome (3.15C). The deletions were further confirmed by sequencing (Appendix 1).

The three mutants were assayed for *lacZ* expression. The deletion of *vicK, vicX* or both genes did not affect the production of LacZ from the *vicR* promoter in either HTVG or $TVG_{6.0}$ when compared to the parent strain (Fig 3.16). Furthermore, both the Δ*vicK* and Δ*vicX* mutants displayed similar levels of X-Gal hydrolysis compared to the parent strain in the presence of either penicillin G, vancomycin, or polymyxin B when tested by the disc diffusion assay (data not shown). Therefore, our results suggest that the VicRKX system does not autoregulate its expression.

3.2.3 The LiaFSR TCS Controls the Expression of *vicR*

Li et al. (2002) previously indicated that the Hk11/Rr11 TCS, recently renamed LiaSR, was required for acid adaptation and might act as a pH sensor. The LiaSR system is a member of the intramembrane-sensing histidine kinase family (IM-HK) which are

Fig 3.15. Genetic organization and PCR amplification of the *vicRKX* locus in the parent, and the Δ*vicK*, Δ*vicX* and Δ*vicKX* mutants. (A) Genetic organization of the *vicRKX* locus in the parent, and the Δ*vicK*, Δ*vicX* and Δ*vicKX* mutants. Genes deleted with the *ermAM* cassette are indicated in their respective mutants. Primer locations (arrows) and amplicons are indicated between arrows. (B) Genomic DNA of the parent, and the Δ*vicK*, Δ*vicX* and Δ*vicKX* mutants served as templates in the PCR. The primer pairs SL160/180 (160-180) and SL160-SL179 (160-179) were selected to amplify the region containing the *vicK* and *vicX* genes, respectively. (C) PCR-amplification of *ermAM* cassette using the primer pair SL550-551 (550-551) and genomic DNA of the parent, and the Δ*vicK*, Δ*vicX* and Δ*vicKX* mutants as templates. The image of the genetic map was adapted from the Gene Image Map application available at the Oral Pathogen Sequence Databases (http://www.oralgen.lanl.gov/oralgen/).

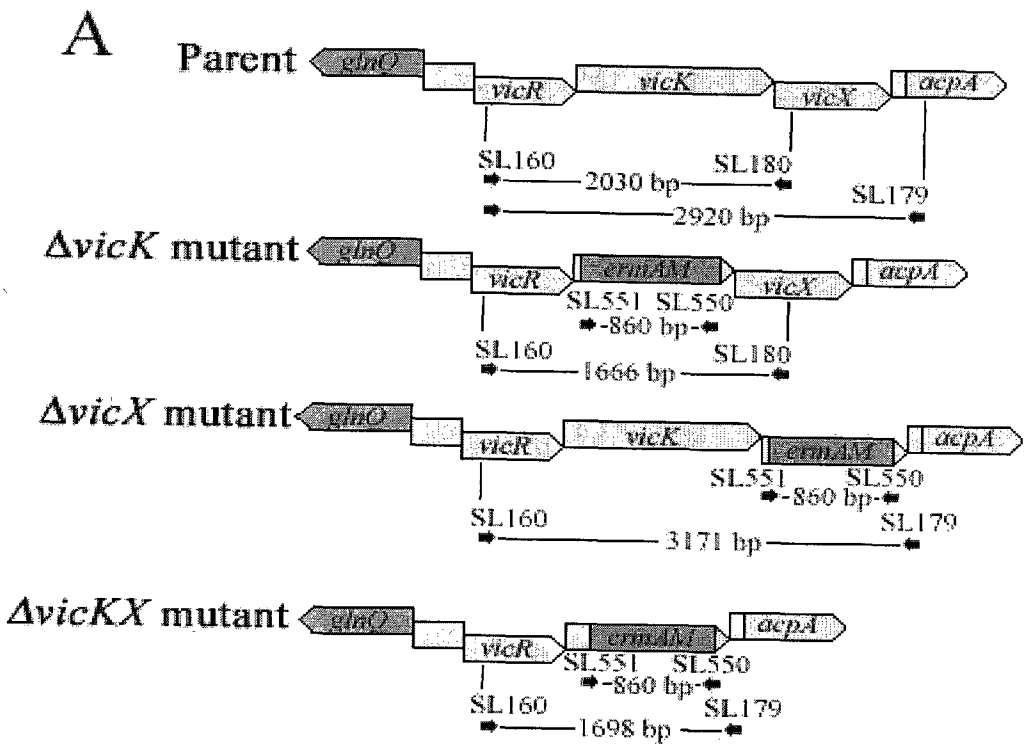
A
Parent
glnQ
vicR
vicK
vicX
acpA
SL160
SL180
SL179
2030 bp
2920 bp
ΔvicK mutant
ermAM
SL551
SL550
-860 bp-
1666 bp
ΔvicX mutant
3171 bp
ΔvicKX mutant
1698 bp

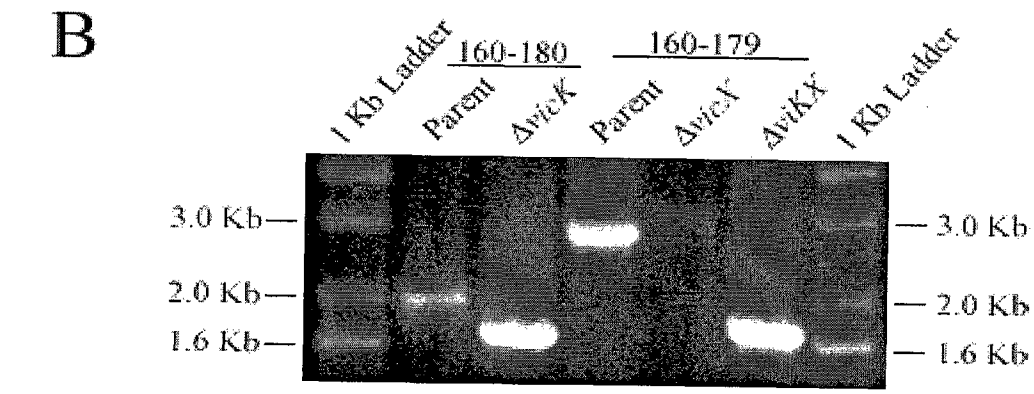
B
1 Kb Ladder
160-180
160-179
Parent
ΔvicK
ΔvicX
ΔviKX
3.0 Kb
2.0 Kb
1.6 Kb

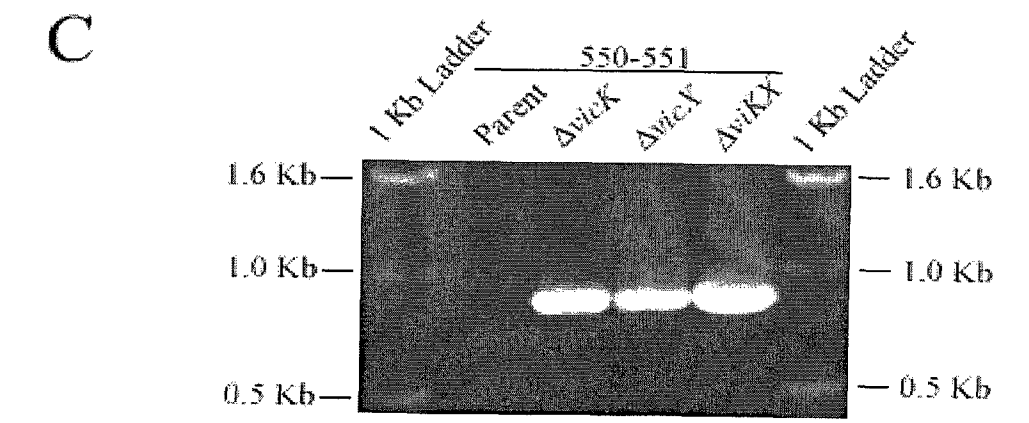
C
1 Kb Ladder
550-551
Parent
ΔvicK
ΔvicX
ΔviKX
1.6 Kb
1.0 Kb
0.5 Kb

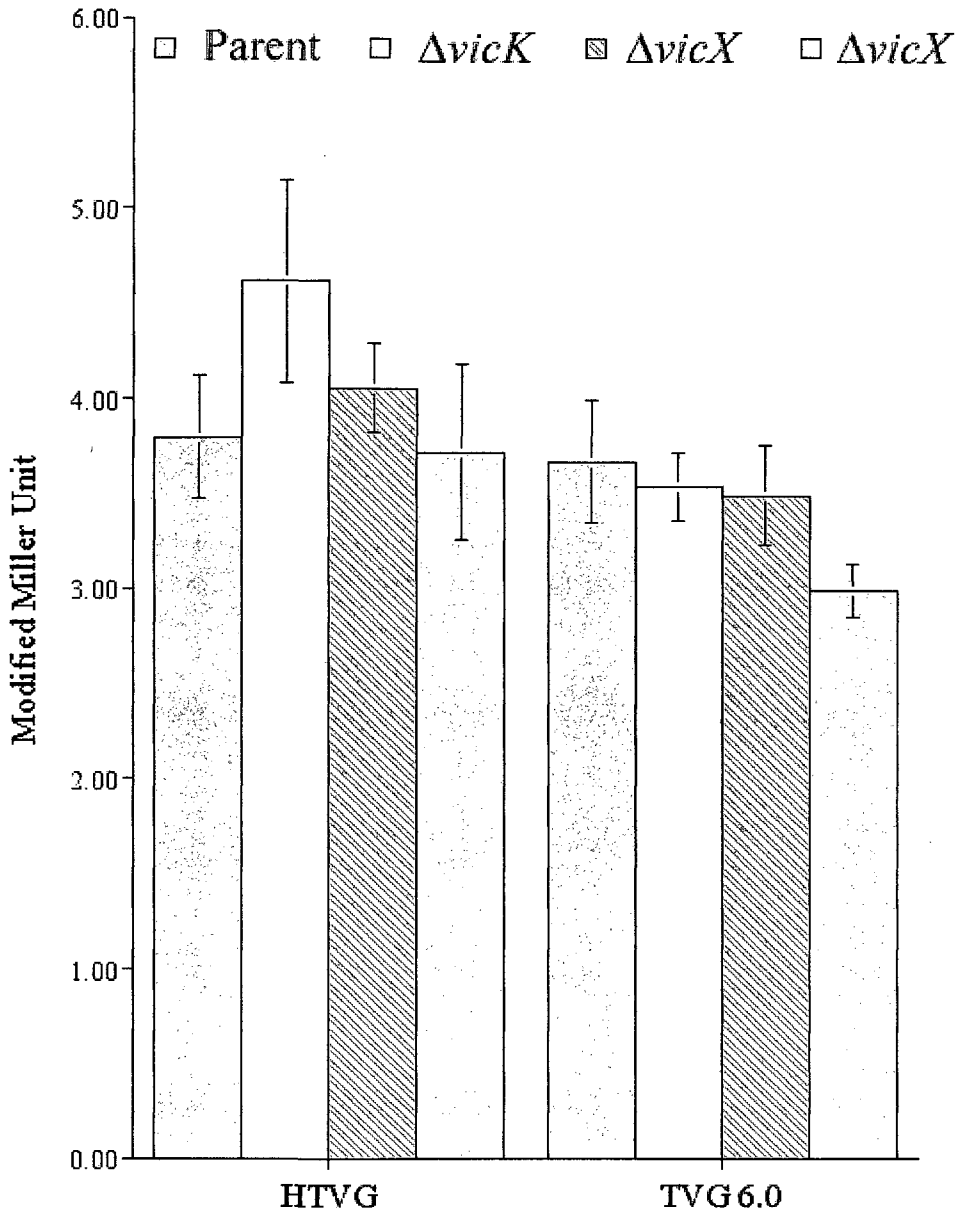

Fig 3.16, Impact of *vicK* and *vicX* deletion on *lacZ* expression in the parent, and the Δ*vicK*, Δ*vicX* and Δ*vicKX* mutants cultured in TVG 6.0 and HTVG to mid-exponential phase. The results represent the means (± SE) of two independent experiments with each experiment consisting of triplicate cultures.

important for controlling the cell-envelope response caused by antibacterial agents and, in some cases, for intrinsic resistance to antibacterial agents (Mascher, 2006). To examine the role of the LiaFSR system in *vicR* expression, the associated genes were deleted. To confirm the deletions, the mutants were first analyzed by PCR (Fig 3.17). In the case of the *liaF* deletion, the PCR with primer pair SL565/SL623 yielded a 1.2 kb and a 1.1 kb amplicon for LiaFSR$^-$ mutant and the parent, respectively, indicating that *liaF* was deleted (Fig 3.17B). In the case of the *liaS* deletion, the amplicons resulting from a PCR with primer pair SL591/SL358 were 1.6 kb for both the parent, and Δ*liaS* mutant (Fig 3.17B). The Δ*liaS* mutant was further analyzed and PCR yielded a 1.5 kb and a 1.0 kb amplicon, which were absent in the parent, when primer pairs SL550/SL358 and SL591/SL551 were used, respectively (Fig 3.18B). These results indicated that *liaS* was deleted. In the case of the *liaR* deletion, primer pair SL569/SL570 amplified a 0.5 kb and a 1.0 kb product in the parent and Δ*liaR* mutant, respectively, indicating that *liaR* was deleted (Fig 3.17B). All three mutants were PCR-positive for the *ermAM* cassette which was absent in the parent (3.18C). The deletions were further confirmed by sequencing (Appendix 1).

3.2.3.1 LacZ Assay

The three resulting mutants were assayed for *lacZ* expression from the *vicR* promoter. When grown in HTVG, the Δ*liaS* mutant exhibited the highest level of expression (200-300% of the parent level; $P<0.05$) (Fig 3.18). The LiaFSR$^-$ mutant also showed a higher *lacZ* expression than the parent ($P<0.05$). Consistent with earlier results, *lacZ* expression was much lower when cells were grown in low pH media ($TVG_{6.0}$), although Δ*liaS* mutant still produced significantly more LacZ than the parent.

Fig 3.17. Genetic organization and PCR amplification of the *liaFSR-ppiB-pnpB* locus in the parent, and the LiaFSR$^-$, Δ*liaS* and Δ*liaR* mutants. (A) Genetic organization of the *liaFSR-ppiB-pnpB* locus in the parent, and the LiaFSR$^-$, Δ*liaS* and Δ*liaR* mutants. Genes deleted with the *ermAM* cassette are indicated in their respective mutant. The promoter of the *liaFSR-ppiB-pnpB* locus is also indicated by a bent arrow. Primer location (arrows) and amplicons are indicated between arrows. (B) Genomic DNA of the parent, and the LiaFSR$^-$, Δ*liaS* and Δ*liaR* mutants served as templates in PCR. The primer pairs SL565/623 (565-623), SL591/358 (591-358) and SL569/570 (569-570) were selected to amplify the region containing the *liaF*, *liaS* and *liaR* genes, respectively. Primer pairs SL550/358 (550-358) and SL591/SL551 (591-551) were used amplify the *ermAM* cassette ligated to the *liaR* gene and *liaF* gene, respectively, in the Δ*liaS* mutant. (C) PCR-amplification of *ermAM* cassette using the primer pair SL550-551 (550-551), and the genomic DNA of the parent, and the LiaFSR$^-$, Δ*liaS* and Δ*liaR* mutants was used as templates. The image of the genetic map was adapted from the Gene Image Map application available at the Oral Pathogen Sequence Databases (http://www.oralgen.lanl.gov/oralgen/).

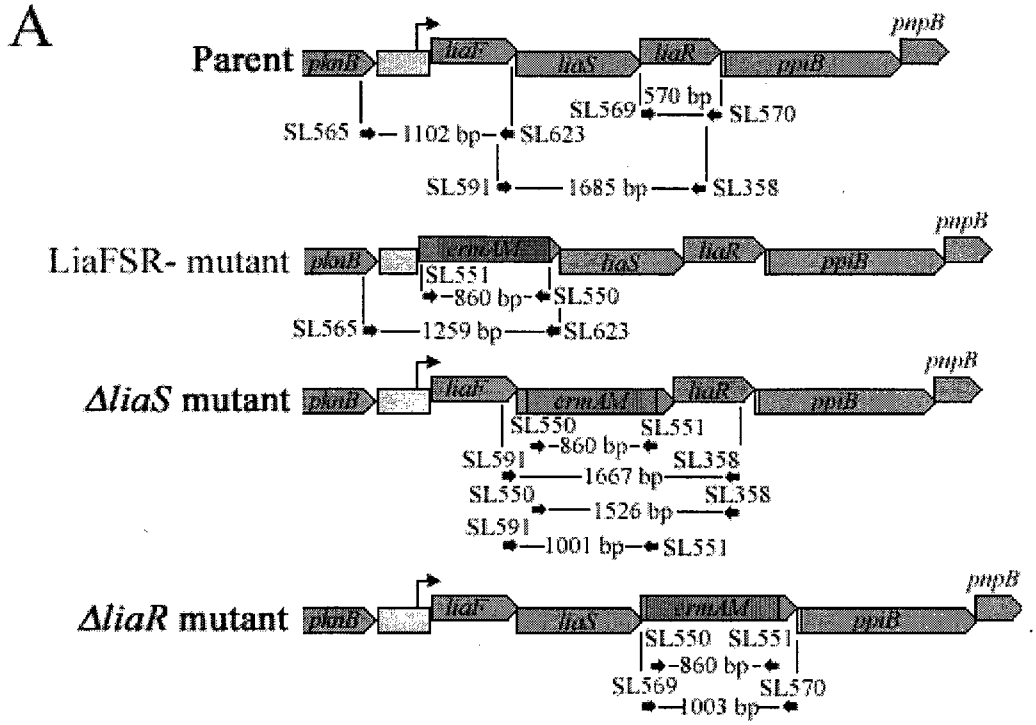
A
Parent
pknB
liaF
liaS
liaR
ppaB
pnpB
SL565
1102 bp
SL623
SL569
570 bp
SL570
SL591
1685 bp
SL358
LiaFSR- mutant
ermAM
SL551
860 bp
SL550
1259 bp
ΔliaS mutant
1667 bp
1526 bp
1001 bp
ΔliaR mutant
1003 bp

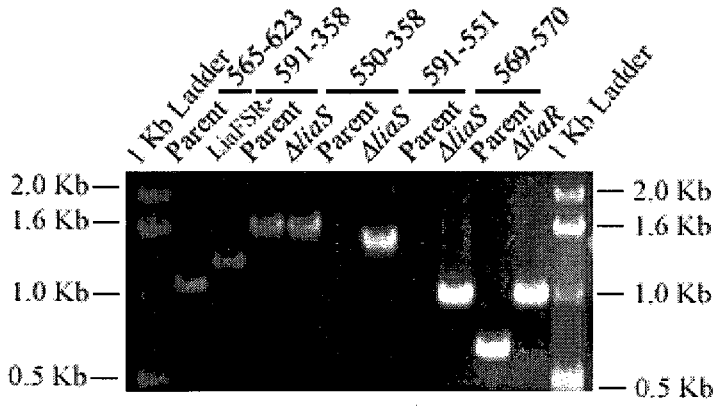
B
1 Kb Ladder
Parent
LiaFSR-
ΔliaS
ΔliaR
565-623
591-358
550-358
591-551
569-570
2.0 Kb
1.6 Kb
1.0 Kb
0.5 Kb

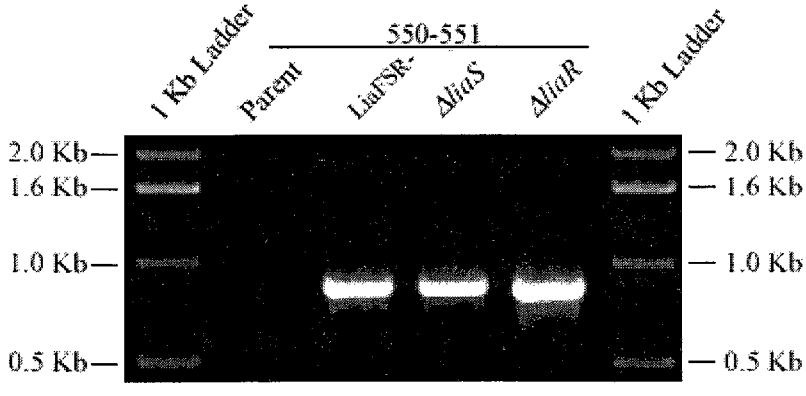
C
1 Kb Ladder
550-551
Parent
LiaFSR-
ΔliaS
ΔliaR
2.0 Kb
1.6 Kb
1.0 Kb
0.5 Kb

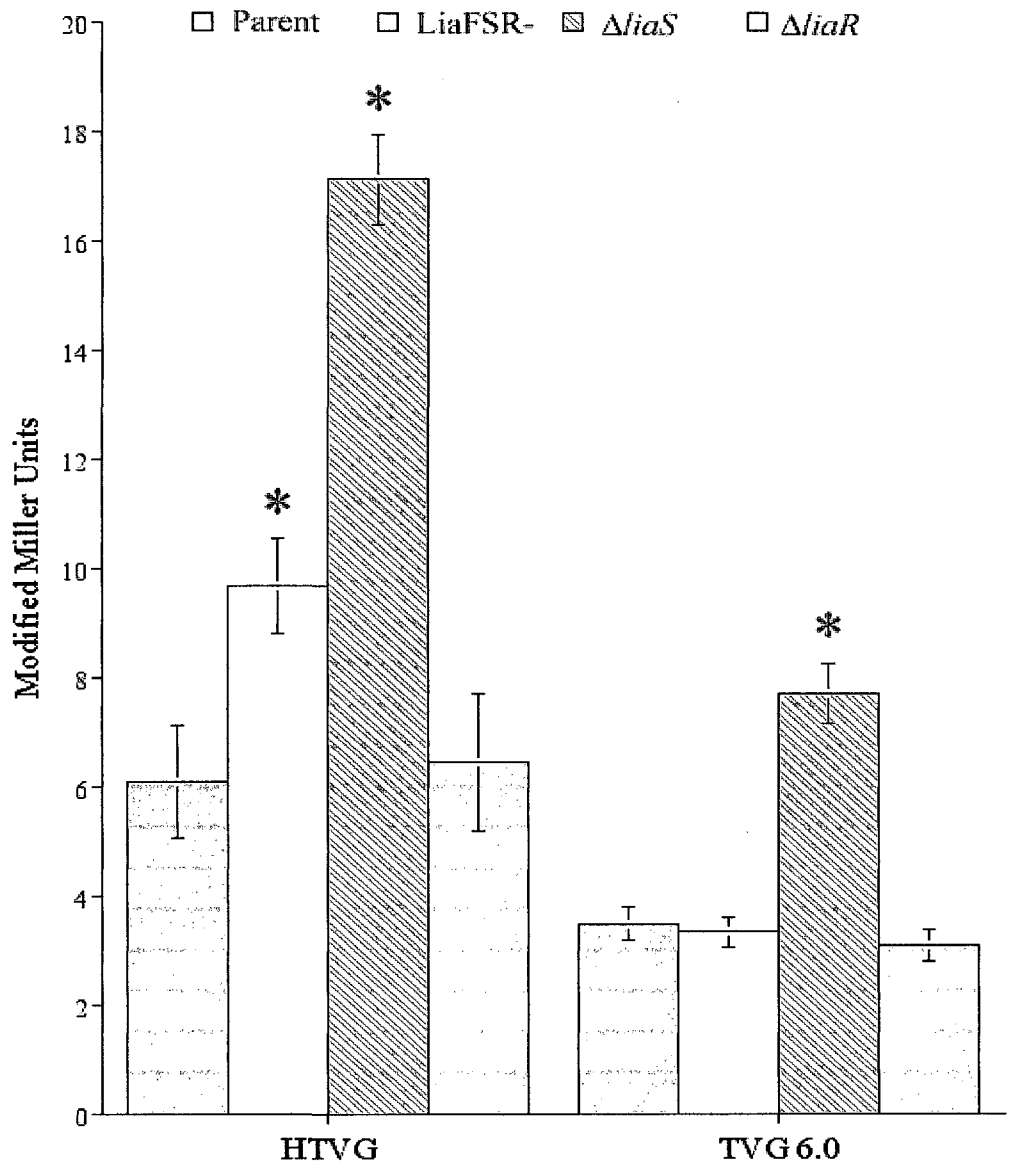

Fig 3.18. Impact of *liaF*, *liaS*, *liaR* deletion on P_{vicR} activity in the parent, and the LiaFSR$^-$, Δ*liaS* and Δ*liaR* mutants cultured in TVG 6.0 and HTVG to mid-exponential phase. The results represent the means (± SE) of two independent experiments with each experiment consisting of triplicate cultures. * indicate $P<0.05$ between the mutant and the parent.

3.2.3.2 RNA and Protein Level

To confirm the observation made with the LacZ assays, RNA and proteins were isolated from each strain and analyzed for levels of *vicR* transcript (Fig 3.19) and protein (Fig 3.20). Consistent with the LacZ assay, the Δ*liaS* mutant produced more *vicR* RNA when grown in HTVG (Fig 3.19); however, there was no consistent increase in *vicR* expression in the LiaFSR$^-$ mutant. In $TVG_{6.0}$, the level of *vicR* transcript also appeared to marginally increase in Δ*liaS* mutant and marginally decrease in the LiaFSR$^-$, and Δ*liaR* mutants. This was inconsistent, to a certain extent, with the results of the LacZ assay.

In contrast, changes in VicR levels were not always consistent with either RNA level and LacZ assay. For example, the level of VicR protein (Fig 3.20) did not increase as much in Δ*liaS* mutant cultured in HTVG when compared to RNA level (Fig 3.19) and the LacZ assay (Fig 3.16). However, consistently higher levels of VicR (1.5 fold; Fig 3.18 and 3.19) were observed in the LiaFSR$^-$ mutant cultured in HTVG. Unfortunately, higher VicR levels in the Δ*liaS* mutant cultured in HTVG or $TVG_{6.0}$ were not observed (Fig 3.20). Additionally, fold changes in VicR expression in the Δ*liaS* mutant were not consistent with the fold changes observed in the LacZ assay (Fig 3.21). Furthermore, VicR polypeptides were also notably up-regulated in the Δ*liaS* mutant cultured in $TVG_{6.0}$ whereas *vicR* RNA transcript was notably downregulated in the LiaFSR$^-$ mutant cultured in $TVG_{6.0}$. VicR levels (Fig 3.20) in the Δ*liaR* mutant cultured in $TVG_{6.0}$ were, however, consistent with the RNA analysis. Specifically, VicR production was decreased in the Δ*liaR* mutant.

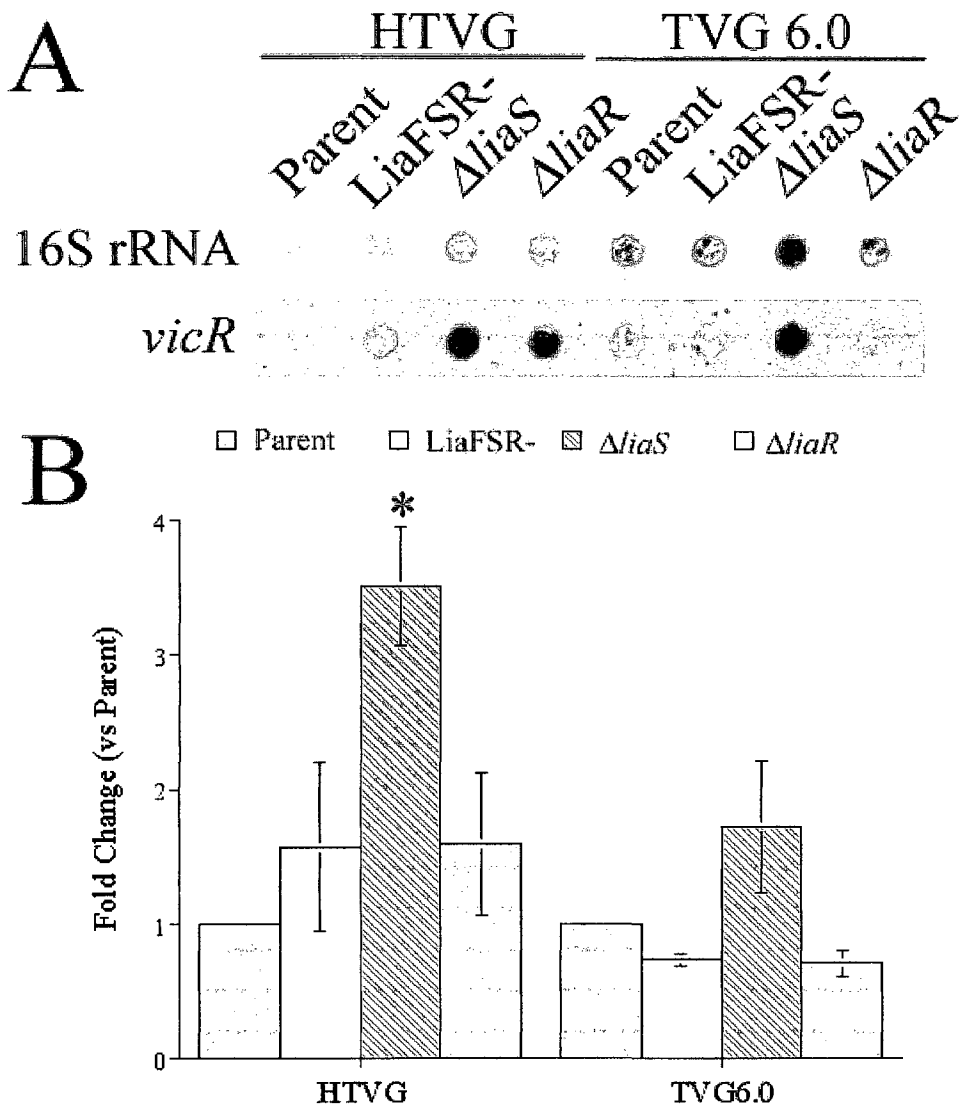

Fig 3.19. Level of *vicR* RNA produced by the parent, and the LiaFSR⁻, Δ*liaS* and Δ*liaR* mutants cultured in $TVG_{6.0}$ and HTVG to mid-exponential phase. RNA dot blot of *vicR* and *16S rRNA* transcripts from the parent, and the LiaFSR⁻, Δ*liaS* and Δ*liaR* mutants cultured in $TVG_{6.0}$ (TVG6.0) and HTVG (A). The intensities of the *vicR* transcripts were normalized against the intensities of 16S rRNA transcripts and the results are presented as the mean (± SE) fold changes compared to the parent from three independent experiments (B). * indicate $P<0.05$ between the mutant and the parent.

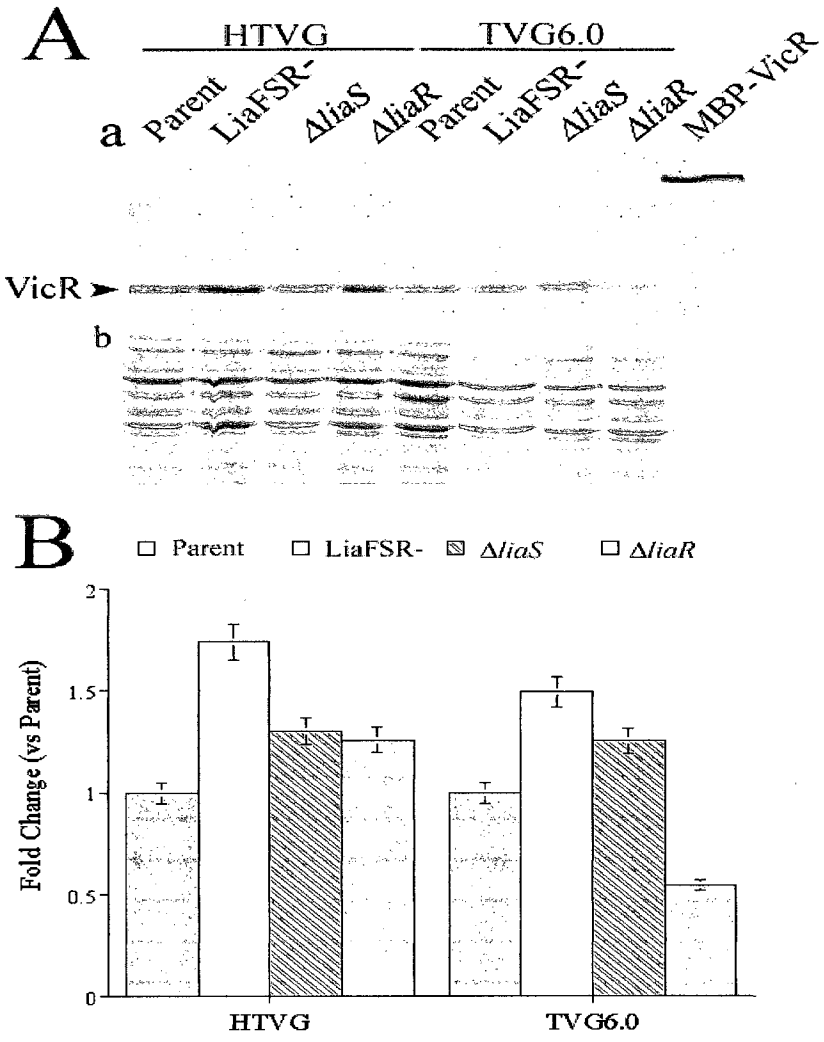

Fig 3.20. Level of VicR protein in the parent, and the LiaFSR$^-$, Δ*liaS* and Δ*liaR* mutants cultured in $TVG_{6.0}$ and HTVG to mid-exponential phase. Cytoplasmic proteins isolated from the parent, and the LiaFSR$^-$, Δ*liaS* and Δ*liaR* mutants cultured in $TVG_{6.0}$ (TVG6.0) and HTVG were analyzed by western immunoblot for the presence of VicR (Aa). The intensities of the VicR protein as analyzed by western immunoblot (Aa) were normalized against Coomassie stained proteins (Ab) and the results are presented as the mean (± SE) fold changes compared to the parent from three independent experiments (B). The purified MBP-VicR was used as a positive control.

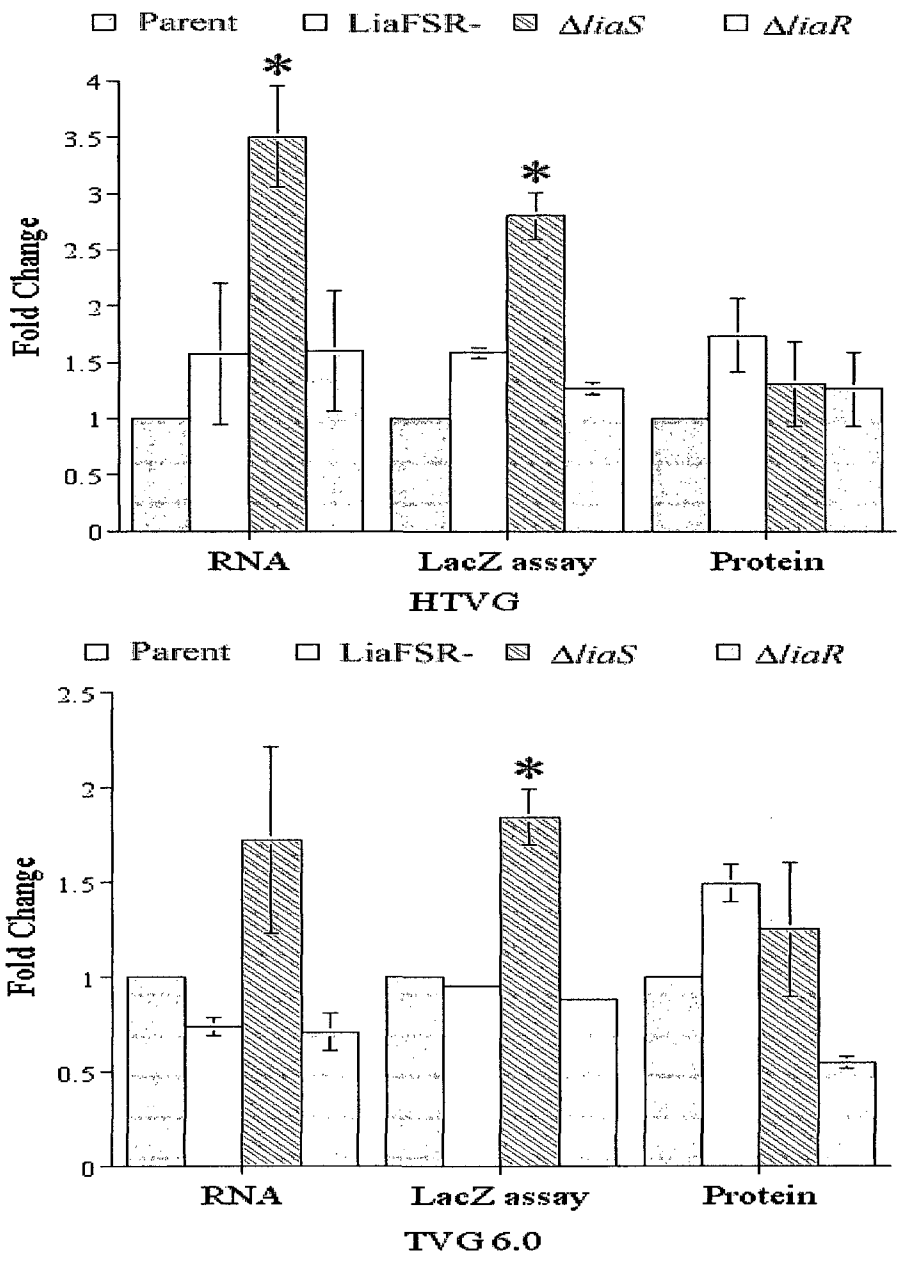

Fig 3.21. Summary of fold changes in *vicR* expression as determined by *lacZ* reporter gene assay, and RNA and protein level in the parent, and the LiaFSR$^-$, *ΔliaS* and *ΔliaR* mutants cultured in $TVG_{6.0}$ and HTVG. The results are the means (± SE) of three independent experiments. * indicate $P<0.05$ between the mutants and the parent.

3.2.4 The Expression *vicR* is Down-Regulated by Exogenous CSP in a ComX-Independent Manner

Senadheera and Cvitkovitch (2005) have reported that the addition of CSP stimulated the expression of *vicR* and *vicK* in the absence of the CSP-specific HK (ComD) and RR (ComE). Furthermore, previous studies by Senadheera et al. (2005; 2007) have shown that deletion of *vicX* results in decreased transformation efficiency in the absence of the CSP. They also showed that the addition of exogenous CSP did not increase the transformation efficiency of a Δ*vicK* mutant or a mutant overexpressing *vicRKX* to the same level as the parent. To test if the regulation involved more elements in the signal CSP-pathway, *comX* was deleted. To confirm the deletion of *comX*, the *comX* locus was first analyzed by means of PCR (Fig 3.22). PCR with primer pair SL573/SL574 yielded a 1.5 kb and a 2.0 kb amplicon for parent and the Δ*comX* mutant, respectively (Fig 3.22B), these results indicate that *comX* was deleted. Furthermore, the *ermAM* cassette was also amplified using the Δ*comX* mutant genomic DNA but not with the parent genomic DNA (3.18C). The deletion was further confirmed by sequencing (Appendix 1).

It was observed that the Δ*comX* mutant produced significantly more LacZ only when grown to early-exponential phase in $TVG_{6.0}$ (Fig 3.23A). A small increase in LacZ production in the Δ*comX* mutant was observed when grown to early-exponential phase in HTVG but the difference was not significant. Change in LacZ production was not observed in cells harvested in the mid-exponential phase (Fig 3.23B). It appears that the expression of *vicR* is ComX-independent and the observed increase in $TVG_{6.0}$ may not have a biological relevance.

Fig 3.22. Genetic organization and PCR amplification of *comX* in the parent and the Δ*comX* mutant. (A) Genetic organization of *comX* locus in the parent and the Δ*comX* mutant. Primer locations (arrows) and amplicons are indicated between arrows. (B) Genomic DNA of the parent and the Δ*comX* mutant served as templates in PCR. The primer pair SL573/574 (573-574) was selected to amplify the region containing the *comX* gene. (C) PCR-amplification of *ermAM* cassette using the primer pair SL550-551 (550-551) and genomic DNA of the parent or the Δ*comX* mutant as templates. The image of the genetic map was adapted from the Gene Image Map application available at the Oral Pathogen Sequence Databases (http://www.oralgen.lanl.gov/oralgen/).

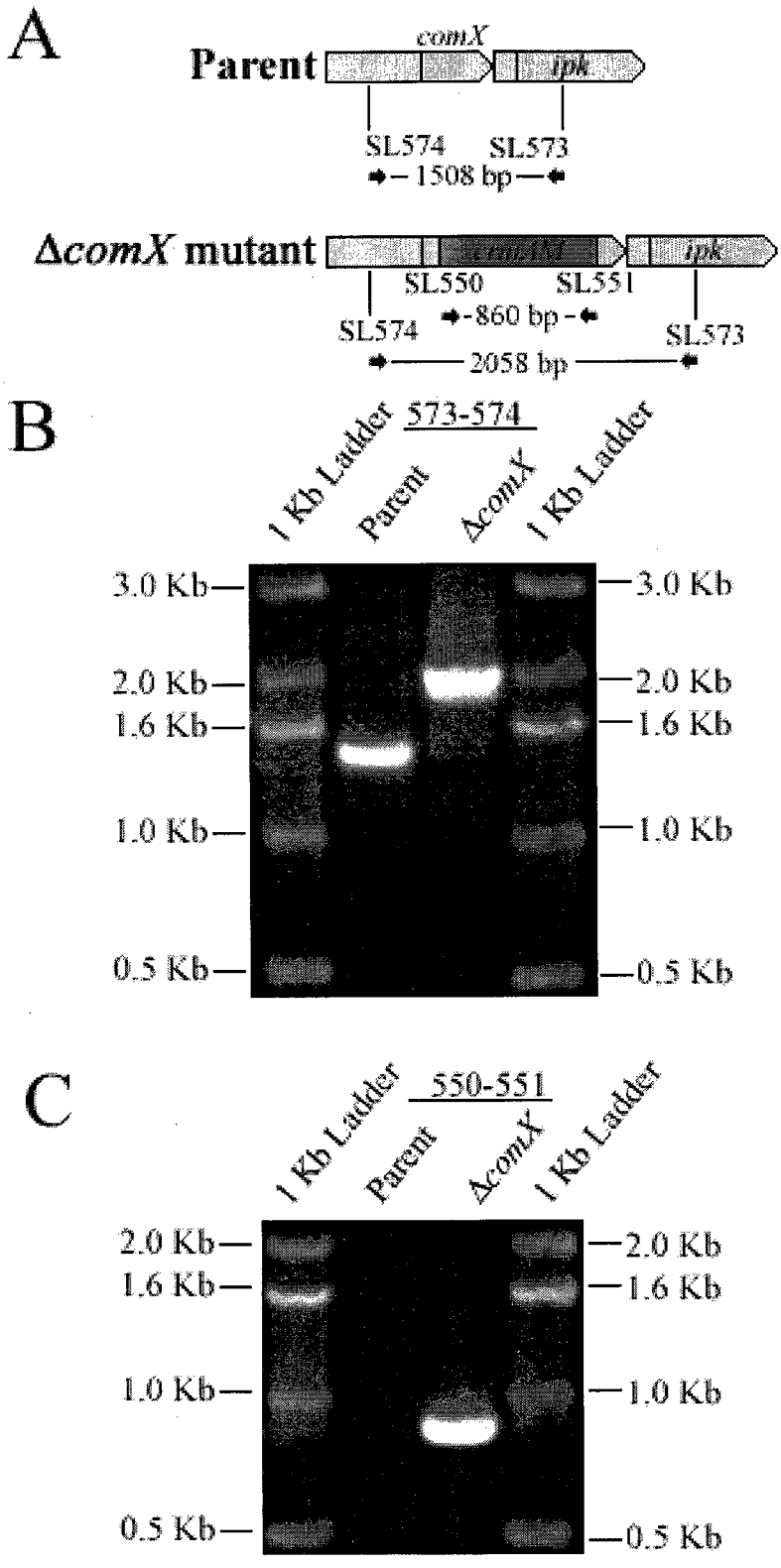
A
Parent
comX
tpk
SL574
SL573
1508 bp
ΔcomX mutant
SL550
SL551
SL574
860 bp
SL573
2058 bp
B
573-574
1 Kb Ladder
Parent
ΔcomX
1 Kb Ladder
3.0 Kb
2.0 Kb
1.6 Kb
1.0 Kb
0.5 Kb
C
550-551
1 Kb Ladder
Parent
ΔcomX
1 Kb Ladder
2.0 Kb
1.6 Kb
1.0 Kb
0.5 Kb

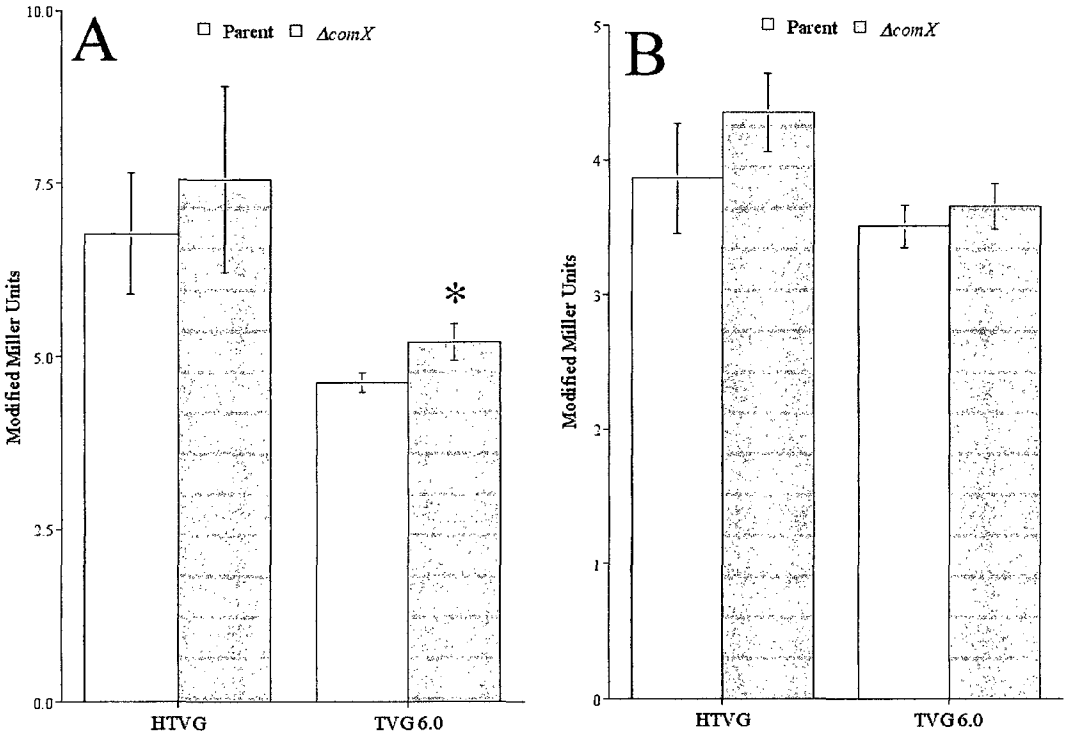

Fig 3.23. Impact of a *comX* mutation on P_{vicR} activity in comparison to the parent when cultured in $TVG_{6.0}$ and HTVG to early-exponential phase (A) and mid-exponential phase (B). The results represent the means (± SE) of two independent experiments with each experiment consisting of triplicate cultures. * indicate $P<0.05$.

To further investigate the role of the CSP signaling pathway, CSP was added to the parent and the Δ*comX* mutant cells cultured to early-exponential phase in HTVG or $TVG_{6.0}$. The CSP caused a decrease in LacZ production in both the parent and the Δ*comX* mutant cells cultured in HTVG (Fig 3.24). No significant changes were observed for the parent cultured in $TVG_{6.0}$ with or without the CSP. These results suggest that CSP downregulates expression of *vicR* in the presence of ComD and ComE and that the signaling employs a ComX-independent pathway.

To further examine the CSP-signaling pathway, a pSL derivative containing the promoter of *comDE* (pYH2) was introduced into *S. mutans* strain UA159. YDNT011 was cultured in HTVG and $TVG_{6.0}$, and harvested at early-exponential phase. It was observed that strain YDNT011 produced significantly more LacZ when culture in HTVG than in $TVG_{6.0}$ (Fig 3.25). An increase in expression of *comDE* in HTVG suggests that the bacteria would be more responsive to CSP under such growth conditions.

3.3 Characterization of the LiaFSR TCS Mutants

The role of the HK LiaS and the RR LiaR has been previously charaterized (Li et al., 2002a); however, the role of LiaF in *S. mutans* has yet to be investigated. The results described in section 3.2 clearly demonstrate that the deletion of components of the LiaFSR system resulted in differential expression of *vicR*. Therefore, further characterization of the $LiaFSR^-$ mutant was warranted.

3.3.1 Deletion of *liaF* is Polar

A study recently reported that the *liaF* gene was erroneously annotated and the new start codon of *liaF* would be located 123-bp downstream from the annotated genome

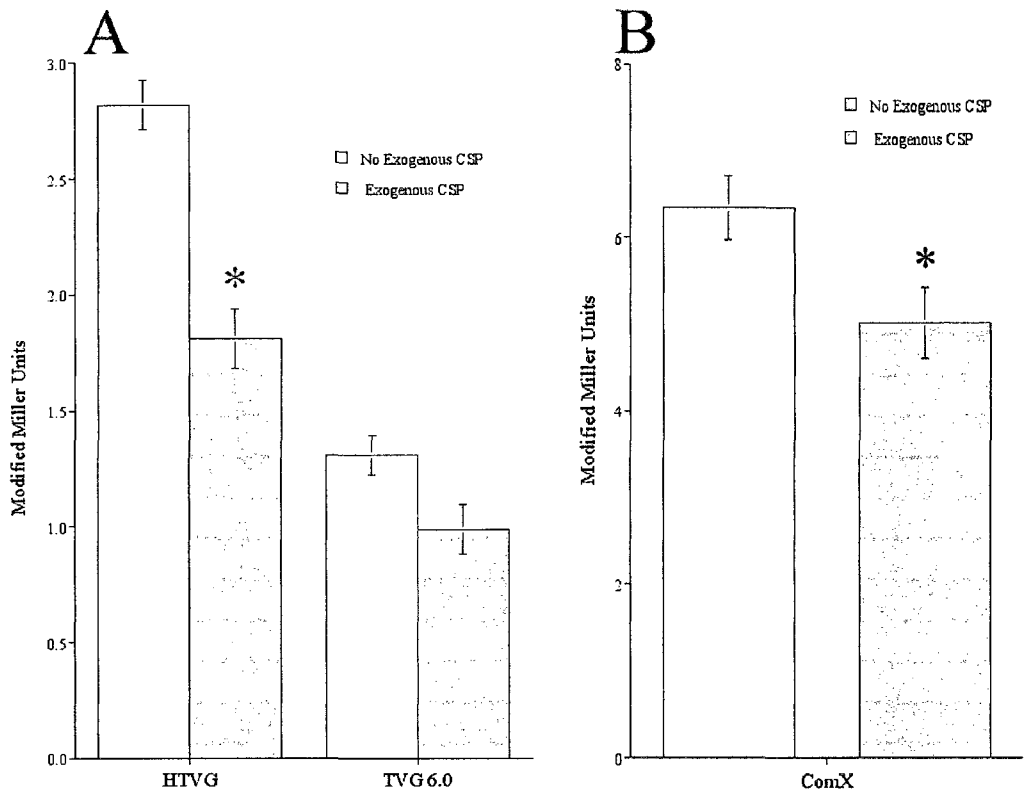

Fig 3.24. Impact of the CSP on P_{vicR} activity in strain HLO002 or the Δ*comX* mutant. (A) Strain HLO002 cultured in HTVG or $TVG_{6.0}$ and (B) the Δ*comX* mutant cultured in HTVG. In both cases, cells were grown to early-exponential phase and the CSP was added. After 1 h, cells were harvested. The results represent the means (± SE) of two independent experiments with each experiment consisting of triplicate cultures. * indicate $P<0.05$.

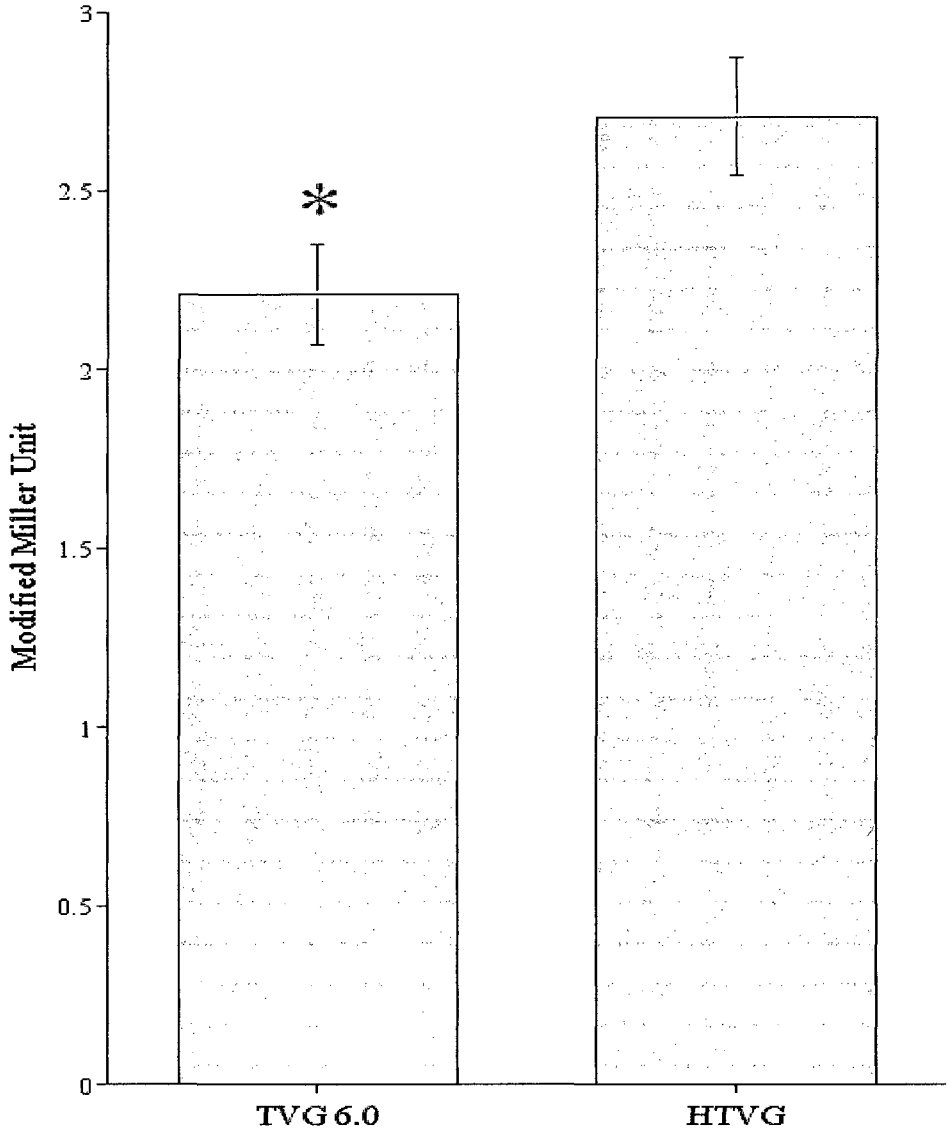

Fig 3.25. Expression of *lacZ* fused to P_{comDE} in strains cultured in TVG 6.0 and HTVG to early-exponential phase. The results represent the means (± SE) of two independent experiments with each experiment consisting of triplicate cultures. * indicate $P<0.05$.

(Suntharalingam et al., 2009). Therefore, the promoter of the *liaFSR-ppiB-pnpB* operon would be located within the newly realized 123-bp intergenic region located between *pknB* and *liaF*. Based on this information, it was noted that the design of the LiaFSR$^-$ mutant resulted in deletion both the newly-identified promoter region and the *liaF* gene. To test if the deletion inactivated expression of genes downstream of *liaF*, cytoplasmic proteins isolated from the parent, and the LiaFSR$^-$, Δ*liaS* and Δ*liaR* mutants were analyzed for the presence of LiaR by means of western immunoblot. The results indicate that both the parent and the Δ*liaS* mutant produced LiaR when cultured in HTVG or $TVG_{6.0}$ (Fig 3.26). As expected, the LiaR polypeptide was not detected in Δ*liaR* mutant (Fig 3.26). Additionally, the LiaFSR$^-$ mutant did not produce LiaR (Fig 3.26) suggesting that the deletion of the promoter resulted in the inactivation of the *liaFSR-ppiB-pnpB* operon.

3.3.2 Expression Levels of *liaF, liaS* and *liaR* in the Parent, and the LiaFSR$^-$, Δ*liaS* and Δ*liaR* Mutants Cultured in $TVG_{6.0}$ and HTVG

To characterize the LiaFSR TCS component mutants, the transcript levels of the three genes were measured (Fig 3.27). The level of *liaS* RNA appeared to be below the detection level in the parent strain and in all three mutants cultured in either HTVG or $TVG_{6.0}$. Similarly, *liaR* transcript could not be detected in the parent strain, LiaFSR- or as expected Δ*liaR* mutant. However, a higher level of *liaR* transcript was observed in Δ*liaS* mutant but the increase does not appear to result in an increase in the production of LiaR (Fig 3.26) Unlike the expression of *liaS* and *liaR*, *liaF* transcript was detected in the parent, Δ*liaS* and Δ*liaR* mutants.

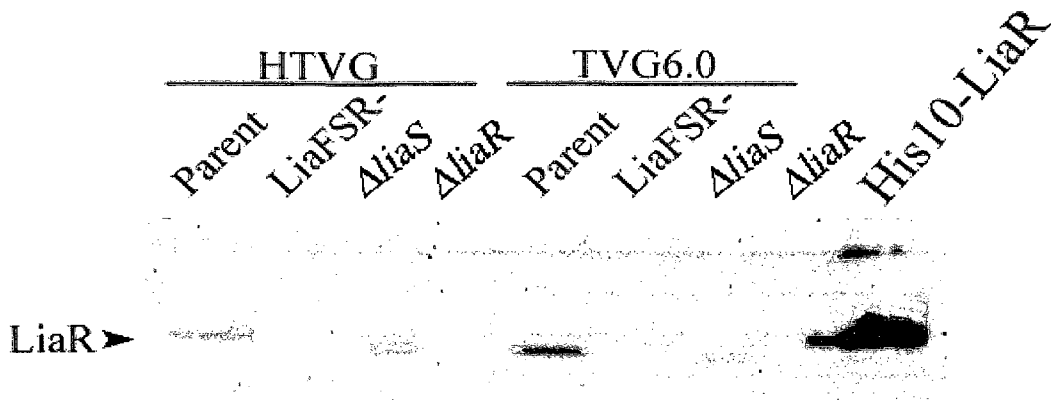

Fig 3.26. Production of LiaR in the parent, and the LiaFSR$^-$, Δ*liaS* and Δ*liaR* mutants cultured in $TVG_{6.0}$ and HTVG to mid-exponential phase. Cytoplasmic proteins isolated from the parent, and the LiaFSR$^-$, Δ*liaS* and Δ*liaR* mutants cultured in $TVG_{6.0}$ (TVG6.0) and HTVG were analyzed by western immunoblot for the presence of LiaR. A purified His_{10}-LiaR (His10-LiaR) was used as a positive control.

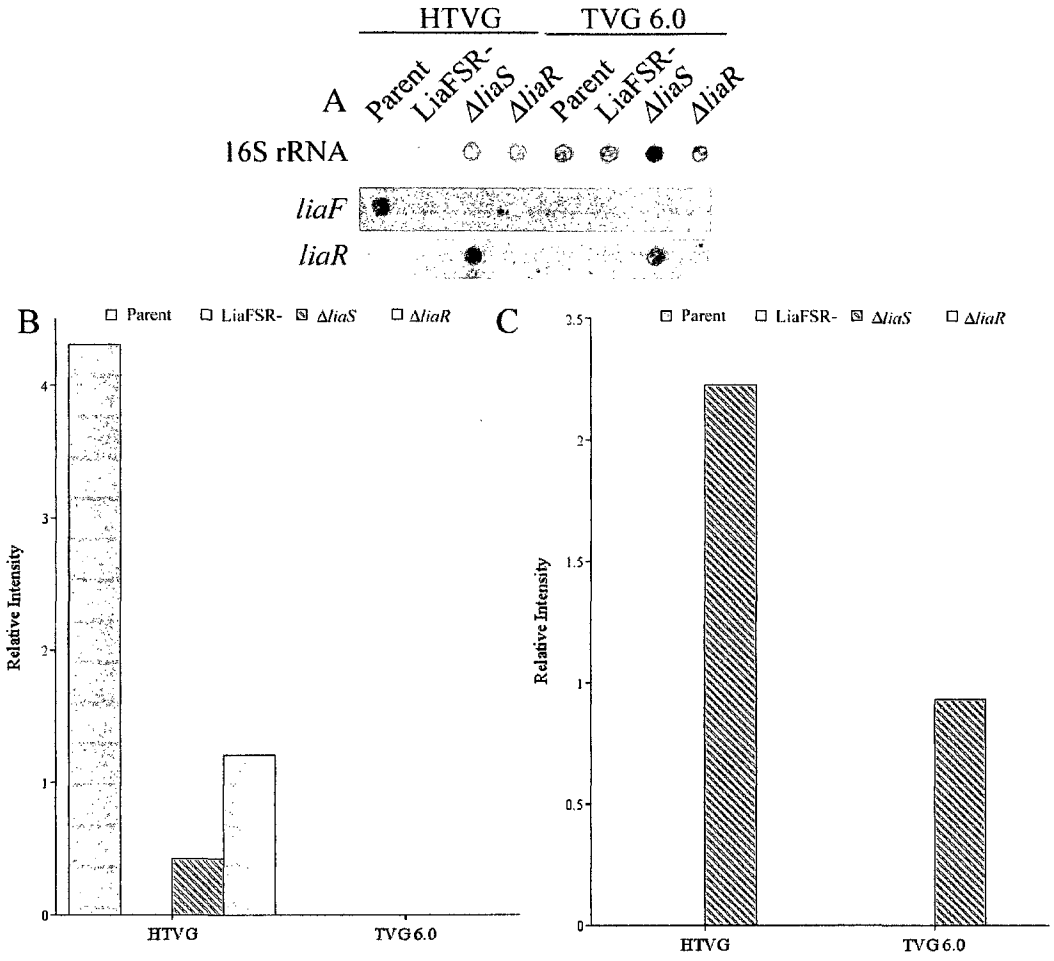

Fig 3.27. Expression levels of *liaF, liaS* and *liaR* in the parent, and the LiaFSR$^-$, Δ*liaS* and Δ*liaR* mutants cultured in TVG$_{6.0}$ and HTVG. RNA dot blot of *liaF*, *liaS*, *liaR* and *16S rRNA* transcripts isolated from the parent, and the LiaFSR$^-$, Δ*liaS* and Δ*liaR* mutants cultured in HTVG and TVG$_{6.0}$ (A). This experiment and the experiment in Fig 3.19 share the 16S rRNA blot because both experiments were performed in parallel. The blot probed with the *liaS* probe is not included because no *liaS* transcript could be detected for any strains under either growth condition. The intensities of the *liaF* (B) and *liaR* (C) transcripts were normalized against the intensities of 16S rRNA transcripts and the absence of a bar means that no transcript could be detected.

3.3.3 Growth of the LiaFSR$^-$, Δ*liaS* and Δ*liaR* mutants

Growth of the mutants in different culture media was measured. The LiaFSR$^-$ and Δ*liaS* mutants had a longer lag phase when the initial pH was above 7.0 (HTVG and TVG; Fig 3.28 and 3.29) and all three mutants had a longer lag phase when the initial pH was 6.0 ($TVG_{6.0}$; Fig 3.30). Additionally, the LiaFSR$^-$ mutant entered stationary phase at a much lower density than any of the strains tested when cultured TVG and $TVG_{6.0}$ (Fig 3.28 and Fig 3.29). The Δ*liaR* mutant also initiated its entrance into stationary phase at a lower density when cutured in TVG and $TVG_{6.0}$. Therefore, both LiaFSR$^-$ and Δ*liaR* mutants 9 reached a lower final density than the parent. In contrast, the Δ*liaS* mutant only appeared to enter stationary phase at a lower density when cultured in HTVG resulting in a lower final density than the parent. In TVG and $TVG_{6.0}$, a reduced final density for the Δ*liaS* mutant was also observed; however, it is possible that the mutant did not finish its growth cycle since the density had not yet plateaued. Therefore, it can only be conclusively stated that Δ*liaS* mutant had a lower final density in HTVG. In addition to affecting lag-phase and transitional phase, the generation time of the LiaFSR$^-$, Δ*liaS* and Δ*liaR* mutants was also impacted. In HTVG, the Δ*liaS* mutant exhibited the longest generation time followed by the LiaFSR$^-$ mutant, the parent and the Δ*liaR* mutant (Table 3.3). When cultured in TVG, the Δ*liaS* mutant had with the longest generation time whereas the parent, the LiaFSR$^-$ mutant, and the Δ*liaR* mutant had similar generation time (Table 3.3). In $TVG_{6.0}$, the growth rates of all strains were similar (Table 3.3).

3.3.4 Autolysis and Autolysin Production by the LiaFSR$^-$, Δ*liaS* and Δ*liaR* Mutants

Gardete et al. (2006) demonstrated that wild-type *S. aureus* and *S. aureus* Δ*vraS*

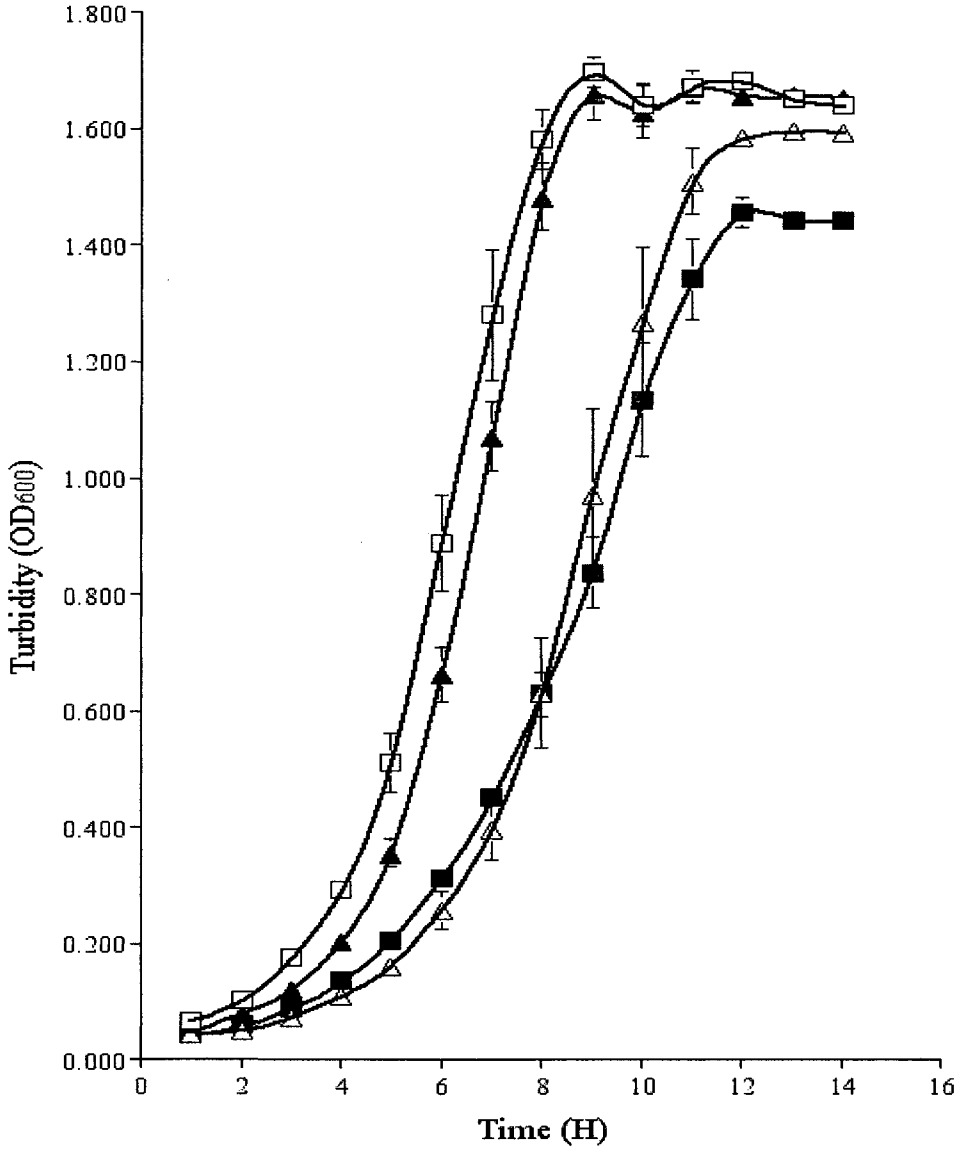

Fig 3.28. Growth kinetics of the parent, the LiaFSR$^-$, Δ*liaS* and Δ*liaR* mutants cultured in HTVG. Growth kinetics of the parent (open squares), and the LiaFSR$^-$ (open triangles), Δ*liaS* (closed squares) and Δ*liaR* (closed triangles) mutants cultured in HTVG. Culture turbidity values are the means of triplicates from two independent experiments. The error bars represent the standard error.

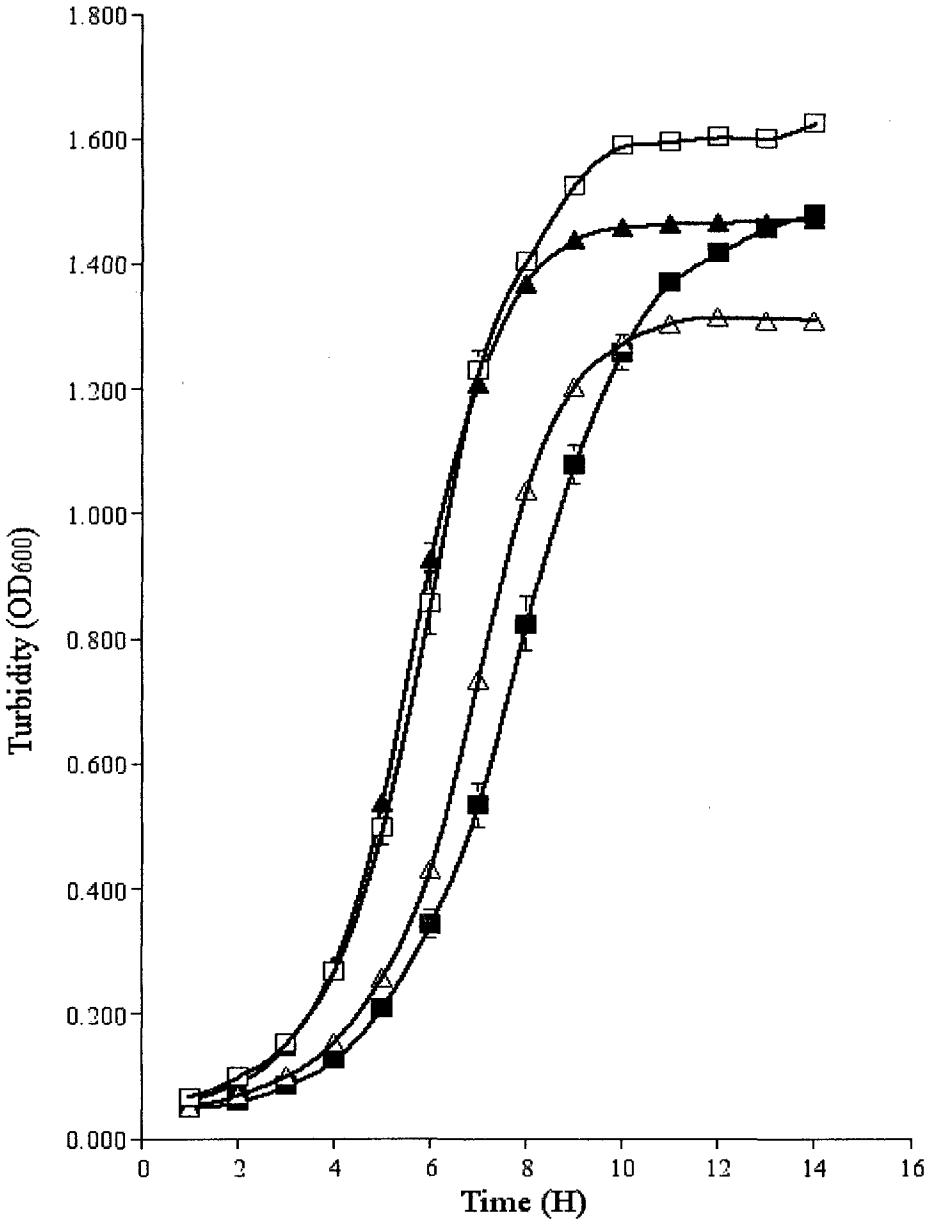

Fig 3.29. Growth kinetics of the parent, the LiaFSR$^-$, Δ*liaS* and Δ*liaR* mutants cultured in TVG. Growth kinetics of the parent (open squares), and the LiaFSR$^-$ (open triangles), Δ*liaS* (closed squares) and Δ*liaR* (closed triangles) mutants cultured in TVG. Culture turbidity values are the means of triplicates from two independent experiments. The error bars represent the standard error.

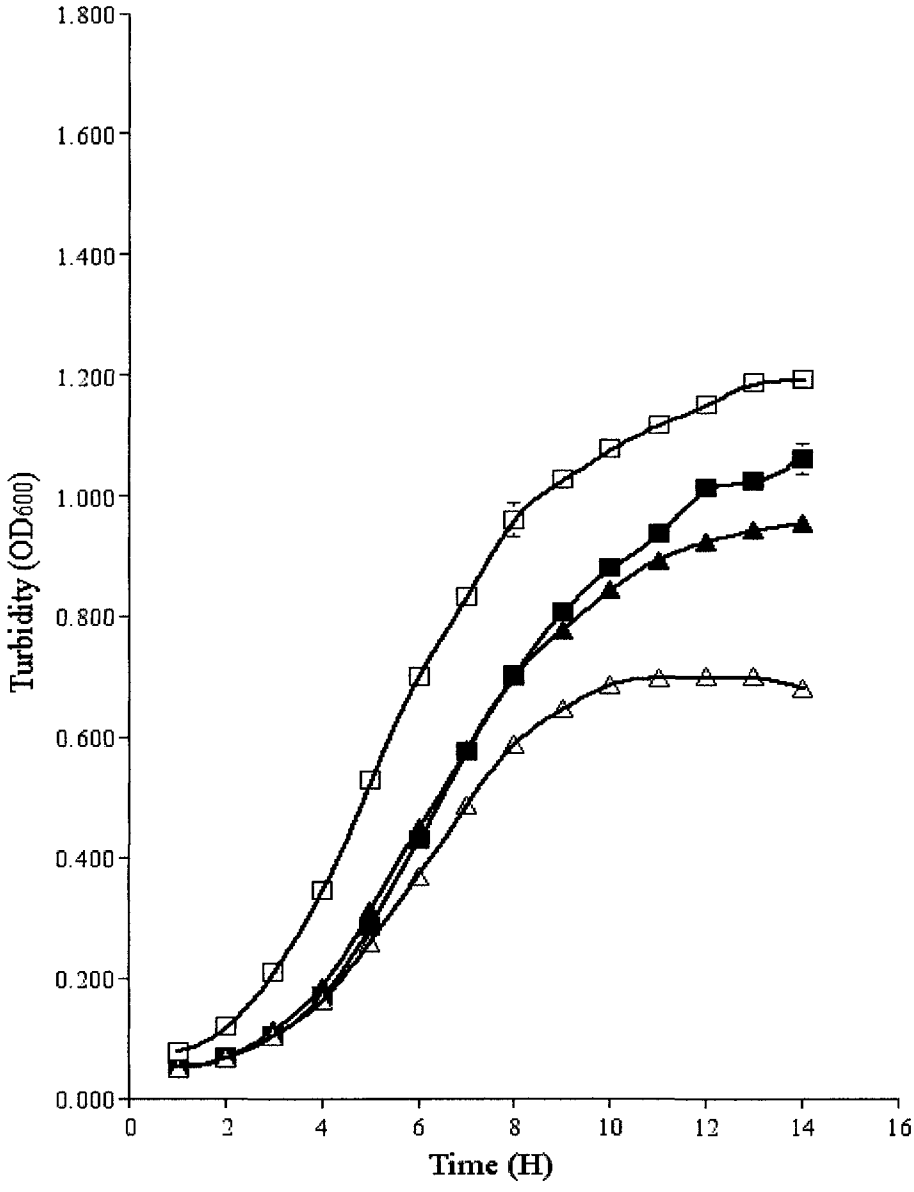

Fig 3.30. Growth kinetics of the parent, the LiaFSR$^-$, Δ*liaS* and Δ*liaR* mutants cultured in TVG$_{6.0}$. Growth kinetics of the parent (open squares), and the LiaFSR$^-$ (open triangles), Δ*liaS* (closed squares) and Δ*liaR* (closed triangles) mutants cultured in TVG$_{6.0}$. Culture turbidity values are the means of triplicates from two independent experiments. The error bars represent the standard error.

Table 3.3. Generation time of the parent, the LiaFSR$^-$, *ΔliaS* and *ΔliaR* mutants cultured in HTVG, TVG and $TVG_{6.0}$

Strains	HTVG	TVG	$TVG_{6.0}$
Parent	1h 50min	1h 31min	2h 00min
LiaFSR$^-$	2h 23min	1h 33min	1h 54min
Δ*liaS*	2h 48min	1h 58min	1h 57min
Δ*liaR*	1h 27min	1h 42min	2h 05min

(liaS homologue*)* mutant had differences in their cell-wall composition. It has also been shown that the *L. lactis* LiaFSR system controls O-acetylation of peptidoglycan which reduces hydrolysis of peptidoglycan by lyzozymes (Velgaetal et al., 2007). In *S. mutans*, biofilm formation is deficient in the absence of autolysin (Brown et al., 2005; Shibata et al. 2005) and defects in biofilm formation is one of the observable phenotypes of the Δ*liaS* or Δ*liaR* mutants (Li et al., 2002a). Therefore, it was hypothesized that deletion of LiaFSR TCS genes in the LiaFSR$^-$, Δ*liaS* and Δ*liaR* mutants would result in cell-wall modification that would reduce or prevent hydrolysis of peptidoglycan by *S. mutans* autolysins and consequently would result in defective autolysis. To test this hypothesis, the autolysis kinetics and autolysin expression of the parent and the *liaFSR* mutant strains were analyzed.

When cultured in HTVG, all three mutants exhibited a decrease in autolysis when compared to the parent (Fig 3.31). In TVG, a decrease autolysis was also observed for the LiaFSR$^-$, and Δ*liaS* mutants but not for the Δ*liaR* mutant (Fig 3.32). No autolysis occured in any of strains when cultured in $TVG_{6.0}$ (Fig 3.33).

To further examine the autolytic activity, zymogram analysis using cell wall from strain UA159 as the substrate was performed. Autolysin expression was highest in bacteria grown in HTVG, moderate in bacteria grown in TVG and barely detectable in bacteria grown in $TVG_{6.0}$ (Fig 3.34A). Additionally, the Δ*liaS* mutant cultured in HTVG also exibited reduced level of autolysin production. In addition to zymogram analysis, autolysin extracts were visualized using colloidal Coomassie blue staining (Fig 3.34B). It was observed that an equivalent amount of protein was loaded for each sample. Visualization of the extract also revealed that a polypeptide at approximately 80 kDa was

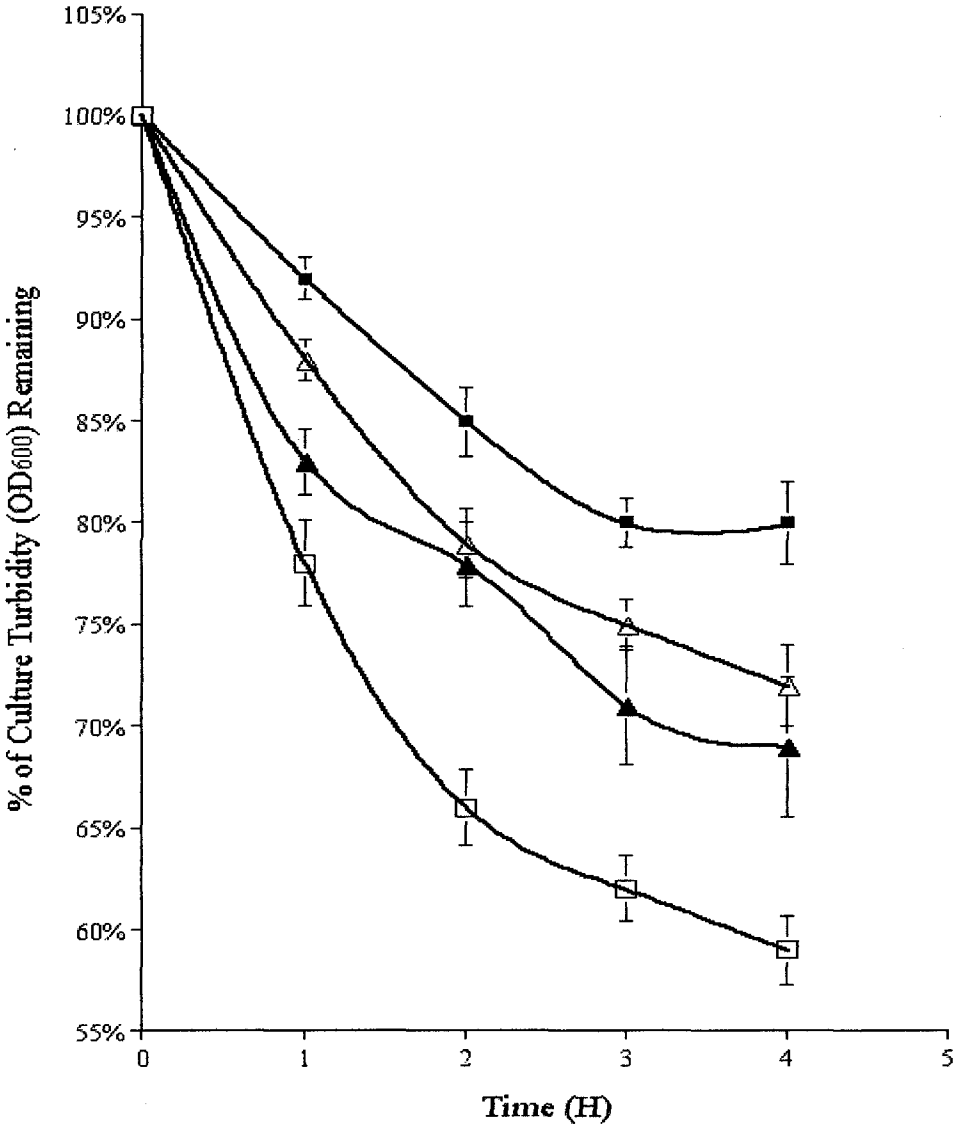

Fig 3.31. Autolysis kinetics of the parent, and the LiaFSR⁻, Δ*liaS* and Δ*liaR* mutants cultured in HTVG. Autolysis kinetics of the parent (open squares), and the LiaFSR⁻ (open triangles), Δ*liaS* (closed squares) and Δ*liaR* (closed triangles) mutants cultured in HTVG. Culture density remaining was calculated as a percentage of OD_{600} at t=X, where X is desired time point, over OD_{600} at t=0h. The results are the means of triplicates from two independent experiments. The error bars represent the standard error.

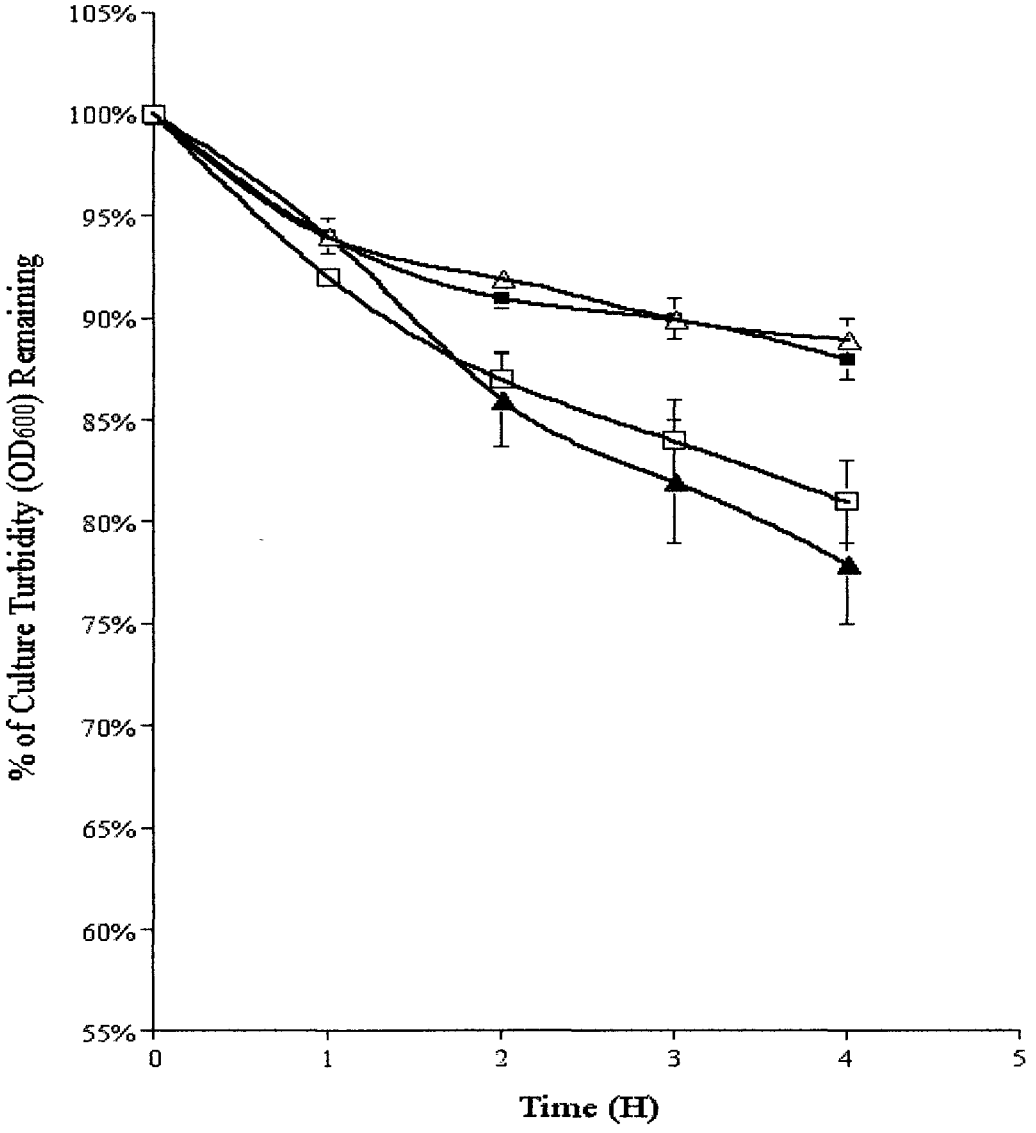

Fig 3.32. Autolysis kinetics of the parent, and the LiaFSR⁻, Δ*liaS* and Δ*liaR* mutants cultured in TVG. Autolysis kinetics of the parent (open squares), and the LiaFSR⁻ (open triangles), Δ*liaS* (closed squares) and Δ*liaR* (closed triangles) mutants cultured in TVG. Culture density remaining was calculated as a percentage of OD_{600} at t=X, where X is desired time point, over OD_{600} at t=0h. The results are the means of triplicates from two independent experiments. The error bars represent the standard error.

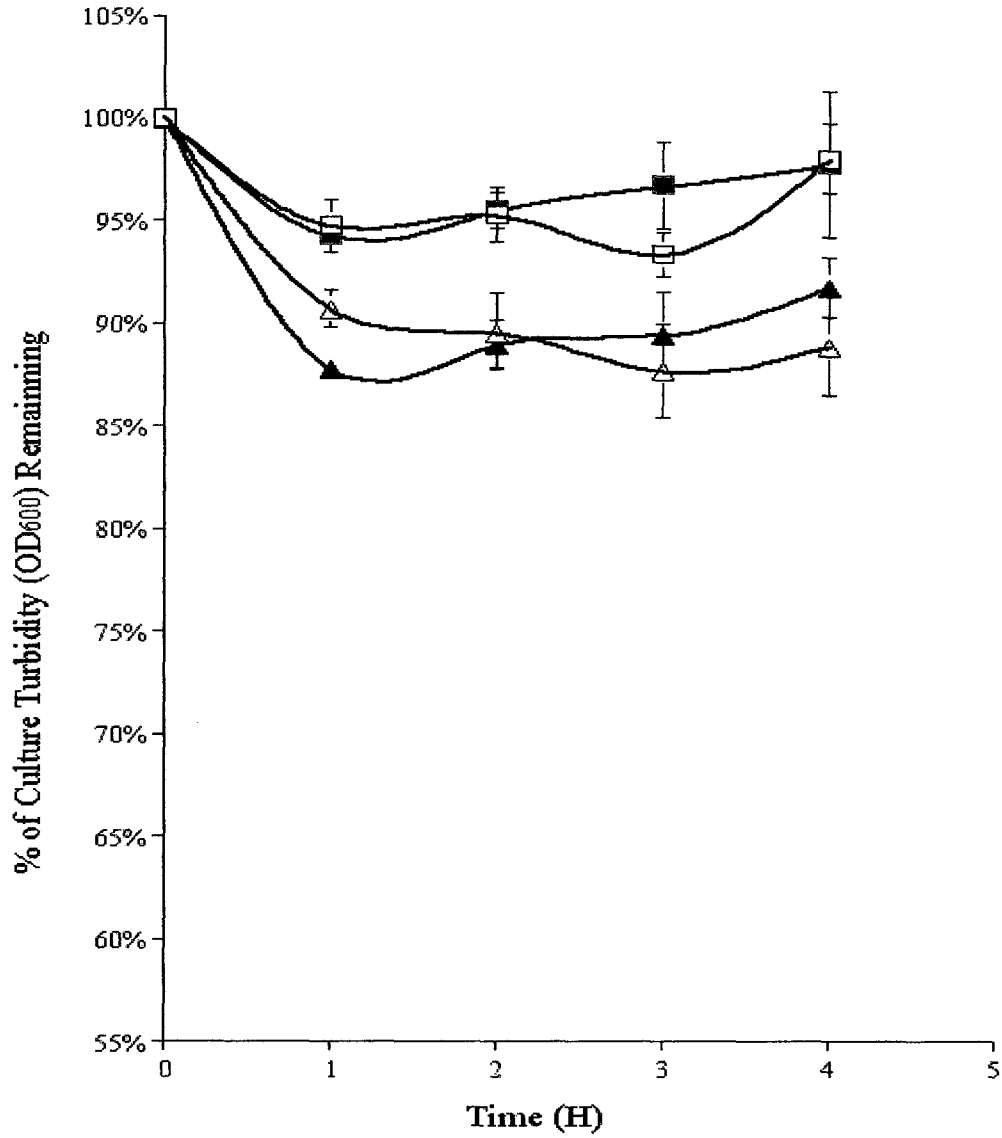

Fig 3.33. Autolysis kinetics of the parent, and the LiaFSR$^-$, Δ*liaS* and Δ*liaR* mutants cultured in $TVG_{6.0}$. Autolysis kinetics of the parent (open squares), and the LiaFSR$^-$ (open triangles), Δ*liaS* (closed squares) and Δ*liaR* (closed triangles) mutants cultured in $TVG_{6.0}$. Culture density remaining was calculated as a percentage of OD_{600} at t=X, where X is desired time point, over OD_{600} at t=0h. The results are the means of triplicates from two independent experiments. The error bars represent the standard error.

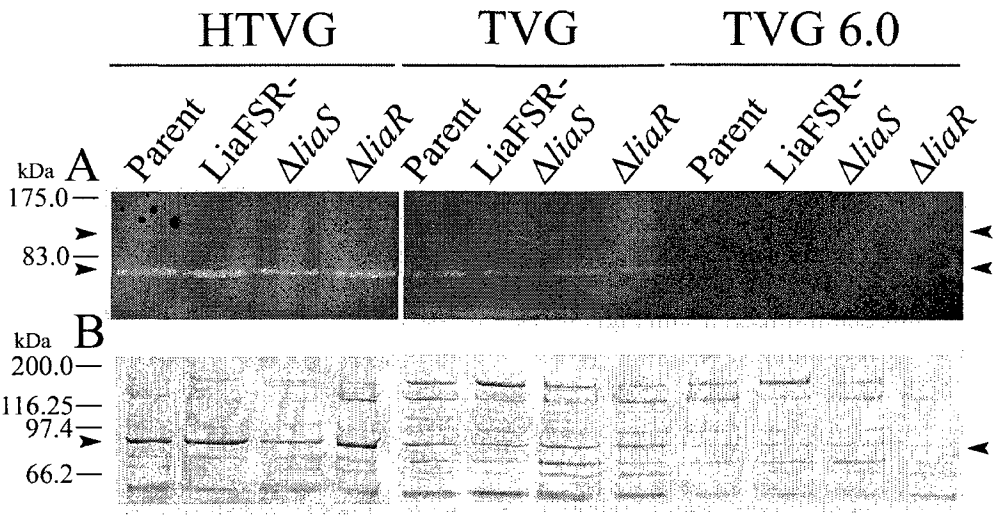

Fig 3.34. Zymogram analysis of the parent, and the LiaFSR⁻, Δ*liaS* and Δ*liaR* mutants cultured in HTVG, TVG, and $TVG_{6.0}$. Crude autolysin extracts of the parent, and the LiaFSR⁻, Δ*liaS* and Δ*liaR* mutants cultured in HTVG, TVG and $TVG_{6.0}$ were separated on a 10% SDS-polyacrylamide gel with (A) or without (B) cell wall of *S. mutans* strain UA159. Gels containing no cell wall were stained by colloidal Coomassie blue and those containing cell wall were stained with methylene blue. The Coomassie-stained gels were used to ensure equal loading between samples. The numbers refer to the sizes (kDa) and positions of protein standards. The arrows indicate the major (~80 kDa) or minor (~107 kDa) isoforms of the autolysin.

differentially expressed. The 80 kDa polypeptide corresponded to the size of a previously characterized autolysin (Ahn and Burne, 2006; Yoshimura et al., 2006). The 80 kDa polypeptide from the parent and the Δ*liaR* mutant sample was excised from the gel and analyzed by liquid chromatography followed by tandem mass spectrometry (LC-MS/MS). The analysis confirmed that the differentially expressed peptide was the major autolysin (Fig 3.35).

In summary, it was observed that autolysin expression strongly correlated with the rate of autolysis. For example, cells with the highest autolysin expression also displayed the highest rate of autolysis. However, the differences in autolysis between strains did not always correlate with the level of autolysin; the Δ*liaS* mutant cultured in HTVG appears to be the exception. The Δ*liaS* mutant produced less autolysin.

3.3.5 Biofilm Formation by the LiaFSR$^-$, Δ*liaS* and Δ*liaR* Mutants

The ability of the LiaFSR$^-$, Δ*liaS* and Δ*liaR* mutants to form biofilm was analyzed using two different approaches: SEM and a microwell plate assay. For SEM, the parent and mutant strains were grown in 70% FMC and biofilm were examined after 16 h and 24 h of growth. After 16 h, all three mutants clearly showed a deficiency in structured biofilm formation (Fig 3.36, 3.37, 3.38 and 3.39). When compared to Δ*liaS* and Δ*liaR* mutants, the LiaFSR$^-$ mutant appeared to have a more severe defect in forming biofilm. All three mutants were able to attach and form some, but very limited, tertiary structure. Furthermore, the biofilm formed by the mutants lacked extensive tertiary structure such as "water channels" (Fig 3.36, 3.37, 3.38 and 3.39). After 24h, the biofilm formed by the parent lost some biomass and tertiary structure when compared to the 16-h biofilm. In

A
1 MKSKTYLMIP LALTLFMAAN KISADEQNQS LSASEVISSD ATSVSELPAT
51 TAQISQEVRN NGQDSTIQLQ QTQEQSDPIT STSETTVSSM KAATNGSPAK
101 ANETETVPSQ ASTASSVQTP DQILTVPSVK AETTSTADQL QSTSSAPLDQ
151 QTDAKRLSNK MTPASSVQAR SSLTQDKQVQ AQEVTSAVVE EKGIKLQYNG
201 QIARNTKIQF AVWSARNDQD DLQWYTANNM GAAYAEFKNH REYGTYYVHT
251 YANQNGKMIG LNATTLTIAQ PQVQTNIQRK SATNFELTVS NVPNTISGIM
301 VPVWSDQNGQ DDIKWYNARK ADDGSYKVLI DTKNHKNDLG HYEAHIYGYS
351 TVTQSQIGLA VSSGFDRNDT RPNARISVAN YDQNKTTFDV VVEGSSDTKT
401 VSAVNIAVWS EDKGQDDLKW YSPKIVDNKA TVTINIANHS NTSDKYNVHV
451 YTDYTDGTHS GTILGAYQIN KPLEKNTVSA DLTSDGIALK LDSNTVTDYT
501 KVRFAVWSDQ NGQDDLKWYS ANSDGTATAA YSNHSGYGLY HIHTYIIKDG
551 KMVGLNGKTI TINQPSAKVD IAKESDALYK VTVSNLPAYI SSVVIPVWTD
601 KNNQDDIQWI PATKQGDGTY AAQIQLADHN GETGHYNVHV YGQSKFDNKA
651 VGLAATDGFN VAETRNAVIA ASNYNASAGT IDMIVKQEAG GKAIKEVRIA
701 AWSEADQSNL HWYVSSTIID GKVTVTINEK NHQYIKGNYN IHVYVDYTDG
751 TSSGTNIGNY SLNADKPAVA LPSYFIDISS HNGIISVAEF NSLKQQGIQG
801 VVVKLTEGTS YINPYASSQI ANARAAGIKV SAYHYAHYTS AAGAQEEARY
851 FANAARSFGL EASTVMVNDM EESSMVNNIN NNVQAWQDEM RRQGYSNLIH
901 YTMASWLDIR GGQVDTARFG INNFWVAHYA KGYTYMTQEE AKSLNYYANA
951 AAWQYTSVSS KLSHALDENI DYTGRFTQQ

B
1 MKSKTYLMIP LALTLFMAAN KISADEQNQS LSASEVISSD ATSVSELPAT
51 TAQISQEVRN NGQDSTIQLQ QTQEQSDPIT STSETTVSSM KAATNGSPAK
101 ANETETVPSQ ASTASSVQTP DQILTVPSVK AETTSTADQL QSTSSAPLDQ
151 QTDAKRLSNK MTPASSVQAR SSLTQDKQVQ AQEVTSAVVE EKGIKLQYNG
201 QIARNTKIQF AVWSARNDQD DLQWYTANNM GAAYAEFKNH REYGTYYVHT
251 YANQNGKMIG LNATTLTIAQ PQVQTNIQRK SATNFELTVS NVPNTISGIM
301 VPVWSDQNGQ DDIKWYNARK ADDGSYKVLI DTKNHKNDLG HYEAHIYGYS
351 TVTQSQIGLA VSSGFDRNDT RPNARISVAN YDQNKTTFDV VVEGSSDTKT
401 VSAVNIAVWS EDKGQDDLKW YSPKIVDNKA TVTINIANHS NTSDKYNVHV
451 YTDYTDGTHS GTILGAYQIN KPLEKNTVSA DLTSDGIALK LDSNTVTDYT
501 KVRFAVWSDQ NGQDDLKWYS ANSDGTATAA YSNHSGYGLY HIHTYIIKDG
551 KMVGLNGKTI TINQPSAKVD IAKESDALYK VTVSNLPAYI SSVVIPVWTD
601 KNNQDDIQWI PATKQGDGTY AAQIQLADHN GETGHYNVHV YGQSKFDNKA
651 VGLAATDGFN VAETRNAVIA ASNYNASAGT IDMIVKQEAG GKAIKEVRIA
701 AWSEADQSNL HWYVSSTIID GKVTVTINEK NHQYIKGNYN IHVYVDYTDG
751 TSSGTNIGNY SLNADKPAVA LPSYFIDISS HNGIISVAEF NSLKQQGIQG
801 VVVKLTEGTS YINPYASSQI ANARAAGIKV SAYHYAHYTS AAGAQEEARY
851 FANAARSFGL EASTVMVNDM EESSMVNNIN NNVQAWQDEM RRQGYSNLIH
901 YTMASWLDIR GGQVDTARFG INNFWVAHYA KGYTYMTQEE AKSLNYYANA
951 AAWQYTSVSS KLSHALDENI DYTGRFTQQ

Fig 3.35. Identification of the 80 kDa polypeptide by mass spectrometry as the AtlA autolysin. The 80 kDa polypeptides isolated from the parent (A) and the Δ*lia*R mutant (B) samples. The matched peptides generated by trypsin digest and identified by LC-MS/MS are underlined. The Mascot scores are 1472 and 1412 for the parent (A) and the Δ*liaR* mutant (B) samples, respectively.

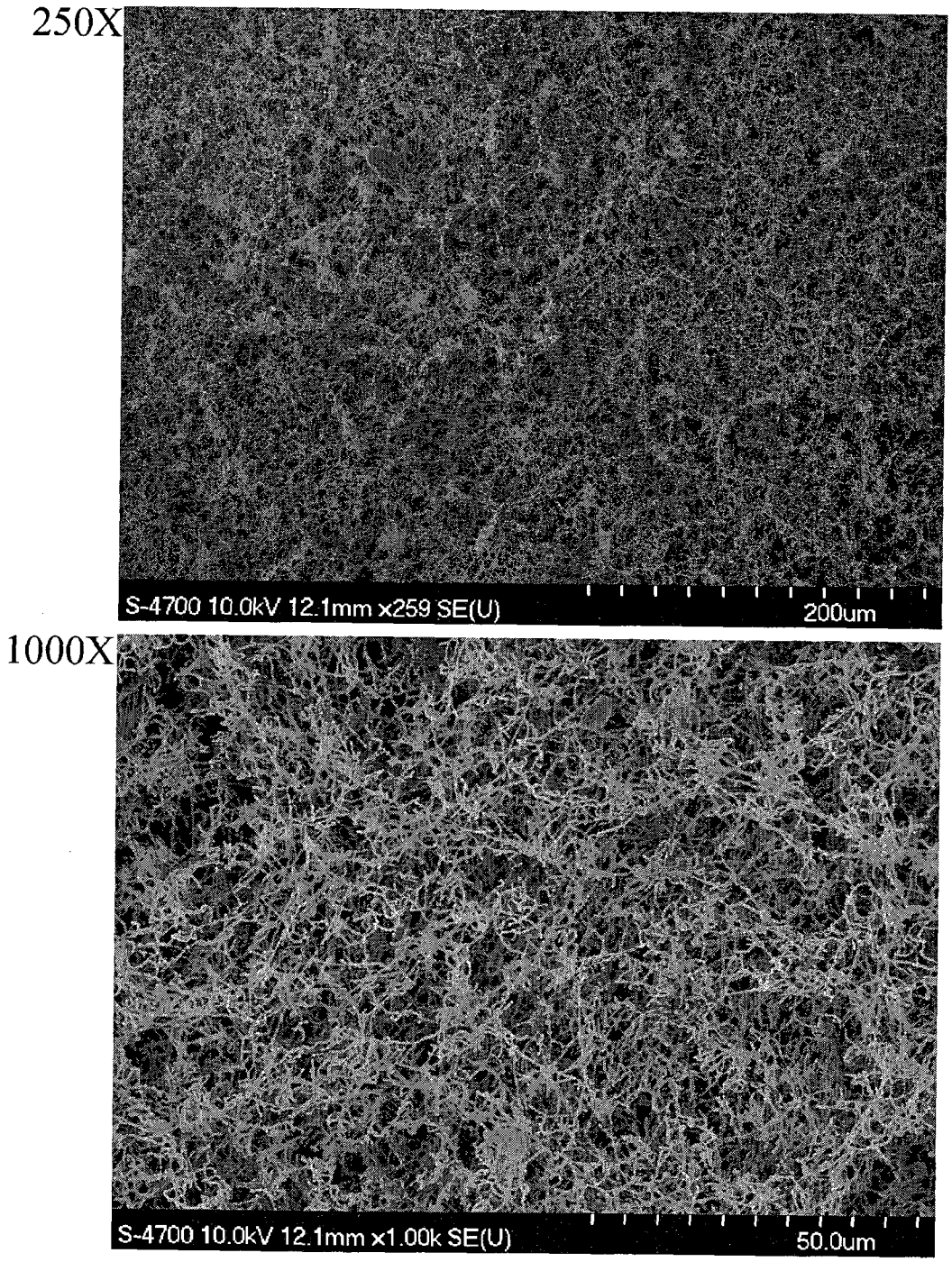

Fig 3.36. SEM of a 16-hour biofilm formed by the parent cultured in 70% FMC.

Representative fields of view at 250X and 1000X.

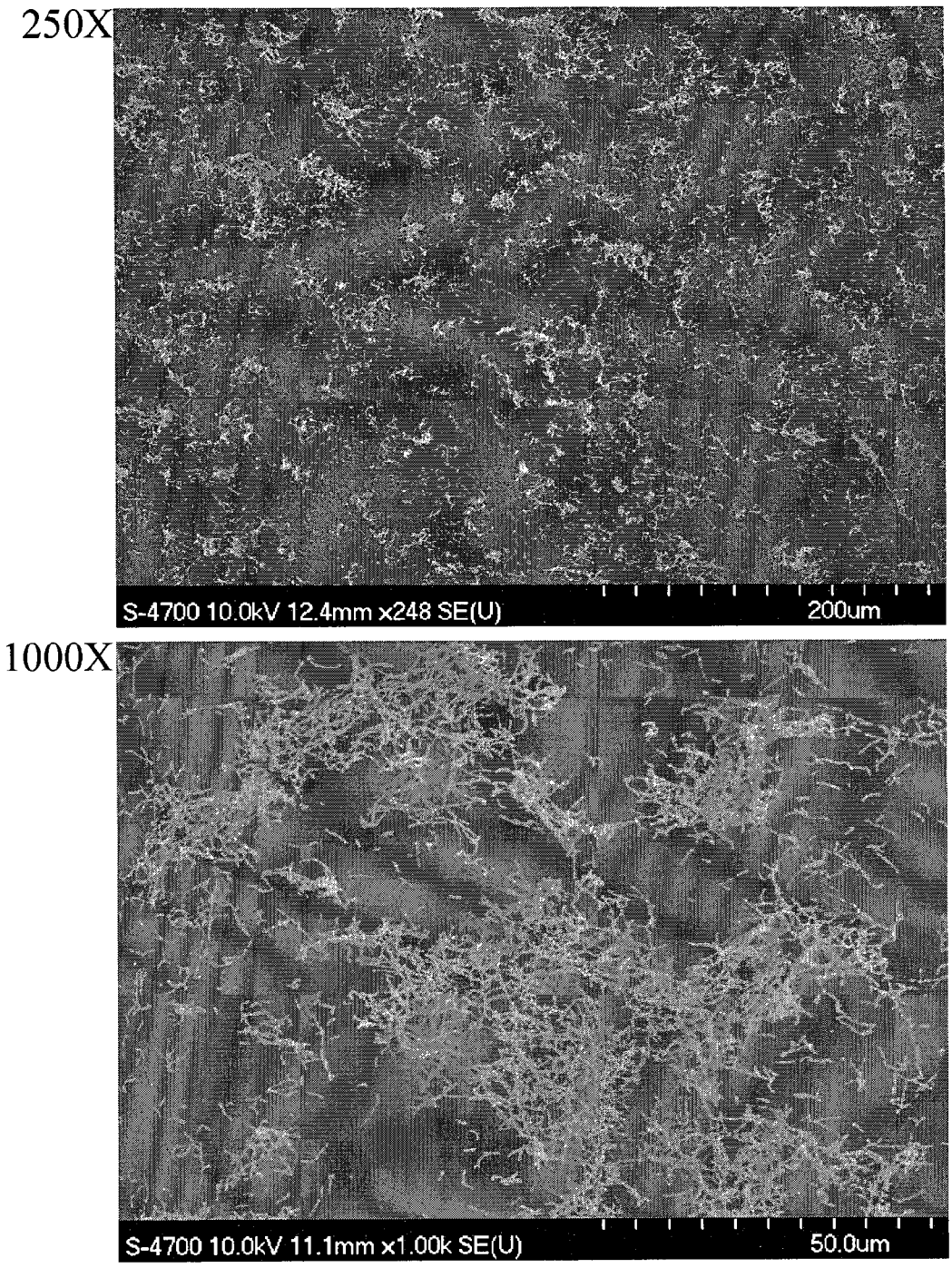

Fig 3.37. SEM of a 16-hour biofilm formed by the LiaFSR$^-$ mutant cultured in 70% FMC. Representative fields of view at 250X and 1000X.

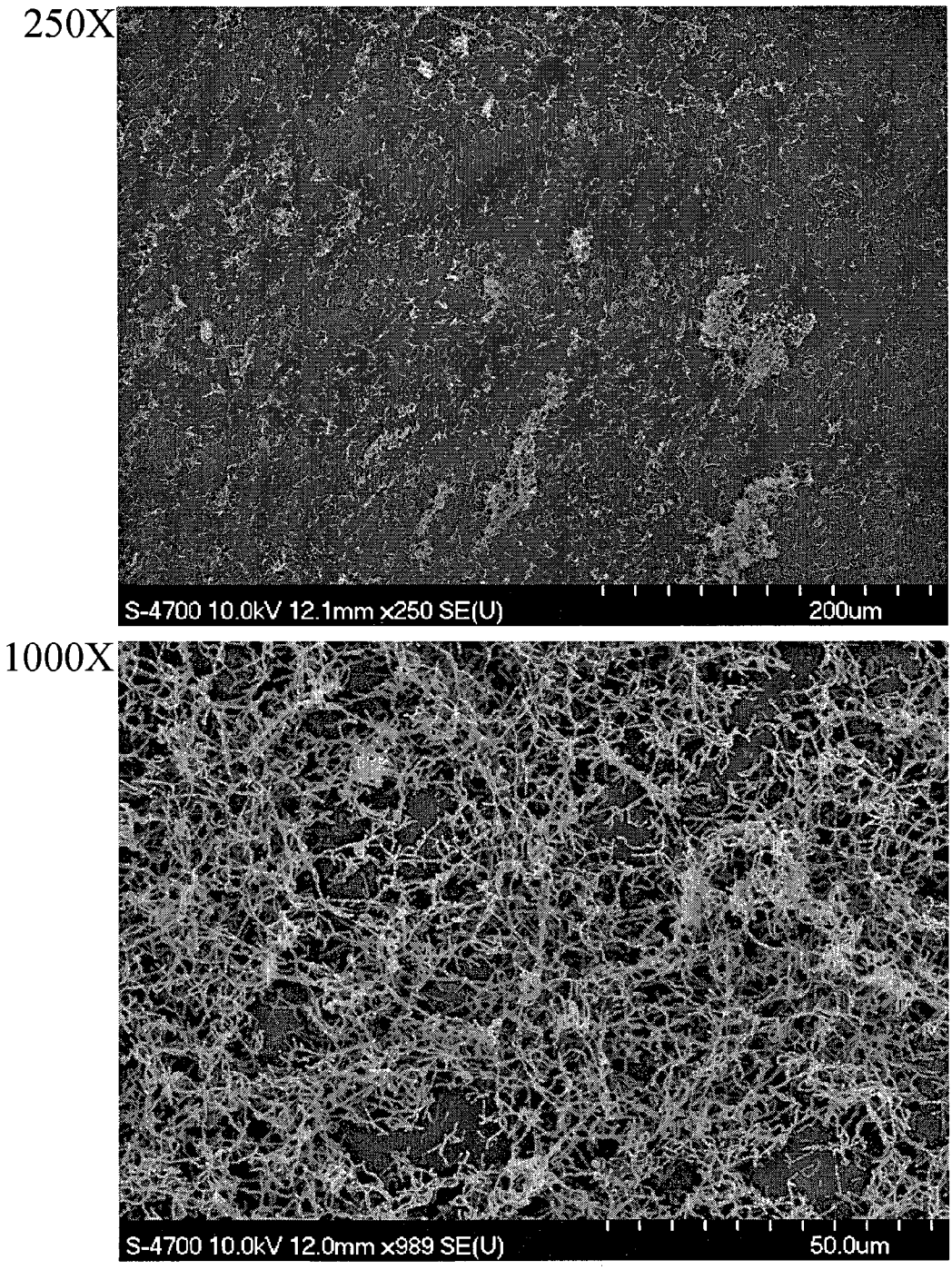

Fig 3.38. SEM of a 16-hour biofilm formed by the Δ*iaS* mutant cultured in 70% FMC. Representative fields of view at 250X and 1000X.

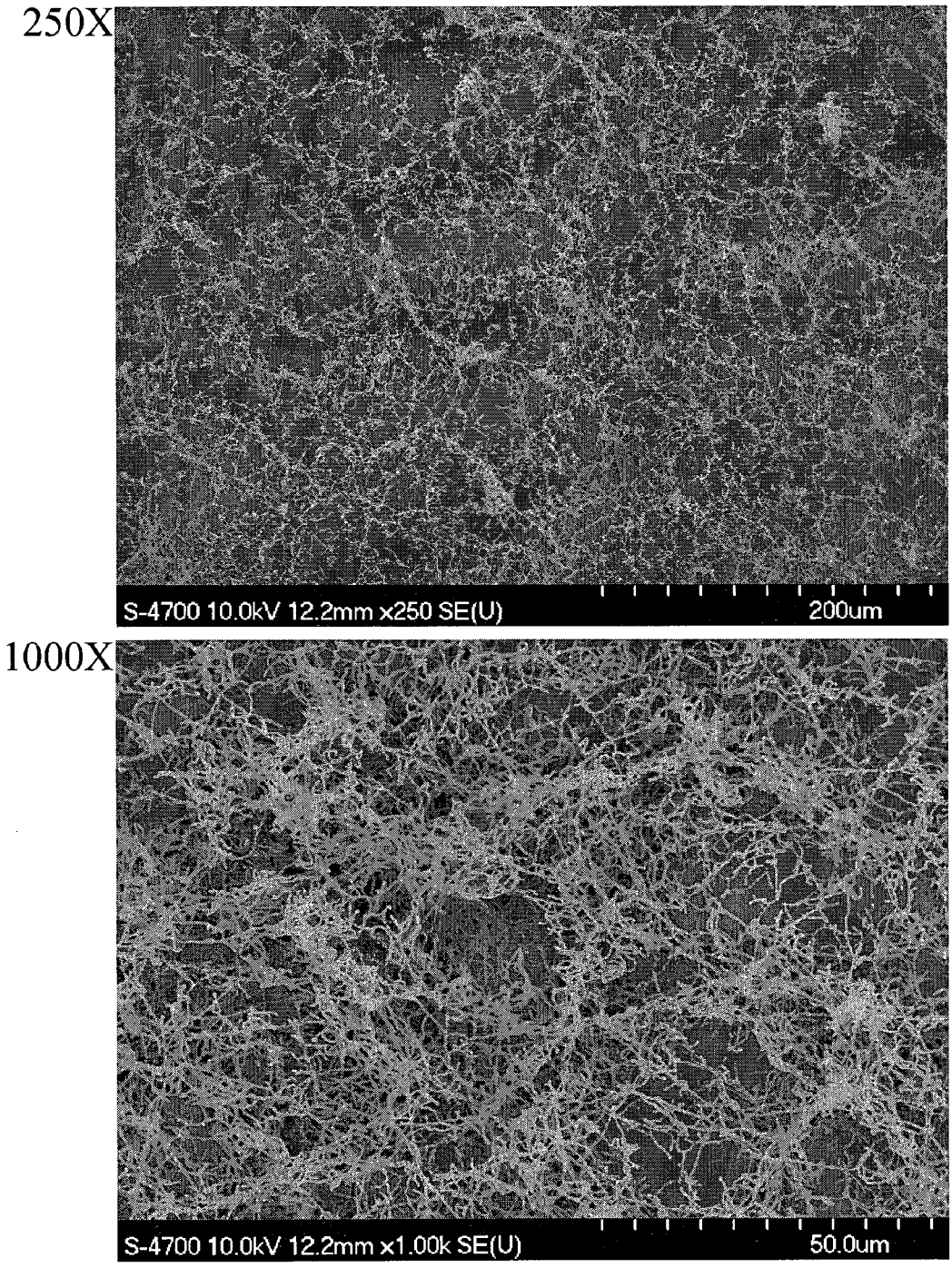

Fig 3.39. SEM of a 16-hour biofilm formed by the Δ*liaR* mutant cultured in 70% FMC. Representative fields of view at 250X and 1000X.

contrast, the biofilms formed by any of the three mutants did not contain any tertiary structures and appeared as clusters of bacterial cells partially covering the surface (Fig 3.40, 3.41, 3.42 and 3.43). Additionally, the biofilms formed by the mutants also contained less cells at 24 h than 16 h. The results clearly show that, like the Δ*liaS* and Δ*lia*R mutans, the LiaFSR$^-$ mutant has limited ability to form biofilm. Furthermore, aging of the biofilm was characterized and demonstrated that no mutants were able to maintain their limited biofilm as it aged.

In parallel, the ability of the mutants strains to form biofilm under different growth conditions was assessed using a microwell-plate. Although the microwell-plate assay has been previously used to assess biofilm formation, the results of the assay did not correlate with the results from the SEM analysis. In a microwell plate assay, the LiaFSR$^-$, Δ*liaS* and Δ*lia*R mutans did not show any impairment in biomass accumulation when grown in 70% FMC as compared to the parent (Fig 3.44). The SEM data clearly showed a reduced ability to properly form a well-structured biofilm. In DBM, the LiaFSR- consistently accumulated less biomass than the Δ*liaS* mutant, althought there was no statistical difference in biomass accumulation between the parent strain and the mutant strains. The results (Fig 3.44) clearly demonstrate that the LiaFSR$^-$, Δ*liaS* and Δ*lia*R mutans did not fully lose their ability to attach and accumulate biomass. Additionally, the rates of detachment of the parent and all three mutants, as determined by using the Calgary Biofilm Device, were similar (Fig 3.45).

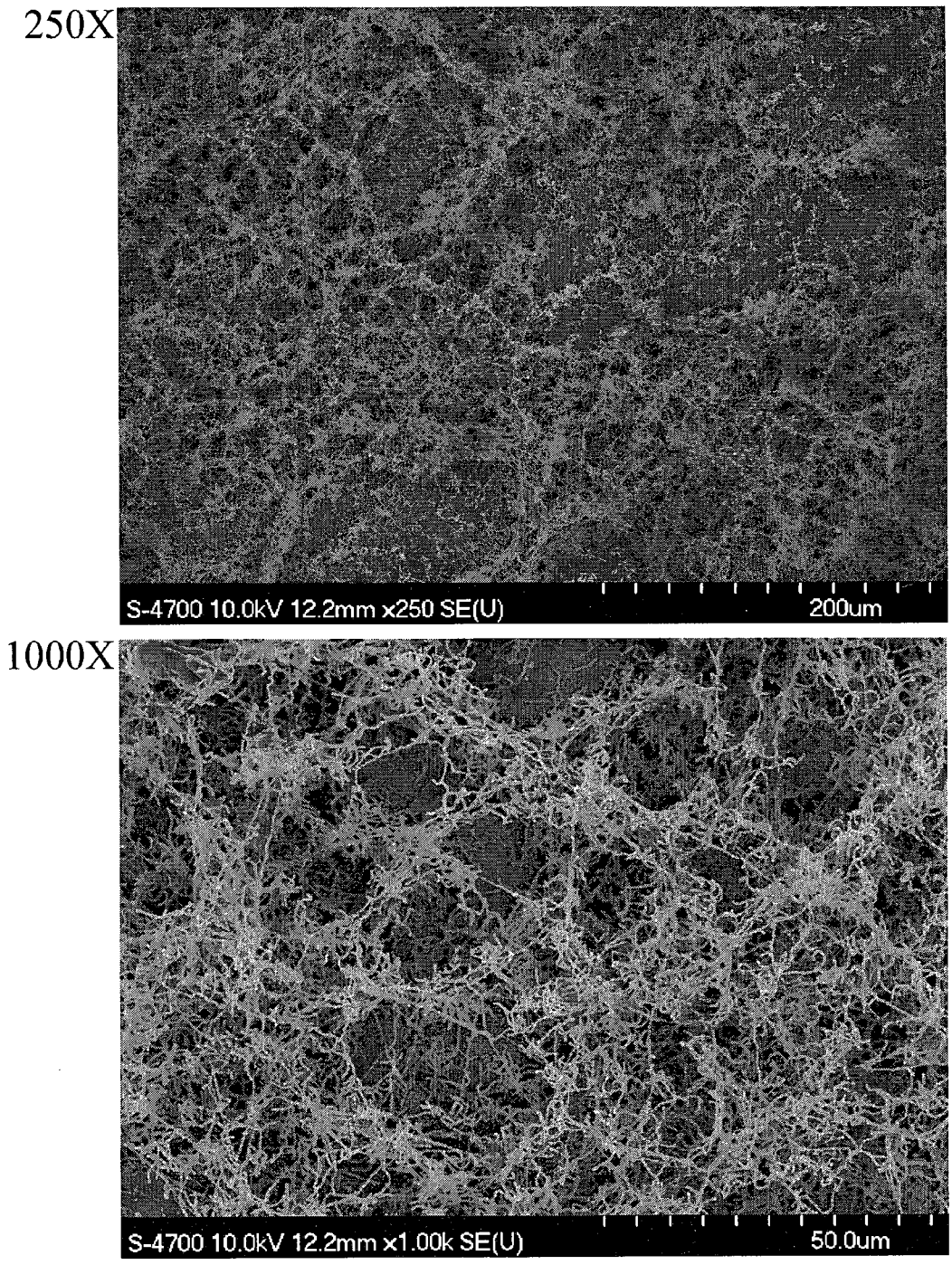

Fig 3.40. SEM of a 24-hour biofilm formed by the parent cultured in 70% FMC.

Representative fields of view at 250X and 1000X.

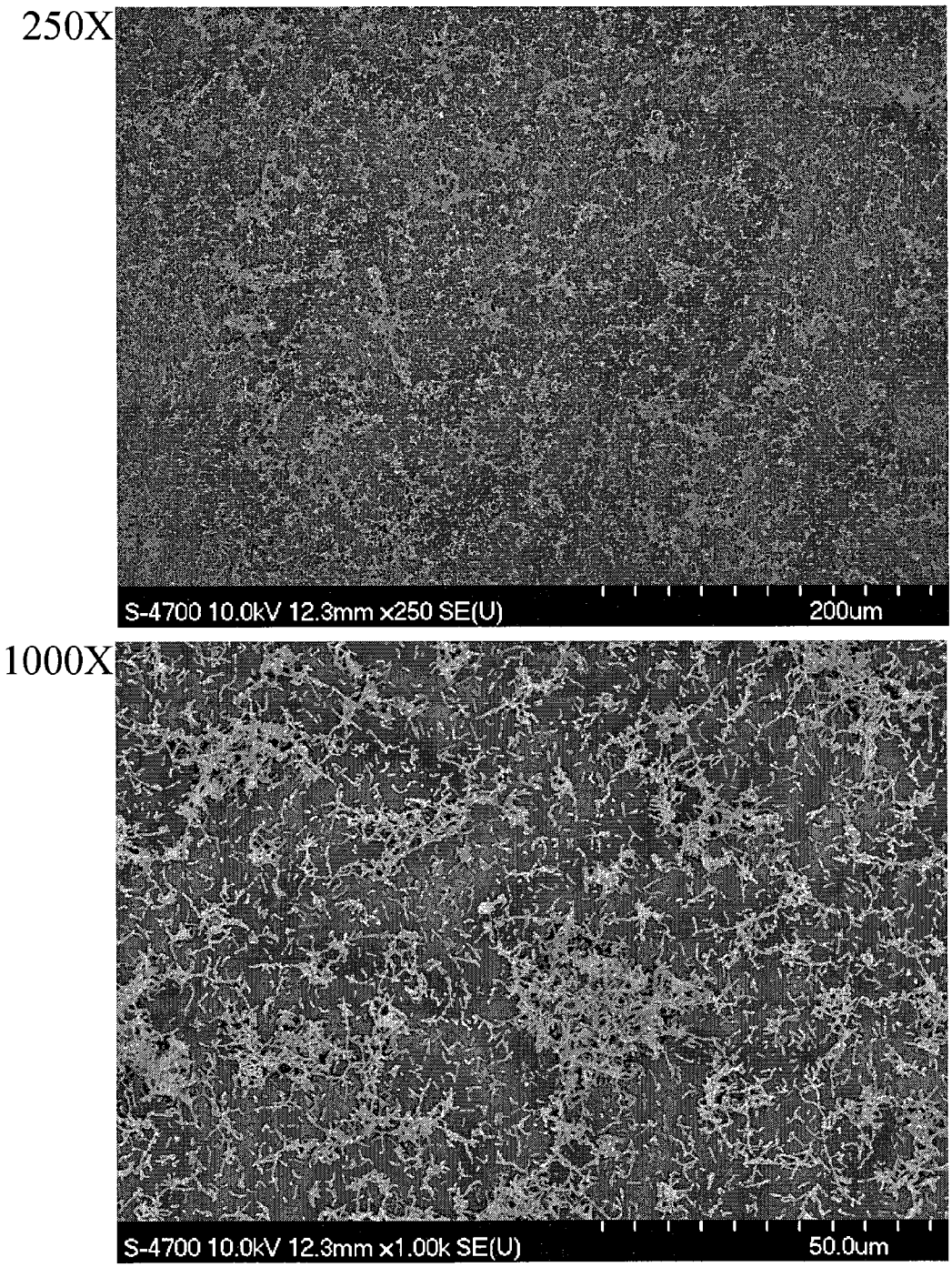

Fig 3.41. SEM of 24-hour biofilm formed by the LiaFSR$^-$ mutant cultured in 70% FMC. Representative fields of view at 250X and 1000X.

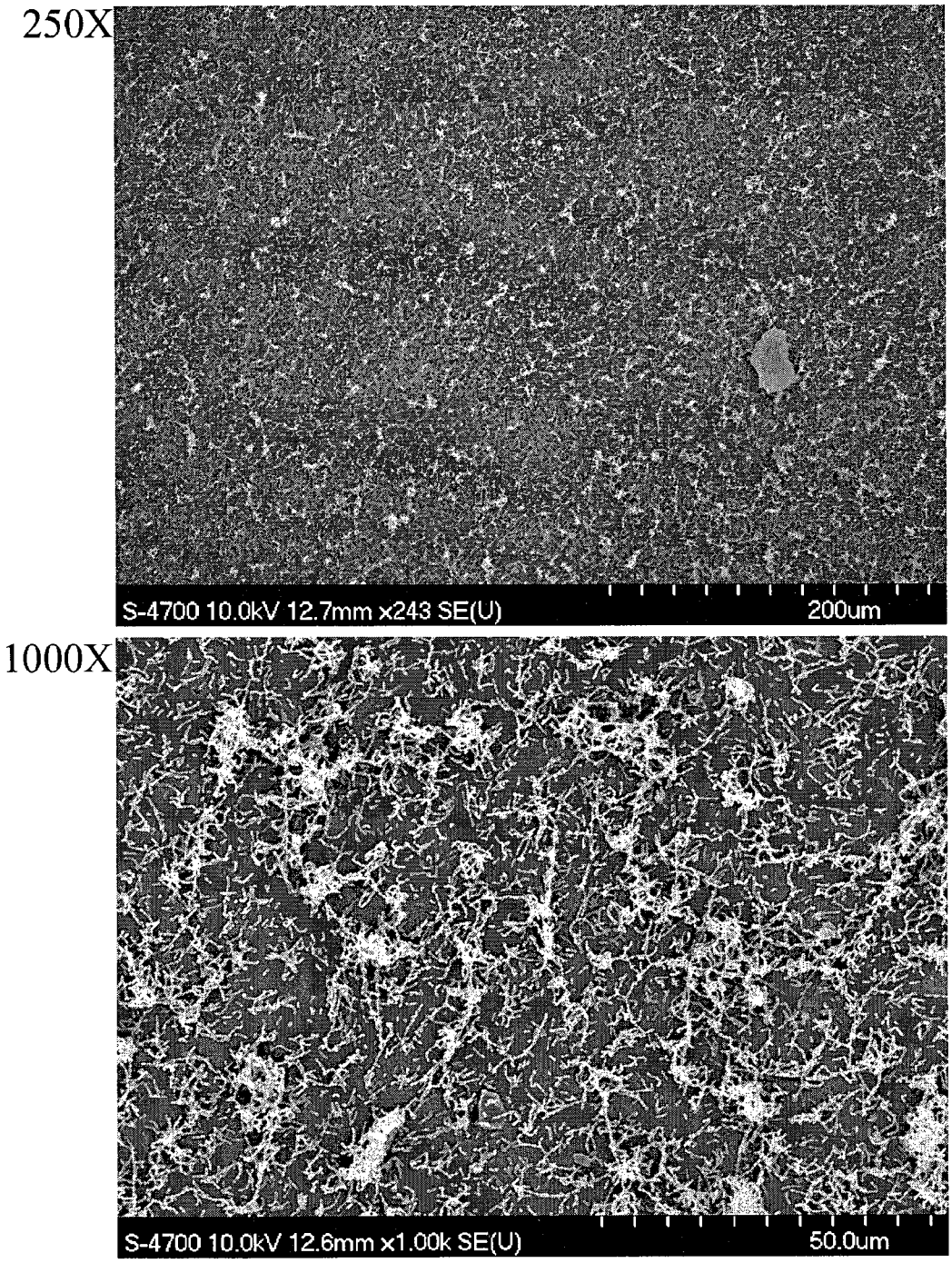

Fig 3.42. SEM of a 24-hour biofilm formed by the Δ*iaS* mutant cultured in 70% FMC. Representative fields of view at 250X and 1000X.

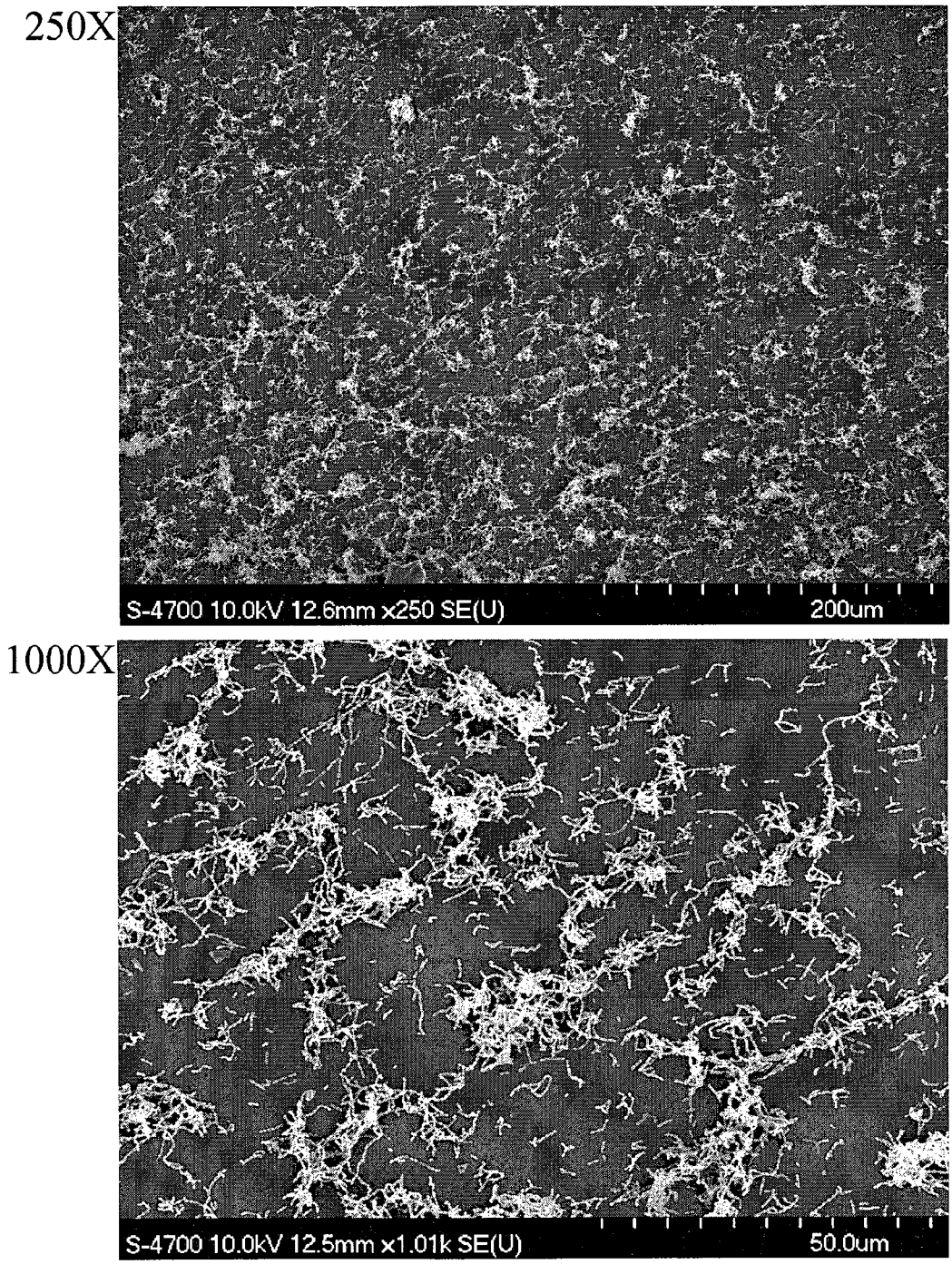

Fig 3.43. SEM of a 24-hour biofilm formed by the Δ*liaR* mutant cultured in 70% FMC. Representative fields of view at 250X and 1000X.

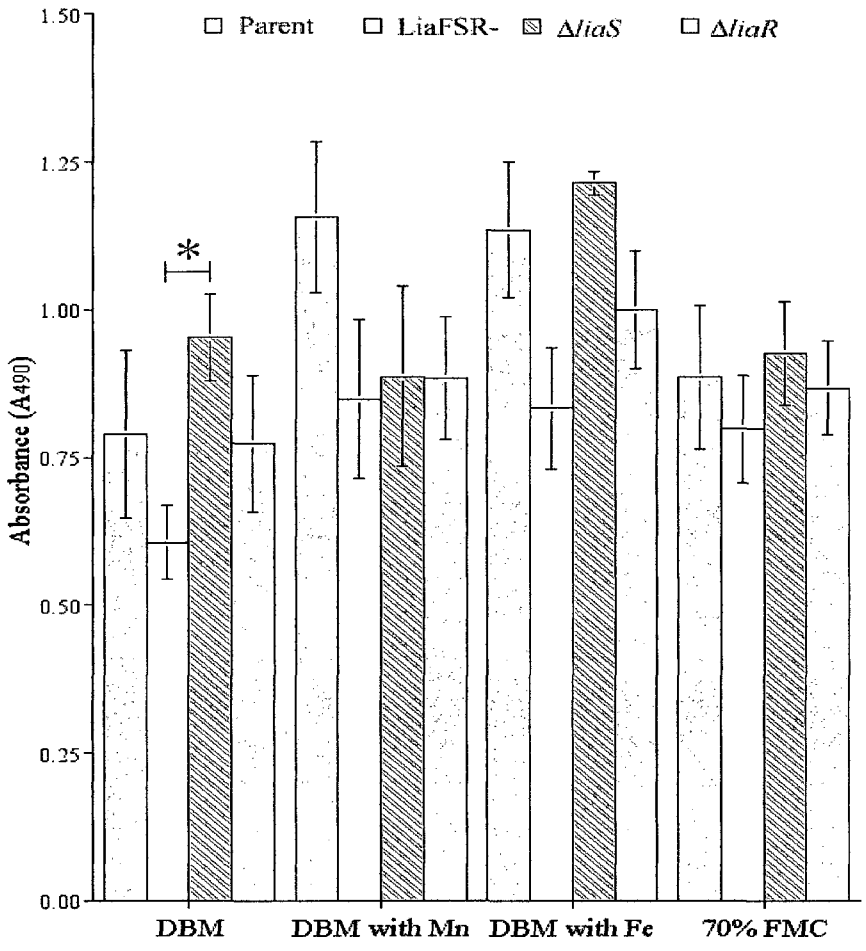

Fig 3.44. Biomass accumulation assay of the parent, and the LiaFSR⁻, Δ*liaS* and Δ*liaR* mutants cultured in DBM, DBM with different metal ions and 70% FMC for 16 hours. *S. mutans* strains were cultured in DBM, DBM supplemented with 25 μM of manganese sulfate (DBM with Mn), DBM supplemented with 5 μM of ferrous sulfate (DBM with Fe) or 70% FMC. The graph represents the level of stain absorbed and released by the biofilms. The results are the average of six replicates and representative of three independent experiments. The error bars represent the standard deviation. * indicates $P<0.05$. Stastical significance is only shown for samples that were statistically significant in all three experiments

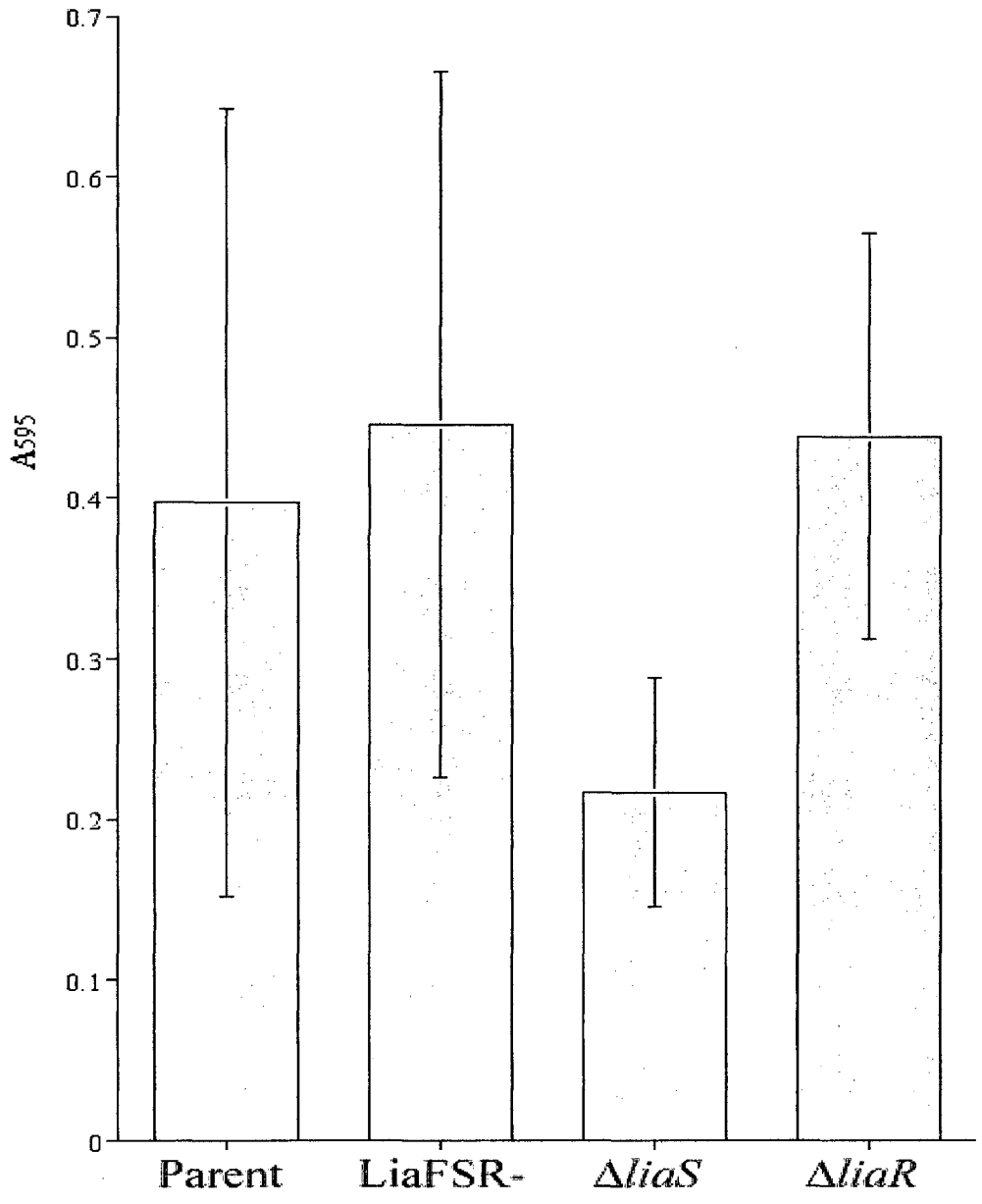

Fig 3.45. Biofilm detachment assay of the parent and the LiaFSR$^-$, Δ*liaS* and Δ*liaR* mutants cultured in 70% FMC. *S. mutans* strains were cultured in 70% FMC on a Calgary Biofilm Device. The graph represents the level of stain absorbed and released by the biofilm formed by the detached cells. The results are the average of sixteen replicates and representative of three independent experiments. The error bars represent the standard deviation.

3.3.6 Acid Stress and Adaptation

The mutants were initially examined for acid sensitivity, a well-characterized phenotype of the Δ*liaS* and Δ*liaR* mutants of strain NG8 (Li et al., 2002). At pH 5.0, both the LiaFSR$^-$, and Δ*liaS* mutants showed greatly diminished growth when compared to the parent. The Δ*liaR* mutant grew as well as the parent (Fig 3.46). The three mutants and parent showed no difference in growth at pH 7.0. These results indicate that all three mutants of strain UA159 behaved identically to those of strain NG8 (Li et al., 2002).

The LiaFSR$^-$, Δ*liaS* and Δ*liaR* mutants were further examined for their ability to adapt to an acidic environment. Non-adapted cells of the LiaFSR$^-$, Δ*liaS* and Δ*liaR* mutants were more sensitive to acid shock than the parent (Fig 3.47). These results are consistent with those reported by Li et al. (2002). Furthermore, passaging the cells for a minimum of 2 h at pH 5.5 improved the survival of all strains equally (Fig 3.47). These results suggest that the LiaFSR$^-$, Δ*liaS* and Δ*liaR* mutants were not deficient in the ability to adapt to an acidic condition.

3.3.7 Antibiotic Sensitivity of the LiaFSR$^-$, Δ*liaS* and Δ*liaR* Mutants

Since the LiaFSR system is thought to respond to antibiotics that disturb lipid II cycles and has been associated with resistance to some antibiotics (Boyle-Vavra et al., 2006; Gardete et al., 2006; Goldstein et al., 2007), the sensitivity to vancomycin, penicillin G and polymyxin B of the mutants relative to the parent strain was tested. None of the mutants had increased sensitivity to penicillin G and vancomycin; however, a noticeable increase in sensitivity to polymyxin B was observed for all three mutants when cultured in all media tested (Table 3.4).

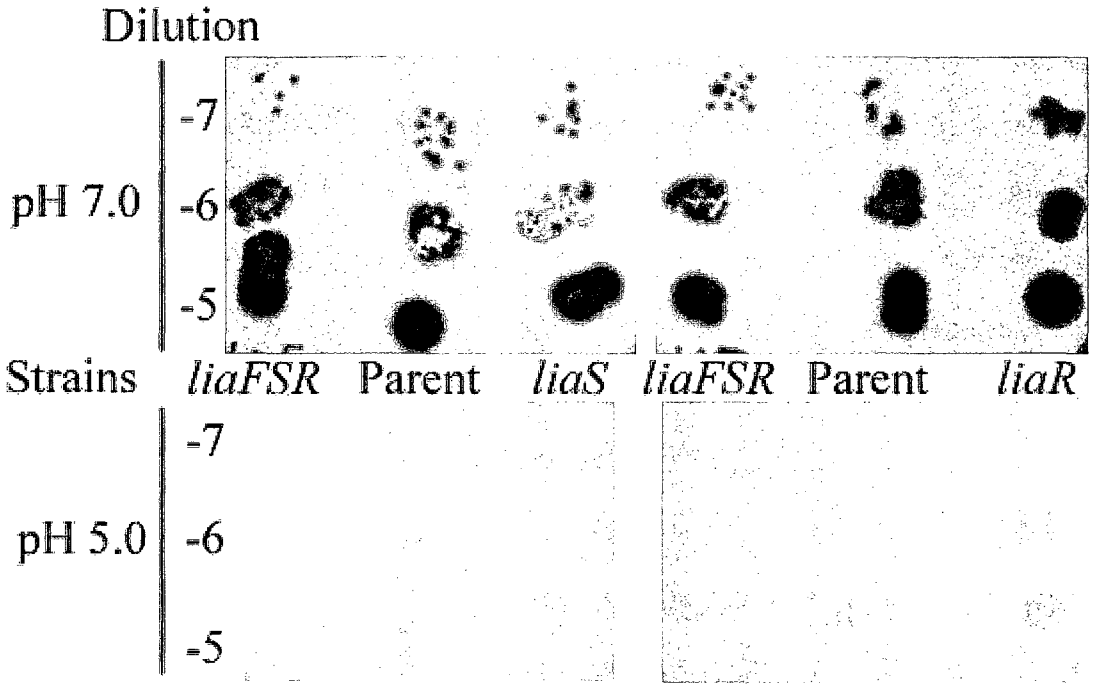

Fig 3.46. Effect of pH on the growth of the LiaFSR$^-$, Δ*liaS* and Δ*liaR* mutants. The parent, and the LiaFSR$^-$ (*liaFSR*), Δ*liaS* (*liaS*) and Δ*liaR* (*liaR*)mutants were cultured in HTVG to mid-exponential phase, serially diluted and spot plated on TVG at pH 7.0 or 5.0.

Fig 3.47. Acid stress and adaptation of the LiaFSR$^-$, Δ*liaS* and Δ*liaR* mutants. *S. mutans* strains were cultured in HEPES-buffered TYEG (pH 7.8) to mid-exponential phase before being transferred to citrate-buffered TYEG (pH 3.5) medium. The adapted cells were cultured for 2 h in MES-buffered TYEG (pH 5.5) medium prior to acid killing at pH 3.5. Non-adapted cells were subjected to acid killing without the 2-h treatment at pH 5.5. Percentage survival was determined using the ratio of CFU after 1.5 h of acid killing over the CFU at the start of the acid killing. The values of the non-adapted cells represents the typical pattern observed from at least 3 independent experiments with triplicate culture. For the adapted cells with 1.5h killing, the results represent the average of two independent experiments with triplicate culture. For the adapted cell with 1.0h killing, the results represent only one experiment with an acid killing time of 1 h. The error bars represent the standard error.

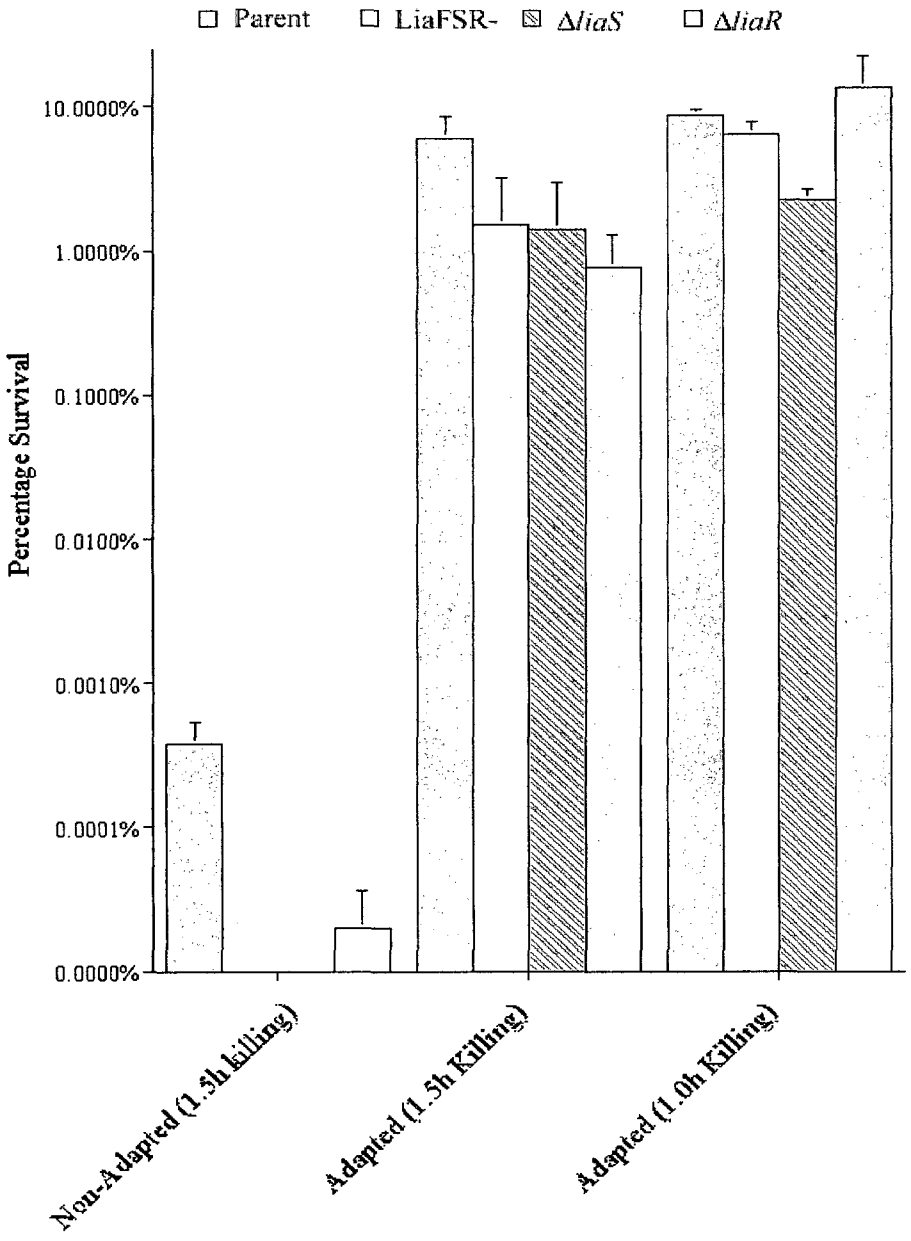
Parent
LiaFSR-
ΔliaS
ΔliaR
Percentage Survival
10.0000%
1.0000%
0.1000%
0.0100%
0.0010%
0.0001%
0.0000%
Non-Adapted (1.5h killing)
Adapted (1.5h Killing)
Adapted (1.0h Killing)

Table 3.4. Antibiotic susceptibility of the LiaFSR⁻, Δ*liaS* and Δ*liaR* mutants.

Strains	Polymyxin B						Van[3]	Pen G[4]
	Disc assay[1]			Liquid Assay[2]			Etest[2]	
	15000 U	7500 U	3750 U	TVG	$TVG_{6.0}$	HTVG		
Parent	3 mm	1 mm	≤ 1 mm	100	100	50	2	0.032
LiaFSR⁻	4.5 mm	2.5 mm	≤ 1 mm	50	50	50	2	0.032
Δ*liaS*	4.5 mm	3 mm	≤ 1 mm	25	50	25	2	0.032
Δ*liaR*	4 mm	3 mm	≤ 1 mm	50	100	50	2	0.032

[1]Distance from the edge of the disc to the edge of the zone of inhibition

[2]Concentration in μg/mL

[3]Vancomycin

[4]Pennicilin G

3.3.8 Mutacin Production of the LiaFSR$^-$, Δ*liaS* and Δ*liaR* Mutants

Two previous studies have reported that the deletion of *liaS* impaired the production of mutacin I in strain UA140 (Tsang et al., 2005) and production of mutacin IV in strain UA159 (Chong et al., 2008). To test if mutacin production was also affected by the inactivation of the LiaFSR TCS, the deferred antagonism assay was performed. When cultured on solid THY, it was observed that both the parent and the Δ*liaR* mutant produced a mutacin that was active against *S. gordonii* strain DL1 which was cultured in solid THY or HTVG (Table 3.5). Mutacin production was abolished in the LiaFSR$^-$, and Δ*liaS* mutants (Table 3.5). On the other hand, mutacin production was not detected for any of the strains when *S. mutans* was cultured on solid HTVG. Based on these results, it is tempting to suggest that control of mutacin production is modulated by the LiaFSR system only under specific conditions.

3.3.9 Cytoplasmic Protein Expression Profile of the LiaFSR$^-$, Δ*liaS* and Δ*liaR* Mutants

To gain insight into the proteins affected by the deletion of the LiaFSR TCS components, the cytoplasmic proteins of the parent and the three mutants were analyzed by 2DGE (Fig 3.48, 3.49, 3.50, 3.51, 3.52, 3.53, 3.54 and 3.55, Table 3.6 and Appendix 2). Several protein spots were observed to be differentially regulated in Δ*liaS* and Δ*liaR* mutants cultured in HTVG; however, no differentially-expressed proteins were identified in the LiaFSR$^-$ mutant. The major differences were the clear decreases of phosphoglycerate kinase (Spot 419) in Δ*liaS* mutant and the change in the dominant isoform of fructose-bisphosphate aldolase (Spots 219 and 220) in Δ*liaR* mutant.

Table 3.5. Results from the deferred antagonism assay for the LiaFSR$^-$, Δ*liaS* and Δ*liaR* mutants against *S. gordonii.*

	THY[1]		HTVG[1]	
Tester Strains	THY Overlay[2]	HTVG Overlay[2]	THY Overlay	HTVG Overlay
Parent	1-2 mm[3]	1-2 mm	≤ 1mm	≤ 1mm
LiaFSR$^-$	≤ 1mm	≤ 1mm	≤ 1mm	≤ 1mm
Δ*liaS*	≤ 1mm	≤ 1mm	≤ 1mm	≤ 1mm
Δ*liaR*	2-3 mm	2-3 mm	≤ 1mm	≤ 1mm

[1]Growth media for the tester strains

[2]Growth media for *S. gordonii*

[3]Distance from the edge of the colony to the edge of the zone of inhibition

Fig 3.48. Two-dimensional (pH 4-7) gel analysis of cytoplasmic proteins isolated from the parent strain cultured in HTVG. Cytoplasmic proteins isolated from the parent strain cultured in HTVG were analyzed. Proteins that are differentially expressed in the parent as compared to the samples from the mutants are highlighted with an arrow head and numbered. Two representative gels are shown. The numbers at the top and on the left represent the pH of the Immobiline Dry Strip and the sizes and positions of protein standards, respectively.

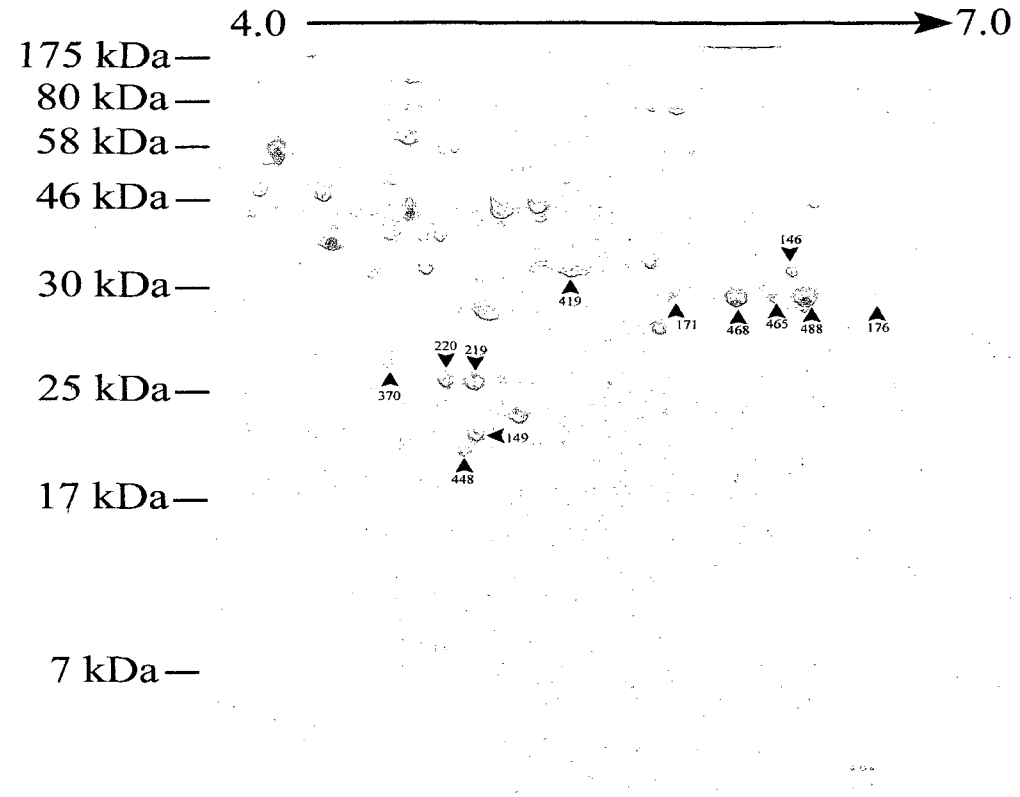
4.0
7.0
175 kDa
80 kDa
58 kDa
46 kDa
30 kDa
25 kDa
17 kDa
7 kDa
146
419
171
468
465
488
176
220
219
370
149
448

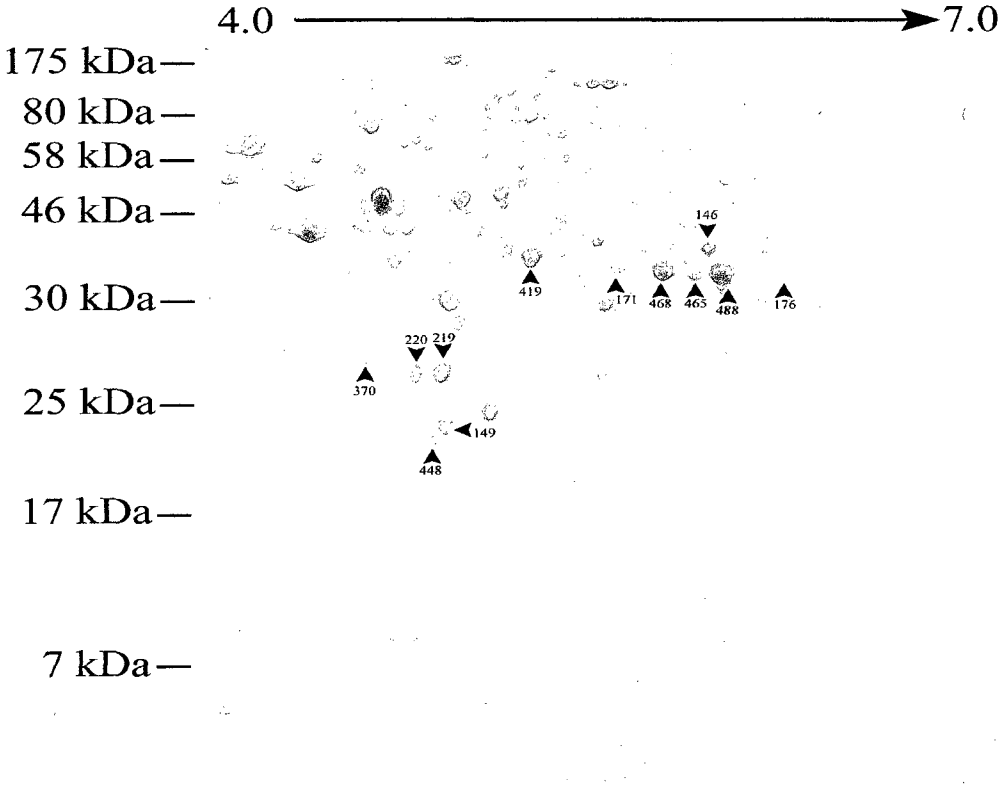
4.0
7.0
175 kDa
80 kDa
58 kDa
46 kDa
30 kDa
25 kDa
17 kDa
7 kDa
146
419
171
468
465
488
176
220
219
370
149
448

Fig 3.49. Two-dimensional (pH 4-7) gel analysis of cytoplasmic proteins isolated from the LiaFSR$^-$ mutant cultured in HTVG. Cytoplasmic proteins isolated from the LiaFSR$^-$ mutant cultured in HTVG were analyzed. Proteins that are differentially expressed in the mutant as compared to the samples from the parent are highlighted with an arrow head and numbered. Two representative gels are shown. The numbers at the top and on the left represent the pH of the Immobiline Dry Strip and the sizes and positions of protein standards, respectively.

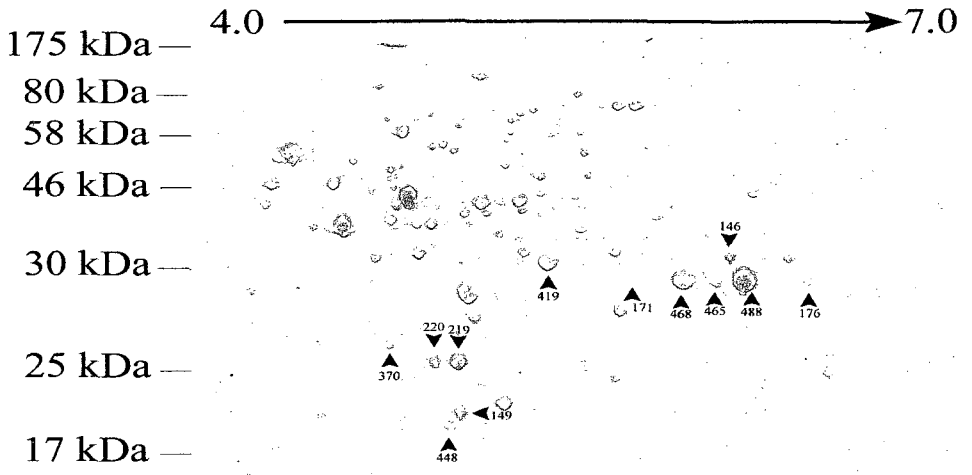
4.0
7.0
175 kDa
80 kDa
58 kDa
46 kDa
30 kDa
25 kDa
17 kDa
7 kDa
146
419
171
468
465
488
176
220
219
370
149
448

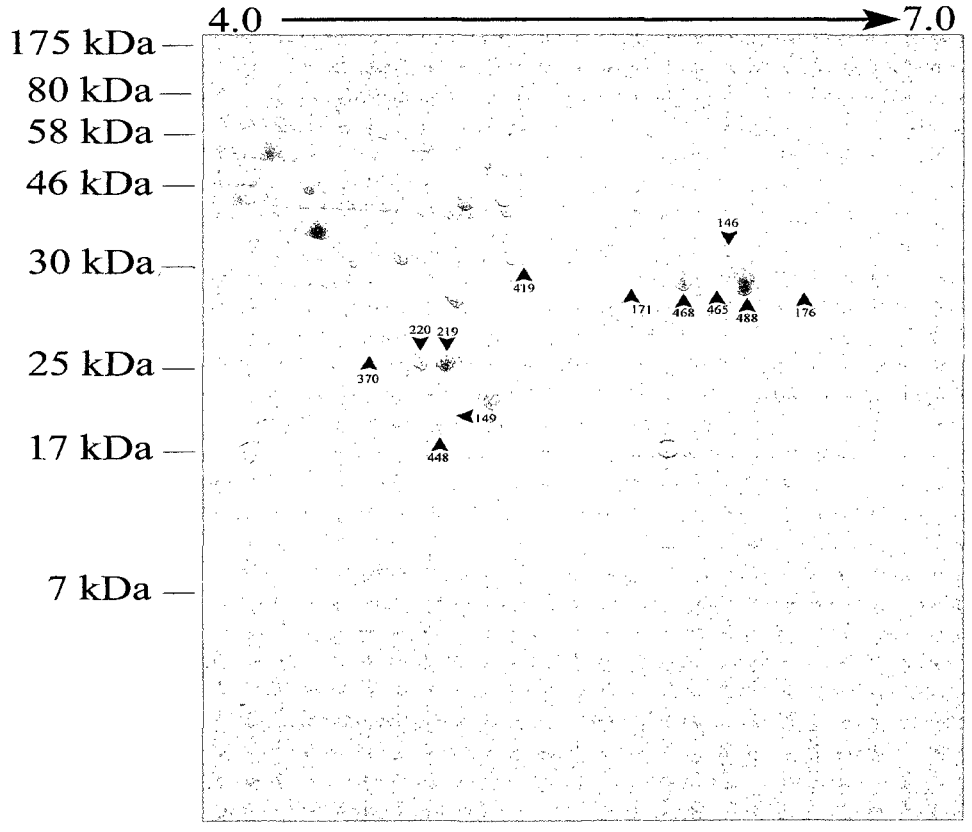
4.0
7.0
175 kDa
80 kDa
58 kDa
46 kDa
30 kDa
25 kDa
17 kDa
7 kDa
146
419
171
468
465
488
176
220
219
370
149
448

Fig 3.50. Two-dimensional (pH 4-7) gel analysis of cytoplasmic proteins isolated from the Δ*liaS* mutant cultured in HTVG. Cytoplasmic proteins isolated from the Δ*liaS* mutant cultured in HTVG were analyzed. Proteins that are differentially expressed in the mutant as compared to the samples from the parent are highlighted with an arrow head and numbered. Two representative gels are shown. The numbers at the top and on the left represent the pH of the Immobiline Dry Strip and the sizes and positions of protein standards, respectively.

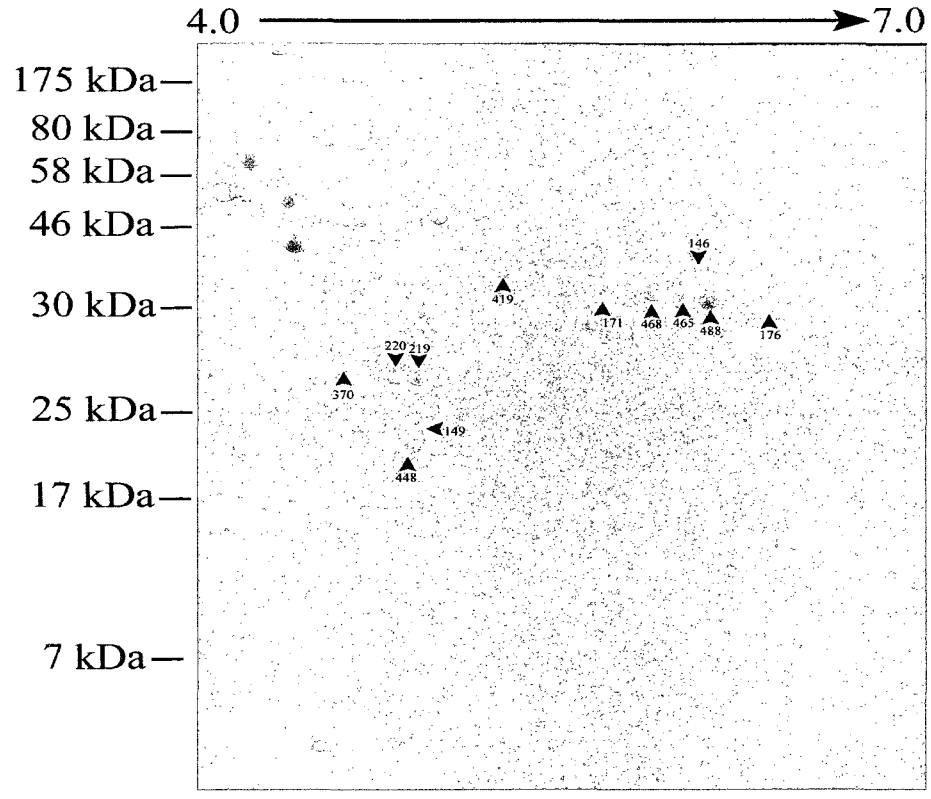
4.0
7.0
175 kDa
80 kDa
58 kDa
46 kDa
30 kDa
25 kDa
17 kDa
7 kDa
146
419
171
468
465
488
176
220
219
370
149
448

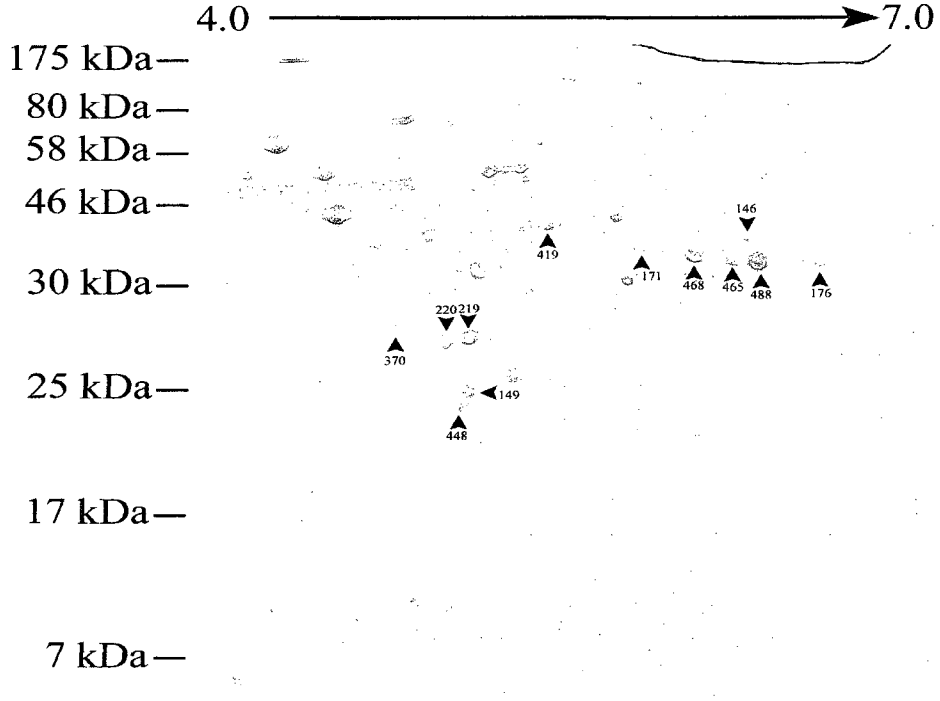
4.0
7.0
175 kDa
80 kDa
58 kDa
46 kDa
30 kDa
25 kDa
17 kDa
7 kDa
146
419
171
468
465
488
176
220
219
370
149
448

Fig 3.51. Two-dimensional (pH 4-7) gel analysis of cytoplasmic proteins isolated from the *ΔliaR* mutant cultured in HTVG. Cytoplasmic proteins isolated from the *ΔliaR* mutant cultured in HTVG were analyzed. Proteins that are differentially expressed in the mutant as compared to the samples from the parent are are highlighted with an arrow head and numbered. Two representative gels are shown. The numbers at the top and on the left represent the pH of the Immobiline Dry Strip and the sizes and positions of protein standards, respectively.

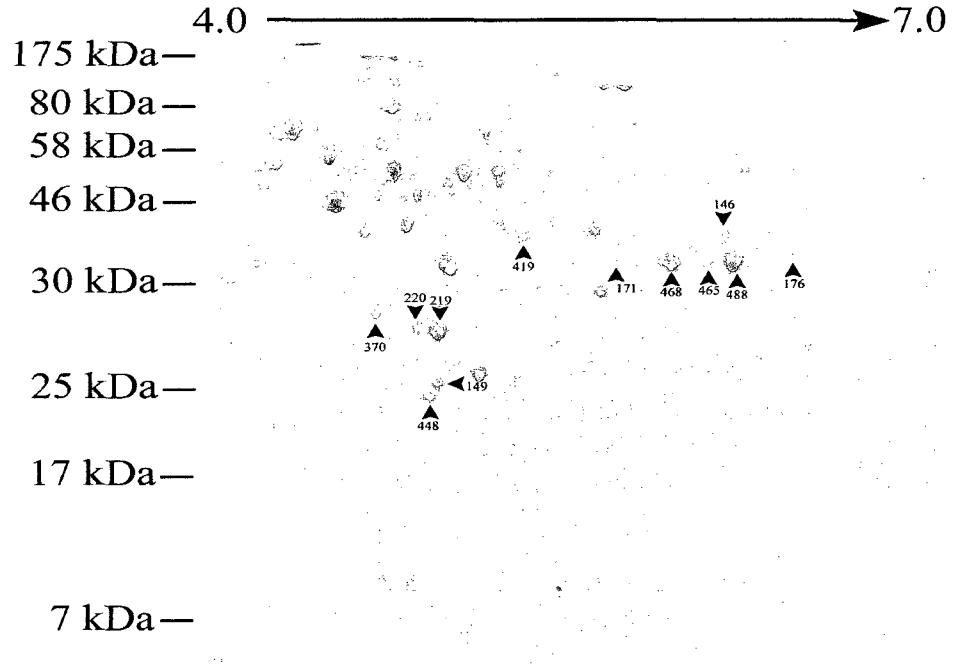
4.0
7.0
175 kDa
80 kDa
58 kDa
46 kDa
30 kDa
25 kDa
17 kDa
7 kDa
146
419
171
468
465
488
176
220
219
370
149
448

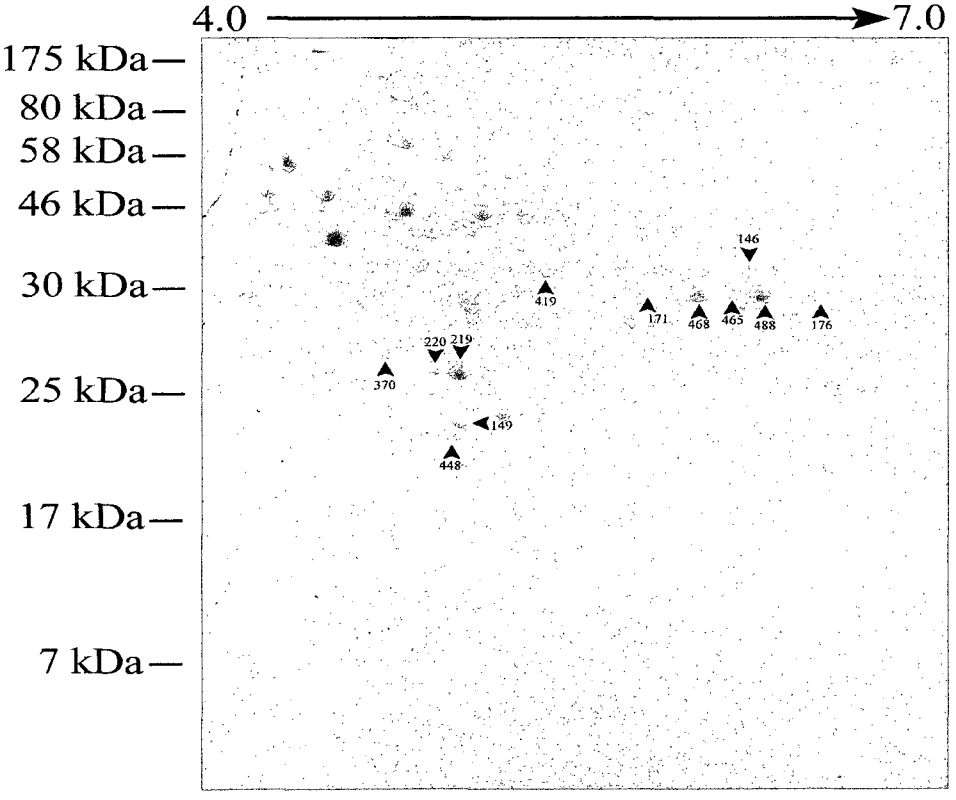
4.0
7.0
175 kDa
80 kDa
58 kDa
46 kDa
30 kDa
25 kDa
17 kDa
7 kDa
146
419
171
468
465
488
176
220
219
370
149
448

Fig 3.52. Two-dimensional (pH 4-7) gel analysis of cytoplasmic proteins isolated from the parent strain cultured in $TVG_{6.0}$. Cytoplasmic proteins isolated from the parent strain cultured in HTVG were analyzed. Proteins that are differentially expressed in the parent as compared to the samples from the mutants are highlighted with an arrow head and numbered. Two representative gels are shown. The numbers at the top and on the left represent the pH of the Immobiline Dry Strip and the sizes and positions of protein standards, respectively.

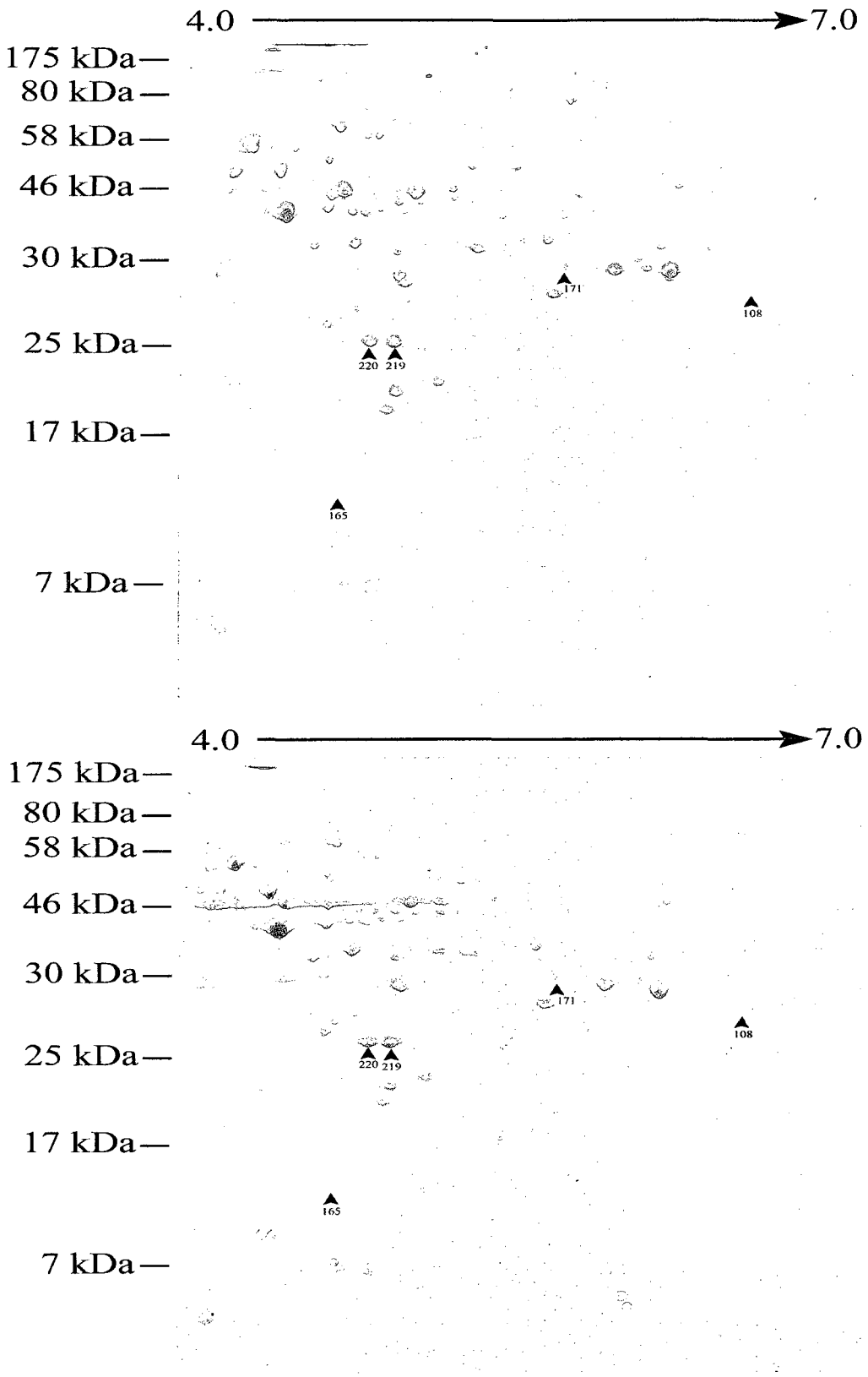
4.0
7.0
175 kDa
80 kDa
58 kDa
46 kDa
30 kDa
25 kDa
17 kDa
7 kDa
171
108
220
219
165
4.0
7.0
175 kDa
80 kDa
58 kDa
46 kDa
30 kDa
25 kDa
17 kDa
7 kDa
171
108
220
219
165

Fig 3.53. Two-dimensional (pH 4-7) gel analysis of cytoplasmic proteins isolated from the LiaFSR$^-$ mutant cultured in $TVG_{6.0}$. Cytoplasmic proteins isolated from the LiaFSR$^-$ mutant cultured in $TVG_{6.0}$ were analyzed. Proteins that are differentially in the mutant expressed as compared to the samples from the parent are highlighted with an arrow head and numbered. Two representative gels are shown. The numbers at the top and on the left represent the pH of the Immobiline Dry Strip and the sizes and positions of protein standards, respectively.

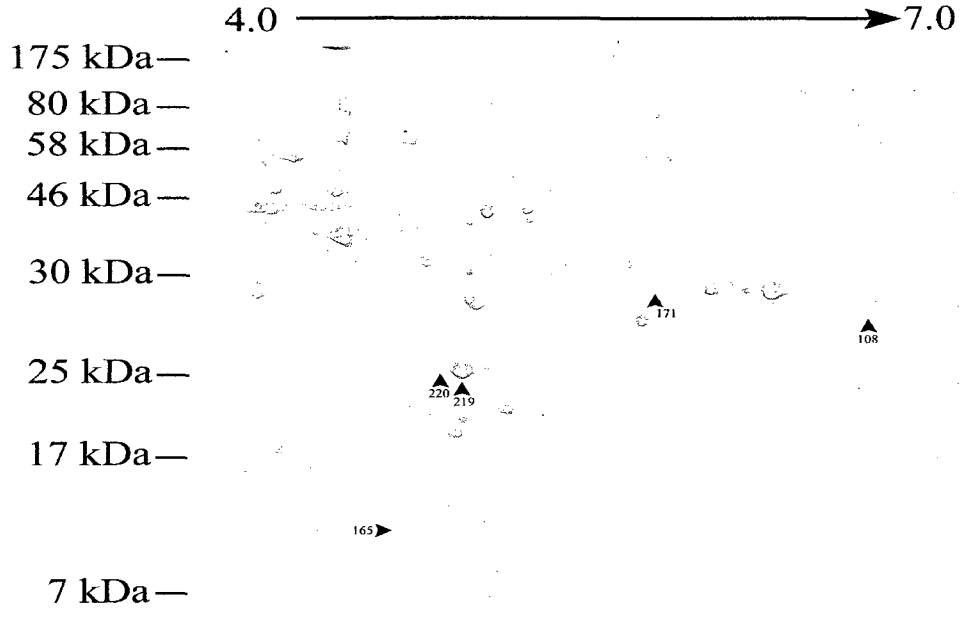
4.0
7.0
175 kDa
80 kDa
58 kDa
46 kDa
30 kDa
25 kDa
17 kDa
7 kDa
171
108
220
219
165

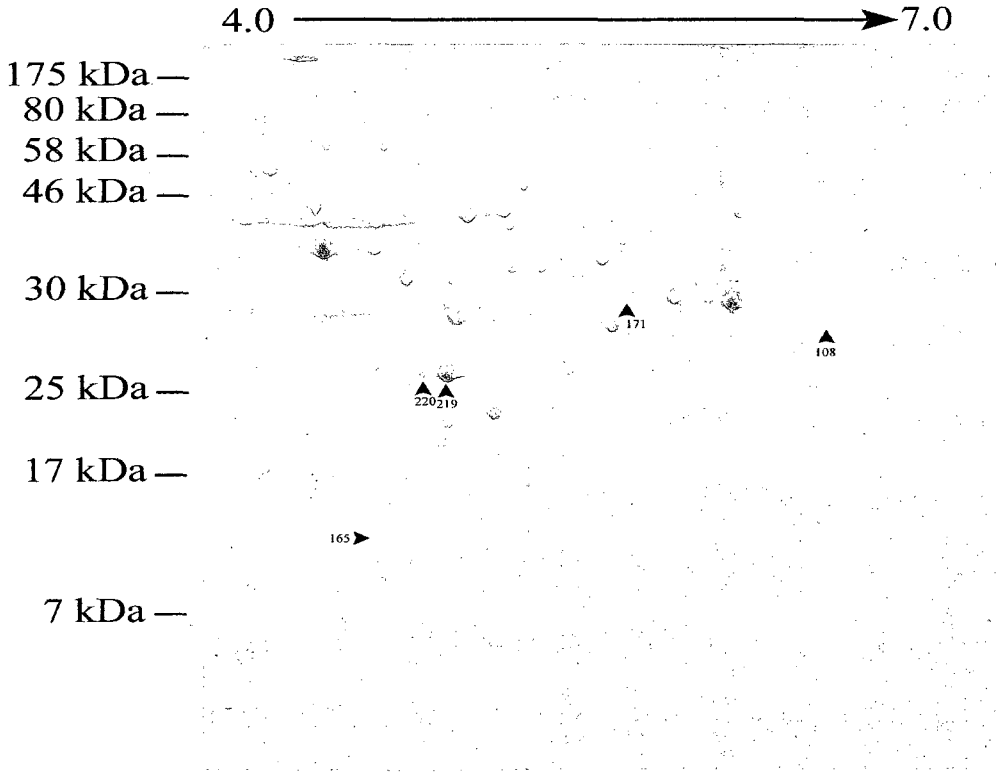
4.0
7.0
175 kDa
80 kDa
58 kDa
46 kDa
30 kDa
25 kDa
17 kDa
7 kDa
171
108
220
219
165

Fig 3.54. Two-dimensional (pH 4-7) gel analysis of cytoplasmic proteins isolated from the Δ*liaS* mutant cultured in $TVG_{6.0}$. Cytoplasmic proteins isolated from the Δ*liaS* mutant cultured in $TVG_{6.0}$ were analyzed. Proteins that are differentially expressed in the mutant as compared to the samples from the parent are highlighted with an arrow head and numbered. Two representative gels are shown. The numbers at the top and on the left represent the pH of the Immobiline Dry Strip and the sizes and positions of protein standards, respectively.

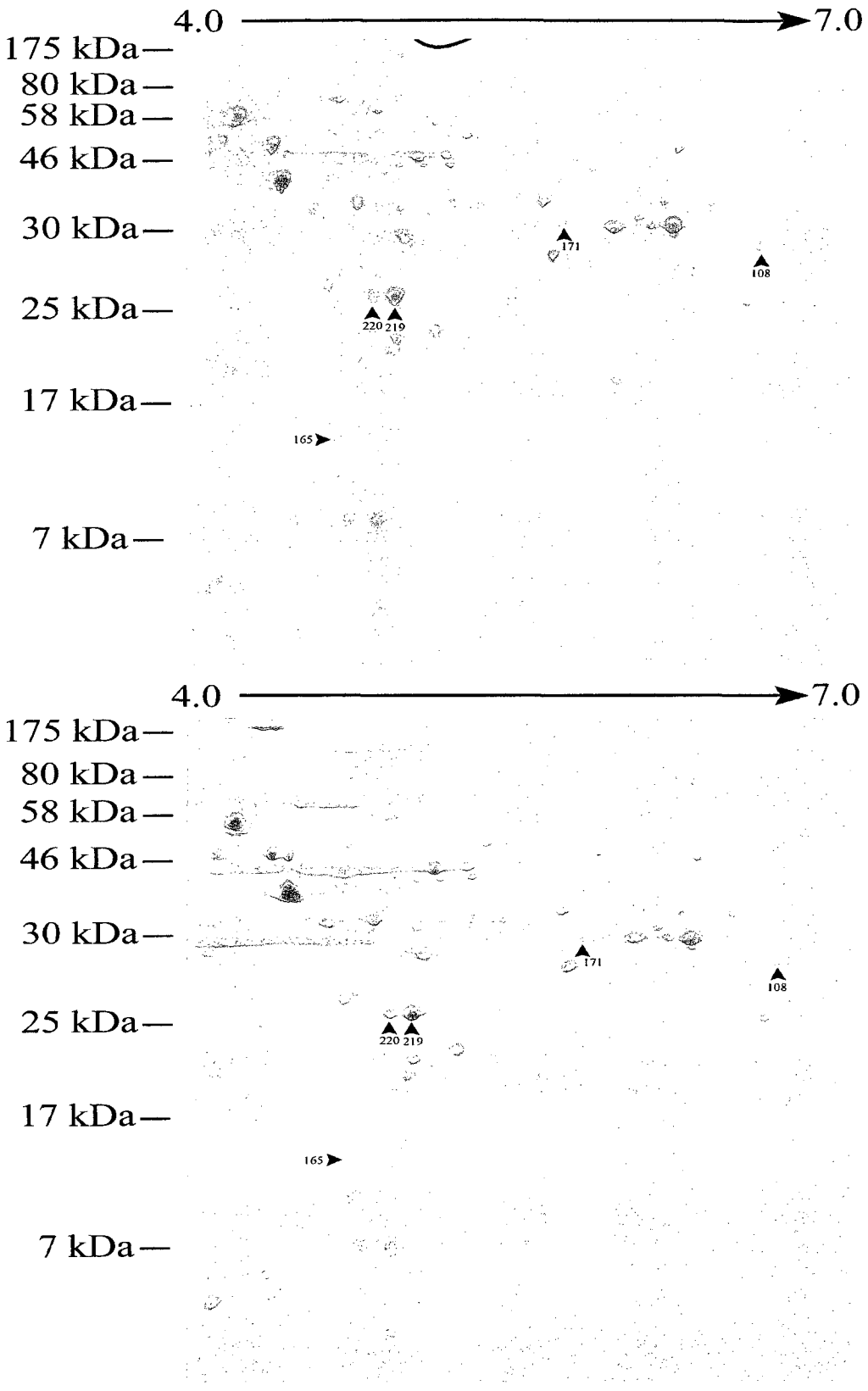
4.0
7.0
175 kDa
80 kDa
58 kDa
46 kDa
30 kDa
25 kDa
17 kDa
7 kDa
171
108
220
219
165
4.0
7.0
175 kDa
80 kDa
58 kDa
46 kDa
30 kDa
25 kDa
17 kDa
7 kDa
171
108
220
219
165

Fig 3.55. Two-dimensional (pH 4-7) gel analysis of cytoplasmic proteins isolated from the *ΔliaR* mutant cultured in $TVG_{6.0}$. Cytoplasmic proteins isolated from the *ΔliaR* mutant cultured in $TVG_{6.0}$ were analyzed. Proteins that are differentially expressed in the mutant as compared to the samples from the parent are highlighted with an arrow head and numbered. Two representative gels are shown. The numbers at the top and on the left represent the pH of the Immobiline Dry Strip and the sizes and positions of protein standards, respectively.

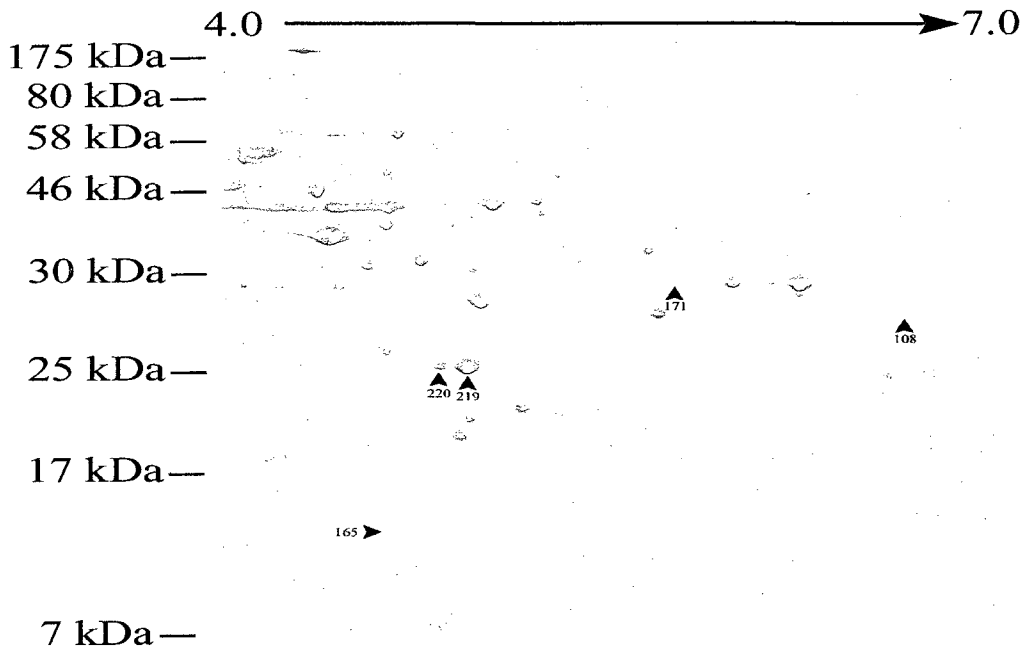
4.0
7.0
175 kDa
80 kDa
58 kDa
46 kDa
30 kDa
25 kDa
17 kDa
7 kDa
171
108
220
219
165

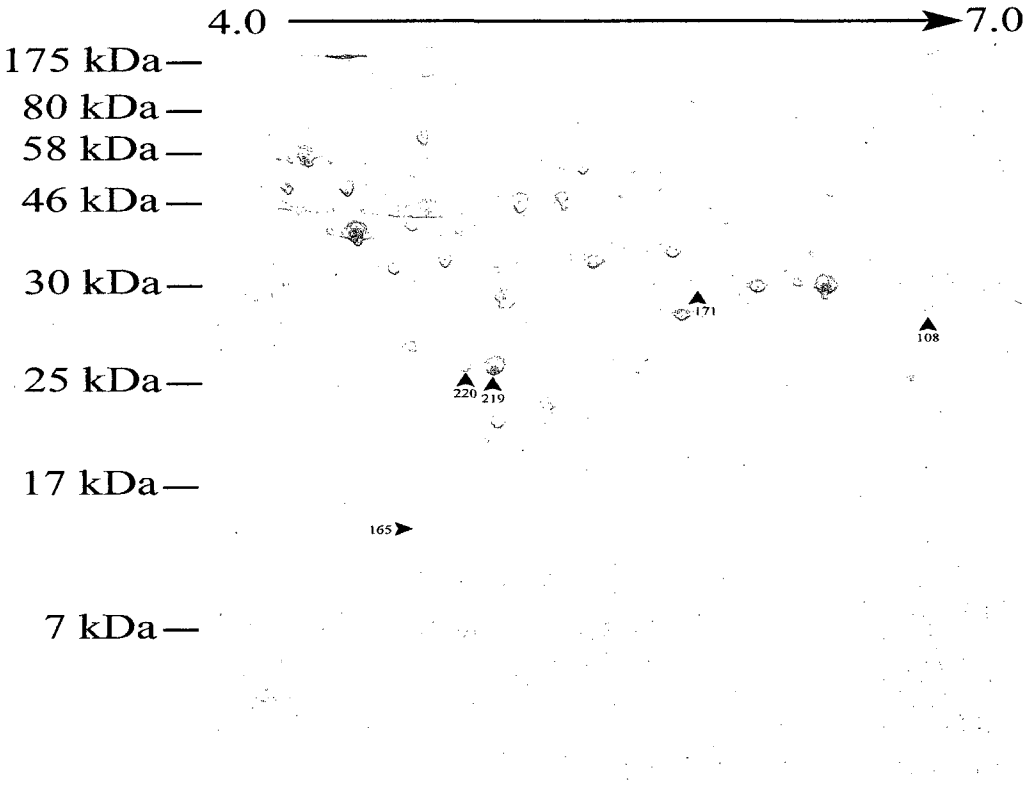
4.0
7.0
175 kDa
80 kDa
58 kDa
46 kDa
30 kDa
25 kDa
17 kDa
7 kDa
171
108
220
219
165

Table 3.6. Summary of two-dimensional gel electrophoresis and mass spectrometry analysis.

Strains	Media	Protein name - function	Gene ID[1]	Spot ID	Fold Change
LiaFSR$^-$	HTVG	No differentially expressed protein spots identified			
	$TVG_{6.0}$	GapC - glyceraldehyde-3-phosphate dehydrogenase	SMu0325	171	-1.75
		CysK - cysteine synthetase A	SMu0449	108	-2.85
		FbaA - fructose-bisphosphate aldolase	SMu0088	220	-1.8
		FbaA - fructose-bisphosphate aldolase	SMu0088	219	+1.3
		GreA - transcription elongation factor	SMu1574	165	-1.85
ΔliaS	HTVG	RmlB - dTDP-glucose-4,6-dehydratase	SMu1327	465	-1.75
		GapC - glyceraldehyde-3-phosphate dehydrogenase	SMu0325	488	-1.8
				468	-2.7
				171	-2.95
		Pgk - phosphoglycerate kinase	SMu0326	419	-5.55
		PpaC - manganese-dependent inorganic pyrophosphatase	SMu1537	370	-1.7
		TpiA – triosephosphate isomerase	SMu0652	149	-2.0
		SodA – superoxide dismutase	SMu0571	448	-1.38
		FabF - 3-oxoacyl-(acyl-carrier-protein) synthase	SMu1585	146	-2.5
	$TVG_{6.0}$	FbaA - fructose-bisphosphate aldolase	SMu0088	220	-1.8

Strains	Media	Protein name - function	Gene ID[1]	Spot ID	Fold Change
		FbaA - fructose-bisphosphate aldolase	SMu0088	219	+1.3
ΔliaR	HTVG	RmlB - dTDP-glucose-4,6-dehydratase	SMu1327	465	-1.75
		GapC - glyceraldehyde-3-phosphate dehydrogenase	SMu0325	488	-1.8
				176	-2.85
		FbaA - fructose-bisphosphate aldolase	SMu0088	220	-2.0
		FbaA - fructose-bisphosphate aldolase	SMu0088	219	+2.0
	$TVG_{6.0}$	GapC - glyceraldehyde-3-phosphate dehydrogenase	SMu0325	171	-2.0
		FbaA - fructose-bisphosphate aldolase	SMu0088	220	-1.8
		FbaA - fructose-bisphosphate aldolase	SMu0088	219	+1.3

[1] The LC-MS/MS analyses are included in Appendix 2

Additionally, a decrease in the level of several isoforms of glyceraldehyde-3-phosphate dehydrogenase was observed in the Δ*liaS* (Spots 171, 468 and 488) and Δ*liaR* mutants (Spots 176 and 488) cultured in HTVG. Furthermore, the production of triosephosphate isomerase (Spot 149) was also reduced in the Δ*liaS* mutant cultured in HTVG. The enzymes mentioned above are involved in the glycolysis pathway.

In addition to enzymes involved in the glycolysis pathway, four other proteins potentially involved in cell-envelope metabolism or oxidative stress were identified. The first protein, RlmB (Spot 465), showed reduced levels in both the Δ*liaS* and Δ*liaR* mutants cultured in HTVG. RlmB is involved in rhamnose synthesis required for exopolysaccharides (Tsukioka et al., 1997). The second protein, PpaC (Spot 379), was down-regulated in the Δ*liaS* mutant cultured in HTVG. PpaC is also known as Dlt5 and appears to be part of the *dlt* operon of *S. mutans* (Spatafora et al., 1999). The third protein identified is SodA (Spot 448), a superoxide dismutase, and Δ*liaS* mutant cultured in HTVG exhibited a lower production of SodA. The fourth protein was 3-oxoacyl-(acyl-carrier-protein) synthase (Spot 146), it was as down-regulated in the Δ*liaS* mutant cultured in HTVG.

In contrast to what was seen when the LiaFSR$^-$ mutant was cultured in HTVG, there was reduced production of several proteins when the LiaFSR$^-$ mutant was cultured in $TVG_{6.0}$. One of the identified proteins was CysK (Spot 108), which is a protein involved in cystein synthesis; another is GreA (Spot 165), which a transcription elongation factor. Additionally, it was observed that the LiaFSR$^-$ mutant cultured in $TVG_{6.0}$ differentially produced only one of the glyceraldehyde-3-phosphate dehydrogenase isoforms (Spot 171) which was at a lower level than the parent. The

Δ*liaR* mutant cultured in TVG6.0 exhibited the same reduction for Spot 171. Unlike the other two mutants, the Δ*liaS* mutant cultured in TVG6.0 did not show a differential production of the glyceraldehyde-3-phosphate dehydrogenase isoforms. The only common protein differentially regulated in all three mutants cultured in $TVG_{6.0}$ was the dominant isoform of fructose-bisphosphate aldolase (Spots 219 and 220).

3.3.10 Phosphoglycerate Kinase Activity is Reduced in the Absence of LiaS

To confirm some of the 2DGE data, phosphoglycerate kinase, glyceraldehyde-3-phosphate dehydrogenase and triosephosphate isomerase enzymatic activity was measured for both HLO002 and the Δ*liaS* mutant cultured in HTVG. Phosphoglycerate kinase activity was decreased in the the Δ*liaS* mutant when compared to its parental strain (Fig 3.56). No change in activity was observed for glyceraldehyde-3-phosphate dehydrogenase and triosephosphate isomerase.

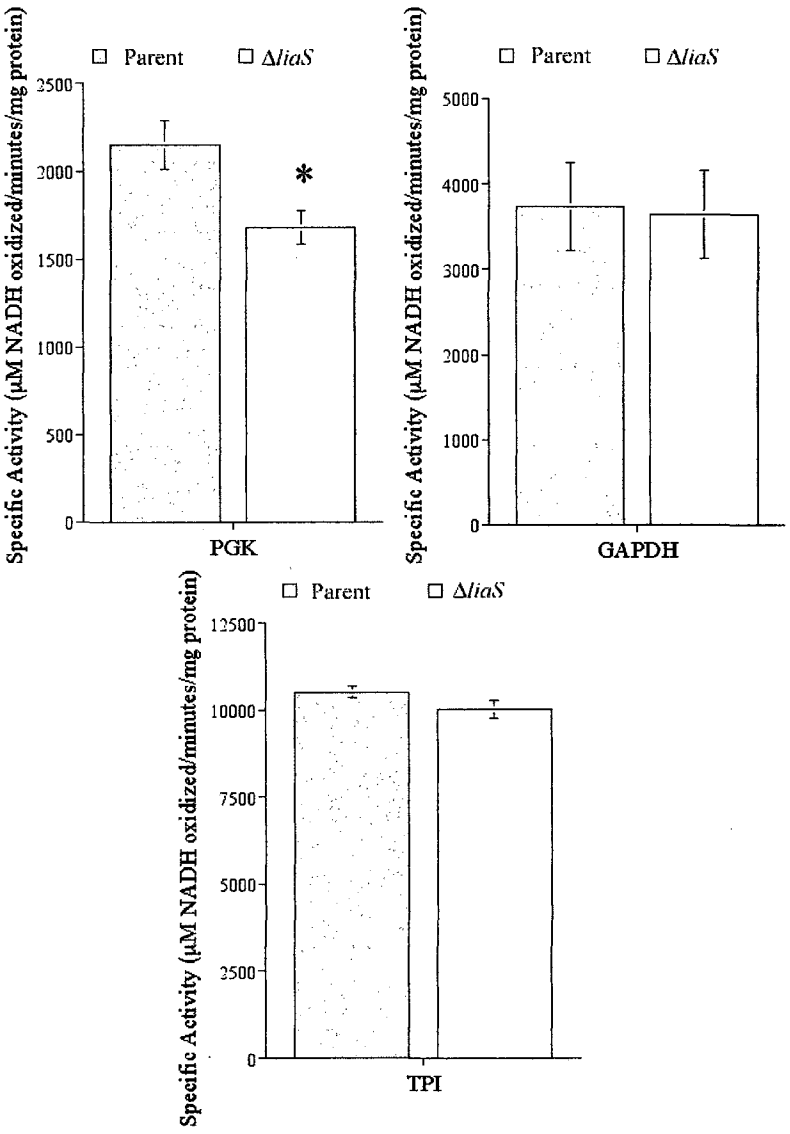

Fig 3.56. Phosphoglycerate kinase, glyceraldehyde-3-phosphate dehydrogenase and triosephosphate isomerase activity in the parent and the *ΔliaS* mutant cultured in HTVG. Cytoplasmic proteins isolated from the parent and the *ΔliaS* mutant were assayed for phosphoglycerate kinase (PGK), glyceraldehyde-3-phosphate dehydrogenase (GAPDH) and triosephosphate isomerase (TPI) activity. The results represent the means (± SE) of two independent experiments with each experiment consisting of triplicate cultures. * indicate $P<0.05$ between the mutant and the parent.

Chapter 4. Discussion

4.1 Analysis of the *murA1* Mutant Phenotypes

A previous attempt to inactivate the *vicRKX* operon resulted in the creation of a mutant exhibiting up-regulation of FTF in the absence of sucrose, overproduction of an extracellular carbohydrate containing glucose and glucuronic acid, and autoaggregation. Additonally, the mutant did not grow in culture media at pH 5.5 and showed a reduced cell density at pH 6.0 (Lee et al., 2004). Although the resulting mutant was identified as a *vicRKX* mutant, subsequent analysis revealed that the suicide vector did not insert into the targeted location (Senadheera et al., 2005). Using a combination of primer walking sequencing, PCR and an *E. coli* clone library, the site of insertion was identified to be located within the *murA1* gene. This gene encodes a UDP-N-acetylglucosamine 1-carboxyvinyltransferase which performs the first committed step of peptidoglycan synthesis. The insertion occured via the pBR325 region of pCovR/981, which has a 9-bp homology with the *murA1* gene. The length of the homologous region was surprisingly small; however, Marvo et al. (1983) reported that, in *E coli*, 10 to 13 bp of homology was sufficient for phage A and pBR322, the pBR325 parental plasmid, to recombine. Nonetheless, the presence of a 400-bp *vicR* fragment on pCovR/981 should have yielded a homologous recombination at the targeted site but it did not occur indicating that inactivation of *vicR* is a suicidal event.

To confirm that *murA1* was inactivated, the sensitivity of the mutant to phosphomycin and other antibiotics was tested. The *murA1* mutant was more sensitive to phosphomoycin compared to the parental strain. Given that MurA is the target of phosphomycin (Du et al., 2000) and the deletion of *murA* in *B. anthracis* increased

sensitivity to phosphomycin (Kedar et al., 2008), the increase sensitivity to phosphomycin of the *S. mutans murA1* mutant suggest that *murA1* was inactivated by the insertion of pCovR/981. Additionally, the parent and the *murA1* mutant showed equal sensitivity to polymyxin B, penicillin G, vancomycin and erythromycin. These results suggest that pCovR/981 inserted only within the *murA1* gene.

The insertion of pCovR/981 into *murA1* gene may have a polar effect on downstream gene expression. Analysis of the annotated genome and *in silico* analysis of DNA sequences immediately preceding and following *murA1* suggested that *murA1* is part of an operon with *epuA*, the gene immediately downstream. The *murA1* stop codon and the *epuA* start codon are separated by 2 bp. Analysis of the 200-bp region upstream of *epuA* revealed that typical promoter elements were absent and termination sequences were not observed in the region immediately downstream of *murA1*. In order to clarify the role of *murA1* in the observed phenotype, complementation was attempted. The introduction of the shuttle vector pDL276 carrying a copy of *murA1* in *E. coli* was unsuccessful despite many attempts. Therefore, the complementation could not be carried in *S. mutans*.

Since the previous characterization study had demonstrated that the mutant over-expressed *ftf,* over-produced an exopolysaccharide and autoaggregated, it was hypothesized that the mutant would form a defective biofilm. A biomass accumulation assay was first performed to establish if the mutant was able to attach and accumulate biomass. The mutant was able to attach and accumulate biomass better than the parent. The ability to accumulate more biomass is probably due to the over-production of exopolysaccharide and its ability to autoaggregate. Such an increase in biomass may also indicate a failure of bacterial cells to detach from the biofilm. To assess the detachment

ability of the mutant, the Calgary biofim device was used to measure the rate of detachment and the ability of the detached cells to form a new biofilm. The results from the assay indicated that both the parent and the mutant have the same ability to detach and form new biofilm. SEM analysis showed that, like the parent strain, the mutant strain formed a biomass mat, but the mat appears to be thicker in the mutant. The organization of the biofilm in the mutant also appeared to be more chaotic and lack the usual organized structure of the parental strain. Again, the change in biofilm structure is likely due the over-production of the exopolysaccharide, overexpression of *ftf* and autoaggregation by the mutant. Therefore, it was concluded that the mutant was able to attach, accumulate biomass and detach. Furthermore, the biofilm formed by the mutant had an altered architecture when compared to the biofilm formed by the parent.

Like several Gram-positive bacteria, *S. mutans* possesses two genes encoding UDP-N-acetylglucosamine enolpyruvyl transferases (Ajdic et al., 2002). Du et al., (2000) observed that two UDP-N-acetylglucosamine enolpyruvyl transferases of *S. pneumoniae* were less efficient in catalyzing the transfer of enolpyruvate from phosphoenolpyruvate to UDP-N-acetylglucosamine as compared to the *E. coli* enzyme. It is, therefore, tempting to propose that both enzymes are required for optimal activity in *S. mutans*. The deletion of either enzyme in *S. mutans* would result in a decrease yield of UDP-*N*-acetylglucosamine enolpyruvate creating bottlenecks in the production of cell-wall precursors and their transpeptidation. Additionally, the decrease in UDP-*N*-acetylglucosamine enolpyruvate could result in the acumulation of the precursor, UDP-N-acetylglucosamine. Consequently, normal cellular processes such as protein anchoring and synthesis of exopolysaccharides would be disrupted. In support of this hypothesis, the *murA1* mutant overproduces an extracellular carbohydrate containing glucose and

glucuronic acid and the mutant was sensitive to acidic pH (Lee et al., 2004). Interestingly, the polymerization of N-acetylglucosamine and glucuronic acid forms hyaluronic acid which is the typical component of *S. pyogenes* capsule. However, *S. mutans* is not known to produce a hyaluronic acid capsule and the carbohydrate identified in the *murA1* mutant did not contain *N*-acetylglucosamine and was not fructan (Lee et al., 2004). In the *murA1* mutant, the accumulation of the carbohydrate increases the microenvironment concentration of glucose and glucuronic acid containing carbohydrates which in turn, induces the expression of *ftf* through a TCS or a phosphoenolpyruvate-sugar phosphotransferase system (PTS). Lee et al. (2004) noted that the overexpression of *ftf* in the *murA1* mutant was eliminated by the introduction of a multi-copy plasmid carrying the *vicRKX* operon (pCovRSX/276). The presence of pCovRSX/276 resulted in a 50% reduction of the extra-cellular carbohydrate. It is tempting to suggest that the introduction of multi-copy pCovRSX/276 likely resulted in the overexpression of *vicRKX*. The VicRK TCS appears to be a system monitoring active cell-wall synthesis (Dubrac et al., 2008). It is, therefore, possible that the up-regulation of VicR resulted in increased expression of genes encoding proteins involved in cell-envelope homeostasis. The VicRK TCS probably sensed the cell-wall defect present in the *murA1* mutant and, thus, the overexpression of *vicRKX* from the plasmid coincidentally increased the amount of enzyme involved in the synthesis of peptidoglycan biosynthetic precursors. Consequently, the increase in cell-wall precursor resulted in a larger amount of components available to attach to the glucuronic-acid-containing carbohydrates and, thus, reduced the amount of extracellular carbohydrates associated with the *murA1* deletion. The reduction of the extracellular carbohydrates

probably reduced the local concentration of glucose and glucuronic acid containing carbohydrates and, thus, reduced the *ftf*-induction level.

4.2 Regulation of *vicR* Expression

Despite recent advancements in the knowledge regarding the role of VicRK TCS, few reports have described the stimuli and environmental conditions influencing the expression of the *vicRKX* operon. At the onset of this study, the growth-phase dependent expression of *vicR* in *B. subtilis* was the only established variable affecting *vicR* expression (Fabret and Hoch, 1998; Fukuchi et al., 2000). Recently, growth-phase dependent expression of *vicR* has been observed in *S. mutans* (Stipp et al., 2008) and it was also established that *vicR* was not differentially expressed in the presence of various carbohydrate sources, with the exception of xylitol (Shemesh et al., 2006). Additionally, two potential inducers of *vicR* have been identified: paraquat (Senadheera et al., 2007) and hydrogen peroxide (Deng et al., 2007). However, the expression of *vicR* by aerobically grown *S. mutans* is only marginally lower than anaerobically grown cells (Ahn and Burne, 2007) suggesting that induction of *vicR* expression by oxidative stress is a transient response.

In order to study the environmental conditions influencing *vicR* expression, the 411-bp region containing the promoter of *vicR* (P_{vicR}) was inserted upstream of a *lacZ* gene. A LacZ-reporter plate assay was initially used to screen conditions that induced or repressed P_{vicR} activity. As observed by Shemesh *et al.* (2006), it was found that the carbohydrates tested did not influence P_{vicR} activity but growth pH did have an impact on the activity of P_{vicR}. To confirm the influence of culture pH, *S. mutans* was cultured in liquid media adjusted to different pH with or without buffer. It was observed that the pH

of the medium had an impact on the activity of P_{vicR} and that buffering the medium allowed for continually high expression of the reporter gene. It was first concluded that the pH of the medium was a key environmental factor influencing the expression of *vicRSX* operon. To confirm the *lacZ* assay results, the levels of *vicR* transcript were measured in *S. mutans* cultured in $TVG_{6.0}$ and HTVG. In agreement with the LacZ assay, up-regulation of *vicR* was observed in the *S. mutans* cultured in HTVG. Additionally, *vicR* expression was also induced at mid- and late-exponential phase supporting the observations made in *S. mutans* (Stipp et al., 2008) and those made *B. subtilis* (Fabret and Hoch, 1998; Fukuchi et al., 2000).

In addition to pH, growth phase and carbohydrate source, the impact of several antibiotics on *vicR* expression was also investigated. Vancomycin, ampicillin, penicillin G, and polymyxin B induced the expression of *vicR*. All four of these antibacterial agents are known to induce the cell-envelope stress response. Such stress in Gram-positive bacteria is modulated by TCS and extracellular function (ECF) sigma factors (Jordan et al., 2008). The induction of *vicR* expression by inducers of cell-envelope stress suggests that the VicRK TCS belongs to the cell-envelope stress response. Despite the fact that the *S. mutans* genome does not appear to encode any ECF sigma factors (Ajdic et al., 2001; Helmann, 2002), two TCS, LiaFSR and MbrCD, have been implicated in the cell-envelope stress response in *S. mutans* (Jordan et al, 2008). Furthermore, it has also been proposed by others that the VicRK TCS plays a role in cell-envelope stress response (Jordan et al., 2008). The LiaFSR TCS was of particular interest because it was linked to acid stress response in *S. mutans* and homologues control the response to vancomycin in *B. subtilis*, *S. aureus* and *S. pneumoniae*. It was hypothesized that the LiaFRS TCS might influence the expression of *vicRKX* operon.

The effects of deleting *vicK* or *vicX* on *vicR* expression were assessed and revealed that VicRK TCS does not autoregulate its expression. This is in agreement with previous studies where it has been reported that VicRK TCS does not autoregulate its expression (Fabret and Hoch, 1999; Ng et al., 2005; Senadheera et al., 2007). However, differential expression of *vicR* was observed in the *liaFSR* deletion strains. Up-regulation of *vicR* was observed in the Δ*liaS* mutant cultured in HTVG. Additionally, the inactivation of the LiaFSR system resulted in the induction of *vicR* in *S. mutans* cultured in HTVG but not in those cultured in $TVG_{6.0}$. The deletion of *liaR* also resulted in the differential regulation of *vicR*; down-regulation was observed in *S. mutans* cultured in $TVG_{6.0}$ whereas no change was observed in *S. mutans* cultured in HTVG. The up-regulation of *vicR* transcription in the Δ*liaS* mutant and down-regulation of *vicR* in Δ*liaR* mutant clearly establishes a link between *vicR* regulation and the LiaFSR TCS. Furthermore, induction of *vicR* expression was associated with the induction of *liaR* expression in the Δ*liaS* mutant. This further supports a link between *vicR* expression and the LiaFSR TCS.

Although differential *vicR* expression patterns were generally consistent for all three approaches, the expression pattern observed in LiaFSR-negative mutant cultured in $TVG_{6.0}$ were inconsistent. For example, the LacZ-reporter assay showed no differential expression whereas the RNA levels of *vicR* were down-regulated and VicR levels were increased. Additionally, fold-increases in protein levels were often not as great as those observed for the *lacZ*-reporter assay and RNA blots. Inconsistencies between transcript and protein levels have also been observed in *B. subtilis*. Specifically, a decrease in *vicRK* transcript during transition from exponential phase to stationary phase did not result in a decrease in the level of VicR and VicK protein in *B. subtilis* (Fabret and Hoch,

1998; Szurmant et al., 2005; Howell et al., 2006). The differences observed in this study support observations made with *B. subtilis* and provide an interesting insight into the regulation of *vicR*. Therefore, it is reasonable to hypothesize that post-transcriptional regulation of *vicR* is occurring.

Differential regulation of *vicR* in the three mutants could indicate that the *vicRKX* operon is a member of the LiaR regulon. An analysis of the promoter of *vicRKS* revealed the absence of a LiaR binding site (Fig 4.1). Additionally,recombinant LiaR did not bind to the promoter of *vicR* in EMSA experiment (data not shown). Based on the absence of a LiaR box, LiaFSR appears to control the expression of *vicR* indirectly.

Results obtained from the disc diffusion assay also support this hypothesis. In the assay, vancomycin induced *vicR* expression in the absence of the LiaFSR TCS components. This is in disagreement with currently published literature. Vancomycin is one of the signals that activate the LiaFSR TCS signalling cascade (see Mascher et al., 2004). It, therefore, suggests that another signalling pathway may control the expression of *vicR* in the presence of cell-envelope stress induced by vancomycin. In the same disc diffusion assay, Penicillin G and polymyxin B did not induce *vicR* expression in the absence of the LiaFSR TCS components. Penicillin G and polymyxin B do not normally induce the expression of the *liaFRS* operon in *B. subtilis* (see Mascher et al., 2004). Thus, the absence of an effect by those antibiotics is consistent with the literature. The inactivation of the LiaFSR system, the HK LiaS and the RR LiaR did not result in observable changes in the expression of the monitored genes in the presence of the inducer. Therefore, LiaFSR TCS probably does not control the expression of *vicR* under penicillin G and polymyxin B induced stress.

Fig 4.1. Promoter analysis of the DNA sequence immediately upstream of *vicR* start codon. (A)The sequence immediately upstream of the start codon of *vicR* was analyzed for promoter elements including the transcription start site (TS), the -10 and -35 box, the ribosome binding site (RBS), inverted repeats stem loop and potential regulatory-protein binding site. (B) Consensus sequence for the DNA-binding site of LiaR as presented by Martinez et al. (2007).

Cell-envelope stress appears to be a theme for the regulation of *vicR* in *S. mutans* and, predictably, other Gram-positive bacteria. This hypothesis is in agreement with the model of VicRK TCS signaling proposed by Dubrac et al. (2008). In their model, Dubrac et al (2008) proposed that the VicRK TCS senses active cell-wall synthesis by detecting peptidoglycan biosynthetic precursors. Furthermore, it has been proposed that the VicRK TCS co-ordinates cell-wall remodelling (Fukushima et al., 2008). During the cell-envelope stress response, the cell envelope is repaired and remodelled (Jordan et al., 2008) and the VicRK could play a key role in monitoring the repair and remodelling process. However, correlation between the growth pH and regulation of *vicR* does not appear to fit within the model. Cell-wall remodelling may occur during ATR but in this study, ATR would only be observed during a limited time period following inoculation. Furthermore, it may be difficult to differentiate between the normal cell-envelope turn-over and stress caused by acid. In the liquid phase LacZ assay, down-regulation of *lacZ* in cells grown in $TVG_{7.8}$ correlated with both a drop of pH below 5.0 and the beginning of stationary phase (t=8h). The identification of acidic pH as stimulus that down-regulated the expression of *vicR* is likely due to the side effects of growing in acidic environment and pH is likely not the signal. During growth kinetics, it was observed that the generation time for *S. mutans* cultured in HTVG (1h 37min) or $TVG_{7.8}$ (1h 34min) was noticeably higher than that observed for *S. mutans* cultured in $TVG_{6.0}$ (2h 12min; see Fig 3.08). An acidic environment leads to a decreased growth rate, which results in the slowing of the cell-envelope turn-over rate. At the opposite end, the highest level of *vicR* expression was obtained during active growth and in media conditions with the highest rate of cell division. Rapid cell division would result in an increase of cell-wall turn-over and genes involved in cell division would be up-regulated during exponential phase to

ensure proper division. The VicRK system is known to regulate expression of genes encoding cell-division proteins and cell-wall synthesis enzymes in several Gram-positive bacteria (Dubrac et al., 2008). Furthermore, it has been shown that decreasing the amount of *vicR* transcript in *S. pneumoniae* results in a population with many large cells and hollow cells (Ng *et al.*, 2003 & 2004). The notion that the level of *vicR* expression is dependent on the rate of cell division and growth is reasonable.

Senadheera *et al.* (2007) and Deng *et al.* (2007) reported that the *vicRKX* operon was up-regulated when *S. mutans* was stressed with paraquat or H_2O_2 and they suggested that oxidative stress affected the expression of *vicRKX*. However, an increase in the expression of *vicR* was not observed when *S. mutans* was grown under aerobic conditions (Ahn and Burne, 2007). This study shows that H_2O_2 did not induce *lacZ* expression in the diffusion disc assay. Therefore, oxidative stress, per se, may not be a key environmental stress inducing the expression of *vicR*. Oxidative stress includes a wide range of non-specific effects caused by different agents or conditions. One of the consequences of oxidative stress is the peroxidation of lipids and, in some cases, the oxidation of NADPH (Bus and Gibson, 1984). Peroxidation of lipids results in an unstable membrane and disrupts lipid cycling, and NADPH is a key factor in lipid synthesis and cycling. Those events would result in cell-envelope stress and the response to those event is likely an immediate and short response. Senadheera *et al.* (2007) and Deng *et al.* (2007) measured *vicR* expression 15 min. and 2 h, respectively, after the induction of the stress. In this study and in Ahn and Burne (2007) study, stress was monitored over a longer period of time. Taken together, this would explained the difference between this study and their studies. Furthermore, it strongly supports the hypothesis *vicR* monitors cell-wall remodelling during growth and cell-envelope stress.

4.2.1 Proposed Model for the Regulation of *vicR* Expression Under Normal Growth Conditions and Cell-envelope Stress

As mentioned above, the level of *vicR* expression appears to be dependent on the rate of cell division and growth when *S. mutans* is not exposed to cell-envelope stresses. The dependence of *vicR* expression on active cell division indicates that the regulation of *vicR* transcription is embedded in the cell division process. Therefore under normal conditions, regulators controlling cell division are likely modulating expression of the *vicRKX* operon. More specifically, it is appropriate to suggest that *vicR* expression is controlled by the number of septums and replication forks at the onset of the C-period of bacterial division (Haeusser and Levin, 2008). The C-period is characterized by the initiation of DNA replication, elongation of bacterial cells, and termination of DNA replication.

The number of replication forks may play a more critical role than the number of septums given that rapidly dividing cells initiate new rounds of DNA replication before completing the previous rounds (Haeusser and Levin, 2008). Furthermore, the expression of *vicR* would be up-regulated at the beginning of the C-period because the VicRK TCS would be required to monitor the elongation stage which would be characterized by an increase in the length of the cell wall. However, it is unlikely that the amount of peptidoglycan biosynthesis precursors control the expression of *vicR* because it has been proposed that peptidoglycan precursors are the environmental signals inducing the VicRK TCS signaling cascade (Dubrac et al., 2008) and the VicRK TCS does not regulate its expression.

Under cell-envelope stress, the first responder class of cell-envelope stress response systems, which includes LiaFSR, are activated and modulate expression of

genes involved in cell-envelope synthesis. Induction of these genes is essential to repair of damage done by the stress (Jordan et al., 2008). In addition to cell-envelope repair activation, the LiaFSR TCS appears to control expression of a *spxB* homologue, which is a regulator that facilitates RNA polymerase binding (Suntharalingam et al., 2009; Veiga et al., 2007). In *L. lactis*, it was observed that expression of the *spxB* homologue was induced by the LiaFSR TCS. Furthermore, it was also observed that SpxB controls the expression of *oatA*, which encodes a protein that *O*-acetylates peptidoglycan, by facilating binding of the RNA polymerase complex to the promoter of *oatA* (Veiga et al., 2007). Deletion of the *spxB* homologue in *S. aureus* results in the reduced expression of *ftsZ*, which is part of the VicR regulon (Pamp et al., 2006). *S. mutans* encodes two potential homologues of SpxB, SMu1891 and SMu1044. It is possible that either or both SMu1891 and SMu1044 participate in the LiaFSR response and regulate *vicR* expression; however this remains to be investigated.

In summary, growth rate influences the number of replication forks and septums and, in turn, this modulates *vicR* expression by influencing. In the presence of cell-envelope stress, *vicR* expression is induced indirectly by the first-responder class of cell-envelope stress responders such as the LiaFSR system. In both cases, the VicRK system is needed to monitor cell-wall elongation and repair by sensing the level of peptidoglycan biosynthetic precursors (Fig 4.2)

4.2.2 Regulation of *vicR* Expression by the ComDE TCS

It was observed that the competence-associated TCS, ComDE, and the competence-stimulating peptide, CSP, were involved in the regulation of *vicR*. Senadheera and Cvitkovitch (2005) have reported that the addition of competence-

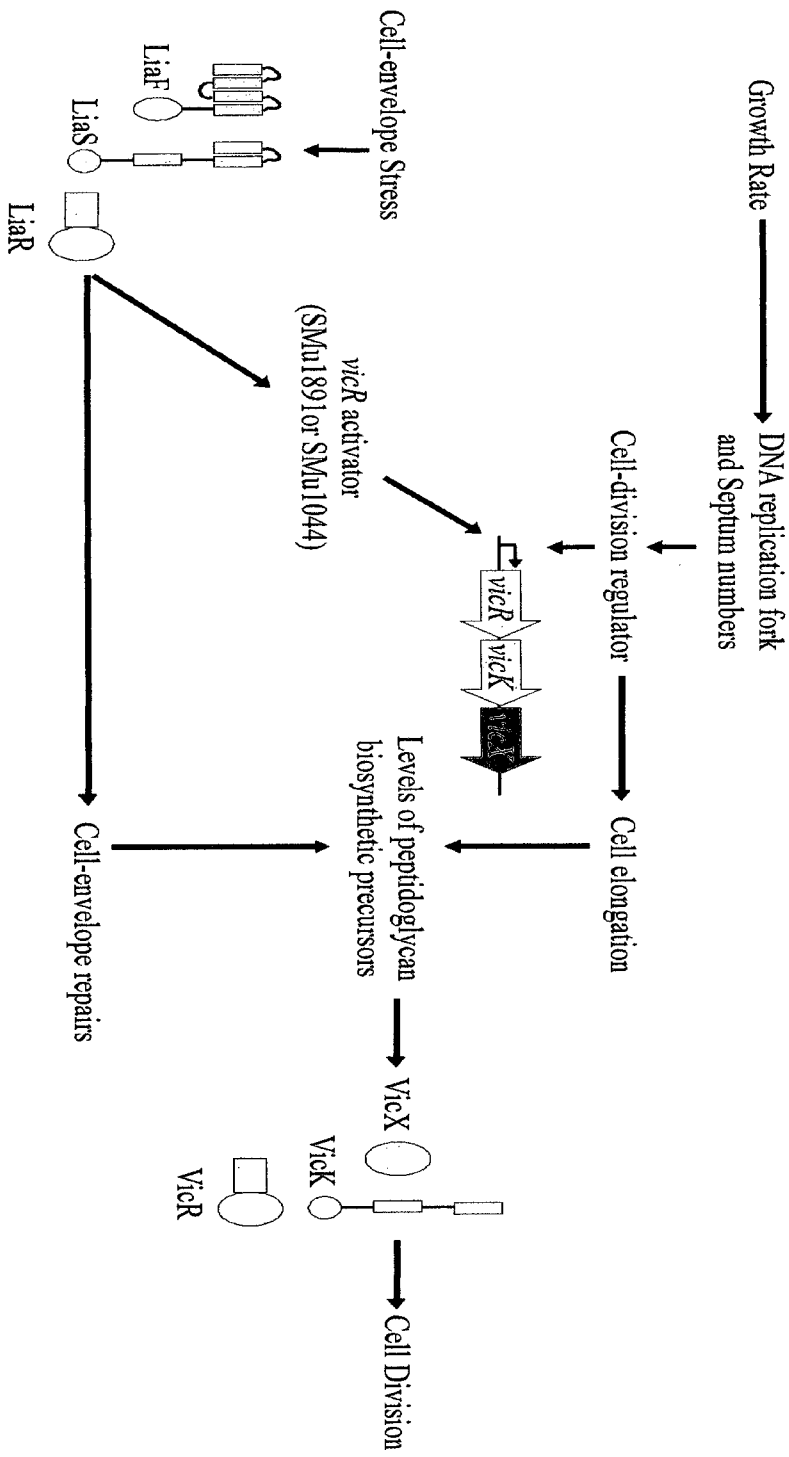

Fig 4.2. Proposed regulation of *vicR* under normal growth conditions and under cell-envelope stress.

stimulating peptide stimulated expression of *vicR* and *vicK* in the absence of the CSP-specific TCS, ComDE. The presence of the ComDE appears to have the opposite effect when exogenous CSP was added to growth media. The expression from P_{vicR} was decreased when the CSP was supplied to cells during early-exponential phase and CSP signaling was independent of ComX. When supplied exogenously, CSP is associated with a significant reduction in the rate of cell-division and even cell death in a ComX-independent manner (Qi *et al.*, 2005). Recently, expression of mutacin and CSP-induced cell death has been shown to be regulated by the ComDE TCS system in a ComX-independent manner. Furthermore, mutacin production induced by CSP results in lysis of *S. mutans* (Perry et al., 2009a). As a consequence, the lysis would result in a reduced rate of cell division which would lead to a decrease in the expression of *vicR*. This hypothesis fits within the proposed model of *vicR* regulation (Fig 4.2).

The addition of CSP results in decreased expression of *vicR* in cells cultured in HTVG and $TVG_{6.0}$ but the decrease was only significant in cells cultured in HTVG. In addition, *lacZ* expression from P_{comDE} was up-regulated in HTVG when compared to cell cultured in $TVG_{6.0}$. Therefore, an increase in expression of *comDE* in HTVG suggests that the bacteria would be more responsive to CSP under such growth conditions. Furthermore, a more drastic decrease in expression might be noticeable when the cells have a higher generation time than a lower one (HTVG vs $TVG_{6.0}$).

CSP did not induce *vicR* expression in the presence of ComDE TCS; however, a report by Senadheera and Cvitkovitch (2005) suggests the involvement of another TCS. In the absence of the ComDE TCS, the CSP is thought to signal through the CiaHR system (Ahn et al., 2006). In *S. mutans*, the CiaHR TCS is involved in competence development and stress tolerance. Additionally, the CiaHR TCS may also be involved in

the cell-envelope stress response. For example, it has been observed that *ciaHR* expression is induced by penicillin G (Rogers et al., 2007) and vancomycin in *S. pneumoniae* (Haas et al., 2005). Both antibiotics were shown to induce *vicR* expression. Furthermore, the CiaRH TCS prevented autolysis triggered by various environmental conditions and it was proposed that CiaHR plays an important role in ensuring cell-wall integrity (Mascher et al., 2006). It is therefore possible that CSP signaling through CiaHR induces *vicR* expression.

4.2.2.1 Hypothetical Model for the Regulation of vicR *Expression by the CSP and the ComDE TCS*

Based on the published results and those obtained in this study, a model for the regulation of *vicR* by the CSP and its associated TCS, ComDE is proposed (summarized in Fig 4.3). When exogenous CSP is added to the growth media and ComDE are present, CSP binds to ComD resulting the ATP-dependent autophosphorylation. The phosphoryl group is then transferred to ComE which activates its DNA-binding ability. ComE then represses the expression of *comC* but induces the expression of mutacin-associated genes and *comX*. Induction of mutacin genes increase mutacin production resulting in cell lysis (Perry et al., 2009a) which then decreases the rate of cell division and consequently, decreases the expression of *vicR*. The effect of mutacin is a part of the ComX-independent pathway. In the ComX-dependent pathway, ComX induces the expression of competence-related genes. In the absence of ComDE (ComDE-independent pathway), the addition of exogenous CSP induces the CiaHR TCS which represses mutacin production but induces *vicR* expression.

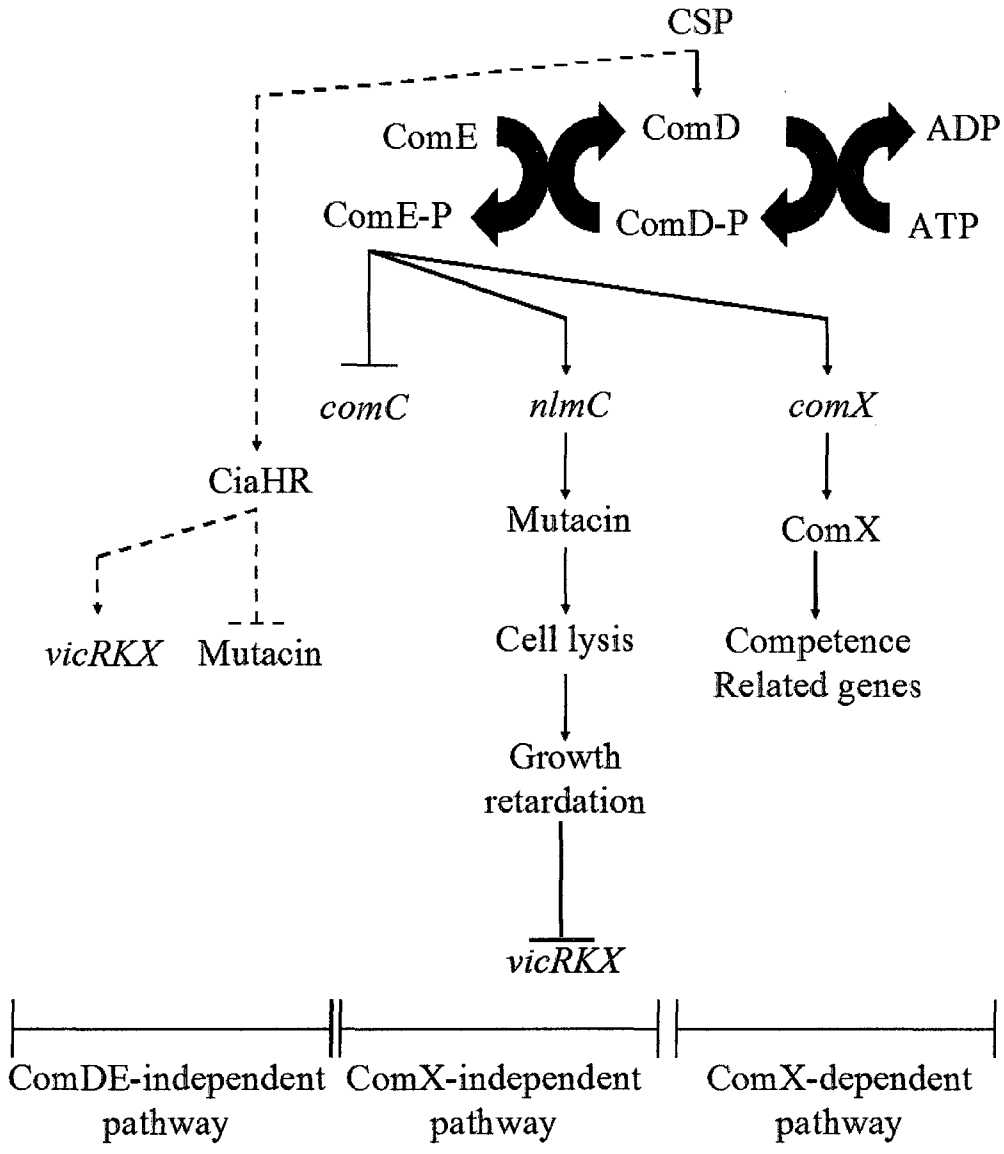

Fig 4.3 Proposed model of the regulation of *vicR* by ComDE system.

4.3 Analysis of LiaFSR TCS Mutant Phenotypes

The role of both LiaS and LiaR in virulence, biofilm formation, acid stress tolerance and mutacin production have been previously characterized in *S. mutans* (Li et al, 2002a; Tsang et al., 2005; Chong et al., 2008a; Li et al., 2008); however the impact of the deletion of the gene (*liaF*) located upstream of *liaS* and *liaR* had yet to be determined. In this study, the objective was to investigate the role of LiaF in biofilm formation, acid stress tolerance and mutacin production. The design of the primers and *erm*-cassette insertion site required for the construction of a Δ*liaF* mutant was based on the information available at the Oral Pathogen Sequence database in 2007. A study has recently reported that the *liaF* gene was erroneously annotated (Suntharalingam et al., 2009). The new start codon of *liaF* is located 123-bp downstream from that of previous reports (Ajdic et al., 2002). Furthermore, the promoter of the *liaFSR-ppiB-pnpB* is located within the newly realized 123-bp inter-genic region. Based on this information, the insertion of the *erm* cassette accidently deleted both the promoter region and the *liaF* gene, and therefore, the deletion of the promoter resulted in the inactivation of the *liaFSR-ppiB-pnpB* operon. Therefore, the phenotypes observed in the created Δ*liaF* mutant is the result of the inactivation of the entire operon rather than a single component.

Investigation into the growth kinetics of the LiaFSR$^-$, Δ*liaS* and Δ*liaR* mutants revealed that all three mutants had a delayed lag phase when cultured in $TVG_{6.0}$. Only the LiaFSR$^-$and Δ*liaS* mutants had a delayed lag phase when cultured HTVG and TVG. Similar delays were observed by Li et al (2002a) for both the Δ*liaS* and Δ*liaR* mutants when cultured in TYEG at pH 7.0 or pH 5.5 but there was a noticeably longer lag phase

in their studies for the Δ*liaR* mutant compared to Δ*liaS* mutant. In this study, the Δ*liaS* mutant had a longer lag phase than the Δ*liaR* mutant. One of the differences between this study and the study by Li et al. (2002a) is the growth media. As noted by Biswas et al. (2008), a Δ*liaS* mutant grew faster than the parent in defined minimal medium whereas growth rate was similar in a complex medium. Therefore, the culture media appears to have an effect on the growth of the Δ*liaS* mutant. It was also observed that the LiaFSR$^-$ and Δ*liaR* mutants cultured in TVG and $TVG_{6.0}$, and the Δ*liaS* mutant cultured in HTVG initiated entry into stationary phase at a lower cell density than the parent. This would indicate that the mutants are defective in their transition from exponentional phase to stationary phase and suggests that the LiaFSR TCS plays a key role during the transition. These observations are in agreement with those obtained in *B. subtilis* (Jordan et al., 2007). In *B. subtilis*, the *liaFSR* operon is up-regulated during the transition to stationary phase indicating that the LiaFSR system plays a role during that phase.

It was also found that the LiaFSR$^-$, and Δ*liaS* mutants autolyzed less than the parent when cultured in TVG and that the LiaFSR$^-$, Δ*liaS* and Δ*liaR* mutants autolyzed less than the parent when cultured in HTVG. The reduction in autolysis was, however, not always correlated with reduced expression of autolysin. The exception was the Δ*liaS* mutant cultured in HTVG in which the mutant appeared to produce less autolysin. Additionally, Li et al. (2002a) noted an increase in the length of the cell-chains formed by the Δ*liaS* and Δ*liaR* mutants. This would indicate a defect in cell separation and, thus, a decrease in autolysis. The change in autolysis profile in the absence of changes in autolysin-expression profile may help to provide a mechanism by which the LiaFSR system is linked to biofilm formation. Based on data accumulated in this study, it can be hypothesized that cell-wall modification in the mutants reduces the ability of the

autolysin, AtlA, to hydrolyse peptidoglycan. Such a hypothesis is supported by the fact that observable differences in cell-wall compositions between a wild-type *S. aureus* and *S. aureus* Δ*vraS (liaS* homologue*)* mutant have been described (Gardete et al., 2006). Furthermore, it has been demonstrated that the *L. lactis* LiaFSR systems controls O-acetylation of peptidoglycan. Increase O-acetylation of peptidoglycan results in reduction in hydrolysis of peptidoglycan by lyzozymes (Veiga et al., 2007). Additionally, it was observed that all three mutants were more sensitive to polymyxin B. Polymyxin B is a cationic anti-bacterial peptide and an increased sensitivity would indicate changes in the overall charge of the cell envelope as observed in *S. gordonii* (Chan et al., 2007). Change in cell-envelope charge is often indicative of cell-wall modification. In the case of the three mutants, the cell-wall modifications would be deregulated and would thus occur in the absence of stress. Such modifications would result in a decrease in hydrolysis of the peptidoglycan by AtlA. Reduction of cell-wall hydrolysis can have several consequences and in the case of *S. mutans*, deletion of *atlA* results in defective biofilm formation (Brown et al 2006; Shibata et al 2005).

One of the major phenotypic characterizations of the *liaS* and *liaR* deletion mutants was their inability to form proper biofilm. In this study, all three mutants failed to form a proper biofilm and the inactivation of the *liaFSR-ppiB-pnpB* operon had the greatest effect on biofilm fomation which clearly indicates that the LiaFSR system affect biofilm formation. These results are in agreement with the previously published study by Li et al. (2002a). Appropriately, the same authors hypothesized that the LiaFSR system plays a role in biofilm formation. Recently, Chong et al. (2008a) demonstrated that GbpC was up-regulated in a Δ*liaS* mutant but not in a *liaR* deletion mutant. Up-regulation of GbpC would offer an explanation for the lack of proper biofilm formation in the *liaS*

deletion mutant. However, GpbC expression has been shown to be directly regulated by the orphan RR CovR (Sato et al., 2000; Idone et al., 2003) and, recently, by IrvR (Niu et al., 2008). However, the data obtained in this study suggest an alternative hypothesis in which the LiaFSR system does not participate in the regulation of biofilm formation. Specifically, the LiaFSR system is thought to regulate cell-envelope modifications and homeostasis, and it has only been linked to biofilm formation in *S. mutans*. Furthermore, deletion of *atlA* results in changes in the profile of cell-surface-associated proteins (Ahn and Burne, 2006). It is therefore tempting to hypothesis that the cell-wall modification occurring in the LiaFSR$^-$, Δ*liaS* and Δ*liaR* mutants would reduce autolysis which would consequently modify the cell-surface-associated protein profile and the combined effects would result in poor biofilm formation. In conclusion, the LiaFSR system probably does not participate in biofilm formation.

The notion that the LiaFSR system controls cell-envelope homeostasis is further supported by the data collected using 2D-gel analysis. First, the 3-oxoacyl-(acyl-carrier-protein) synthase was identified as being down-regulated in the Δ*liaS* mutant cultured in HTVG. This enzyme is an important player in the metabolism of fatty acid and phospholipid and down-regulation of the enzyme could influence cell-envelope homeostasis. Second, all the enzymes and some related isoforms involved in transforming β-D-fructose $6P_2$ to glycerate $3P_2$ during glycolysis were identified as being differentially regulated in one or more of the mutants (Fig 4.4). The greatest difference was the shift from two equal FbaA isoforms (spot 219 and 220) in the parent to a dominant FbaA isofrom (spot 219) in all mutants cultured in $TVG_{6.0}$ and the Δ*liaR* mutant cultured in HTVG. As identified by 2DGE, the production of phosphoglycerate

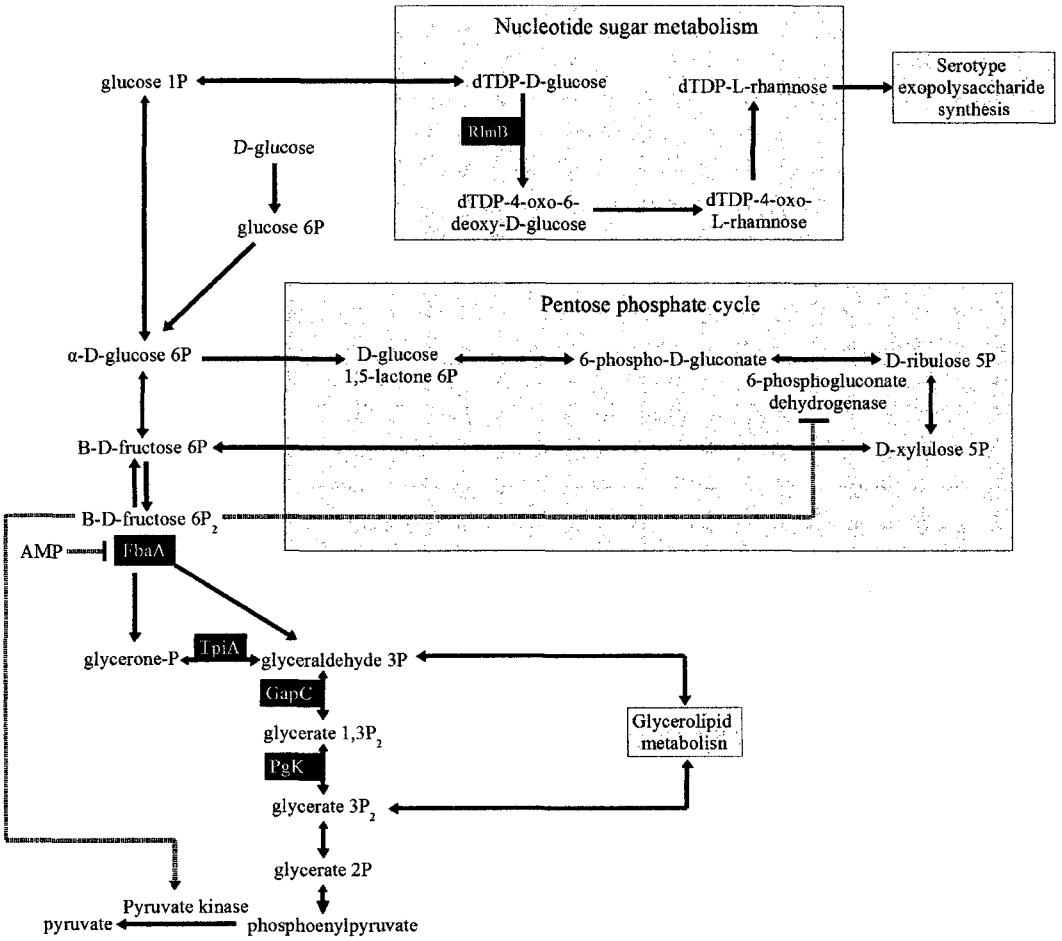

Fig 4.4. Glycolysis and related pathways impacted by the deletion of the LiaFSR system. Proteins that were identified as differently regulated by the inactivation of one or more of the LiaFSR TCS genes are boxed in black. Regulation is indicated by dashed lines.

kinase was also greatly reduced in the Δ*liaS* mutant cultured in HTVG. This reduction also resulted in a decreased in enzymatic in the same mutant. This part of the glycolysis pathway is of particular interest because glyceraldehyde 3P, a product generated by the enzymatic activity of FbaA, and glycerate $3P_2$ are intermediates used in glycerolipid metabolism which is required for cell-wall and cell-membrane component synthesis. Additionally, a search for a LiaR-binding site in the promoter of the gene encoding the glycolysis-pathway enzyme revealed that none of the promoters had a strong match for the LiaR-binding site. Thus, it appears that the LiaFSR system does not directly regulate the glycolysis pathway and that the changes observed are likely indirect effects caused by changes in glycerolipid metabolism and fatty-acid turn over.

Changes in the level of enzyme involved in the glycolysis pathway are also of particular interest for another phenotype of these three mutants: acid sensitivity. A recent study by Korithoski et al. (2008) identified pyruvate dehydrogenase E1α sub-unit as a key enzyme improving acid tolerance. This enzyme converts pyruvate to acetyl-CoA which is subsequently catalyzed into ethanol and acetate to yield additional ATP. The proposed change in glycerolipid metabolism would hijack the intermediates converted during glycolysis. A reduction in glycolysis intermediates would results in a reduce amount of pyruvate available for the production of ATP. This consequently predisposes the mutants to be more sensitive to acid shock by reducing the ability of *S. mutans* to produce and store ATP given that aciduricity in *S. mutans* is largely mediated by a F_1F_0-ATPase proton pump. A reduced pool of ATP during an acid shock would reduce the ability of *S. mutans* to quickly initiate the ATR. This predisposition is probably made worse by the uncontrolled cell-wall modifications occurring in all three mutants. Therefore, the sensitivity of the mutants to acid is likely to be multifactorial and it is

unlikely that the LiaFSR directly controls acid adaptation because all three mutants were able to grow in and adapt to an acidic condition.

Other proteins that were identified as differentially regulated help support the idea that the sensitivity of the mutants to acid shock is multifactorial. A dTDP-D-glucose 4,6 dehydratase (RmlB) was identified as being down-regulated. RlmB appears to be required for growth in the presence of sucrose. When cultured in the presence of sucrose, the dTNP-rhamnose synthesis-deficient mutant recombines *gtfB* and *gtfC* and creates a *gtfBC* hybrid gene (Yamashita et al., 1999). The recombination of *gtfB* and *gtfC* has been implicated with increased fitness of the glucan-binding protein A (*gbpA*) mutant when grown in a medium that acidifies (Banas et al., 2007). The recombination of both *gtfB* and *gtfC* is thought to alleviate the stress-induced by a malformed biofilm by changing biofilm morphology and preventing acid-killing. Therefore, RlmB down-regulation could result in increased acid-shock sensitivity. Furthermore, PpaC a member the *dlt* operon was identified as being downregulated, suggesting that the entire operon is also downregulated. The gene products of the *dlt* operon add D-alanine ester to lipoteichoic acid and improves the survival of *S. mutans* when grown under acidic conditions (Boyd et al., 2000). Therefore, the lipoteichoic acids of the Δ*liaS* mutant probably have a reduced level of D-alanine and could potentially explain the sensitivity of the Δ*liaS* mutant to acid shock. Additionally, the expression of a cystein synthesase was down-regulated in the LiaFSR$^-$ mutant cultured in $TVG_{6.0}$. This enzyme was identified as up-regulated during acid shock by Li et al. (2002a) and in biofilm (Rathsam et al., 2005). Furthermore, the promoter of *cysK* possessed a strong match for a LiaR-binding site suggesting that it might be directly regulated by the LiaFSR TCS.

Two other down-regulated proteins are SodA and GreA, both proteins could play a role in the overall homeostatic state of the cell. Superoxide dismutases (SodA) are involved in the detoxification of toxic oxygen species and are up-regulated when *S. mutans* is grown aerobically (Martin et al., 1984). The growth kinetics of the parent and mutant strains were established in atmospheric oxygen. Cytoplasmic proteins were isolated from bacteria cultured under these conditions. Therefore, down-regulation of SodA might explain the reduced growth rate of the *ΔliaS* mutant cultured in HTVG due to an increase in toxic oxygen species. Second, GreA was identified as being down-regulated in the LiaFSR$^-$ mutant cultured in $TVG_{6.0}$. GreA is required to ensure optimal transcription (Artsimovitch et al., 2004). Thus, a reduced amount of GreA could explain the poor response of the LiaFSR$^-$ mutant cells. Specifically, the LiaFSR$^-$ mutant cells cultured in $TVG_{6.0}$ would be in sub-optimal transcriptional state which results in the sub-optimal response to stress.

The hypothesis that the LiaFSR system does not control acid adaptation is clearly supported by the fact that the LiaFSR$^-$ mutant was able to adapt to an acidic environment despite the inactivation of the LiaFSR TCS. The hypothesis is clearly in disagreement with the results reported by Li et al. (2002a). The discrepancy may be explained by the differences in methodology. For example, when using the method for acid adaptation described by Li et al. (2002a) in this study, it yielded inconsistent results and it was impossible to reach similar results and conclusion. However, a detailed analysis of two studies by the same group (Li et al., 2001a and 2002a) suggest possible pitfalls in their analysis. Li et al. (2001a) described that acid adaptation of *S. mutans* was dependent on density and growth phase. In a later study, the authors used a fixed time (2h) for all strains as a measure of growth phase rather than culture density (Li et al., 2002a). It is

clear from the results of their study and this study that the LiaFSR$^-$, Δ*liaS* and Δ*liaR* mutants have different growth kinetics. Therefore, Li et al. (2002a) probably compared the adaptation of cells during different growth phases. Another reason for the discrepancy is the difference in buffers used. The phosphate-citrate (40 mM) buffer used by Li et al. (2002a) does not have the capability to maintain pH above 7.0 (data not shown). Furthermore, the variation of growth phase mentioned above would have influenced the pH of the culture at the time of the shock and could have influenced the ability of the strains to survive an acid shock. Therefore, all the above-mentioned confounding factors would have influenced the results of Li et al. (2002a) leading the group to reach the conclusion that the LiaFSR TCS controls acid adaptation in *S. mutans*.

The SEM results clearly demonstrate that, like the Δ*liaS* and Δ*liaR* mutants, the LiaFSR$^-$ mutant had impaired biofilm formation and this is in agreement with the results reported by Li et al. (2002a). However, the results from the microwell asssay was noticeably different than those previously reported in the literature (Bhagwat et al., 2001; Li et al. 2002a). For example, Li et al. (2002a) observed a decrease in biomass accumulation for both the Δ*liaS* and Δ*liaR* mutants whereas Bhagwat et al. (2001) showed an increase in the accumulation of biomass by a Δ*liaR* mutants. In both studies, the authors used a semi-defined medium similar the DBM used in the study. The key difference is that Bhagwat et al. (2001) and Li et al. (2002a) added Casamino Acids instead of individual amino acids and that Li et al. (2002a) omitted Mn in their medium. Casamino acids may contain metals. Trace metals such as Mn have been reported to affect the accumulation of biomass by *S. mutans* (Arirachakaran et al., 2007a). The effect of trace elements, such as calcium, have also been observed in the biofilm formation of a Δ*ciaX* mutant. This mutant was not able to create a biofilm in the absence of calcium (He

et al., 2008). An additional difference between this and previous studies was the dye used to measure biomass. In this study and the one by Li et al. (2002a), safranin was used to stain the biofilm, whereas in the study by Bhagwat et al. (2001), crystal violet was used. Each stain binds to different bacterial components and therefore, differences in dye absorption by the biofilm may be due to differentially regulated components. The results obtained in this and previous studies clearly show the limitations of analyzing biofilm formation of *S. mutans* using a microwell approach. The approach is likely better suited to characterize mutants or growth conditions that completely abrogate any biofilm formation (all-or-none phenotypes).

At a first glance, the regulation of mutacin appears not to fit into the cell-envelope stress model; however, a focus look at the microbial ecology of the mouth offer an explanation. Several oral bacteria produce bacteriocins against competing oral bacteria and bacteriocins often attack the cell envelope (Kreth et al., 2008b). Given that the LiaFSR is thought to sense disturbances in the cell-envelope, the damage caused by bacteriocins would induce the LiaFSR system and indicate the presence of competing oral bacteria. In response to the threat, *S. mutans* would differentially regulate mutacin production to either eliminate the threat. The production is, however, probably indirectly controlled by the LiaFSR TCS. Two proteins, IrvR and IrvA, have been associated with the control of mutacin production (Niu et al., 2008; Tsang et al., 2006). IrvR has been identified as the repressor of *irvA*. The expression of *irvR* is repressed by the LiaFSR TCS (Tsang et al., 2006). IrvA is also a repressor of mutacin I-associated gene, *mutA*. It has been proposed that IrvR activity would be regulated by stress signals and IrvA and IrvR would act as a regulatory pair. Therefore it would appear that the LiaFSR TCS directly regulates the expression of *irvR*. The potential differential regulation of *irvR*

would provide an explanation for the lack of mutacin production observed in a Δ*liaS* mutant. However, the LiaFSR$^-$ mutant did not produce mutacin in the absence of LiaR, whereas the Δ*liaR* mutant produces mutacin in the absence of LiaR. Therefore, it appears that LiaR is not the only component of the LiaFSR system controlling the expression of *irvR* or mutacin expression. It is clear that the LiaFSR system participates in mutacin production but the role of its individual components should be investigated in greater detail.

Despite the major phenotypes exhibited by the mutants of the LiaFSR TCS, the expression of *liaF*, *liaS* and *liaR* was below the detection threshold in mid-exponential phase cells cultured in $TVG_{6.0}$ and the *liaF* transcript was the only one detected in cells cultured in HTVG to mid-exponential phase. The low levels of *liaF*, *liaS* and *liaR* transcript has been reported in *S. aureus* cultured in the absence of stress (Yin et al., 2006). Furthermore, the expression of *liaFSR* in *B. subtilis* is up-regulated during the transition from exponential phase to stationary phase (Jordan et al., 2007). This suggests that the expression of *liaFSR* would be repressed during mid-exponential phase. Additionally, only the *liaF* transcript was detected. Furthermore, up-regulation of *liaR* in YDNT005 was not associated with a similar up-regulation of *liaF*. This suggests that at least *liaF* can be transcribed independently of *liaS* and *liaR* and that *liaR* can be expressed from a different promoter. The regions preceding and immediately following the *liaF*, *liaS* and *liaR* genes were analyzed for the presence of promoter and terminator sequences (Fig 4.5 and 4.6). All three genes had possible promoter elements but the strongest matches were found in the regions preceding *liaF* (Fig 4.5A). Based on a recent study (Suntharalingam et al., 2009), the promoter region is likely 123-bp downstream of the currently annotated start codon of *liaF* (Fig 4.5B). The region preceding *liaS* also has

Fig 4.5. Promoter Analysis of the DNA sequence immediately upstream of *liaF, liaS* and *liaR* start codon. The sequence immediately upstream of the annotated start codon of *liaF* (A), the alternative start codon of *liaF* proposed by Suntharalingam et al. (2009) (B), *liaS* (C) and *liaR* (D) were analyzed for promoter elements including the transcription start site (TS), the -10 and -35 box, the ribosome binding site (RBS), inverted repeats stem loops and potential regulatory-protein binding site. The LiaR-binding site in panel (A) represents the best potential match based on the predicted postion of the -35 site and the presence of inverted repeats immediately upstream of the -35 site. The similarity score is 6/14 (20%) and the proposed sequence is 2-bp longer than the 14-bp consensus (see Fig 4.1). The LiaR-binding site in panel (B) is the sequence proposed by Suntharalingam et al. (2009) and it has a similarity score 9/14 (64%).

A

TAAATAAAGAAATAGGTAAAACAAGGACTGAGAAGAATCTTCTCAATCCTTGT
TTTTATATATCATGGCTCGAACTATTGAATGATATAGGCGGTTAATTATATGATTT
ATTAGGTCATCATGTCAATTCAAGTTATGTTTATGATCTGTTGATAATAATGGTTA
Predicted *E. coli* PhoP binding site
TCTAATGCAGGTATACTCATATGTTGTAGTTATTATATTTATAAGTTTAAGGTTCTT
GCCTCAGCCTCCTTGTTTGAAGAGATAACTTTTTTGTTATCAAACTTGTATCCGT
LiaR-binding site -35
CTAGGATTAAGACTGTATAAGATTGATGTATGATAACTAAGCT**ATG**-*liaF*
-10 TS RBS

B

Annotated Start Codon

ATGGCGTCTTTGATATTTGAAAAATTCTCTTTATCTTTAGTGTTATTTGGTCTAG
LiaR-binding site
ATCAAGAGGTGAAATTTATCCTAAATTTTGATACAATGACTAATAATTGTAGAA
-35 -10 TS
CTGAAGGAAGCCTT**ATG**-*liaF*
RBS

C

CAGCATCTATGGCTATGTTCGCTTTTTTGATGCACCAGAATATGATTTGCGCA
Predicted *E. coli* OxyR-binding site
ATGAGGAAATTAGACTGTCTGATCATATAGATGGAAGAACCAAATCTGTAAA
-35
AATTATCATCAATGTCATTGCGGGCTTGGTGGAGGTAGAACGTATATG-*liaS*
-10 TS RBS

D

TTGGTTTTGATATGGATGTCGTTCGAGATTTGAGTTACGGCTTGAAAAACAT
CGAAGATCGCGTTAATGATTTAGCTGGGACAGTAAAGTTTTTAAGTGCTGAA
-35
AATAAGGGGGTTGTTATGGATATCCATGTACCAATAATGAAAGGGG**ATG**-*liaR*
-10 Stem-loop TS RBS

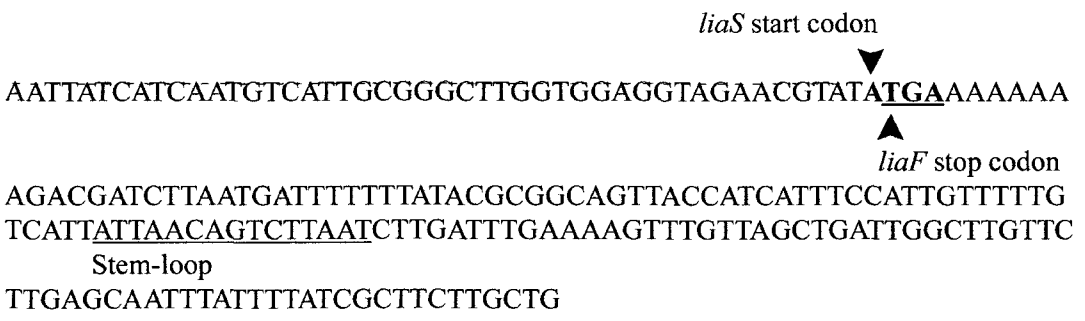

Fig 4.6. Sequence analysis of the the DNA sequence immediately downstream of *liaF* stop codon. The sequence immediately downstream of the stop codon of *liaF* was analyzed for stem loops and Rho transcription termination sequences. The *liaS* start codon and the *liaF* stop codon are indicated.

strong promoter sequences (Fig 4.5C). Additionally, a stem-loop was present in the region immediately downstream of the *liaF* stop codon (Fig 4.6). The presence of a stem-loop would suggest that *liaF* transcription can be terminated in a Rho-independent manner. The expression and the *in silico* analysis suggest that at least two promoters and at least two transcripts exits. The first transcript would be initiated from the promoter preceding *liaF* and would only encode for *liaF*. A second transcript would be iniated from the promoter preceding *liaF* and would encode the entire operon (*liaFSR-ppiB-pnpB*). A third possible transcript would be initiated from the *liaS* promoter and encode for *liaSR-ppiB-pnpB*. Different transcript sizes have been observed in *S. aureus* and include one with the complete operon but also one transcript containing only *liaS* and *liaR* (Yin et al., 2006). However, transcription appears to be driven from only one promoter, although a secondary but minor transcription start site was observed.

An alternative hypothesis to transcription driven from a secondary promoter is post-transciptional processing of the *liaSR-ppiB-pnpB* transcript. Such processing has been reported for the *LEE4* operon of enterohemorrhagic *E. coli* (Lodato and Kaper, 2009). In the example mentioned, the post-transcriptional processing was characterized by an inverted repeat resembling a Rho-independent transcription terminator that was located within an open reading frame. Such an inverted repeat is found in the *S. mutans liaS* gene (Fig 4.6). Interestingly, the deletion of the *S. aureus liaSR* was associated with disapearance of most transcripts with the exception of the transcript encoding the whole operon (Yin et al., 2006).

Alternatively, the up-regulation of *liaR* in the Δ*liaS* mutant may be due to a polar effect caused by the insertion of the *erm* cassette. Yin et al. (2006) also noted the disapearance LiaR due the insertion of the *erm* cassette in *liaS*. Furthermore, the

introduction of a kanamycin resistance marker in *ciaH* was also associated with up-regulation of the upstream gene, *ciaR*, in *S. mutans* (He et al., 2008). Therefore, a polar effect caused by the insertion of the *ermAM* cassette in *liaS* cannot be excluded.

Despite the possibility of a polar effect, the phenotypes associated with the Δ*liaS* mutant are clearly influenced by the over-expression of *liaR*. Futhermore, it indicates that the LiaFSR TCS autoregulates its expression unless over-expression is due to a polar effect. In contrast to the Δ*liaS* mutant phenotype, the phenotypes of the LiaFSR$^-$ and Δ*liaR* mutants are associated with the absence of *liaR* transcripts.

4.3.1 Proposed Model for the Regulation Cascade of the LiaFSR System

Based on the information gathered, a preliminary model for the regulation by the LiaFSR TCS is proposed (summarized in Fig 4.7). In the absence of stress and during exponential growth, *liaF* is transcribed from its promoter at a very low level and transcription is stopped at the stem-loop found in *liaS*. Both *liaS* and *liaR* are also expressed but at a much lower level than *liaF*. Despite the low level expression, the LiaFSR system is crucial for sensing a stimulus during exponential growth. The nature of the signal is unknown but Butcher et al. (2007) identified a small peptide and an associated ABC-transporter that induced the LiaFSR TCS signaling pathway in *B. subtilis*. Butcher et al. (2007) did not identify a homologue in *S. mutans* but bidirectional analysis of the annotated genome revealed that *S. mutans* encodes a homologue of *yycH*, one of the genes located in the *B. subtilis* ABC transporter and small peptide locus. This homologue, SMu0340, is located in locus encoding an ABC transporter (SMu0335 and SMu0336), two small peptides (SMu0342 and SMu 0343), an oxidoreductase (SMu0341) and an aminotransferase (Smu0339). In *B. subtilis,* an oxidoreductase and an

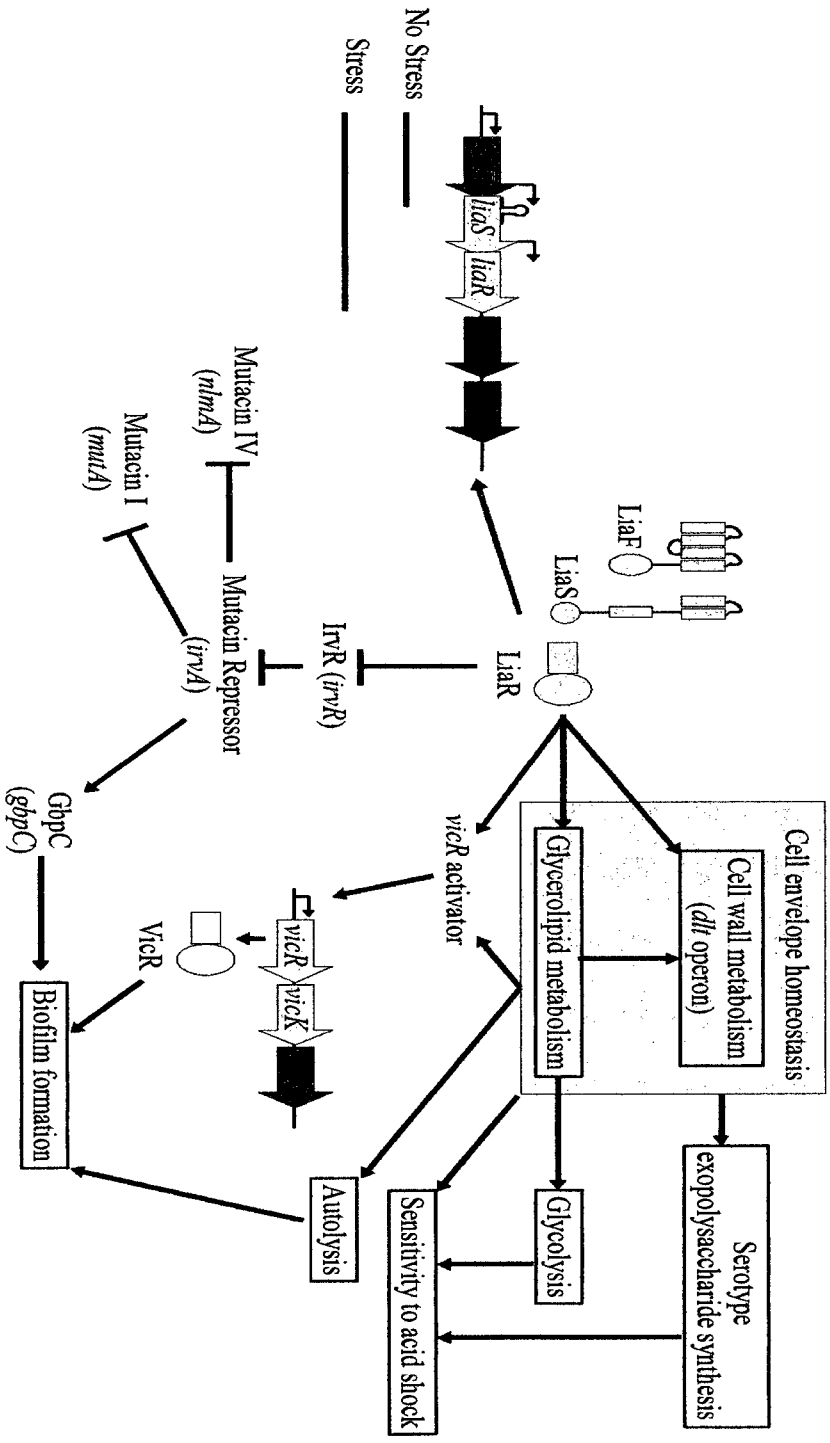

Fig 4.7. Proposed model of regulation by the LiaFSR system.

aminotransferase are involved in processing of the small peptide. Hypothetically, this locus possibly produces a peptide that is sensed by the LiaFSR system. Furthermore, the peptide expression is induced at the onset of the transition from exponential phase to stationary phase (Butcher et al., 2007). The peptide is expressed during the growth phase when expression of the *liaFSR* operon is activated and when the LiaFSR TCS is thought to play a key role.

LiaS activity also appears to be important during exponential phase. In the absence of LiaS, *liaR* transcript was more abundant and regulation of *liaFSR* expression by LiaR has been implicated in *B. subtilis* (Jordan et al., 2006) and *L. lactis* (Martinez et al., 2007). Given that LiaR DNA-binding activity is optimal when phosphorylated and dimerized (Belcheva and Golemi-Kotra, 2008), the activation of gene expression by LiaR would require phosphorylation of the RR by LiaS or another phosphoryl donor. Furthermore, it has been established that LiaS possesses both kinase and phosphatase activity (Belcheva and Golemi-Kotra, 2008). Therefore, LiaR may be phosphorylated by LiaS in the presence of stresses and dephosphorylated by LiaS in the absence of stress. In the absence of LiaS, LiaR would be phosphorylated by another phosphoryl donor regardless of the condition and the active phosphorylated LiaR form would become the dominant isoform. This would activate gene expression in an uncontrolled manner. The LiaR regulon in *S. mutans* has yet to be established but it is known that LiaR in other Gram-positive organisms controls the expression of genes encoding proteins associated with cell-wall synthesis (Jordan et al., 2008). In *S. mutans*, LiaR appears to repress *irvR* which in turn, represses mutacin production. Assuming the LiaR regulon is fairly conserved, the LiaFSR TCS would maintain cell-envelope homeostasis in the presence of a stress and mutants of the TCS would deregulate the homeostasis. Changes in

homeostasis would impact the composition of the cell wall, as observed in *S. aureus* (Gardete et al., 2006). Furthermore, changes in the composition of the cell-wall would decrease the ability of autolysins to digest the cell wall resulting in a decreased level of autolysis. Decreases in autolysis would also impact surface protein expression and decrease biofilm formation as noted previously (Brown et al 2006; Shibata et al 2005; Ahn and Burne, 2006). In addition to affecting biofilm formation, the imbalance in cell-envelope homeostasis would affect glycolysis and exopolysaccharides synthesis as observed in the 2D-gel data. Additionally, the effect on glycolysis and synthesis of exopolysaccharide, and changes in cell-wall composition would predispose *S. mutans* to acid shock.

To summarize, an activated LiaFSR TCS represses the expression of *irvR* which results in the repression of mutacin and modulates the level of GbpC. The level of GbpC impacts biofilm formation. In addition to *irvR*, the TCS induces the expression of yet-to-be-identified *vicR* activatior which induces *vicR* expression resulting in proper monitoring of cell-wall repair. The activated LiaR also modulates cell-envelope homeostasis which impacts cell-wall composition. Modifications to cell-wall composition reduces autolysis and prevents the lysis of *S. mutans* during stress.

4.4 General Conclusion

In this thesis, it was established that the suicide vector, pCovR/981, inserted into the *murA1* gene (SMu1386) and not in the *vicR* gene as previously thought (Lee et al., 2004). This clearly indicates that the VicRK TCS was not responsible for the phenotypes observed in the mutant.

When identifying environmental and bacterial factors affecting *vicR* expression, it was established for the first time that *vicR* expression is induced by cell-envelope stressors. The LiaFSR TCS was identified as a regulator of *vicR* expression. Furthermore, it was also confirmed that the expression of *vicR* is growth-phase dependent. It was concluded that in the absence of stress, *vicR* expression was growth-phase dependent. Additionally, results obtained in this thesis indicate that the stimulus activating the VicRK TCS signaling cascade is different from the environmental factor inducing *vicR* expression. This thesis provides a preliminary hypothetical model in which the expression of *vicR* is embedded in the cell-division process and is possibly controlled by general regulators of cell division. This model fits and complements the current VicRK signaling-cascade model suggested by Dubrac et al. (2008). Given that *vicR* is widely conserved among the the *Bacilli* class, this model can probably be applied to most members the class. Furthermore, the LiaFSR TCS is possibly a regulator of *vicR* in other members of *Bacilli* class because this TCS is widely conserved among several members of the class.

Mutants lacking components of the LiaFSR system were also characterized with respect to several processes such as mutacin production and biofilm formation. These experiments indicated that the mutants have cell-wall modifications resulting in defects in several biological processes. The observation made in this thesis provides a preliminary model and framework for identifying the causes of the *liaFSR* mutant phenotype. This model possibly applies only to *S. mutans* and related oral streptococci; however, certain elements of the model can be used to make inferences for other Gram-positive bacteria.

4.5 Future Directions

The work presented in this thesis has provided insights into the regulation of the RR *vicR* and the role of the LiaFSR system. Over the course of this thesis, several hypotheses were formulated which require testing. Several of these hypotheses can be tested using biochemical assays and basic molecular biology tools. In the case of the *murA1* mutant, it was suggested that peptidoglycan biosynthetic precursors accumulate. Therefore, the *murA1* mutant should be analyzed for the accumulation of petidoglycan precursors. Furthermore, it is important that the novel carbohydrate secreted by the *murA1* mutant be identified because it will help formulate a better hypothesis.

In the case of *vicR* expression, it was hypothesized that SMu1891 and SMu1044 expression is induced by the LiaFSR TCS and that either protein can participate in the up-regulation of *vicR* expression. Therefore, the genes encoding SMu1891 and SMu1044 proteins should be deleted in the *S. mutans* Δ*liaS* mutant carrying the P_{vicR}-*lacZ* fusion.

It was also hypothesized that CSP signals throught another TCS which is involved in the regulation of *vicR* expression. To test this hypothesis, the activity of the *vicR* promoter should be measured in a Δ*comD*, Δ*comE* and Δ*comDE* mutants. in the presence and absence of the CSP. Furthermore, the gene encoding the RR CiaR or the HK CiaH should be deleted in the *S. mutans* strain carrying the P_{vicR}-*lacZ* fusion. The activity of the *vicR* promoter should then be measured in these mutants.

It was hypothesized that the composition of the cell wall and cell membrane would different in the *liaFSR* TCS mutants. Therefore, the composition of both bacterial components could be analyzed to test this hypothesis. Additionally, a zymogram using the cell wall of the LiaFSR$^-$, Δ*liaS* and Δ*liaR* mutants cultured in HTVG could be done to

test autolysin activity of strain UA159. It has also been suggested that cell-envelope proteins are differential regulated in the LiaFSR$^-$, Δ*liaS* and Δ*liaR* mutants. Therefore, 2DGE analysis should be done on cell-wall proteins and cell-membrane proteins of the parental and mutant strains. It was also observed that the LiaFSR$^-$, Δ*liaS* and Δ*liaR* mutants could not maintain the integrity of their biofilms as they aged. Recently, Perry et al. (2009b) identified DNA as an important component of the *S. mutans* biofilm and highlighted the importance of cell lysis during biofilm maturation. Therefore the biofilm of the LiaFSR$^-$, Δ*liaS* and Δ*liaR* mutants should be analyzed for their DNA content.

Appendix 1. Unedited DNA Sequences from the PCR Confirming the Deletion mutants.

The DNA sequence was analyzed using the BLASTN function found on the NCBI website and the oral pathogen database website. *S. mutans* genomic sequences are bolded and the *ermAM* sequence is shaded in gray. Arrows delineate specific DNA-sequence regions. Start or stop codons are in capital letters. Restriction site are underlined.

> YDNT006 - primer SL160

cctgacttgattatattggacttaatgttaccagaactagacggtcttgaagtggctaaggaagttagaaaaaacagcca
→*vicR*
tgttccaattattatgttatcagctaaagacagtgagtttgataaggttattggtcttgaaattggtgctgatgattatgtga
ctaaacctttttctaatcgtgaattactggcgcgtgtaaaagcgcatcttcgccgtactgaaaatattgaatccgcagtgg
ctgaggaaaatgcttcaggtatacctgaaattattattggggacttgcaaatcttaccagatgcttttgttgctaaaaaac
gtggaacagaggtagagttaactcaccgtgagtttgagttgttgcatcacttagcgacacacacaggtcaggtgatgac
gcgtgaacatttacttgaaacggtttggggctatgattattttggagatgtccgtactgttgatgttactgttcgtcgtctgc
gtgaaaaaattgaagatacacctagtcgtccagagtacattttgacgcgacgcggtgttggttattacatgaaatcat<u>A</u>
vicK→
<u>TGacTAA</u>tgtgtttgaatcaagtccctgggg<u>cctccggccgg</u>tatactggccggcagcgactcatagaattatttcctccc
vicR← *vicK ←* SfiI cut site *→ ermAM*
gttaaataatagataactattaaaaatagacaatacttgctcataagtaacggtacttaaattgtttactttggcgtgtttcattgcttgat
gaaactgatttttagtaaacNNNNgacgatattctcgattgacccattttgNNacaaNgtacgtatat

> YDNT006 - primer SL180

gattcgtcttcatcttcttcccattcatcaattgcatcattatcgttttcacaaggtaaaacgatggtaaaggtcgacccttc
gccttcctcactattggcccaggcggccgggcccaaaatttttgatttgtatcttaaaatttgtataataggaattgaagttaaat
vicK ← SfiI cut site *→ ermAM*
tagatgctaaaaatttgtaattaagaaggagtgattacatgaacaaaaatataaaatattctcaaaacttttaacgagtgaaaaagt
actcaaccaaataataaaacaattgaatttaaaagaaaccgataccgtttacgaaattggaacaggtaaagggcatttaacgaN
NNaaNtggctgaaataagtaaacaggtaacgtctattgaattagacagtcatctattcaacttatcgtcagaaaaattaaaactg
aatactcgtgtcactttaactcaccaagatgttctacagtttcaattccctaacaaacagaggtataaaattgttgggagtattccttac
catttaagcacacaaattattaaaaaagtggtttttgaaagccatgcgtctgacatctatctgattgttgaaNNaggattctacaag
cgtaccttggatattcaccgaacactagggttgctcttgcacactcaagtctcgattcaNNaattgcttaagctgccagcggaat
gctttcatcctaaaccaaaagtaaacagtgtcttaataaaacttacccgccataccacNNNNNNtccggNNNaatattgN
NNNNtatataNNNNNtttgttNNNNNNNgggtcaatNNNNNNNNNcgtcaactgttNNNNNaaaat
c

> YDNT004 - primer SL179

tcctttcttNNNccttagacctttctattatagcaaaaatcacccagaacaaccatttccgagtaatctttgtttttcattct
tccttttaagctgtcca<u>CTA</u>gatttttgctaatggtaaagcagtatctggcgggtatcNNN<u>gcccaggcggccgggcc</u>
→ vicX *vicX←* SfiI cut site

caaaatttgtttgatttgtatcttaaaattttgtataataggaattgaagttaaattagatgctaaaaatttgtaattaagaaggagtgatt
→ *ermAM*
acatgaacaaaaatataaaatattctcaaaactttttaacgagtgaaaaagtactcaaccaaataataaaacaattgaatttaaaaga
aaccgataccgtttacgaaattggaacaggtaaagggcatttaacgacgaaactggctgaaataagtaaacaggtaacgtctatt
gaattagacagtcatctattcaacttatcgtcagaaaaattaaaactgaatactcgtgtcactttaactcaccaagatgttctacagttt
caattccctgacaaacagaggtataaaattgttgggagtattccttaccatttaagcacacaaattattaaaaaagtggtttttgaaag
ccatgcgtctgacatctatctgattgttgaagaaggattctacaagcgtaccttggatattcaccgaacactagggttgctcttgcac
actcaagtctcgattcagcaattgcttaagctgccagcggaatgctttcatcctaaaccaaaagtaaacagtgtcttaataaaactta
cccgccataccacaggtgttccggataaatattggaagctatatacgtactttgttNNNNNNtgggtcaatcgNNNNNa
ccgtcaactgtttactNNNaatcagtttcatcaagcaatgaaaNNNNNcaaagtaaacaatttaagtaccgttacttatgN
NNNNgtattNNNNNNNNNNNNNNNNNctattNNNNNacg

> YDNT016 - primer SL160
atcctgacttgattatattggacttaatgttaccagaactagacggtcttgaagtggctaaggaagttagaaaaaacagc
→*vicR*
catgttccaattattatgttatcagctaaagacagtgagtttgataaggttattggtcttgaaatgggtgctgatgattatgt
gactaaacctttttctaatcgtgaattactggcgcgtgtaaaagcgcatcttcgccgtactgaaaatattgaatccgcNN
tggctgaggaaaatgcttcaggtatacctgaaattattattggggacttgcaaatcttaccagatgcttttgttgctaaaaa
acgtggaacagaggtagagttaactcaNcgtgagtttgagttgttgcatcacttagcgacacacacaggtcaggtgatg
acgcgtgaacatttacttgaaacggtttggggctatgattattttggagatgtccgtactgttgatgttactgttcgtcgtct
gcgtgaaaaaattgaagatacacctagtcgtccagagtacattttgacgcgacgcggtgttggttattacatgaaatcat

ATGacTAAtNtgtttgaatcaagtccctggggcctccggccggtatactggccggcagcgactcNNNNNattattt
vicK→ *vicR*← *vicK* ← SfiI cut site → *ermAM*
cctcccgttaaataatagataactattaaaaatagacaatacttgcccataggtaacggtacttaaattgtttactttggcgtgtttcatt
gcttgatgaaactgatttttagtaaacagttgacgatattctcgattgacccattttgaaacaaNNNacgtataNNNcttccaat
atttatcNgNaNcatctgtggtatgNcNNNtNNNNtttaNNNNNNNNctgtttNNNtttggttt

> YDNT016 - primer SL179
tcctttcttNNNccttagacctttctattatagcaaaaatcacccagaacaaccatttccgagtaatctttgtttttcattct
tccttttaagctgtccaCTAgatttttgctaatggtaaagcagtatctggcgggtatcagggcccaggcggccgggccca
→ *vicX* *vicX*← SfiI cut site
aaatttgtttgatttgtatcttaaaattttgtataataggaattgaagttaaattagatgctaaaaatttgtaattaagaaggagtgattac
→ *ermAM*
atgaacaaaaatataaaatattctcaaaactttttaacaagtgaaaaagtactcaaccaaataataaaacaattgaatttaaaagaaa
ccgataccgtttacgaaattggaacaggtaaagggcatttaacgacgaaactggctgaaataagtaaacaggtaacgtctattga
attagacagtcatctattcaacttatcgtcagaaaaattaaaactgaatactcgtgtcactttaactcaccaagatgttctacagtttca
attccctaacaaacagaggtataaaattgttgggaatattccttaccatttaagcacacaaattattaaaaaagtggtttttgaaagcc
atgcgtctgacatctatctgattgttgaagaaggattctacaagcgtaccttggatattcaccgaacactagggttgctcttgcacac
tcaagtctcgattcagcaattgcttaagctgccagcggaatgctttcatcctaaaccaaaagtaaacagtgtcttaataaaacttacc
cgccataccacagatgttccggataaatattggaagctatatacgtactttgtttNNNNNtgggtcaatcgaNNatatcgtca
actgtttactNNNNatcagtttcNNNNNNcaatgaaacacgNcaaagtaaacaatttaagtaccgttacctatgggcaa
gtattgtc

> LiaFSR- - primer SL565

ttcttaatNagataggtNNNNNggactgagaaNNNNttcNNNtccttgtttttatatatcatggctcgaactatt
gaatgatataggcggttaattatatgatgttattaggtcatcatgtcaattcaagttatgtttatgatctgttgataataatgt
tatctaatgcaggtatactcatatgttgtagttattatatttataagtttaaggttcttgcctcagcctccttgtttgaNNNg
ataacttttttgttatcaaacttgtatccgtctaggattaaaactgtataNNNttgatgtatgataactaagctATGgc

→P_{liaF}

gtctttgatatttgaaaaattctggggcctcccctggccggcctggccggcagcgactcataaaattatttcctcccgttaaata

P_{liaF}← SfiI cut site → *ermAM*

atagataactattaaaaatagacaatacttgctcataagtaacggtacttaaattgtttactttggcgtgtttcattgcttgatgaaactg
atttttagtaaacagttgacgatattctcgattgacccattttgaaacaaagtacgtatatagcttccaatatttatccggaacatctgtg
gtatggcgggtaagttttattaNNNcactgtttacttttggtttaggatgaaagcattccgctggcagcttaagcaattgctgaatc
gagacttgagtgtgcaNNNgcaaccctagtgttcggtgaatatccaaggtacgcttgtNNNatccttcttcaacaatcNNN
tNgatgtcNNNNNcatggctttcaaaaaccacttttttaataatttNNNNNNcNNNaNtgNtNNNgaatacNNN
NNNNNNNNtttatacctctgtttgtNNNNgaattgaaactNNNNNNNNatctt

> LiaFSR- - primer SL622

attgcttNNNtcgttttaggaagttccccaatatcttccttataaacaacctcaatattactcttatcagttaattctctaN
NaatcatagcaagtccttctgaaagtgtctttccttctaattctgtaggacgcaaatgcagtaaaaggactNgcaagtca
ttctgagcattgttgagcatatcttcaatagctaataattgtgtctgcagttgttttttttccaattgatcaagattatgNNN
aacacctgacaaaatcatagaaaaggcaaacagtccttgactcactgtgtcatgtaaatctcgagcaatgcgttttctctc
ctttttgacaatttcctgactgctggcaatataggtattttccgtcttttgcaaattattNgNtaactgctgcatttta NNN
NNaNNNNNNttaacgtttttccctaattcggtatcatcttcctgtgtgatggcctgatNNNNcaaaatgcgtttta
aattttggttgaggtggcgtttgctattatcatctaaaatcatccataccaacagtaaaagaaaagtcaaggaaataaag
gcagcaNNNNNNgNtaaaataaattgctcaggaacaNNccaatcNNNtaacaaacttttcaaatcNNNNt
taaNNctgttaataatgacaaaaacaatggaaatgatNNNNNcNNNNNNNNNNaaaaaaatcatNNN

liaS←

NNNcNNNttttttt

> YDNT005 - primer SL591

tctgtaaNNNNNcatcaatgtcattgcgggcttggtggaggtagaacgtatATGAaaaaaaagacgatcttaat

→ *liaF* *liaF* ← → *liaS*

gatttttttatacgcggcagttaccatcatttccggggcgcgcccggggcccaaaatttgtttgatttgtatcttaaaattttgtata

liaS ← AscI cut site →*ermAM*

ataggaattgaagttaaattagatgctaaaaatttgtaattaagaaggagtgattacatgaacaaaaatataaaatattctcaaaactt
tttaacgagtgaaaaagtactcaaccaaataataaaacaattgaatttaaaagaaaccgataccgtttacgaaattggaacaggta
aagggcatttaacgacgaaactggctgaaataagtaaacaggtaacgtctattgaattagacagtcatctattcaacttatcgtcag
aaaaattaaaactgaatactcgtgtcactttaactcaccaagatgttctacagtttcaattccctaacaaacagaggtataaaattgtt
gggagtattccttaccatttaagcacacaaattattaaaaaagtggtttttgaaagccatgcgtctgacatctatctgattgttgaaga
aggattctacaagcgtaccttggatattcaccgaacactagggttgctcttgcacactcaagtctcgattcagcaattgcttaagct
gccagcggaatgctttcatcctaaaccaaaagtaaacagtgtcttaataaaacttacccgccataccacagatgttccggataaat
attggaagctatatacgtactttgtttcaaaatgggtcaatcgNNNNtatcgtcaactgtttactaaaaatcagtttcatcaagca
NtgaaaNNNNNNNaNgtaaacaatttNNNtaccgttNNNtatgNgcaagta

> YDNT005 - primer SL358

ttagaNNNNgtgttttgNNNtcttcaaagaaatgaaaagctcatcagcaatcgtttggttatcataacccttagcaa
→*liaR*
gtaaagccaaaatgtctcgttcacgcgctgttaaatcttcatgcaaatcaggattattatgatgatccttgattttcttatca
acttctgttttaatcgctaaatctcccttagctacttttttgaatggcattcaaaatttcagctgcactggaagttttcaacata
taacctttagcacctgcttcaatgacaggataaatttttttcgttatctaaataactggttaaaactagaattttggcttctttc
caatcttttagaagttcaagagtggcttctacaccatccatttctggcataaccaagtccatgacaacaacgtctggtttta
attttaaagccaagccaatacctttgacggccattgctagcctcaccgataacttctacattatcttgtaaattaagaaaact
tttcaaacccaatcgaaccatttcatgatcatcaaccagtataacttttgttttactaATCagCATctcctttcattattg
liaS → ←*liaR*
gtacatggatatccataacaacccccttattttcagcacttggccggccagtcggcagcgactcatagaattatttcctcccgt
liaS←FseI cut site →*ermAM*
taaataatagataactattaaaaatagacaatacttgctcataagtaacggtacttaaattgtttactttggcgtgtttcattgcttgatg
aaactgatttttagtaaacagttgacgatattctcgattgacccattttgaaacaaagtacgtatatagcttccaatatttatccggaac
atctgtggtatggcgggtaagttttattaNNNcactgtttacttttggtttaNNNNNNNNNNcattccgctgNcNNNttta
agcaattgctgaNNNNN

> YDNT009 - primer SL569

tgaNtggttcgattgggtttgaaagttttcttaatttacaagataatgtagaagttatcggtgaggcggcgcgccccgggc
→*liaR* *liaR*←AscI cut site
ccaaaatttgtttgatttgtatcttaaaattttgtataataggaattgaagttaaattagatgctaaaaatttgtaattaagaaggagtgat
→*ermAM*
tacatgaacaaaaatataaaatattctcaaaacttttaacgagtgaaaaagtactcaaccaaataataaaacaattgaatttaaaag
aaaccgataccgtttacgaaattggaacaggtaaagggcatttaacgacgaaactggctaaaataagtaaacaggtaacgtctat
tgaactagacagtcatctattcaacttatcgtcagagaaattaaaactgaatactcgtgtcactttaattcaccaagatattctacagtt
tcaattccctaacaaacagaggtataaaattgttgggagtattccttaccatttaagcacacaaattattaaaaaagtggtttttgaaa
gccatgcgtctgacatctatctgattgttgaagaaggattctacaagcgtaccttggatattcaccgaacactagggttgctcttgca
cactcaagtctcgattcagcaattgcttaagctgccagcggaatgctttcatcctaaaccaaaagtaaacagtgtcttaataaaactt
acccgccataccacagatgttccagataaatattggaagctatatacgtactttgtttcaaaatgggtcaatcgagaatatcgtcaa
ctgtttactaaaaatcagtttcatcaagcaatgaaacacgccaaagtaaacaatttaagtaccgttacttatgagcaagtattNtcta
NNNttaNNNgNtatctaNNNNNtaaNNNNagg

> YDNT009 - primer SL550

ggaattgaagNNNattagatgctaaaaatttgtaattaagaaggagtgattacatgaacaaaaatataaaatattctcaaaacttttt
→*ermAM*
taacgagtgaaaaagtactcaaccaaataataaaacaattgaatttaaaagaaaccgataccgtttacaaaattggaacaggtaaa
gggcatttaacgaNNNaactggctaaaataagtaaacaggtaacgtctattgaactNNNcagtcatctattcaacttatcgtc
NNNNNaattaaaactgaatactcgtgtcactttaattcaccaagatattctacagtttcaattccctaacaaacagaggtataaa
attgttgggagtattccttaccatttaagcacacaaattattaaaaaagtggtttttgaaagccatgcgtctgacatctatctgattgttg
aaaaaggattctacaagcgtaccttggatattcaccgaacactagggttgctcttgcacactcaagtctcgattcagcaattgctta
agctgccagcggaatgctttcatcctaaaccaaaagtaaacagtgtcttaataaaacttacccgccataccacNNNtgttccaa
ataaatattggaagctatatacgtactttgtttcaaaatgggtcaatNNNNNatatcgtcaactgtttactaaaaatcagtttcatc
aagcaatgaaacaNNNcaaagtaaacaatttaagtaccgttacttatgagcaagtattNtctatttttaNNNgttatctattattt
aacgggaggaaataattctatgNNNcNctgccNNNNNgccggccNNNcccttcNNNatcatt

> YDNT008 - primer SL573

gcacatataggtatcttttttgaagagatattttgagccccgttgagatatggtatctcctctttagaagatgagcagcttt
ataaacatcatttttcggtttaaaggtaatttgcaattatttgattctacaactatcttatcctcagcaatttctgtaatagtc
aaataatcatttaaatcaacactggccataatcattgacaattcgtgaaaaccatcttgatattttccagcaatatcaaga
ccaagattgattttagccggagctttttcaataatttcCATaatatgccttccctgaaaactgttaaacacattatatcaa
SMu1813←
aaggtttgataatatggcatgttaaaccaataatttataataacttttcttaattttcaaccaaaaagaatggtacaatcac
atgttccattctttccctttttaaCTAttttttccttaaaatcacttaatttttttacgtaaatctttcagcatactttgccttccca
→*comX*
aaaagtgggccggccagtcggcagcgactcatagaattatttcctcccgttaaataatagataactattaaaaatagacaatactt
← FseI cut site →*ermAM*
gctcataagtaacggtacttaaattgtttactttggcgcgtttcattgcttgatgaaactgatttttagtaaacagttgacgatattctcg
attgacccattttgaaacaaagtacgtatatagcctccaatatttatctggaacatctgtggtatggcgggtaagttttattaNNNc
actgtttacttttggtttNNNNtgaaagcattccgccgNcagcttaagcaattgctgaatcgNNNcttgagtgtgcaNNN
NNaaccctagtgttcggtNaNtatNNNNNNNNNcgcttgtNNNNNccttcNNNNNNNaatcNNNNNNNN
tgtc

> YDNT008 - primer SL574

ttatagtgcagacggttttgagatttgttatatttaataagttaatgtatcgtccaaattggttaagtacatggaggtaaaa
atatgattgtatgcgcggcgattagtttttgtttcttgtgaactttgatttgttgatattgttctcgaattgggcgtgttcgaca
taccctgctttatcttgaattttgatcctcttaattttcaatctgtgaattgaatgtttcagggaatttgtccaatttcaaataat
gagaaccgtgtggatctacttatcaaaatttttttgcgtaaaataaaggatctgcttaagtgttttattagtttgtaatgcgag
gtgatgttttgtttaaaaagaaactgtttaatctgttagtcagaggttgtaaataaaacagccagttaagatgggacattt
atgtcctgttcttaaagtctttttcgttttataataattttattataaaaggaggtcatcgtaatagATGgaagaagatttt
→*comX*
gaaattgtttttaataaggttaagccaattgtatggaaattaagccgttattactttattaaaatgtggactcgtgaagatt
ggcaacaaggcgcgccccgggcccaaaatttgtttgatttgtatcttaaaattttgtataattggaattgaagttaaattagatgcta
←AscI cut site →*ermAM*
aaaatttgtaattaagaaggagtgattacatgaacaaaaatataaaatattctcaaaacttttaacgagtgaaaaagtactcaacca
aataataaaacaattgaatttaaaagaaaccgataccgtttaNNNNNNtggaacaNNtaaagggcatttaacgaNNNa
NctggctNNNNtNagtaaacaggtaacgtctaNNNaattNNNNNgtcatctattcaacttatcgtcNNNNNNN
NNNaactgaatactNNNNtcactt

Appendix 2. Summary of the LC-MS/MS Analysis Performed on the Protein Spots Identified as Differentially Expressed in the 2DGE Analysis.

The matched peptides are underlined and the the Mascot scores and sequence coverage are included

Spot 419 - Phosphoglycerate kinase

```
  1 MAKLTVKDVD LKGKKVLVRV DFNVPVKDGV ITNDNRITAA LPTIKYIIEH
 51 GGRAVLFSHL GRVKEEADKK GKSLAPVAAD LAKKLVQEVV FPGVTRGEQL
101 EAAINALKNG EVLLVENTRF EDVDGKKESK NDPELGKYWA SLGDGIFVND
151 AFGTAHRAHA SNVGISANVD KAVAGFLLEN EIAYIQEAVD NPVRPFIAIL
201 GGSKVSDKIG VIENLLKKAD KVLIGGGMTY TFLKAQGIEI GDSLVEEDKL
251 DIAKDLLAKA NGKLILPVDS KEANAFADYT EVKDTEGAAV DPGFLGLDIG
301 PKSIAKFDDE LTGAKTVVWN GPMGVFENPD FQAGTIGVMD AIVKQPGVKS
351 IIGGGDSAAA AINLGRADKF SWISTGGGAS MELLEGKVLP GLAALTEK
```

Sequence Coverage: 66%

Mascot Score: 1560

Spot 468 - Glyceraldehyde-3-phosphate dehydrogenase

```
  1 MVVKVGINGF GRIGRLAFRR IQNVEGVEVT RINDLTDPNM LAHLLKYDST
 51 QGRFDGNVEV KEGGFEVNGK FVKVSAERDP EQIDWAADGV EIVLEATGFF
101 ASKAAAEKHL HANGGAKKVV ITAPGGNDIK TIVFNTNHDV LDGTETVISG
151 ASCTTNCLAP MAKALHDNFS IKEGLMTTIH AYTGDQMVLD GPHRKGDLRR
201 ARAAAANIVP NSTGAAKAIG LVIPELNGKL DGAAQRVPVP TGSVTELVAV
251 LDKKVTVDEV NAAMKAAANE SYGYTEDPIV SSDIVGMSFG SLFDATQTKV
301 LDVDGKQLVK VVSWYDNEMS YTSQLVRTLE YFAKIAK
```

Sequence Coverage: 32%

Mascot Score: 551

Spot 465 - dTDP-glucose-4,6-dehydratase

```
  1 MTEYKNIIVT GGAGFIGSNF VHYVYNNHPD VHVTVLDKLT YAGNRANLEE
 51 ILGDRVELVV GDIADSELVD KLAAKADAIV HYAAESHNDN SLKDPSPFIY
```

101 TNFVGTYILL EAARKYDIRF HHVSTDEVYG DLPLREDLPG HGEGPGEKFT
151 AETKYNPSSP YSSTKAASDL IVKAWVRSFG VKATISNCSN NYGPYQHIEK
201 FIPRQITNIL SGIKPKLYGE GKNVRDWIHT NDHSTGVWAI LTKGRIGETY
251 LIGADGEKNN KEVLELILEK MSQPKNAYDH VTDRAGHDLR YAIDSTKLRE
301 ELGWKPQFTN FEEGLEDTIK WYTEHEDWWK AEKEAVEANY AKTQKILN

Sequence Coverage: 46%

Mascot Score: 867

Spot 488 - Glyceraldehyde-3-phosphate dehydrogenase

1 MVVKVGINGF GRIGRLAFRR IQNVEGVEVT RINDLTDPNM LAHLLKYDST
51 QGRFDGNVEV KEGGFEVNGK FVKVSAERDP EQIDWAADGV EIVLEATGFF
101 ASKAAAEKHL HANGGAKKVV ITAPGGNDIK TIVFNTNHDV LDGTETVISG
151 ASCTTNCLAP MAKALHDNFS IKEGLMTTIH AYTGDQMVLD GPHRKGDLRR
201 ARAAAANIVP NSTGAAKAIG LVIPELNGKL DGAAQRVPVP TGSVTELVAV
251 LDKKVTVDEV NAAMKAAANE SYGYTEDPIV SSDIVGMSFG SLFDATQTKV
301 LDVDGKQLVK VVSWYDNEMS YTSQLVRTLE YFAKIAK

Sequence Coverage: 34%

Mascot Score: 709

Spot 176 - Glyceraldehyde-3-phosphate dehydrogenase

1 MVVKVGINGF GRIGRLAFRR IQNVEGVEVT RINDLTDPNM LAHLLKYDST
51 QGRFDGNVEV KEGGFEVNGK FVKVSAERDP EQIDWAADGV EIVLEATGFF
101 ASKAAAEKHL HANGGAKKVV ITAPGGNDIK TIVFNTNHDV LDGTETVISG
151 ASCTTNCLAP MAKALHDNFS IKEGLMTTIH AYTGDQMVLD GPHRKGDLRR
201 ARAAAANIVP NSTGAAKAIG LVIPELNGKL DGAAQRVPVP TGSVTELVAV
251 LDKKVTVDEV NAAMKAAANE SYGYTEDPIV SSDIVGMSFG SLFDATQTKV
301 LDVDGKQLVK VVSWYDNEMS YTSQLVRTLE YFAKIAK

Sequence Coverage: 32%

Mascot Score: 612

Spot 146 - 3-oxoacyl-(acyl-carrier-protein) synthase, FabF

1 MTLKRVVVTG YGVTSPIGHT PEDFWNSLHD GKIGIKPITK FDASEIPVFN
51 AGEIQDFPFD KYFVKKDKNR MDTYSLYAIY AAMEAIENAA LDMAQEIRDR
101 VGVIVSSGIG GLQELEDQII RMHERGMKRI KPMFIPKALS NMGAGNIALK
151 IGAQGVCKSI TTACASANDA IGEAFREIKY GFHDVILAGG SEASITKIGI

201 GGFNALTALS TTEDPARSAI PFDKDRNGFV MGEGAAVLIL ESLEHAQKRG
251 ARILAEVVGY GSNCDAYHMT TPTPDGSGAA KAIKLAINEA GISPEEVNYV
301 NAHGTSTQAN EKGESKAIVA VLGKDVPVSS TKSFTGHLLG AAGGVEAIAT
351 IEAIRNHFVP MTAGTKELSE DIEANVVYGQ GQEAVIKYAI SNTFGFGGHN
401 AVLAFKRWED

Sequence Coverage: 76%

Mascot Score: 1275

Spot 220 - Fructose-bisphosphate aldolase

1 MAIVSAEKFV QAARDNGYAV GGFNTNNLEW TQAILRAAEA KKAPVLIQTS
51 MGAAKYMGGY KLCKVLIETL VESMGITVPV AIHLDHGHYE DALECIEVGY
101 TSIMFDGSHL PVEENLEKAK EVVAKAHAKG ISVEAEVGTI GGEEDGIIGR
151 GELAPIDDAK AMVETGIDFL AAGIGNIHGP YPANWEGLDL DHLKKLTEAV
201 PGFPIVLHGG SGIPDDQIRA AIKLGVAKVN VNTECQIAFA NATRKFAAEY
251 EANEAEYDKK KLFDPRKFLK PGFEAITEAV EERIDVFGSE GKA

Sequence Coverage: 47%

Mascot Score: 888

Spot 219 - Fructose-bisphosphate aldolase

1 MAIVSAEKFV QAARDNGYAV GGFNTNNLEW TQAILRAAEA KKAPVLIQTS
51 MGAAKYMGGY KLCKVLIETL VESMGITVPV AIHLDHGHYE DALECIEVGY
101 TSIMFDGSHL PVEENLEKAK EVVAKAHAKG ISVEAEVGTI GGEEDGIIGR
151 GELAPIDDAK AMVETGIDFL AAGIGNIHGP YPANWEGLDL DHLKKLTEAV
201 PGFPIVLHGG SGIPDDQIRA AIKLGVAKVN VNTECQIAFA NATRKFAAEY
251 EANEAEYDKK KLFDPRKFLK PGFEAITEAV EERIDVFGSE GKA

Sequence Coverage: 42%

Mascot Score: 1051

Spot 171 - Glyceraldehyde-3-phosphate dehydrogenase

1 MVVKVGINGF GRIGRLAFRR IQNVEGVEVT RINDLTDPNM LAHLLKYDST
51 QGRFDGNVEV KEGGFEVNGK FVKVSAERDP EQIDWAADGV EIVLEATGFF
101 ASKAAAEKHL HANGGAKKVV ITAPGGNDIK TIVFNTNHDV LDGTETVISG
151 ASCTTNCLAP MAKALHDNFS IKEGLMTTIH AYTGDQMVLD GPHRKGDLRR
201 ARAAAANIVP NSTGAAKAIG LVIPELNGKL DGAAQRVPVP TGSVTELVAV
251 LDKKVTVDEV NAAMKAAANE SYGYTEDPIV SSDIVGMSFG SLFDATQTKV

301 LDVDGKQLVK **VVSWYDNEMS YTSQLVR**TLE YFAKIAK

Sequence Coverage: 47%

Mascot Score: 758

Spot 370 - Manganes-dependent inorganic pyrophosphatase PpaC

1 SK**ILVFGHQN PDSDAIGSSX AYAYLK**RQLG VDAQAVALGN PNEETAFVLD
51 YFGIQAPPVV KSAQAEGAKQ VILTDHNEFQ QSIADIR**EVE VVEVVDHHRV**
101 **ANFETANPLY XRLEPVGSAS SIVYR**LYK**EN GVAIPK**EIAG VXLSGLISDT
151 LLLK**SPTTHA SDPAVAEDLA KIAGVDLQEY GLAXLK**AGTN LASK**TAAQLV**
201 **DIDAKTFELN GSQVRVAQVN TVDINEVLER QNEIEEAIK**A SQAANGYSDF
251 VLXITDILNS NSEILALGNN TDK**VEAAFNF TLKNNHAFLA GAVSR**KK**QVV**
301 **PQLTESFNG**

Sequence Coverage: 58%

Mascot Score: 1116

Spot 149 - Triosephosphate isomerase

1 **MSRKPIIAGN WKMNKTAAEA REFIDAVKNN IPSNNLVDTV IGSPALFLEG**
51 **MK**KGVKGTEL QVAAQNCYWE DFGAFTGETS PAALAALGVD YVIIGHSERR
101 **DYFHETDQEI NKK**AHAIFKH K**MTPILCCGE SLETYEAGK**T AEWIEGQITA
151 DLK**GLSAEQV SSMVIAYEPI WAIGTGKSAD ANIADDICGV VR**ATVEKLYG
201 K**EVAQAVRIQ YGGSVKPENV AEYMAK**ENVD GALVGGASLQ ADSFLALLDF
251 VK

Sequence Coverage: 53%

Mascot Score: 580

Spot 165 - Transcription elongation factor GreA

1 **MSEKTYPMTL AEKEQLEQEL EELKLVRRPE VIERIKIARS YGDLSENSEY**
51 EAAK**DEQAFV EGQISSIETK** IR**YAEIVDSD AVAK**NEVAIG KTVIVR**EVGT**
101 **NDEDTYSIVG AAGADVFAGK ISNESPIAQA LIGK**KTGDK**V MIESPAGSYQ**
151 **VEIVK**VKKTK

Sequence Coverage: 62%

Mascot Score: 429

Spot 108 - Cysteine kinase A

```
  1 MAKIYNNITE LIGNTPIVKL NNVVPEDAAD VYVKLEAFNP GSSVKDRIAL
 51 SMIEDAEKRG LIKPGDTIVE PTSGNTGIGL SWVGAAKGYN VIITMPETMS
101 VERRKIIQAY GAKLVLTPGS AGTKGAIDKA HEIAKEVGGW VPLQFDNPAN
151 PKIHELTTGP EILEAFGSHG LDAVVAGIGT GGTITGISRA LKKDNPDIKI
201 YGLEADESAV LSGDKPGPHK IQGISTGFIP AALDTHSYDE VIRVKSDDAL
251 ATGRYFGGKE GFLLGISASA AVWAALEVAK KLGKGKKVLA IAPDNGERYL
301 STALYEFN
```

Sequence Coverage: 50%

Mascot Score: 763

Spot 448 - Glyceraldehyde-3-phosphate dehydrogenase

```
  1 MAILLPDLPY AYDALEPYID AETMTLHHDK HHATYVANAN AALEKHPEIG
 51 ENLEVLLADV EQIPADIRQS LINNGGGHLN HALFWELLSP EKTKVTAEVA
101 AAINEAFGSF DDFKAAFTAA ATTRFGSGWA WLVVDKEGKL EVTSTANQDT
151 PISQGLKPIL ALDVWEHAYY LNYRNVRPNY IKAFFEVINW NTVARLYAEA
201 LTK
```

Sequence Coverage: 50%

Mascot Score: 564

References

Ahn, S.J., and Burne, R.A. 2007. Effects of oxygen on biofilm formation and the AtlA autolysin of *Streptococcus mutans*. J. Bacteriol. **189**(17): 6293-6302.

Ahn, S.J., and Burne, R.A. 2006. The *atlA* operon of *Streptococcus mutans*: role in autolysin maturation and cell surface biogenesis. J. Bacteriol. **188**(19): 6877-6888.

Ahn, S.J., Wen, Z.T., and Burne, R.A. 2006. Multilevel control of competence development and stress tolerance in *Streptococcus mutans* UA159. Infect. Immun. **74**(3): 1631-1642.

Ahn, S.J., Lemos, J.A., and Burne, R.A. 2005. Role of HtrA in growth and competence of *Streptococcus mutans* UA159. J. Bacteriol. **187**(9): 3028-3038.

Ajdic, D., McShan, W.M., McLaughlin, R.E., Savic, G., Chang, J., Carson, M.B., Primeaux, C., Tian, R., Kenton, S., Jia, H., Lin, S., Qian, Y., Li, S., Zhu, H., Najar, F., Lai, H., White, J., Roe, B.A., and Ferretti, J.J. 2002. Genome sequence of *Streptococcus mutans* UA159, a cariogenic dental pathogen. Proc. Natl. Acad. Sci. U. S. A. **99**(22): 14434-14439.

Allan, E., Hussain, H.A., Crawford, K.R., Miah, S., Ascott, Z.K., Khwaja, M.H., and Hosie, A.H. 2007. Genetic variation in *comC*, the gene encoding competence-stimulating peptide (CSP) in *Streptococcus mutans*. FEMS Microbiol. Lett. **268**(1): 47-51.

Alves, R., and Savageau, M.A. 2003. Comparative analysis of prototype two-component systems with either bifunctional or monofunctional sensors: differences in molecular structure and physiological function. Mol. Microbiol. **48**(1): 25-51.

Anderson, N. L. 1991. Two Dimensional Gel Electrophoresis: Operation of the ISO-DALT System, 2nd Ed., Large Scale Biology Press, Rockville, M.D.

Aravind, L., and Ponting, C.P. 1999. The cytoplasmic helical linker domain of receptor histidine kinase and methyl-accepting proteins is common to many prokaryotic signalling proteins. FEMS Microbiol. Lett. **176**(1): 111-116.

Arirachakaran, P., Benjavongkulchai, E., Luengpailin, S., Ajdic, D., and Banas, J.A. 2007b. Manganese affects *Streptococcus mutans* virulence gene expression. Caries Res. **41**(6): 503-511.

Arirachakaran, P., Luengpailin, S., Banas, J.A., Mazurkiewicz, J.E., and Benjavongkulchai, E. 2007a. Effects of manganese on *Streptococcus mutans* planktonic and biofilm growth. Caries Res. **41**(6): 497-502.

Artsimovitch, I., Patlan, V., Sekine, S., Vassylyeva, M.N., Hosaka, T., Ochi, K., Yokoyama, S., and Vassylyev, D.G. 2004. Structural basis for transcription regulation by alarmone ppGpp. Cell **117**(3): 299-310.

Banas, J.A. 2004. Virulence properties of *Streptococcus mutans*. Front. Biosci. **9**: 1267-1277.

Banas, J.A., Hazlett, K.R., and Mazurkiewicz, J.E. 2001. An in vitro model for studying the contributions of the *Streptococcus mutans* glucan-binding protein A to biofilm structure. Methods Enzymol. **337**: 425-433.

Banas, J.A., Potvin, H.C., and Singh, R.N. 1997. The regulation of *Streptococcus mutans* glucan-binding protein A expression. FEMS Microbiol. Lett. **154**(2): 289-292.

Banas, J.A., Miller, J.D., Fuschino, M.E., Hazlett, K.R., Toyofuku, W., Porter, K.A., Reutzel, S.B., Florczyk, M.A., McDonough, K.A., and Michalek, S.M. 2007. Evidence that accumulation of mutants in a biofilm reflects natural selection rather than stress-induced adaptive mutation. Appl. Environ. Microbiol. **73**(1): 357-361.

Bates, C.S., Toukoki, C., Neely, M.N., and Eichenbaum, Z. 2005. Characterization of MtsR, a new metal regulator in group A *Streptococcus*, involved in iron acquisition and virulence. Infect. Immun. **73**(9): 5743-5753.

Beg, A.M., Jones, M.N., Miller-Torbert, T., and Holt, R.G. 2002. Binding of *Streptococcus mutans* to extracellular matrix molecules and fibrinogen. Biochem. Biophys. Res. Commun. **298**(1): 75-79.

Belcheva, A., and Golemi-Kotra, D. 2008. A close-up view of the VraSR two-component system. A mediator of *Staphylococcus aureus* response to cell wall damage. J. Biol. Chem. **283**(18): 12354-12364.

Belli, W.A., and Marquis, R.E. 1991. Adaptation of *Streptococcus mutans* and *Enterococcus hirae* to acid stress in continuous culture. Appl. Environ. Microbiol. **57**(4): 1134-1138.

Bhagwat, S.P., Nary, J., and Burne, R.A. 2001. Effects of mutating putative two-component systems on biofilm formation by *Streptococcus mutans* UA159. FEMS Microbiol. Lett. **205**(2): 225-230.

Bijlsma, J.J., and Groisman, E.A. 2003. Making informed decisions: regulatory interactions between two-component systems. Trends Microbiol. **11**(8): 359-366.

Birnboim, H.C., and Doly, J. 1979. A rapid alkaline extraction procedure for screening recombinant plasmid DNA. Nucleic Acids Res. 7(6): 1513-1523.

Bisicchia, P., Noone, D., Lioliou, E., Howell, A., Quigley, S., Jensen, T., Jarmer, H., and Devine, K.M. 2007. The essential YycFG two-component system controls cell wall metabolism in *Bacillus subtilis*. Mol. Microbiol. **65**(1): 180-200.

Biswas, I., Drake, L., and Biswas, S. 2007. Regulation of *gbpC* expression in *Streptococcus mutans*. J. Bacteriol. **189**(18): 6521-6531.

Biswas, I., Drake, L., Erkina, D., and Biswas, S. 2008. Involvement of sensor kinases in the stress tolerance response of *Streptococcus mutans*. J. Bacteriol. **190**(1): 68-77.

Biswas, S., and Biswas, I. 2006. Regulation of the glucosyltransferase (*gtfBC*) operon by CovR in *Streptococcus mutans*. J. Bacteriol. **188**(3): 988-998.

Biswas, S., and Biswas, I. 2005. Role of HtrA in surface protein expression and biofilm formation by *Streptococcus mutans*. Infect. Immun. **73**(10): 6923-6934.

Bowen, W.H., Schilling, K., Giertsen, E., Pearson, S., Lee, S.F., Bleiweis, A., and Beeman, D. 1991. Role of a cell surface-associated protein in adherence and dental caries. Infect. Immun. **59**(12): 4606-4609.

Boyd, D.A., Cvitkovitch, D.G., Bleiweis, A.S., Kiriukhin, M.Y., Debabov, D.V., Neuhaus, F.C., and Hamilton, I.R. 2000. Defects in D-alanyl-lipoteichoic acid synthesis in *Streptococcus mutans* results in acid sensitivity. J. Bacteriol. **182**(21): 6055-6065.

Boyle-Vavra, S., Yin, S., and Daum, R.S. 2006. The VraS/VraR two-component regulatory system required for oxacillin resistance in community-acquired methicillin-resistant *Staphylococcus aureus*. FEMS Microbiol. Lett. **262**(2): 163-171.

Brady, L.J., Piacentini, D.A., Crowley, P.J., Oyston, P.C., and Bleiweis, A.S. 1992. Differentiation of salivary agglutinin-mediated adherence and aggregation of mutans streptococci by use of monoclonal antibodies against the major surface adhesin P1. Infect. Immun. **60**(3): 1008-1017.

Brown, T.A.,Jr, Ahn, S.J., Frank, R.N., Chen, Y.Y., Lemos, J.A., and Burne, R.A. 2005. A hypothetical protein of *Streptococcus mutans* is critical for biofilm formation. Infect. Immun. **73**(5): 3147-3151.

Burne, R.A., Chen, Y.Y., and Penders, J.E. 1997. Analysis of gene expression in *Streptococcus mutans* in biofilms in vitro. Adv. Dent. Res. **11**(1): 100-109.

Burne, R.A., Wen, Z.T., Chen, Y.Y., and Penders, J.E. 1999. Regulation of expression of the fructan hydrolase gene of *Streptococcus mutans* GS-5 by induction and carbon catabolite repression. J. Bacteriol. **181**(9): 2863-2871.

Bus, J.S., and Gibson, J.E. 1984. Paraquat: model for oxidant-initiated toxicity. Environ. Health Perspect. **55**: 37-46.

Butcher, B.G., Lin, Y.P., and Helmann, J.D. 2007. The *yydFGHIJ* operon of *Bacillus subtilis* encodes a peptide that induces the LiaRS two-component system. J. Bacteriol. **189**(23): 8616-8625.

Cao, M., Wang, T., Ye, R., and Helmann, J.D. 2002. Antibiotics that inhibit cell wall biosynthesis induce expression of the *Bacillus subtilis* sigma(W) and sigma(M) regulons. Mol. Microbiol. **45**(5): 1267-1276.

Chan, K.G., Mayer, M., Davis, E.M., Halperin, S.A., Lin, T.J., and Lee, S.F. 2007. Role of D-alanylation of *Streptococcus gordonii* lipoteichoic acid in innate and adaptive immunity. Infect. Immun. **75**(6): 3033-3042.

Chen, A., Hillman, J.D., and Duncan, M. 1994. L-(+)-lactate dehydrogenase deficiency is lethal in *Streptococcus mutans*. J. Bacteriol. **176**(5): 1542-1545.

Chen, P.M., Chen, J.Y., and Chia, J.S. 2006. Differential regulation of *Streptococcus mutans gtfBCD* genes in response to copper ions. Arch. Microbiol. **185**(2): 127-135.

Chia, J.S., Yeh, C.Y., and Chen, J.Y. 2000. Identification of a fibronectin binding protein from *Streptococcus mutans*. Infect. Immun. **68**(4): 1864-1870.

Chia, J.S., Chang, L.Y., Shun, C.T., Chang, Y.Y., Tsay, Y.G., and Chen, J.Y. 2001. A 60-kilodalton immunodominant glycoprotein is essential for cell wall integrity and the maintenance of cell shape in *Streptococcus mutans*. Infect. Immun. **69**(11): 6987-6998.

Chong, P., Drake, L., and Biswas, I. 2008a. LiaS regulates virulence factor expression in *Streptococcus mutans*. Infect. Immun. **76**(7): 3093-3099.

Chong, P., Drake, L., and Biswas, I. 2008b. Modulation of *covR* expression in *Streptococcus mutans* UA159. J. Bacteriol. **190**(13): 4478-4488.

Churchward, G. 2007. The two faces of Janus: virulence gene regulation by CovR/S in group A *Streptococci*. Mol. Microbiol. **64**(1): 34-41.

Clausen, V.A., Bae, W., Throup, J., Burnham, M.K., Rosenberg, M., and Wallis, N.G. 2003. Biochemical characterization of the first essential two-component signal transduction system from *Staphylococcus aureus* and *Streptococcus pneumoniae*. J. Mol. Microbiol. Biotechnol. **5**(4): 252-260.

Claverys, J.P., Dintilhac, A., Pestova, E.V., Martin, B., and Morrison, D.A. 1995. Construction and evaluation of new drug-resistance cassettes for gene disruption mutagenesis in *Streptococcus pneumoniae*, using an ami test platform. Gene **164**(1): 123-128.

Crowley, P.J., Brady, L.J., Michalek, S.M., and Bleiweis, A.S. 1999. Virulence of a *spaP* mutant of *Streptococcus mutans* in a gnotobiotic rat model. Infect. Immun. **67**(3): 1201-1206.

Crowley, P.J., Brady, L.J., Piacentini, D.A., and Bleiweis, A.S. 1993. Identification of a salivary agglutinin-binding domain within cell surface adhesin P1 of *Streptococcus mutans*. Infect. Immun. **61**(4): 1547-1552.

Dashper, Stuart G., and Reynolds, Eric C. 1996. Lactic acid excretion by *Streptococcus mutans*. Microbiol. **142**(1): 33-39

Dashper, S.G., and Reynolds, E.C. 1992. pH regulation by *Streptococcus mutans*. J. Dent. Res. **71**(5): 1159-1165.

Demuth, D.R., and Irvine, D.C. 2002. Structural and functional variation within the alanine-rich repetitive domain of streptococcal antigen I/II. Infect. Immun. **70**(11): 6389-6398.

Deng, D.M., Liu, M.J., ten Cate, J.M., and Crielaard, W. 2007. The VicRK system of *Streptococcus mutans* responds to oxidative stress. J. Dent. Res. **86**(7): 606-610.

Distler, W., and Kroncke, A. 1981. The lactate metabolism of the oral bacterium *Veillonella* from human saliva. Arch. Oral Biol. **26**(8): 657-661.

Douglas, C.W., and Russell, R.R. 1982. Effect of specific antisera on adherence properties of the oral bacterium *Streptococcus mutans*. Arch. Oral Biol. **27**(12): 1039-1045.

Du, W., Brown, J.R., Sylvester, D.R., Huang, J., Chalker, A.F., So, C.Y., Holmes, D.J., Payne, D.J., and Wallis, N.G. 2000. Two active forms of UDP-N-acetylglucosamine enolpyruvyl transferase in Gram-positive bacteria. J. Bacteriol. **182**(15): 4146-4152.

Duarte, S., Klein, M.I., Aires, C.P., Cury, J.A., Bowen, W.H., and Koo, H. 2008. Influences of starch and sucrose on *Streptococcus mutans* biofilms. Oral Microbiol. Immunol. **23**(3): 206-212.

Dubrac, S., Bisicchia, P., Devine, K.M., and Msadek, T. 2008. A matter of life and death: cell wall homeostasis and the WalKR (YycGF) essential signal transduction pathway. Mol. Microbiol. **70**(6): 1307-1322.

Dunning, D.W., McCall, L.W., Powell, W.F.,Jr, Arscott, W.T., McConocha, E.M., McClurg, C.J., Goodman, S.D., and Spatafora, G.A. 2008. SloR modulation of the *Streptococcus mutans* acid tolerance response involves the GcrR response regulator as an essential intermediary. Microbiology **154**(Pt 4): 1132-1143.

Echenique, J.R., and Trombe, M.C. 2001. Competence repression under oxygen limitation through the two-component MicAB signal-transducing system in *Streptococcus pneumoniae* and involvement of the PAS domain of MicB. J. Bacteriol. **183**(15): 4599-4608.

Ernst, R.K., Guina, T., and Miller, S.I. 1999. How intracellular bacteria survive: surface modifications that promote resistance to host innate immune responses. J. Infect. Dis. **179 Suppl 2**: S326-30.

Fabret, C., and Hoch, J.A. 1998. A two-component signal transduction system essential for growth of *Bacillus subtilis*: implications for anti-infective therapy. J. Bacteriol. **180**(23): 6375-6383.

Federle, M.J., McIver, K.S., and Scott, J.R. 1999. A response regulator that represses transcription of several virulence operons in the group A *Streptococcus*. J. Bacteriol. **181**(12): 3649-3657.

Ferretti, J.J., Gilpin, M.L., and Russell, R.R. 1987. Nucleotide sequence of a glucosyltransferase gene from *Streptococcus sobrinus* MFe28. J. Bacteriol. **169**(9): 4271-4278.

Fozo, E.M., and Quivey, R.G.,Jr. 2004. Shifts in the membrane fatty acid profile of *Streptococcus mutans* enhance survival in acidic environments. Appl. Environ. Microbiol. **70**(2): 929-936.

Francesca, B., Ajello, M., Bosso, P., Morea, C., Andrea, P., Giovanni, A., and Piera, V. 2004 Both lactoferrin and iron influence aggregation and biofilm formation in *Streptococcus mutans*. BioMetals **17**(3): 271-278.

Fujita, K., Matsumoto-Nakano, M., Inagaki, S., and Ooshima, T. 2007. Biological functions of glucan-binding protein B of *Streptococcus mutans*. Oral Microbiol. Immunol. **22**(5): 289-292.

Fukuchi, K., Kasahara, Y., Asai, K., Kobayashi, K., Moriya, S., and Ogasawara, N. 2000. The essential two-component regulatory system encoded by *yycF* and *yycG* modulates expression of the *ftsAZ* operon in *Bacillus subtilis*. Microbiology **146 (Pt 7)**(Pt 7): 1573-1583.

Fukushima, K., Ikeda, T., and Kuramitsu, H.K. 1992. Expression of *Streptococcus mutans* gtf genes in *Streptococcus milleri*. Infect. Immun. **60**(7): 2815-2822.

Fukushima, T., Szurmant, H., Kim, E.J., Perego, M., and Hoch, J.A. 2008. A sensor histidine kinase co-ordinates cell wall architecture with cell division in *Bacillus subtilis*. Mol. Microbiol. **69**(3): 621-632.

Funane, K., Shiraiwa, M., Hashimoto, K., Ichishima, E., and Kobayashi, M. 1993. An active-site peptide containing the second essential carboxyl group of dextransucrase from *Leuconostoc mesenteroides* by chemical modifications. Biochemistry **32**(49): 13696-13702.

Galperin, M.Y. and M. Gomelsky. 2005. Bacterial signal transduction modules: From genomics to biology. Features. *ASM News* **71**: 326-333.

Galperin, M.Y. 2004. Bacterial signal transduction network in a genomic perspective. Environ. Microbiol. **6**(6): 552-567.

Gao, R., Mack, T.R., and Stock, A.M. 2007. Bacterial response regulators: versatile regulatory strategies from common domains. Trends Biochem. Sci. **32**(5): 225-234.

Gardete, S., Wu, S.W., Gill, S., and Tomasz, A. 2006. Role of VraSR in antibiotic resistance and antibiotic-induced stress response in *Staphylococcus aureus*. Antimicrob. Agents Chemother. **50**(10): 3424-3434.

Goldstein, F., Perutka, J., Cuirolo, A., Plata, K., Faccone, D., Morris, J., Sournia, A., Kitzis, M.D., Ly, A., Archer, G., and Rosato, A.E. 2007. Identification and phenotypic characterization of a beta-lactam-dependent, methicillin-resistant *Staphylococcus aureus* strain. Antimicrob. Agents Chemother. **51**(7): 2514-2522.

Goodman, S.D., and Gao, Q. 2000. Characterization of the *gtfB* and *gtfC* promoters from *Streptococcus mutans* GS-5. Plasmid **43**(1): 85-98.

Graham, M.R., Smoot, L.M., Migliaccio, C.A., Virtaneva, K., Sturdevant, D.E., Porcella, S.F., Federle, M.J., Adams, G.J., Scott, J.R., and Musser, J.M. 2002. Virulence control in group A *Streptococcus* by a two-component gene regulatory system: global expression profiling and in vivo infection modeling. Proc. Natl. Acad. Sci. U. S. A. **99**(21): 13855-13860.

Gravesen, A., Kallipolitis, B., Holmstrom, K., Hoiby, P.E., Ramnath, M., and Knochel, S. 2004. pbp2229-mediated nisin resistance mechanism in *Listeria monocytogenes* confers cross-protection to class IIa bacteriocins and affects virulence gene expression. Appl. Environ. Microbiol. **70**(3): 1669-1679.

Groisman, E.A. 1998. The ins and outs of virulence gene expression: Mg2+ as a regulatory signal. Bioessays **20**(1): 96-101.

Gutierrez, J.A., Crowley, P.J., Brown, D.P., Hillman, J.D., Youngman, P., and Bleiweis, A.S. 1996. Insertional mutagenesis and recovery of interrupted genes of *Streptococcus mutans* by using transposon Tn917: preliminary characterization of mutants displaying acid sensitivity and nutritional requirements. J. Bacteriol. **178**(14): 4166-4175.

Gutierrez, J.A., Crowley, P.J., Cvitkovitch, D.G., Brady, L.J., Hamilton, I.R., Hillman, J.D., and Bleiweis, A.S. 1999. *Streptococcus mutans* ffh, a gene encoding a homologue of the 54 kDa subunit of the signal recognition particle, is involved in resistance to acid stress. Microbiology **145 (Pt 2)**(Pt 2): 357-366.

Haas, W., and Banas, J.A. 2000. Ligand-binding properties of the carboxyl-terminal repeat domain of *Streptococcus mutans* glucan-binding protein A. J. Bacteriol. **182**(3): 728-733.

Haas, W., Kaushal, D., Sublett, J., Obert, C., and Tuomanen, E.I. 2005. Vancomycin stress response in a sensitive and a tolerant strain of *Streptococcus pneumoniae*. J. Bacteriol. **187**(23): 8205-8210.

Haeusser, D.P., and Levin, P.A. 2008. The great divide: coordinating cell cycle events during bacterial growth and division. Curr. Opin. Microbiol. **11**(2): 94-99.

Hajishengallis, G., Koga, T., and Russell, M.W. 1994. Affinity and specificity of the interactions between *Streptococcus mutans* antigen I/II and salivary components. J. Dent. Res. **73**(9): 1493-1502.

Hamilton, I.R., and Buckley, N.D. 1991. Adaptation by *Streptococcus mutans* to acid tolerance. Oral Microbiol. Immunol. **6**(2): 65-71.

Han, T.K., Zhang, C., and Dao, M.L. 2006. Identification and characterization of collagen-binding activity in *Streptococcus mutans* wall-associated protein: a possible implication in dental root caries and endocarditis. Biochem. Biophys. Res. Commun. **343**(3): 787-792.

Hazlett, K.R., Mazurkiewicz, J.E., and Banas, J.A. 1999. Inactivation of the gbpA gene of *Streptococcus mutans* alters structural and functional aspects of plaque biofilm which are compensated by recombination of the *gtfB* and *gtfC* genes. Infect. Immun. **67**(8): 3909-3914.

Hazlett, K.R., Michalek, S.M., and Banas, J.A. 1998. Inactivation of the *gbpA* gene of *Streptococcus mutans* increases virulence and promotes in vivo accumulation of recombinations between the glucosyltransferase B and C genes. Infect. Immun. **66**(5): 2180-2185.

He, X., Wu, C., Yarbrough, D., Sim, L., Niu, G., Merritt, J., Shi, W., and Qi, F. 2008. The *cia* operon of *Streptococcus mutans* encodes a unique component required for calcium-mediated autoregulation. Mol. Microbiol. **70**(1): 112-126.

Heiner, C.R., Hunkapiller, K.L., Chen, S.M., Glass, J.I., and Chen, E.Y. 1998. Sequencing multimegabase-template DNA with BigDye terminator chemistry. Genome Res. **8**(5): 557-561.

Helmann, J.D. 2002. The extracytoplasmic function (ECF) sigma factors. Adv. Microb. Physiol. **46**: 47-110.

Hoch, J.A. 2000. Two-component and phosphorelay signal transduction. Curr. Opin. Microbiol. **3**(2): 165-170.

Homonylo-McGavin, M.K., and Lee, S.F. 1996. Role of the C terminus in antigen P1 surface localization in *Streptococcus mutans* and two related cocci. J. Bacteriol. **178**(3): 801-807.

Howell, A., Dubrac, S., Noone, D., Varughese, K.I., and Devine, K. 2006. Interactions between the YycFG and PhoPR two-component systems in *Bacillus subtilis*: the PhoR kinase phosphorylates the non-cognate YycF response regulator upon phosphate limitation. Mol. Microbiol. **59**(4): 1199-1215.

Howell, A., Dubrac, S., Andersen, K.K., Noone, D., Fert, J., Msadek, T., and Devine, K. 2003. Genes controlled by the essential YycG/YycF two-component system of *Bacillus subtilis* revealed through a novel hybrid regulator approach. Mol. Microbiol. **49**(6): 1639-1655.

Huang, M., Meng, L., Fan, M., Hu, P., and Bian, Z. 2008. Effect of biofilm formation on virulence factor secretion via the general secretory pathway in *Streptococcus mutans*. Arch. Oral Biol. **53**(12): 1179-1185.

Hudson, M.C., and Curtiss, R.,3rd. 1990. Regulation of expression of *Streptococcus mutans* genes important to virulence. Infect. Immun. **58**(2): 464-470.

Idone, V., Brendtro, S., Gillespie, R., Kocaj, S., Peterson, E., Rendi, M., Warren, W., Michalek, S., Krastel, K., Cvitkovitch, D., and Spatafora, G. 2003. Effect of an orphan response regulator on *Streptococcus mutans* sucrose-dependent adherence and cariogenesis. Infect. Immun. **71**(8): 4351-4360.

Jacobson, G.R., Lodge, J., and Poy, F. 1989. Carbohydrate uptake in the oral pathogen *Streptococcus mutans*: mechanisms and regulation by protein phosphorylation. Biochimie **71**(9-10): 997-1004.

Jayaraman, G.C., Penders, J.E., and Burne, R.A. 1997. Transcriptional analysis of the *Streptococcus mutans hrcA*, *grpE* and *dnaK* genes and regulation of expression in response to heat shock and environmental acidification. Mol. Microbiol. **25**(2): 329-341.

Jiang, S.M., Cieslewicz, M.J., Kasper, D.L., and Wessels, M.R. 2005. Regulation of virulence by a two-component system in group B *Streptococcus*. J. Bacteriol. **187**(3): 1105-1113.

Jordan, S., Hutchings, M.I., and Mascher, T. 2008. Cell envelope stress response in Gram-positive bacteria. FEMS Microbiol. Rev. **32**(1): 107-146.

Jordan, S., Junker, A., Helmann, J.D., and Mascher, T. 2006. Regulation of LiaRS-dependent gene expression in *Bacillus subtilis*: identification of inhibitor proteins, regulator binding sites, and target genes of a conserved cell envelope stress-sensing two-component system. J. Bacteriol. **188**(14): 5153-5166.

Jordan, S., Rietkotter, E., Strauch, M.A., Kalamorz, F., Butcher, B.G., Helmann, J.D., and Mascher, T. 2007. LiaRS-dependent gene expression is embedded in transition state regulation in *Bacillus subtilis*. Microbiology **153**(Pt 8): 2530-2540.

Kara, D., Luppens, S.B., and Cate, J.M. 2006. Differences between single- and dual-species biofilms of *Streptococcus mutans* and *Veillonella parvula* in growth, acidogenicity and susceptibility to chlorhexidine. Eur. J. Oral Sci. **114**(1): 58-63.

Kara, D., Luppens, S.B., van Marle, J., Ozok, R., and ten Cate, J.M. 2007. Microstructural differences between single-species and dual-species biofilms of *Streptococcus mutans* and *Veillonella parvula*, before and after exposure to chlorhexidine. FEMS Microbiol. Lett. **271**(1): 90-97.

Kedar, G.C., Brown-Driver, V., Reyes, D.R., Hilgers, M.T., Stidham, M.A., Shaw, K.J., Finn, J., and Haselbeck, R.J. 2008. Comparison of the essential cellular functions of the two *murA* genes of *Bacillus anthracis*. Antimicrob. Agents Chemother. **52**(6): 2009-2013.

Korithoski, B., Levesque, C.M., and Cvitkovitch, D.G. 2008. The involvement of the pyruvate dehydrogenase E1alpha subunit, in *Streptococcus mutans* acid tolerance. FEMS Microbiol. Lett. **289**(1): 13-19.

Kremer, B.H., van der Kraan, M., Crowley, P.J., Hamilton, I.R., Brady, L.J., and Bleiweis, A.S. 2001. Characterization of the sat operon in *Streptococcus mutans*: evidence for a role of Ffh in acid tolerance. J. Bacteriol. **183**(8): 2543-2552.

Kreth, J., Zhang, Y., and Herzberg, M.C. 2008b. Streptococcal antagonism in oral biofilms: *Streptococcus sanguinis* and *Streptococcus gordonii* interference with *Streptococcus mutans*. J. Bacteriol. **190**(13): 4632-4640.

Kreth, J., Zhu, L., Merritt, J., Shi, W., and Qi, F. 2008a. Role of sucrose in the fitness of *Streptococcus mutans*. Oral Microbiol. Immunol. **23**(3): 213-219.

Kreth, J., Merritt, J., Zhu, L., Shi, W., and Qi, F. 2006. Cell density- and ComE-dependent expression of a group of mutacin and mutacin-like genes in *Streptococcus mutans*. FEMS Microbiol. Lett. **265**(1): 11-17.

Kreth, J., Hung, D.C., Merritt, J., Perry, J., Zhu, L., Goodman, S.D., Cvitkovitch, D.G., Shi, W., and Qi, F. 2007. The response regulator ComE in *Streptococcus mutans* functions both as a transcription activator of mutacin production and repressor of CSP biosynthesis. Microbiology **153**(Pt 6): 1799-1807.

Kuroda, M., Kuroda, H., Oshima, T., Takeuchi, F., Mori, H., and Hiramatsu, K. 2003. Two-component system VraSR positively modulates the regulation of cell-wall biosynthesis pathway in *Staphylococcus aureus*. Mol. Microbiol. **49**(3): 807-821.

Lamy, M.C., Zouine, M., Fert, J., Vergassola, M., Couve, E., Pellegrini, E., Glaser, P., Kunst, F., Msadek, T., Trieu-Cuot, P., and Poyart, C. 2004. CovS/CovR of group B *Streptococcus*: a two-component global regulatory system involved in virulence. Mol. Microbiol. **54**(5): 1250-1268.

Lau, P.C., Sung, C.K., Lee, J.H., Morrison, D.A., and Cvitkovitch, D.G. 2002. PCR ligation mutagenesis in transformable streptococci: application and efficiency. J. Microbiol. Methods **49**(2): 193-205.

Lee, H.Y., Cho, S.A., Lee, I.S., Park, J.H., Seok, S.H., Baek, M.W., Kim, D.J., Lee, S.H., Hur, S.J., Ban, S.J., Lee, Y.K., Han, Y.K., Cho, Y.K., and Park, J.H. 2007. Evaluation of *phoP* and *rpoS* mutants of *Salmonella enterica* serovar *Typhi* as attenuated typhoid vaccine candidates: virulence and protective immune responses in intranasally immunized mice. FEMS Immunol. Med. Microbiol. **51**(2): 310-318.

Lee, S.F., and Boran, T.L. 2003. Roles of sortase in surface expression of the major protein adhesin P1, saliva-induced aggregation and adherence, and cariogenicity of *Streptococcus mutans*. Infect. Immun. **71**(2): 676-681.

Lee, S.F., Delaney, G.D., and Elkhateeb, M. 2004. A two-component *covRS* regulatory system regulates expression of fructosyltransferase and a novel extracellular carbohydrate in *Streptococcus mutans*. Infect. Immun. **72**(7): 3968-3973.

Lee, S.F., Progulske-Fox, A., Erdos, G.W., Piacentini, D.A., Ayakawa, G.Y., Crowley, P.J., and Bleiweis, A.S. 1989. Construction and characterization of isogenic mutants of *Streptococcus mutans* deficient in major surface protein antigen P1 (I/II). Infect. Immun. **57**(11): 3306-3313.

Lemos, J.A., and Burne, R.A. 2002. Regulation and Physiological Significance of ClpC and ClpP in *Streptococcus mutans*. J. Bacteriol. **184**(22): 6357-6366.

Lemos, J.A., Chen, Y.Y., and Burne, R.A. 2001. Genetic and physiologic analysis of the *groE* operon and role of the HrcA repressor in stress gene regulation and acid tolerance in *Streptococcus mutans*. J. Bacteriol. **183**(20): 6074-6084.

Levesque, C.M., Mair, R.W., Perry, J.A., Lau, P.C., Li, Y.H., and Cvitkovitch, D.G. 2007. Systemic inactivation and phenotypic characterization of two-component systems in expression of *Streptococcus mutans* virulence properties. Lett. Appl. Microbiol. **45**(4): 398-404.

Levin, J.C., and Wessels, M.R. 1998. Identification of *csrR/csrS*, a genetic locus that regulates hyaluronic acid capsule synthesis in group A *Streptococcus*. Mol. Microbiol. **30**(1): 209-219.

Li, Y., and Burne, R.A. 2001. Regulation of the *gtfBC* and *ftf* genes of *Streptococcus mutans* in biofilms in response to pH and carbohydrate. Microbiology **147**(Pt 10): 2841-2848.

Li, Y.H., Tian, X.L., Layton, G., Norgaard, C., and Sisson, G. 2008. Additive attenuation of virulence and cariogenic potential of *Streptococcus mutans* by simultaneous inactivation of the ComCDE quorum-sensing system and HK/RR11 two-component regulatory system. Microbiology **154**(Pt 11): 3256-3265.

Li, Y.H., Hanna, M.N., Svensater, G., Ellen, R.P., and Cvitkovitch, D.G. 2001a. Cell density modulates acid adaptation in *Streptococcus mutans*: implications for survival in biofilms. J. Bacteriol. **183**(23): 6875-6884.

Li, Y.H., Lau, P.C., Lee, J.H., Ellen, R.P., and Cvitkovitch, D.G. 2001b. Natural genetic transformation of *Streptococcus mutans* growing in biofilms. J. Bacteriol. **183**(3): 897-908.

Li, Y.H., Lau, P.C., Tang, N., Svensater, G., Ellen, R.P., and Cvitkovitch, D.G. 2002a. Novel two-component regulatory system involved in biofilm formation and acid resistance in *Streptococcus mutans*. J. Bacteriol. **184**(22): 6333-6342.

Li, Y.H., Tang, N., Aspiras, M.B., Lau, P.C., Lee, J.H., Ellen, R.P., and Cvitkovitch, D.G. 2002b. A quorum-sensing signaling system essential for genetic competence in *Streptococcus mutans* is involved in biofilm formation. J. Bacteriol. **184**(10): 2699-2708.

Liu, M., Hanks, T.S., Zhang, J., McClure, M.J., Siemsen, D.W., Elser, J.L., Quinn, M.T., and Lei, B. 2006. Defects in *ex vivo* and *in vivo* growth and sensitivity to osmotic stress of group A *Streptococcus* caused by interruption of response regulator gene *vicR*. Microbiology **152**(Pt 4): 967-978.

Lodato, P.B., and Kaper, J.B. 2009. Post-transcriptional processing of the *LEE4* operon in enterohaemorrhagic *Escherichia coli*. Mol. Microbiol. **71**(2): 273-290.

Loesche, W.J. 1986. Role of *Streptococcus mutans* in human dental decay. Microbiol. Rev. **50**(4): 353-380.

Love, R.M., McMillan, M.D., and Jenkinson, H.F. 1997. Invasion of dentinal tubules by oral streptococci is associated with collagen recognition mediated by the antigen I/II family of polypeptides. Infect. Immun. **65**(12): 5157-5164.

Lukat, G.S., McCleary, W.R., Stock, A.M., and Stock, J.B. 1992. Phosphorylation of bacterial response regulator proteins by low molecular weight phospho-donors. Proc. Natl. Acad. Sci. U. S. A. **89**(2): 718-722.

Luppens, S.B., Kara, D., Bandounas, L., Jonker, M.J., Wittink, F.R., Bruning, O., Breit, T.M., Ten Cate, J.M., and Crielaard, W. 2008. Effect of *Veillonella parvula* on the antimicrobial resistance and gene expression of *Streptococcus mutans* grown in a dual-species biofilm. Oral Microbiol. Immunol. **23**(3): 183-189.

Lynch, D.J., Fountain, T.L., Mazurkiewicz, J.E., and Banas, J.A. 2007. Glucan-binding proteins are essential for shaping *Streptococcus mutans* biofilm architecture. FEMS Microbiol. Lett. **268**(2): 158-165.

Ma, J.K., Kelly, C.G., Munro, G., Whiley, R.A., and Lehner, T. 1991. Conservation of the gene encoding streptococcal antigen I/II in oral streptococci. Infect. Immun. **59**(8): 2686-2694.

Ma, P., Yuille, H.M., Blessie, V., Gohring, N., Igloi, Z., Nishiguchi, K., Nakayama, J., Henderson, P.J., and Phillips-Jones, M.K. 2008. Expression, purification and activities of the entire family of intact membrane sensor kinases from *Enterococcus faecalis*. Mol. Membr. Biol. **25**(6-7): 449-473.

MacGregor, E.A., Janecek, S., and Svensson, B. 2001. Relationship of sequence and structure to specificity in the alpha-amylase family of enzymes. Biochim. Biophys. Acta **1546**(1): 1-20.

MacGregor, E.A., Jespersen, H.M., and Svensson, B. 1996. A circularly permuted alpha-amylase-type alpha/beta-barrel structure in glucan-synthesizing glucosyltransferases. FEBS Lett. **378**(3): 263-266.

Martin, B., Quentin, Y., Fichant, G., and Claverys, J.P. 2006. Independent evolution of competence regulatory cascades in streptococci? Trends Microbiol. **14**(8): 339-345.

Martin, M.E., Strachan, R.C., Aranha, H., Evans, S.L., Salin, M.L., Welch, B., Arceneaux, J.E., and Byers, B.R. 1984. Oxygen toxicity in *Streptococcus mutans*: manganese, iron, and superoxide dismutase. J. Bacteriol. **159**(2): 745-749.

Martin, P.K., Li, T., Sun, D., Biek, D.P., and Schmid, M.B. 1999. Role in cell permeability of an essential two-component system in *Staphylococcus aureus*. J. Bacteriol. **181**(12): 3666-3673.

Martinez, B., Zomer, A.L., Rodriguez, A., Kok, J., and Kuipers, O.P. 2007. Cell envelope stress induced by the bacteriocin Lcn972 is sensed by the Lactococcal two-component system CesSR. Mol. Microbiol. **64**(2): 473-486.

Marvo, S.L., King, S.R., and Jaskunas, S.R. 1983. Role of short regions of homology in intermolecular illegitimate recombination events. Proc. Natl. Acad. Sci. U. S. A. **80**(9): 2452-2456.

Mascher, T. 2006. Intramembrane-sensing histidine kinases: a new family of cell envelope stress sensors in Firmicutes bacteria. FEMS Microbiol. Lett. **264**(2): 133-144.

Mascher, T., Zimmer, S.L., Smith, T.A., and Helmann, J.D. 2004. Antibiotic-inducible promoter regulated by the cell envelope stress-sensing two-component system LiaRS of *Bacillus subtilis*. Antimicrob. Agents Chemother. **48**(8): 2888-2896.

Mascher, T., Margulis, N.G., Wang, T., Ye, R.W., and Helmann, J.D. 2003. Cell wall stress responses in *Bacillus subtilis*: the regulatory network of the bacitracin stimulon. Mol. Microbiol. **50**(5): 1591-1604.

Matsumoto, M., Fujita, K., and Ooshima, T. 2006. Binding of glucan-binding protein C to GTFD-synthesized soluble glucan in sucrose-dependent adhesion of *Streptococcus mutans*. Oral Microbiol. Immunol. **21**(1): 42-46.

Matsumura, M., Izumi, T., Matsumoto, M., Tsuji, M., Fujiwara, T., and Ooshima, T. 2003. The role of glucan-binding proteins in the cariogenicity of *Streptococcus mutans*. Microbiol. Immunol. **47**(3): 213-215.

Mattos-Graner, R.O., Porter, K.A., Smith, D.J., Hosogi, Y., and Duncan, M.J. 2006. Functional analysis of glucan binding protein B from *Streptococcus mutans*. J. Bacteriol. **188**(11): 3813-3825.

Mattos-Graner, R.O., Jin, S., King, W.F., Chen, T., Smith, D.J., and Duncan, M.J. 2001. Cloning of the *Streptococcus mutans* gene encoding glucan binding protein B and analysis of genetic diversity and protein production in clinical isolates. Infect. Immun. **69**(11): 6931-6941.

McCleary, W.R., Stock, J.B., and Ninfa, A.J. 1993. Is acetyl phosphate a global signal in *Escherichia coli*? J. Bacteriol. **175**(10): 2793-2798.

McNeill, K., and Hamilton, I.R. 2003. Acid tolerance response of biofilm cells of *Streptococcus mutans*. FEMS Microbiol. Lett. **221**(1): 25-30.

Merritt, J., Qi, F., Goodman, S.D., Anderson, M.H., and Shi, W. 2003. Mutation of *luxS* affects biofilm formation in *Streptococcus mutans*. Infect. Immun. **71**(4): 1972-1979.

Miller-Torbert, T.A., Sharma, S., and Holt, R.G. 2008. Inactivation of a gene for a fibronectin-binding protein of the oral bacterium *Streptococcus mutans* partially impairs its adherence to fibronectin. Microb. Pathog. **45**(1): 53-59.

Miller, S.I., Kukral, A.M., and Mekalanos, J.J. 1989. A two-component regulatory system (*phoP phoQ*) controls *Salmonella typhimurium* virulence. Proc. Natl. Acad. Sci. U. S. A. **86**(13): 5054-5058.

Mitchell, T.J. 2003. The pathogenesis of streptococcal infections: from tooth decay to meningitis. Nat. Rev. Microbiol. **1**(3): 219-230.

Mitrakul, K., Loo, C.Y., Hughes, C.V., and Ganeshkumar, N. 2004. Role of a *Streptococcus gordonii* copper-transport operon, *copYAZ*, in biofilm detachment. Oral Microbiol. Immunol. **19**(6): 395-402.

Mitrophanov, A.Y., Churchward, G., and Borodovsky, M. 2007. Control of *Streptococcus pyogenes* virulence: modeling of the CovR/S signal transduction system. J. Theor. Biol. **246**(1): 113-128.

Monchois, V., Willemot, R.M., and Monsan, P. 1999. Glucansucrases: mechanism of action and structure-function relationships. FEMS Microbiol. Rev. **23**(2): 131-151.

Mooser, G., Hefta, S.A., Paxton, R.J., Shively, J.E., and Lee, T.D. 1991. Isolation and sequence of an active-site peptide containing a catalytic aspartic acid from two *Streptococcus sobrinus* alpha-glucosyltransferases. J. Biol. Chem. **266**(14): 8916-8922.

Munch, R., Hiller, K., Grote, A., Scheer, M., Klein, J., Schobert, M., and Jahn, D. 2005. Virtual Footprint and PRODORIC: an integrative framework for regulon prediction in prokaryotes. Bioinformatics **21**(22): 4187-4189.

Munro, C., Michalek, S.M., and Macrina, F.L. 1991. Cariogenicity of *Streptococcus mutans* V403 glucosyltransferase and fructosyltransferase mutants constructed by allelic exchange. Infect. Immun. **59**(7): 2316-2323.

Munro, C.L., Michalek, S.M., and Macrina, F.L. 1995. Sucrose-derived exopolymers have site-dependent roles in *Streptococcus mutans*-promoted dental decay. FEMS Microbiol. Lett. **128**(3): 327-332.

Nakai, M., Okahashi, N., Ohta, H., and Koga, T. 1993. Saliva-binding region of *Streptococcus mutans* surface protein antigen. Infect. Immun. **61**(10): 4344-4349.

Nakano, K., Tsuji, M., Nishimura, K., Nomura, R., and Ooshima, T. 2006. Contribution of cell surface protein antigen PAc of *Streptococcus mutans* to bacteremia. Microbes Infect. **8**(1): 114-121.

Nakano, K., Matsumura, M., Kawaguchi, M., Fujiwara, T., Sobue, S., Nakagawa, I., Hamada, S., and Ooshima, T. 2002. Attenuation of glucan-binding protein C reduces the cariogenicity of *Streptococcus mutans*: analysis of strains isolated from human blood. J. Dent. Res. **81**(6): 376-379.

Ng, W.L., and Winkler, M.E. 2004. Singular structures and operon organizations of essential two-component systems in species of *Streptococcus*. Microbiology **150**(Pt 10): 3096-3098.

Ng, W.L., Tsui, H.C., and Winkler, M.E. 2005. Regulation of the *pspA* virulence factor and essential *pcsB* murein biosynthetic genes by the phosphorylated VicR (YycF) response regulator in *Streptococcus pneumoniae*. J. Bacteriol. **187**(21): 7444-7459.

Ng, W.L., Kazmierczak, K.M., and Winkler, M.E. 2004. Defective cell wall synthesis in *Streptococcus pneumoniae* R6 depleted for the essential PcsB putative murein hydrolase or the VicR (YycF) response regulator. Mol. Microbiol. **53**(4): 1161-1175.

Ng, W.L., Robertson, G.T., Kazmierczak, K.M., Zhao, J., Gilmour, R., and Winkler, M.E. 2003. Constitutive expression of PcsB suppresses the requirement for the essential VicR (YycF) response regulator in *Streptococcus pneumoniae* R6. Mol. Microbiol. **50**(5): 1647-1663.

Niu, G., Okinaga, T., Zhu, L., Banas, J., Qi, F., and Merritt, J. 2008. Characterization of *irvR*, a novel regulator of the *irvA*-dependent pathway required for genetic competence and dextran-dependent aggregation in *Streptococcus mutans*. J. Bacteriol. **190**(21): 7268-7274.

O'Connell-Motherway, M., van Sinderen, D., Morel-Deville, F., Fitzgerald, G.F., Ehrlich, S.D., and Morel, P. 2000. Six putative two-component regulatory systems isolated from *Lactococcus lactis* subsp. *cremoris* MG1363. Microbiology **146 (Pt 4)**(Pt 4): 935-947.

Ohta, H., Kato, H., Okahashi, N., Takahashi, I., Hamada, S., and Koga, T. 1989. Characterization of a cell-surface protein antigen of hydrophilic *Streptococcus mutans* strain GS-5. J. Gen. Microbiol. **135**(4): 981-988.

Ooshima, T., Matsumura, M., Hoshino, T., Kawabata, S., Sobue, S., and Fujiwara, T. 2001. Contributions of three glycosyltransferases to sucrose-dependent adherence of *Streptococcus mutans*. J. Dent. Res. **80**(7): 1672-1677.

Pamp, S.J., Frees, D., Engelmann, S., Hecker, M., and Ingmer, H. 2006. Spx is a global effector impacting stress tolerance and biofilm formation in *Staphylococcus aureus*. J. Bacteriol. **188**(13): 4861-4870.

Perry, J.A., Jones, M.B., Peterson, S.N., Cvitkovitch, D.G., and Levesque, C.M. 2009a. Peptide alarmone signalling triggers an auto-active bacteriocin necessary for genetic competence. Mol. Microbiol.

Perry, J.A., Cvitkovitch, D.G., and Levesque, C.M. 2009b. Cell death in Streptococcus mutans biofilms: a link between CSP and extracellular DNA. FEMS Microbiol. Lett. **299**(2): 261-266.

Pestova, E.V., Havarstein, L.S., and Morrison, D.A. 1996. Regulation of competence for genetic transformation in *Streptococcus pneumoniae* by an auto-induced peptide pheromone and a two-component regulatory system. Mol. Microbiol. **21**(4): 853-862.

Petersen, F.C., and Scheie, A.A. 2000. Genetic transformation in *Streptococcus mutans* requires a peptide secretion-like apparatus. Oral Microbiol. Immunol. **15**(5): 329-334.

Petersen, F.C., Fimland, G., and Scheie, A.A. 2006. Purification and functional studies of a potent modified quorum-sensing peptide and a two-peptide bacteriocin in *Streptococcus mutans*. Mol. Microbiol. **61**(5): 1322-1334.

Petersen, F.C., Assev, S., van der Mei, H.C., Busscher, H.J., and Scheie, A.A. 2002. Functional variation of the antigen I/II surface protein in *Streptococcus mutans* and *Streptococcus intermedius*. Infect. Immun. **70**(1): 249-256.

Peterson, S., Cline, R.T., Tettelin, H., Sharov, V., and Morrison, D.A. 2000. Gene expression analysis of the *Streptococcus pneumoniae* competence regulons by use of DNA microarrays. J. Bacteriol. **182**(21): 6192-6202.

Pietiainen, M., Gardemeister, M., Mecklin, M., Leskela, S., Sarvas, M., and Kontinen, V.P. 2005. Cationic antimicrobial peptides elicit a complex stress response in *Bacillus subtilis* that involves ECF-type sigma factors and two-component signal transduction systems. Microbiology **151**(Pt 5): 1577-1592.

Potrykus, J., Mahaney, B., White, R.L., and Bearne, S.L. 2007. Proteomic investigation of glucose metabolism in the butyrate-producing gut anaerobe *Fusobacterium varium*. Proteomics **7**(11): 1839-1853.

Qi, F., Chen, P., and Caufield, P.W. 2000. Purification and biochemical characterization of mutacin I from the group I strain of *Streptococcus mutans*, CH43, and genetic analysis of mutacin I biosynthesis genes. Appl. Environ. Microbiol. **66**(8): 3221-3229.

Qi, F., Merritt, J., Lux, R., and Shi, W. 2004. Inactivation of the *ciaH* Gene in *Streptococcus mutans* diminishes mutacin production and competence development, alters sucrose-dependent biofilm formation, and reduces stress tolerance. Infect. Immun. **72**(8): 4895-4899.

Qi, F., Kreth, J., Levesque, C.M., Kay, O., Mair, R.W., Shi, W., Cvitkovitch, D.G., and Goodman, S.D. 2005. Peptide pheromone induced cell death of *Streptococcus mutans*. FEMS Microbiol. Lett. **251**(2): 321-326.

Quivey, R.G., Kuhnert, W.L., and Hahn, K. 2001. Genetics of acid adaptation in oral streptococci. Crit. Rev. Oral Biol. Med. **12**(4): 301-314.

Quivey, R.G.,Jr, Faustoferri, R., Monahan, K., and Marquis, R. 2000. Shifts in membrane fatty acid profiles associated with acid adaptation of *Streptococcus mutans*. FEMS Microbiol. Lett. **189**(1): 89-92.

Quivey, R.G.,Jr, Faustoferri, R.C., Clancy, K.A., and Marquis, R.E. 1995. Acid adaptation in *Streptococcus mutans* UA159 alleviates sensitization to environmental stress due to RecA deficiency. FEMS Microbiol. Lett. **126**(3): 257-261.

Rathsam, C., Eaton, R.E., Simpson, C.L., Browne, G.V., Valova, V.A., Harty, D.W., and Jacques, N.A. 2005. Two-dimensional fluorescence difference gel electrophoretic analysis of *Streptococcus mutans* biofilms. J. Proteome Res. **4**(6): 2161-2173.

Reese, M.G. 2001. Application of a time-delay neural network to promoter annotation in the *Drosophila melanogaster* genome. Comput. Chem. **26**(1): 51-56.

Rogers, P.D., Liu, T.T., Barker, K.S., Hilliard, G.M., English, B.K., Thornton, J., Swiatlo, E., and McDaniel, L.S. 2007. Gene expression profiling of the response of *Streptococcus pneumoniae* to penicillin. J. Antimicrob. Chemother. **59**(4): 616-626.

Russell, R.R. 1979. Glucan-binding proteins of *Streptococcus mutans* serotype c. J. Gen. Microbiol. **112**(1): 197-201.

Russell, R.R., Coleman, D., and Dougan, G. 1985. Expression of a gene for glucan-binding protein from *Streptococcus mutans* in *Escherichia coli*. J. Gen. Microbiol. **131**(2): 295-299.

Sambrook, J., Fritsch, E.F., and Maniatis, T. 1989. Molecular cloning : a laboratory manual. Cold Spring Harbor Laboratory Press, Cold Spring Harbor, N.Y.

Santelli, E., Liddington, R.C., Mohan, M.A., Hoch, J.A., and Szurmant, H. 2007. The crystal structure of *Bacillus subtilis* YycI reveals a common fold for two members of an unusual class of sensor histidine kinase regulatory proteins. J. Bacteriol. **189**(8): 3290-3295.

Sato, Y., Yamamoto, Y., and Kizaki, H. 2000. Construction of region-specific partial duplication mutants (merodiploid mutants) to identify the regulatory gene for the glucan-binding protein C gene in vivo in *Streptococcus mutans*. FEMS Microbiol. Lett. **186**(2): 187-191.

Sato, Y., Yamamoto, Y., and Kizaki, H. 1997. Cloning and sequence analysis of the *gbpC* gene encoding a novel glucan-binding protein of *Streptococcus mutans*. Infect. Immun. **65**(2): 668-675.

Senadheera, M.D., Lee, A.W., Hung, D.C., Spatafora, G.A., Goodman, S.D., and Cvitkovitch, D.G. 2007. The Streptococcus mutans *vicX* gene product modulates gtfB/C expression, biofilm formation, genetic competence, and oxidative stress tolerance. J. Bacteriol. **189**(4): 1451-1458.

Senadheera, M.D., Guggenheim, B., Spatafora, G.A., Huang, Y.C., Choi, J., Hung, D.C., Treglown, J.S., Goodman, S.D., Ellen, R.P., and Cvitkovitch, D.G. 2005. A VicRK signal transduction system in *Streptococcus mutans* affects *gtfBCD*, *gbpB*, and *ftf* expression, biofilm formation, and genetic competence development. J. Bacteriol. **187**(12): 4064-4076.

Senadheera, M.D. and Cvitkovitch, D.G. 2005. A VicRK signal transduction system responds to the signal peptide pheromone in *Streptococcus mutans.* Euro. Research Group Oral Biol. Conference. 5th. 2005. 17. p13.

Shah, D.S., and Russell, R.R. 2004. A novel glucan-binding protein with lipase activity from the oral pathogen *Streptococcus mutans*. Microbiology **150**(Pt 6): 1947-1956.

Shemesh, M., Tam, A., and Steinberg, D. 2007. Differential gene expression profiling of *Streptococcus mutans* cultured under biofilm and planktonic conditions. Microbiology **153**(Pt 5): 1307-1317.

Shemesh, M., Tam, A., Feldman, M., and Steinberg, D. 2006. Differential expression profiles of *Streptococcus mutans ftf, gtf* and *vicR* genes in the presence of dietary carbohydrates at early and late exponential growth phases. Carbohydr. Res. **341**(12): 2090-2097.

Shibata, Y., Kawada, M., Nakano, Y., Toyoshima, K., and Yamashita, Y. 2005. Identification and characterization of an autolysin-encoding gene of *Streptococcus mutans*. Infect. Immun. **73**(6): 3512-3520.

Smorawinska, M., and Kuramitsu, H.K. 1995. Primer extension analysis of *Streptococcus mutans* promoter structures. Oral Microbiol. Immunol. **10**(3): 188-192.

Spector, T. 1978. Refinement of the Coomassie blue method of protein quantitation. A simple and linear spectrophotometric assay for less than or equal to 0.5 to 50 microgram of protein. Anal. Biochem. **86**(1): 142-146.

Stephenson, K., and Hoch, J.A. 2002. Two-component and phosphorelay signal-transduction systems as therapeutic targets. Curr. Opin. Pharmacol. **2**(5): 507-512.

Stipp, R.N., Goncalves, R.B., Hofling, J.F., Smith, D.J., and Mattos-Graner, R.O. 2008. Transcriptional analysis of *gtfB*, *gtfC*, and *gbpB* and their putative response regulators in several isolates of *Streptococcus mutans*. Oral Microbiol. Immunol. **23**(6): 466-473.

Stock, A.M., Robinson, V.L., and Goudreau, P.N. 2000. Two-component signal transduction. Annu. Rev. Biochem. **69**: 183-215.

Stojiljkovic, I., Baumler, A.J., and Hantke, K. 1994. Fur regulon in Gram-negative bacteria. Identification and characterization of new iron-regulated *Escherichia coli* genes by a fur titration assay. J. Mol. Biol. **236**(2): 531-545.

Suntharalingam, P., Senadheera, M.D., Mair, R.W., Levesque, C.M., and Cvitkovitch, D.G. 2009. The LiaFSR system regulates the cell envelope stress response in *Streptococcus mutans*. J. Bacteriol. **191**(9): 2973-2984.

Syvitski, R.T., Tian, X.L., Sampara, K., Salman, A., Lee, S.F., Jakeman, D.L., and Li, Y.H. 2007. Structure-activity analysis of quorum-sensing signaling peptides from *Streptococcus mutans*. J. Bacteriol. **189**(4): 1441-1450.

Szurmant, H., Bu, L., Brooks, C.L.,3rd, and Hoch, J.A. 2008. An essential sensor histidine kinase controlled by transmembrane helix interactions with its auxiliary proteins. Proc. Natl. Acad. Sci. U. S. A. **105**(15): 5891-5896.

Szurmant, H., Mohan, M.A., Imus, P.M., and Hoch, J.A. 2007. YycH and YycI interact to regulate the essential YycFG two-component system in *Bacillus subtilis*. J. Bacteriol. **189**(8): 3280-3289.

Szurmant, H., Zhao, H., Mohan, M.A., Hoch, J.A., and Varughese, K.I. 2006. The crystal structure of YycH involved in the regulation of the essential YycFG two-component system in *Bacillus subtilis* reveals a novel tertiary structure. Protein Sci. **15**(4): 929-934.

Szurmant, H., Nelson, K., Kim, E.J., Perego, M., and Hoch, J.A. 2005. YycH regulates the activity of the essential YycFG two-component system in *Bacillus subtilis*. J. Bacteriol. **187**(15): 5419-5426.

Taubman, M.A., and Nash, D.A. 2006. The scientific and public-health imperative for a vaccine against dental caries. Nat. Rev. Immunol. **6**(7): 555-563.

Taylor, B.L. 2007. Aer on the inside looking out: paradigm for a PAS-HAMP role in sensing oxygen, redox and energy. Mol. Microbiol. **65**(6): 1415-1424.

Taylor, B.L., and Zhulin, I.B. 1999. PAS domains: internal sensors of oxygen, redox potential, and light. Microbiol. Mol. Biol. Rev. **63**(2): 479-506.

Terleckyj, B., Willett, N.P., and Shockman, G.D. 1975. Growth of several cariogenic strains of oral streptococci in a chemically defined medium. Infect. Immun. **11**(4): 649-655.

Tobian, J.A., Cline, M.L., and Macrina, F.L. 1984. Characterization and expression of a cloned tetracycline resistance determinant from the chromosome of *Streptococcus mutans*. J. Bacteriol. **160**(2): 556-563.

Tong, H., Chen, W., Merritt, J., Qi, F., Shi, W., and Dong, X. 2007. Streptococcus oligofermentans inhibits Streptococcus mutans through conversion of lactic acid into inhibitory H2O2: a possible counteroffensive strategy for interspecies competition. Mol. Microbiol. **63**(3): 872-880.

Troffer-Charlier, N., Ogier, J., Moras, D., and Cavarelli, J. 2002. Crystal structure of the V-region of *Streptococcus mutans* antigen I/II at 2.4 A resolution suggests a sugar preformed binding site. J. Mol. Biol. **318**(1): 179-188.

Tsang, P., Merritt, J., Shi, W., and Qi, F. 2006. IrvA-dependent and IrvA-independent pathways for mutacin gene regulation in *Streptococcus mutans*. FEMS Microbiol. Lett. **261**(2): 231-234.

Tsang, P., Merritt, J., Nguyen, T., Shi, W., and Qi, F. 2005. Identification of genes associated with mutacin I production in *Streptococcus mutans* using random insertional mutagenesis. Microbiology **151**(Pt 12): 3947-3955.

van der Ploeg, J.R. 2005. Regulation of bacteriocin production in *Streptococcus mutans* by the quorum-sensing system required for development of genetic competence. J. Bacteriol. **187**(12): 3980-3989.

Vats, N., and Lee, S.F. 2000. Active detachment of *Streptococcus mutans* cells adhered to epon-hydroxylapatite surfaces coated with salivary proteins in vitro. Arch. Oral Biol. **45**(4): 305-314.

Veiga, P., Bulbarela-Sampieri, C., Furlan, S., Maisons, A., Chapot-Chartier, M.P., Erkelenz, M., Mervelet, P., Noirot, P., Frees, D., Kuipers, O.P., Kok, J., Gruss, A., Buist, G., and Kulakauskas, S. 2007. SpxB regulates O-acetylation-dependent resistance of *Lactococcus lactis* peptidoglycan to hydrolysis. J. Biol. Chem. **282**(27): 19342-19354.

Voyich, J.M., Braughton, K.R., Sturdevant, D.E., Vuong, C., Kobayashi, S.D., Porcella, S.F., Otto, M., Musser, J.M., and DeLeo, F.R. 2004. Engagement of the pathogen survival response used by group A *Streptococcus* to avert destruction by innate host defense. J. Immunol. **173**(2): 1194-1201.

Wagner, C., Saizieu Ad, A., Schonfeld, H.J., Kamber, M., Lange, R., Thompson, C.J., and Page, M.G. 2002. Genetic analysis and functional characterization of the *Streptococcus pneumoniae vic* operon. Infect. Immun. **70**(11): 6121-6128.

Wandersman, C., and Delepelaire, P. 2004. Bacterial iron sources: from siderophores to hemophores. Annu. Rev. Microbiol. **58**: 611-647.

Watanabe, T., Hashimoto, Y., Umemoto, Y., Tatebe, D., Furuta, E., Fukamizo, T., Yamamoto, K., and Utsumi, R. 2003. Molecular characterization of the essential response regulator protein YycF in *Bacillus subtilis*. J. Mol. Microbiol. Biotechnol. **6**(3-4): 155-163.

Wen, Z.T., and Burne, R.A. 2004. LuxS-mediated signaling in *Streptococcus mutans* is involved in regulation of acid and oxidative stress tolerance and biofilm formation. J. Bacteriol. **186**(9): 2682-2691.

Wen, Z.T., and Burne, R.A. 2002. Functional genomics approach to identifying genes required for biofilm development by *Streptococcus mutans*. Appl. Environ. Microbiol. **68**(3): 1196-1203.

Wen, Z.T., Suntharaligham, P., Cvitkovitch, D.G., and Burne, R.A. 2005. Trigger factor in *Streptococcus mutans* is involved in stress tolerance, competence development, and biofilm formation. Infect. Immun. **73**(1): 219-225.

Whittaker, C.J., Clemans, D.L., and Kolenbrander, P.E. 1996. Insertional inactivation of an intrageneric coaggregation-relevant adhesin locus from *Streptococcus gordonii* DL1 (Challis). Infect. Immun. **64**(10): 4137-4142.

Yamashita, Y., Takehara, T., and Kuramitsu, H.K. 1993. Molecular characterization of a *Streptococcus mutans* mutant altered in environmental stress responses. J. Bacteriol. **175**(19): 6220-6228.

Yamashita, Y., Tomihisa, K., Nakano, Y., Shimazaki, Y., Oho, T., and Koga, T. 1999. Recombination between *gtfB* and *gtfC* is required for survival of a dTDP-rhamnose synthesis-deficient mutant of *Streptococcus mutans* in the presence of sucrose. Infect. Immun. **67**(7): 3693-3697.

Yin, S., Daum, R.S., and Boyle-Vavra, S. 2006. VraSR two-component regulatory system and its role in induction of *pbp2* and *vraSR* expression by cell wall antimicrobials in *Staphylococcus aureus*. Antimicrob. Agents Chemother. **50**(1): 336-343.

Yoshida, A., Ansai, T., Takehara, T., and Kuramitsu, H.K. 2005. LuxS-based signaling affects *Streptococcus mutans* biofilm formation. Appl. Environ. Microbiol. **71**(5): 2372-2380.

Yoshimura, G., Komatsuzawa, H., Hayashi, I., Fujiwara, T., Yamada, S., Nakano, Y., Tomita, Y., Kozai, K., and Sugai, M. 2006. Identification and molecular characterization of an N-Acetylmuraminidase, Aml, involved in *Streptococcus mutans* cell separation. Microbiol. Immunol. **50**(9): 729-742.

Yu, H., Nakano, Y., Yamashita, Y., Oho, T., and Koga, T. 1997. Effects of antibodies against cell surface protein antigen PAc-glucosyltransferase fusion proteins on glucan synthesis and cell adhesion of *Streptococcus mutans*. Infect. Immun. **65**(6): 2292-2298.

Zuker, M. 2003. Mfold web server for nucleic acid folding and hybridization prediction. Nucleic Acids Res. **31**(13): 3406-3415.